

A RADIONUCLIDE STUDY OF THE CLYDE SEA AREA

THESIS

submitted for the degree of

DOCTOR OF PHILOSOPHY

of the

UNIVERSITY OF GLASGOW

by

ANGUS BUCHANAN MACKENZIE

Chemistry Department

February 1977

ProQuest Number: 13804111

All rights reserved

INFORMATION TO ALL USERS

The quality of this reproduction is dependent upon the quality of the copy submitted.

In the unlikely event that the author did not send a complete manuscript and there are missing pages, these will be noted. Also, if material had to be removed, a note will indicate the deletion.



ProQuest 13804111

Published by ProQuest LLC (2018). Copyright of the Dissertation is held by the Author.

All rights reserved.

This work is protected against unauthorized copying under Title 17, United States Code
Microform Edition © ProQuest LLC.

ProQuest LLC.
789 East Eisenhower Parkway
P.O. Box 1346
Ann Arbor, MI 48106 – 1346

TABLE OF CONTENTS

PAGE

Acknowledgements

List of Tables

List of Figures

Summary

CHAPTER 1 INTRODUCTION AND THEORY

1.1.	General principles and aims of research	1
1.2.	The Clyde Sea Area	3
1.3.	Radium isotopes in the marine environment	20
1.4.	Radiocaesium in the marine environment	34

CHAPTER 2 EXPERIMENTAL

2.1.	General aspects of analytical procedures	53
2.2.	Hydrographic data	55
2.3.	^{226}Ra analytical and nuclear counting techniques	56
2.4.	^{228}Ra analytical and nuclear counting techniques	66
2.5.	^{226}Ra analysis of water samples	76
2.6.	^{228}Ra analysis of water samples	82
2.7.	Radium analysis of sediment	83
2.8.	Radiocaesium analysis of marine materials	89

CHAPTER 3 RESULTS 100

CHAPTER 4 DISCUSSION AND CONCLUSIONS

4.1.	General aspects of caesium concentrations in Clyde Sea Area water	175
4.2.	General aspects of radium concentrations in Clyde Sea Area water	195
4.3.	Water circulation and residence time in Loch Goil	204

4.4.	Radium and radiocaesium concentrations in Clyde Sea Area sediments	227
4.5.	Radiocaesium budget for the Clyde Sea Area	231
4.6.	Radium budget for the Clyde Sea Area	232
4.7.	General conclusions	233
APPENDIX 1		237
APPENDIX 2	Extraction of trace metals from sea water using manganese dioxide impregnated acrylic fibre.	240
APPENDIX 3	Calculations and computer programs	243
REFERENCES.		250

ACKNOWLEDGEMENTS

I wish to record my sincere gratitude to Dr. M.S. Baxter for his tuition, assistance and advice given willingly during his supervision of this research and in the preparation of this thesis. I am also deeply indebted to Dr. W. Jack for his tuition in γ -spectroscopy and for the use of the facilities of his laboratory.

The project relied upon the Clyde River Purification Board for the provision of sampling facilities and hydrographic data. Of the various members of the Clyde River Purification Board staff who contributed I wish particularly to thank J. Curtis, W. Halcrow, W. Ingram, Dr. T Leatherland, D. Mackay, E. McBride and Dr. A. Newton.

The glassblowing and workshop sections of the Chemistry Department of the University of Glasgow under the supervision of J. Connolly and A. Hislop contributed greatly by the construction and efficient maintenance of necessary equipment in this research.

I was privileged to work with colleagues who provided not only a stimulating scientific environment but also an excellent group of friends including H.M. Blauer, J.A. Campbell, R. Crawford, N. Drndarski, Dr. A.E. Fallick, Dr. J.G. Farmer, Dr. T.D.B. Lyon, K. MacKay, A. Mackie, I.G. McKinley, A. Millar, Dr. M.J. Stenhouse and D.S. Swan. Drs. T. Baird, I. Dale, W.S. Moore and J. Thomson provided advice and assistance with various aspects of my work.

Without the support and continuous encouragement of my parents I could not have performed this research and I wish to express my profound gratitude to them. I am also deeply indebted to my sister-in-law Mrs. E. MacKenzie for her many hours of patient and precise work spent in typing and other aspects of the preparation of this thesis.

I wish finally to express my sincere gratitude to the Natural Environment Research Council who funded both equipment and salaries for this research.

LIST OF TABLES

	PAGE
1. Physical dimensions of the Clyde Sea Area.	5.
2. Fresh water flow in the northern section of the Clyde Sea Area.	6.
3. Some major pollutant inputs to the Clyde Sea Area.	7.
4. Isotopes of radium found in natural waters.	21.
5. Typical ^{226}Ra concentrations in the worlds oceans.	30.
6. Typical ^{228}Ra concentrations in the worlds oceans.	33.
7. Total inventory of artificial radionuclides introduced into the worlds oceans.	35.
8. Radionuclide concentrations from global fallout for seawater, sediments and biological materials.	36.
9. Radionuclide concentrations resulting from the controlled disposal of radioactive wastes from nuclear power production for seawater, sediments and biological materials.	37.
10. Major discharges of liquid radioactive waste to surface and coastal waters during 1972/73.	44 and 45.
11. Mean ^{134}Cs and ^{137}Cs concentrations in sea water from the Irish Sea and its north western approaches 1972/73.	47.
12. Radioactivity in fish and shellfish in the Irish Sea 1972/73.	49.

13.	Radioactivity in seaweed and foreshore materials around the Irish Sea and Western Scotland 1972/73.	50.
14.	^{222}Rn detector backgrounds and efficiencies.	63.
15.	Calibration data for extraction of ^{226}Ra from 60 l standard solutions using manganese dioxide impregnated acrylic fibre.	81.
16.	^{226}Ra and ^{137}Cs concentrations in fractional dissolution of Loch Goil sediment	90.
17.	Decay schemes for ^{134}Cs and ^{137}Cs .	95.
18.	Radium samples from Clyde estuary; 11.12.73.	101.
19.	Radium samples from Gareloch; 14.1.74.	103.
20.	Radium samples from River Clyde; 21.1.74.	105.
21.	Radium samples from Clyde estuary/River Leven; 28.2.74.	107.
22.	Radium samples from Clyde estuary; 9.4.74.	109.
23.	Radium samples from Loch Goil; station 1; 8.5.74.	111.
24.	Radium samples from Skelmorlie Bank; 11.6.74.	114.
25.	Radium samples from Gareloch; 20.6.74.	116.
26.	Radium and caesium samples from Loch Goil; station 1; 18.7.74.	117.
27.	Caesium samples from the Firth of Clyde; 30.7.74.	119.
28.	Radium and caesium samples from Loch Goil; station 1; 10.9.74.	121.
29.	Radium samples from Loch Goil; station 1; 25.10.74.	124.
30.	Caesium samples from firth; 25.2.75.	127.

31.	Caesium samples from the estuary, Gareloch and Loch Long; 4.3.75.	128.
32.	Radium and caesium samples from Loch Goil; station 1; 8.4.75.	130.
33.	Caesium samples from Loch Goil, Loch Long and the Firth of Clyde; 8.4.75.	132.
34.	Radium and caesium samples from Clyde estuary; 1.5.75.	134.
35.	Radium and caesium samples from Clyde estuary; 3.6.75.	136.
36.	Caesium samples from Gareloch; 6.11.75.	138.
37.	Caesium samples from the Firth of Clyde; 14.11.75.	139.
38.	Caesium samples from Loch Long; 4.12.75.	141.
39.	Caesium samples from Loch Goil; station 1; 4.12.75.	142.
40.	Caesium samples from Loch Goil; station 2; 4.12.75.	144.
41.	Caesium samples from Loch Long; 8.1.76.	146.
42.	Caesium samples from Loch Goil; station 1; 8.1.76.	147.
43.	Caesium samples from Loch Goil; station 2; 8.1.76.	149.
44.	Caesium samples from Loch Goil, Loch Long; 4.2.76.	151.
45.	Caesium samples from Loch Fyne (middle and south basins); 17.2.76.	153.
46.	Caesium samples from Loch Fyne (north basin); 17.2.76.	154.

47.	Caesium samples from Loch Long; 8.3.76.	156.
48.	Caesium samples from Loch Goil; station 1; 8.3.76.	157.
49.	Caesium samples from Loch Goil; station 2; 8.3.76.	159.
50.	Caesium samples from Loch Goil; station 1; 1.4.76.	161.
51.	Caesium samples from Loch Goil; station 2; 1.4.76.	163.
52.	Caesium samples from Loch Goil; station 3; 1.4.76.	165.
53.	Miscellaneous caesium samples.	167.
54.	Radium analyses of sediment cores G L G 1 and G L G 2 collected by gravity corer from Gareloch; station 1; 14.1.74.	169.
55.	Radium and caesium analyses of sediment core L G C 2 collected by Craib corer from Loch Goil; station 1; 8.4.75.	170.
56.	Radium and caesium analyses of sediment core L G G 5 collected by gravity corer from Loch Goil; station 1; 8.4.75.	172.
57.	Radium and caesium analyses of sediment core G L C 1 collected by Craib corer from Gareloch; station 2; 6.11.75.	173.
58.	Estimated combined water residence times for the Clyde Sea Area/Irish Sea based on ²²⁶ Ra measurements.	199.
59.	Ministry of Agriculture, Fisheries and Food estimates of northwards flow of water through the North Channel.	201.

60. Estimations of density profiles for Loch
Goil 1974-1976.

210-212.

61. Estimated total inventories of ^{226}Ra and
silicate for Loch Goil during 1974.

218.

LIST OF FIGURES

	PAGE.
1. The Clyde Sea Area.	4.
2. Lateral sections and section along axis of greatest depth for Loch Goil.	10.
3. Lateral sections and section along axis of greatest depth for Gareloch.	11.
4. Surface sediments in the northern section of the Clyde Sea Area.	13.
5. Variation of dissolved oxygen in the bottom water of Loch Goil during 1974.	17.
6. The natural decay series.	22.
7. Component operations in critical pathway analysis.	39.
8. Locations of sites discharging liquid radioactive waste to surface and coastal waters during 1972/73 (c.f. Table 10).	43.
9. Locations of M.A.F.F. sampling sites named in Table 11.	47.
10. Concentrations of ^{137}Cs in British Isles coastal water in 1973.	51.
11. Summary of experimental techniques.	54.
12. ^{222}Rn emanation system.	57.
13. (a) Section through ^{222}Rn detector (b) ^{222}Rn detector/photomultiplier assembly.	60.
14. ^{222}Rn detector plateau.	62.
15. Graph of grow in of ^{222}Rn daughter activity.	64.
16. Graph of decay of ^{222}Rn .	65.
17. Schematic diagram of Tracerlab counter.	71.

18.	Tracerlab counter guard and detector plateaux.	72.
19.	Histogram of 100 minute backgrounds recorded on Tracerlab counter in the period 1972-1976.	73.
20.	Graph of decay of ^{228}Ac .	75.
21.	Shipboard sampling systems.	79.
22.	Sections of gravity and Craib corers.	84.
23.	Freezer/transporter unit for sediment cores.	85.
24.	Summary of dissolution procedure for sediment samples.	88.
25.	Caesium extraction system for 10 l water samples.	93.
26.	Typical γ spectra.	96.
27.	Regression analysis plot for data obtained from analysis of ^{137}Cs spiked 5 l sea water samples.	98.
28.	Location of sampling sites for samples R1-R3.	102.
29.	Map showing location of Gareloch sampling sites.	104.
30.	Location of sampling sites for samples R7-R9.	106.
31.	Location of sampling sites for samples R10-R13.	108.
32.	Location of sampling sites for samples R14-R19.	110.
33.	Map showing location of Loch Goil sampling sites.	112.
34.	Hydrographic and radium profiles for Loch Goil; station 1; 8.5.74.	113.
35.	Location of sampling site for samples R26-R28.	115.

36.	Hydrographic and radium profiles for Loch Goil; station 1; 18.7.74.	118.
37.	Location of sampling sites for samples C2-C15.	120.
38.	(a) Hydrographic profiles for Loch Goil; station 1; 10.9.74.	122.
	(b) Radium and caesium profiles for Loch Goil; station 1; 10.9.74.	123.
39.	(a) Hydrographic profiles for Loch Goil; station 1; 25.10.74.	125.
	(b) Radium profiles for Loch Goil; station 1; 25.10.74.	126.
40.	Location of sampling sites for samples C20-C26.	129.
41.	Hydrographic and radium profiles for Loch Goil; station 1; 8.4.75.	131.
42.	Map showing location of sampling sites in Loch Goil, Loch Long and Firth of Clyde.	133.
43.	Location of sampling sites for samples R56-R61/C39-C44.	135.
44.	Location of sampling sites for samples R62-R66/C45-C49.	137.
45.	Location of sampling sites for samples C52-C60.	140.
46.	Hydrographic and caesium profiles for Loch Goil; station 1; 4.12.75.	143.
47.	Hydrographic and caesium profiles for Loch Goil; station 2; 4.12.75.	145.

48.	Hydrographic and caesium profiles for Loch Goil; station 1; 8.1.76.	148.
49.	Hydrographic and caesium profiles for Loch Goil; station 2; 8.1.76.	150.
50.	Map showing sampling sites in Loch Goil, and Loch Long.	152.
51.	Map showing location of Loch Fyne sampling sites.	155.
52.	Hydrographic and caesium profiles for Loch Goil; station 1; 3.3.76.	158.
53.	Hydrographic and caesium profiles for Loch Goil; station 2; 3.3.76.	160.
54.	Hydrographic and caesium profiles for Loch Goil; station 1; 1.4.76.	162.
55.	Hydrographic and caesium profiles for Loch Goil; station 2; 1.4.76.	164.
56.	Hydrographic and caesium profiles for Loch Goil; station 3; 1.4.76.	166.
57.	Map showing location of sampling sites for miscellaneous caesium samples.	168.
58.	Radium and caesium concentrations in sediment core L G C 2.	171.
59.	Radium and caesium concentrations in sediment core G L C 1.	174.
60.	Mean discharge of ^{137}Cs from the Windscale nuclear fuel processing plant during the period 1965-1975.	

61. (a) Monthly output of ^{137}Cs (normalized to January 1975) for Windscale 1973-1976 (b) Mean Seascale - St Bees sea water concentration of ^{137}Cs 1973-1976 (c) Mean North Channel sea water concentrations of ^{137}Cs , 1973-1976. 178.
62. ^{137}Cs concentrations in sea water 1974-1976 for (a) Clyde Sea Area (20m) (b) Clyde Sea Area (surface concentrations normalized to 35‰ salinity) (c) North Channel. 180.
63. $^{134}\text{Cs}/^{137}\text{Cs}$ activity ratio for (a) Windscale effluent (b) North Channel sea water (c) Clyde Sea Area surface water. 181.
64. Residual ^{137}Cs values for the firth on 30.7.74 after subtraction of the lowest observed value. 192.
65. Residual ^{137}Cs values for the firth on 14.11.75 after subtraction of the lowest observed value. 193
66. Plot of ^{137}Cs concentrations versus salinity for samples collected on 1.5.75. 194.
67. Variation of (a) $^{228}\text{Ra}/^{226}\text{Ra}$ activity ratio (b) mean ^{226}Ra concentration in Clyde Sea Area water during 1974 and 1975. 196.
68. Plot of ^{226}Ra concentrations versus salinity for samples collected on 1.5.75 and 3.6.75. 203.
69. Loch Goil density profiles 1974-1976. 213 and 214.
70. Silicate profiles for Loch Goil during 1974. 217.
71. (a) Total silicate inventory for Loch Goil for 1974 (b) Total ^{226}Ra inventory for Loch Goil for 1974 (c) Plot of total ^{226}Ra inventory versus total silicate inventory for Loch Goil during 1974. 219.

72. $^{228}\text{Ra}/^{226}\text{Ra}$ activity ratio versus silicate
concentration for Loch Goil during 1974. 221 and 222.
73. $^{228}\text{Ra}/^{226}\text{Ra}$ activity ratio versus dissolved
oxygen for Loch Goil during 1974. 223 and 224.
- 74 Silicate concentration versus dissolved
oxygen for Loch Goil during 1974. 225 and 226.

SUMMARY

This thesis presents the sampling and analytical procedures developed and the results obtained in a survey of the concentrations of ^{134}Cs , ^{137}Cs , ^{226}Ra and ^{228}Ra in the waters and sediments of the northern section of the Clyde Sea Area. The suitability of these nuclides as tracers of coastal marine processes is discussed and the results are applied to the estimation of water residence times and mixing rates and to the patterns of sedimentation in the area.

^{226}Ra concentrations are determined both by preconcentration from 60 l samples and by direct analyses of 20 l samples, emanation and α counting of ^{222}Rn being used in both cases. ^{228}Ra assay is performed by non-quantitative extraction of radium from more than 1000 l of sea water onto manganese dioxide impregnated acrylic fibre. The $^{228}\text{Ra}/^{226}\text{Ra}$ activity ratio of the extracted radium is determined and the ^{228}Ra concentration derived by comparison with the previously determined ^{226}Ra concentration.

^{134}Cs and ^{137}Cs concentrations are measured by extraction of caesium from 10 l samples of sea water onto the inorganic ion exchanger potassium hexacyanocobalt (II) ferrate (II) (KCFC). Radiocaesium determination is achieved by direct γ -ray spectrometric analysis of the ion exchange column.

The dominant input of radiocaesium to the Clyde Sea Area is demonstrated to be the effluent from the Windscale nuclear fuel reprocessing facility in Cumbria. Matching of maxima in ^{137}Cs concentrations with the Windscale output and with reported values for the North Channel indicates a water transit time of about 3 months for movement from the North Channel to the northern parts of the Clyde Sea Area. Caesium mass budget calculations indicate a mean water

residence time of about 3.9 months for the area and homogeneous vertical profiles imply rapid vertical mixing. About 23% of the ^{137}Cs discharged from Windscale is estimated to pass through the the Clyde Sea Area with 0.08% to 0.4% being retained in the sediments. Loch Goil is the only part of the region to exhibit a long residence time and radiocaesium data indicate that deep water renewal occurs by exchange with Loch Long water at a depth of about 20m. The transient development of a strong pycnocline below 20m leads to entrainment of the deep water and consequently increased residence times.

Typical ^{226}Ra concentrations are demonstrated to be in the range 100 - 160 dpm/1000 l while $^{228}\text{Ra}/^{226}\text{Ra}$ ratios are normally about 1.5. This enrichment relative to Atlantic concentrations is attributed to diffusion from sediments since river input is shown to supply only about 1% of the ^{226}Ra in the area. Despite the fact that diffusion of radium from sediments is the major input, the biological silicate cycle is demonstrated to exert a controlling influence on the ^{226}Ra concentrations in Loch Goil. The complex behaviour of radium thus demonstrated means that evaluation of water mixing processes is virtually impossible on the basis of radium measurements alone.

Both radium and radiocaesium are shown to exhibit conservative behaviour over the salinity range 0 to 32‰ encountered in the estuary.

^{226}Ra and $^{134}\text{Cs}/^{137}\text{Cs}$ analyses of sediment cores reveal that neither radium nor radiocaesium can be used to establish a sediment chronology in this environment but that both can be used to indicate patterns of sediment accumulation with mixing depths of 4cm and more than 10cm being defined for Loch Goil and Gareloch respectively. The $^{134}\text{Cs}/^{137}\text{Cs}$ ratio is also shown to be very useful in assessing the efficiency of recovery of surface sediment. The enrichment of ^{137}Cs

in Gareloch sediment relative to ambient water concentrations is found to be about 3 times greater than that for Loch Goil. A difference in particulate flux is postulated as a possible reason for this variation. Anomalously high ^{226}Ra concentrations are reported for the top 10cm of Loch Goil, with no obvious cause being apparent from the available information.

CHAPTER 1

INTRODUCTION AND THEORY

1. 1. General principles and aims of research.

The investigation of patterns and rates of water circulation and sediment accumulation constitute major areas of research in oceanography. Direct measurement of these processes using instruments such as current meters, drift bottles and sediment traps can be of value. The methods, however, are often time-consuming and results can be subject to large spatial and temporal variations, thus complicating interpretation. It has therefore become standard practice to study these phenomena indirectly by measurement of some property distribution in the sediment or water (Pickard, 1975).

Water circulation and mixing may be considered to occur by a combination of advective and diffusive mechanisms. Advective processes, in which there is a net flow of water, occur where an unstable density gradient is established in a water column or where some external force such as tidal or wind action induces movement of the water. Diffusive processes, in which there is exchange of properties without net movement of water, are regarded as occurring by a mechanism of random eddies, diffusion by this method occurring at a much faster rate than simple molecular diffusion (Bowden, 1965). The characteristic definitive properties of any sample of sea water are its salinity (‰) and temperature ($^{\circ}\text{C}$). The former can be regarded as the total weight in grams of dissolved solids in one kilogram of sea water and is defined by relationship to the conductivity of the solution (Wallace, 1974). These parameters, in conjunction with pressure, uniquely define the density of the solution (Pickard, 1975). The distribution of salinity

and temperature can often be used, therefore, to establish the major features of water structure and to rationalise and quantify mixing processes in terms of density variations (Sverdrup et al, 1942 ; Bowden, 1965). However, where information on rates of such processes is required or in investigations of mixing within a water mass having only a small variation of salinity and temperature, these measurements are often inadequate and must be used in conjunction with observations of some additional property, or tracer, which varies in magnitude as a function of the process being studied. A variety of physical, chemical and biological properties have been used for this purpose but one of the most successful has been radionuclide content of the water.

Two types of information can be derived from an investigation of radionuclide concentrations in sea water. Firstly, where a water mass becomes 'labelled' with one or more radionuclide, the radioactive species can be used as a 'dye-type' tracer such that variations in concentration quantitatively reflect movement and dispersion processes. Secondly, if the half-life of the nuclide is of the same order of magnitude as the timescale of the mixing process then its decay may be used as a 'radioactive clock' to determine the rate at which the process is occurring (Burton, 1965 ; Broecker, 1974). Both naturally-occurring and man-made radionuclides have been successfully employed to study advective and diffusive processes operating over a wide variety of timescales.

In sedimentation studies, radionuclide concentrations can again provide uniquely valuable information. Relative rates of sedimentation can be obtained by palaeontological, chemical and magnetic analyses of sediment cores. If, however, an unsupported radionuclide of appropriate half-life is incorporated into an accumulating sediment and thereafter

remains in a closed system, its decay provides an absolute method for determination of the time elapsed since formation of any particular section of sediment and so allows calculation of the mean sedimentation rate (Burton, 1965 ; Goldberg, 1974).

It is the object of this research to provide a preliminary survey of the distribution and geochemical behaviour of the radionuclides ^{134}Cs , ^{137}Cs , ^{226}Ra and ^{228}Ra in the waters and sediments of the northern section of the Clyde Sea Area; to evaluate the potential of these species as marine tracers and where possible to apply them in a study of both water mixing and sediment accumulation rates in the area.

1. 2. The Clyde Sea Area.

The term 'Clyde Sea Area', first introduced by Mill (1892), is used to describe the system of salt water bodies of total surface area 2,500 km² lying to the north of a line from Girvan to the Mull of Kintyre ie. 55° 15'N (Figure 1). This area, overlying two of the major geological regimes of southern Scotland and serving the industrial, domestic and recreational needs of about half the population of Scotland has attracted scientific investigation for almost a hundred years, firstly because of the inherent interest of the natural system and secondly to assess the effects of human activity on the region. Since Mill's original survey, considerable interdisciplinary information has been accumulated concerning this area and a synoptic account, outlining the state of present knowledge and future research requirements, was prepared by the Natural Environment Research Council in 1974. Some of the basic data from this and other sources are presented in Tables 1 to 3.

The major bathymetric features of the Clyde Sea Area and the drainage patterns of the surrounding land areas can be related directly

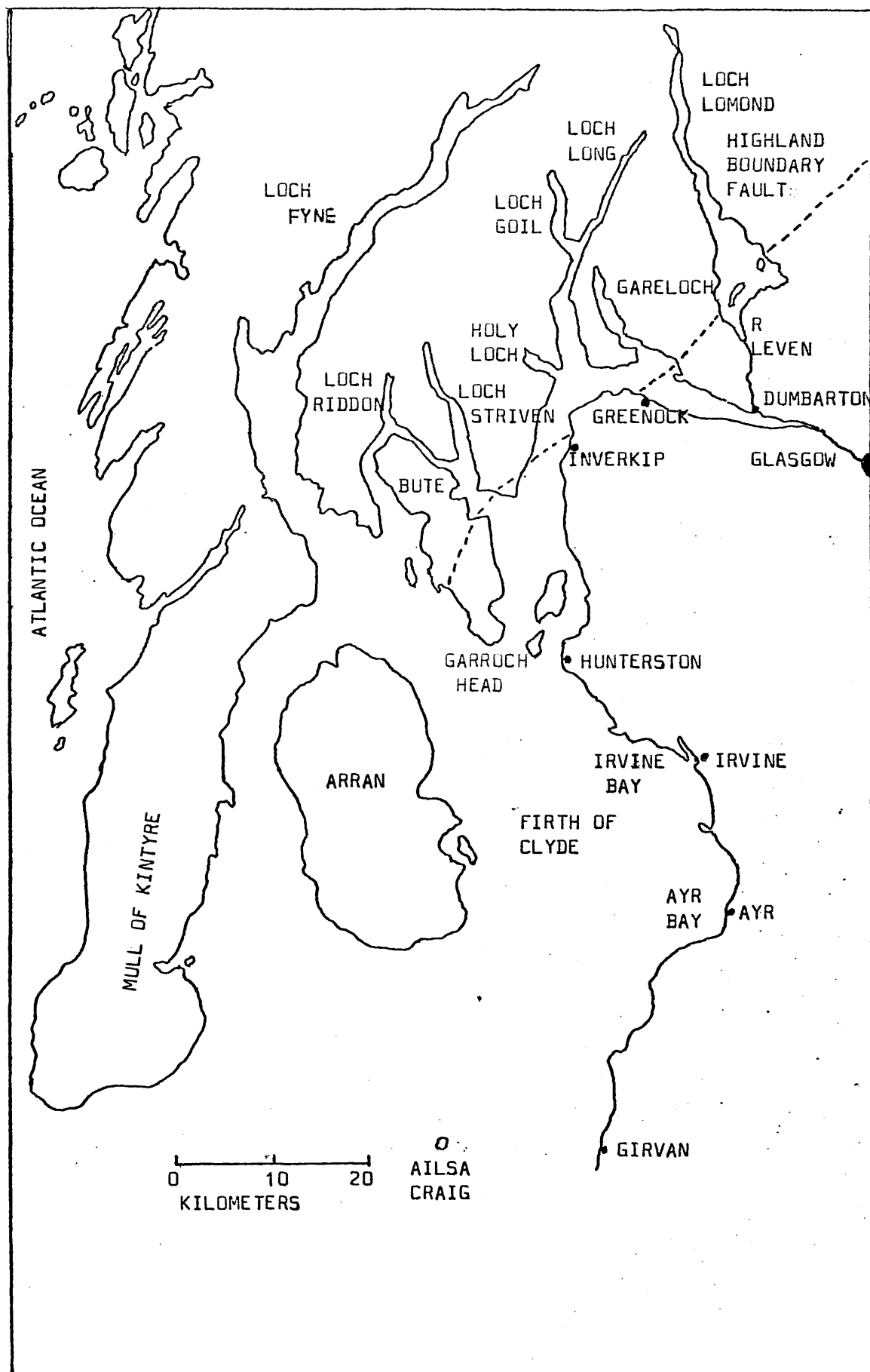


FIGURE 1. The Clyde Sea Area.

Section	Coastline (km)	Area (km ²)	Volume (km ³)
Total Clyde Sea Area		2,500.0*	165.0**
Estuary	170.0	69.0	0.9
Inner Firth		185.0	7.8
Gareloch	33.0	20.5	0.21
Loch Long	57.0	36.2	1.3
Loch Goil		9.0	0.31
Holy Loch	11.0	4.9	0.07
Loch Striven	33.0	15.0	0.5
Loch Riddon/ Kyles of Bute	67.0	44.5	1.27
Loch Fyne	183.0	210.0	13.3

TABLE 1. Physical dimensions of the Clyde Sea Area.

* Natural Environment Research Council, 1974.

** Cambray et al, 1975.

All other information from Clyde River Purification Board baseline data; Leatherland, 1976.

Section	Fresh Water Flow ($\text{m}^3 \text{ sec}^{-1}$)			
	5% exceedence	50% exceedence	95% exceedence	Mean
Estuary	335.0	80.0	28.0	113.0
Inner Firth	17.0	2.4	0.4	
Gareloch	5.7	0.5	0.1	1.9
Loch Long	23.7	2.3	0.3	12.2
Loch Goil	17.8	1.7	0.3	7.8
Holy Loch	31.3	6.8	1.4	11.2
Loch Striven	12.5	1.2	0.2	3.7
Loch Riddon/ Kyles of Bute	23.6	2.3	0.3	7.2
Loch Fyne	129.0	12.3	1.9	38.4
* River Clyde	140.0	23.0	8.0	
* River Kelvin	26.3	5.0	1.4	
* River Carts	28.0	8.5	2.7	
* River Leven	91.0	37.3	14.6	

TABLE 2. Fresh water flow in the northern section of the Clyde Sea Area.

* Natural Environment Research Council, 1974.

Other information from Clyde River Purification

Board baseline data; Leatherland, 1976.

* Sewage:

Section	Estimated input ($\text{m}^3 \text{ day}^{-1}$)
Upper Estuary	10^6
Lower Estuary	0.045×10^6
Firth	0.059×10^6

**Metals:

Metal	Input from River Clyde (tonnes y^{-1})	Sewage sludge deposits (tonnes y^{-1})	Input from Irish Sea (tonnes y^{-1})	Freshwater input from run off (tonnes y^{-1})	Input by rainwater (tonnes y^{-1})
Cu	10.0	25.0	43.0	10.0	50.0
Zn	45.0	60.0	270.0	50.0	250.0
Cd	0.4	0.25	4.0	0.6	1.7
Pb	20.0	25.0	8.0	35.0	60.0

TABLE 3. Some major pollutant inputs to the Clyde Sea Area.

* Natural Environment Research Council, 1974.

** Cambrey et al, 1975.

to the geological structure of the region, the most marked feature of which is the Highland Boundary Fault. To the north of the fault lie the Grampian Highlands composed of quartzose mica schists with subordinate grits, quartzites and limestones, all of which have been subjected to regional metamorphism (Johnstone et al, 1966). South of the fault, the sedimentary sequences of the midland valley, of Old Red Sandstone and Carboniferous age, consist of lavas, mudstones, sandstones and thick coal seams. More recent sediments are poorly represented and geological evidence suggests that these sequences, although initially present, were removed by subsequent erosion (MacGregor and MacGregor, 1948). The present topography of the region resulted largely from the differential erosion of these varied rocks during the Pleistocene glaciation. The obdurate metamorphic rocks of the Grampian Highlands remain as a peneplane of average elevation about 800m deeply dissected by overdeepened glacial depressions and have a thin, peaty soil covering. Drainage is by short, fast rivers and by direct run-off from the hills. The midland valley, composed of less resistant sedimentary rocks, forms an undulating lowland with a surface drift covering of peat, sand, gravel, moraines and boulder clay. Drainage is by longer, meandering rivers flowing west and dominated by the Clyde river system.

The Clyde Sea Area may be divided into three distinct sections, the bathymetries of which closely parallel the underlying rockhead contours. These are:

- (1) A shallow drowned estuary stretching as part of the Clyde river system from a tidal weir in Glasgow westwards for a distance of 38km.
- (2) The deeper open water of the Firth of Clyde.
- (3) A series of fjord-like sea lochs penetrating northwards into the Grampian Highlands.

The estuary has been greatly modified from its natural condition and a dredged channel extends 36km of its length, with progressive deepening recorded since the beginning of the 19th century. The estuary has minimum and average depths of 8.1m and 10m respectively and from Glasgow to 14.5km downstream is totally contained in artificial banks. Downstream from this the estuary broadens and the main dredged channel is flanked by broad, shallow mud flats many of which are exposed at low tide (Collar, 1974). The estuary also receives the freshwater input from the rivers Kelvin, Carts and Leven, the latter being the outlet for the large Loch Lomond catchment area. Data for total freshwater input to the estuary are summarised in Table 2.

Westwards of a line from Greenock to Roseneath Point, the depth of water increases rapidly from about 30m to 60m on moving from the estuary to the firth, the bathymetry of which is marked by the presence of deep trenches leading into the sea lochs in the north. The Loch Fyne depression diverges and flanks each side of the island of Arran, giving rise to the deepest water in the region at 220m. To the south of Arran, at the limit of the Clyde Sea Area, lies a broad submarine plateau of average depth about 40m separating the deep waters of the firth from the deep waters of the North Channel to the south.

The seven sea lochs of the area are all typical glacial trenches with steep sided, flat bottomed, narrow profiles. Loch Goil and Gareloch are enclosed by shallow sills and sections along axes of greatest depth and lateral sections at various points for these lochs are shown in Figures 2 and 3.

In a detailed study of the natural superficial sediment deposits of the firth and sea lochs, Deegan et al (1973) classified the sediments into a distribution of three facies, namely coarse littoral, transitional

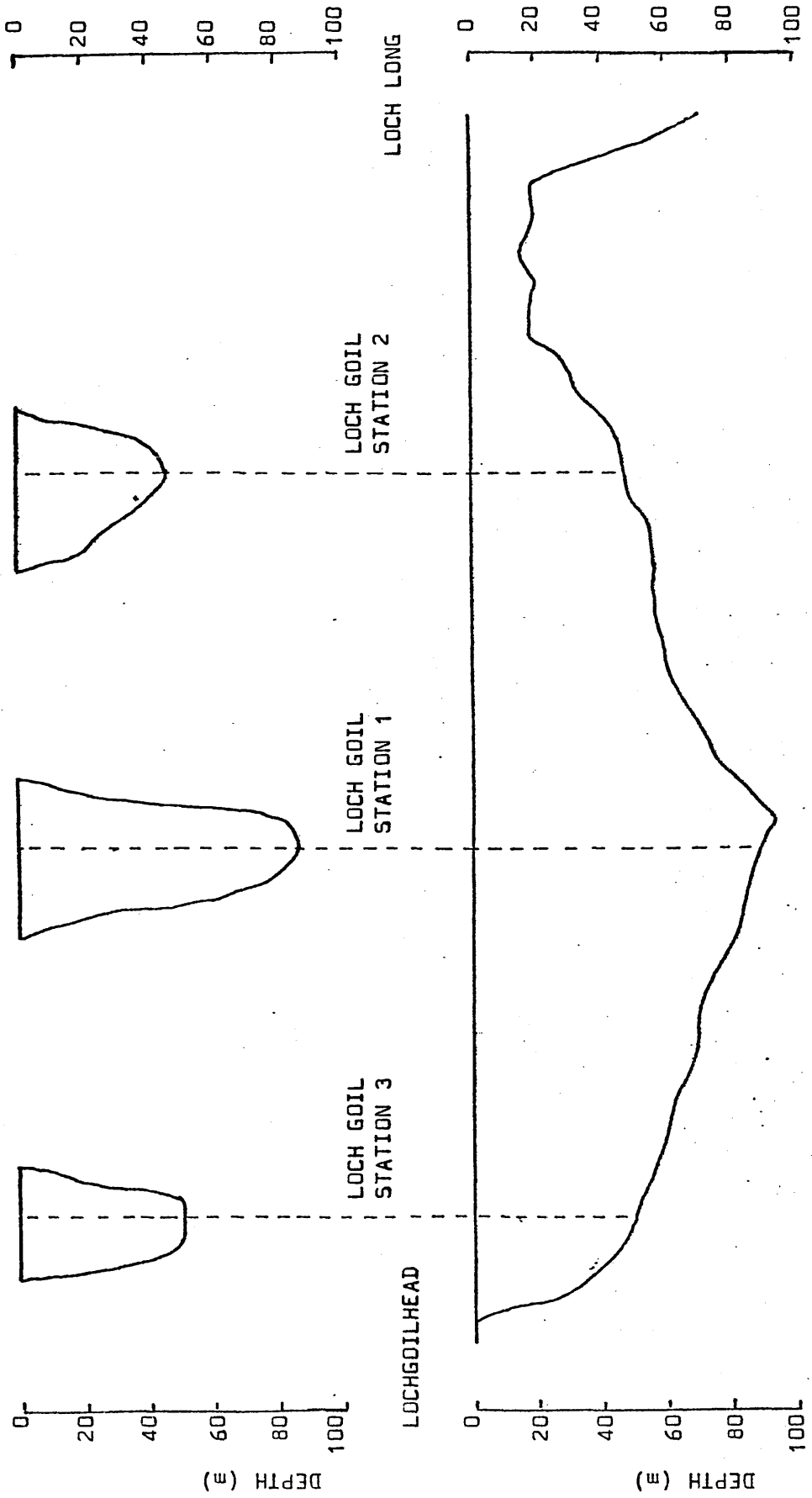


FIGURE 2. Loch Gail: Lateral sections and section along axis of greatest depth. Horizontal scale 1: 50,000; vertical exaggeration X 25. (Based on Admiralty Chart 3746, Haslam 1975).

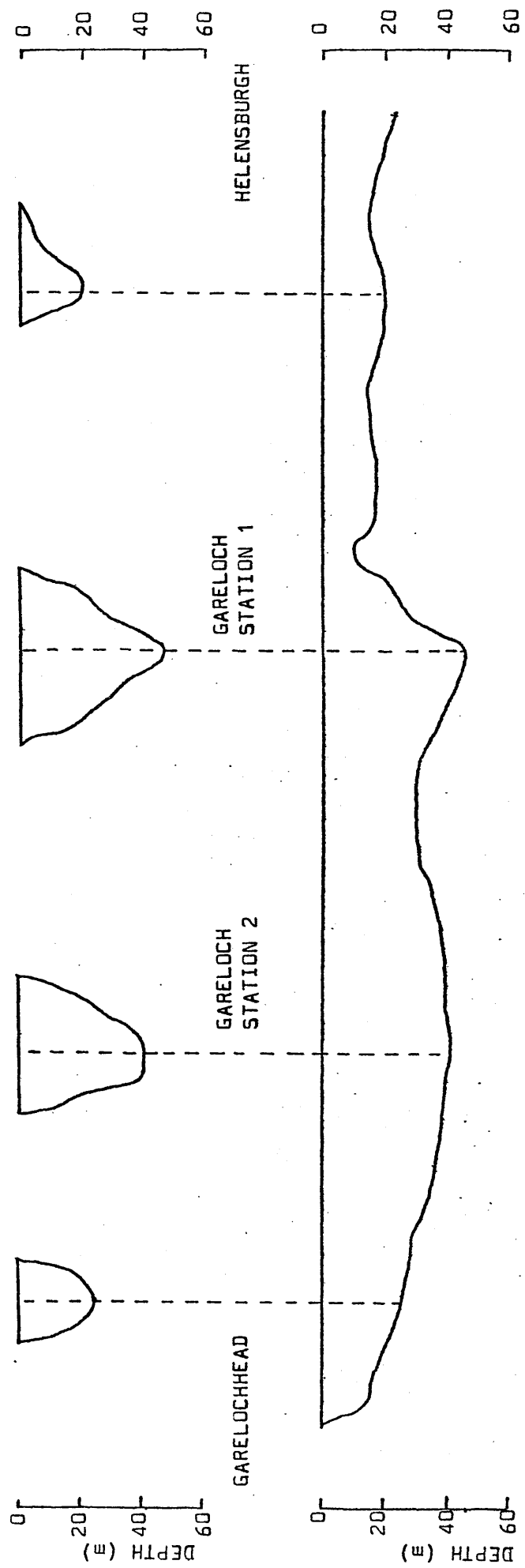


FIGURE 3. Gareloch : lateral sections and section along axis of greatest depth. Horizontal scale 1:50,000; vertical exaggeration X 25 (Based on Admiralty Chart 2000, Hall 1973).

and deep silty clay. The coarse littoral and intermediate facies cover only a limited area as a result of the common occurrence of deep water close to shore whereas the silty clay facies is the most abundant and occurs over most of the firth and sea lochs. The coarse littoral facies is composed of sands, gravels and skeletal carbonates and has greater than 80% of the sample coarser than $62.5\mu\text{m}$. The intermediate facies exhibits major variations in particle size and lithology but is generally similar to the silty clay with added sand and shell materials. Little of the silty clay material is greater than $62.5\mu\text{m}$ and this facies often passes without lithological break into the underlying Flandrian clays. The distribution of surface sediments in the northern section of the area is shown in Figure 4. The total sediment thickness in the firth varies from 160m in the deep trenches to as little as 10m in shallow areas. Sub-surface deposits consist of boulder clay overlain by a variety of sediments including marine clays, beach deposits, outwash gravels and peats depending on the particular local sequence of events during the eustatic sea level and isostatic land level changes at the end of the ice age. The sediments of the estuary have been intensively studied and the input, transport and deposition processes occurring have been well characterised (Gair, 1967 ; Fleming, 1969 ; Collar, 1974). The general conclusion from these investigations was that the estuary receives little or no sediment from the deep waters of the firth but that virtually all of the particulate matter entering at the head of the estuary is deposited within the estuary itself.

The natural patterns of sediment accumulation have been altered by the activity of man, most particularly in the estuary and localised zones of the firth such as the deep water (100m) site to the south of Garroch Head. The estuary receives the bulk of the sewage and

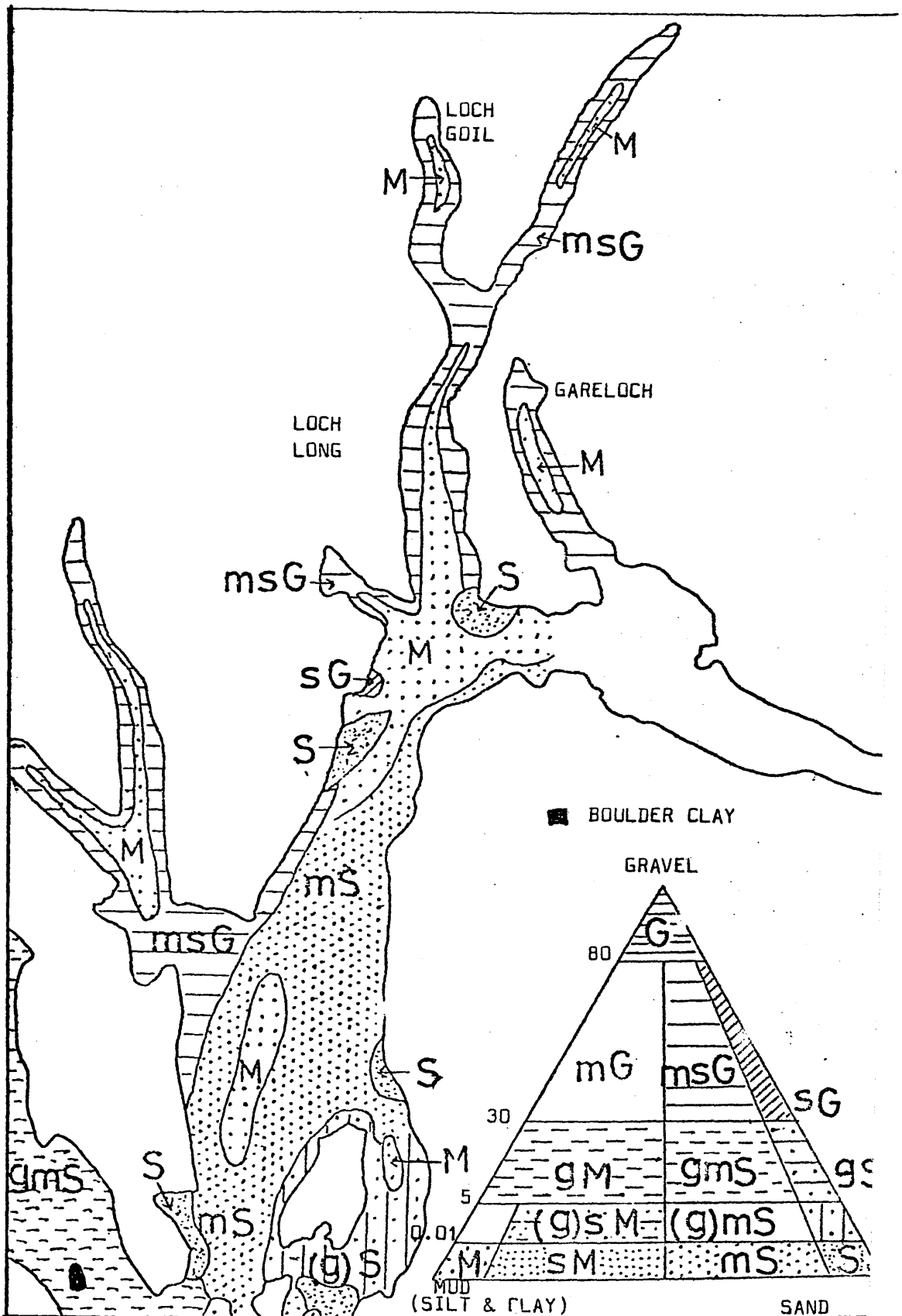


FIGURE 13. Surface sediments in the northern section of the Clyde Sea Area (Deegan et al 1973).

industrial effluent from the densely populated areas of Clydeside, giving rise to heavily polluted sediments in this section (Clyde River Purification Board, 1972, 1973, 1974). Dredging to maintain the navigable channel leads to dispersion of this polluted material to other parts of the system. The sludge from the settling tanks for the treatment of sewage and industrial effluents from the Glasgow area has been dumped in the area to the south of Garroch Head since the start of this century. This has produced a grossly contaminated area of sediment covering some 20km^2 and penetrating to a depth of 40 to 50cm in the sediment (Mackay et al, 1972 ; Halcrow et al, 1973 ; Baxter and Harkness, 1975).

Two quantitative measurements of sedimentation rates in the area have been reported. Moore (1931) measured the sediment flux through the water column to obtain a mean sedimentation rate of about 0.5cm y^{-1} in the Loch Striven area and also noted that the rate of sedimentation varied throughout the year as a function of the diatom population. Baxter and Harkness (1975) using $^{14}\text{C}/^{12}\text{C}$ ratio measurements deduced a modern 'artificial' sedimentation rate of $0.75 \pm 0.2\text{cm y}^{-1}$ for the Garroch Head dumping site and a 'natural' sedimentation rate of 0.3 to 0.6mm y^{-1} for sea lochs in the area. Indirect evidence concerning sedimentation rates can be derived from authigenic formation of manganese as nodules or shell replacements in the area, particularly in the north of the region, along the Kintyre coast and to the south of Arran (Buchanan, 1891 ; Calvert and Price, 1970). Since authigenic manganese generally occurs in areas of low sedimentation rate, Deegan et al (1973) postulated a low rate in this region.

Various methods, including tidal observations, hydrographic surveys, current meter studies and releases of drogues, surface drifters and dyes have been used to investigate water movements in the area.

Tidal observations have been recorded since the middle of the 19th century (Milne, 1974) and the system is well defined, with a small range relative to other estuarine areas in the United Kingdom. For example, at the junction of the estuary and the firth the mean ranges observed are 3.08m springs and 1.89m neaps (Collar, 1974). Tidal variations in the estuary are particularly well characterised and hydraulic modelling of the system has been performed (Thom, 1949 ; Thomson, 1969). Salinity and temperature surveys have also been carried out since the 19th century, in recent years on a regular basis by the Clyde River Purification Board. Salinities decrease from about 32‰ in the northern firth to near zero values at the head of the estuary while vertical profiles show the estuary system to be intermediate between well mixed and partially mixed (Collar, 1974). In the firth, temperature and salinity show only small variations which can largely be related to freshwater input from the estuary and rivers of the Ayrshire coast. For example, in an extensive survey in April 1970, Johnston et al (1974) found that at 3m the ranges of temperature and salinity encountered were 5.96°C in the central firth to 6.30°C off south Bute and 31.5‰ at the mouth of the estuary to 33.74‰ near the Mull of Kintyre. Much of the firth had salinities in the range 33.2‰ to 33.5‰ and vertical profiles of both temperature and salinity showed only small gradients, with water deeper than 50m being about 0.15°C warmer and slightly more saline, at 33.7‰, relative to surface water. These values indicate small density variations throughout the region and consequently a stable system.

Salinity data have been used by Mill (1892) and Craig (1959) to estimate residence times for water in the area. On the basis of observed salinities and calculated freshwater input, Mill estimated the time for water renewal in Loch Fyne to be about 9 days while Craig

obtained a value of 9 months as the mean time for replacement of water in the firth.

Direct measurements of currents by current meters, drogues, drifters and dye releases have been performed mainly in areas receiving a heavy pollution burden such as Ayr and Irvine Bays and to constricted or shallow regions important for navigational purposes (Barnes and Goodley, 1961 ; Johnston et al, 1974 ; Dooley and Steel, 1969 ; Hall, 1973 ; Clyde River Purification Board, 1973). The results of these surveys indicate that surface and nearshore currents are largely wind induced whereas circulation in the open firth is more complex with winds, tides and estuarine circulation contributing. Movement of bottom water has been shown to be weak with a net northward flow.

In monthly surveys of salinity, temperature and dissolved oxygen content of the water in Loch Goil and Gareloch, the Clyde River Purification Board (1974a) has observed an annual cycle with large gradients in vertical profiles being established in summer. This applies particularly to dissolved oxygen and virtually anoxic conditions have been observed in deep water in Loch Goil in late summer. These conditions are generally followed by a rapid increase in dissolved oxygen content in early winter (Figure 5). These observations have been interpreted as a summer stratification of the loch, with very little vertical mixing followed by a 'winter overturn' and this apparent stratification, in conjunction with low freshwater input, has been used to infer long retention times for water in the sea lochs (Clyde River Purification Board, 1974b).

The waters of the Clyde Sea Area can exchange with the Atlantic Ocean and the Irish Sea via the North Channel. Communication with the Atlantic is by way of an 11 mile wide channel between the Mull of Kintyre and the Irish coast while that with the Irish Sea is by the

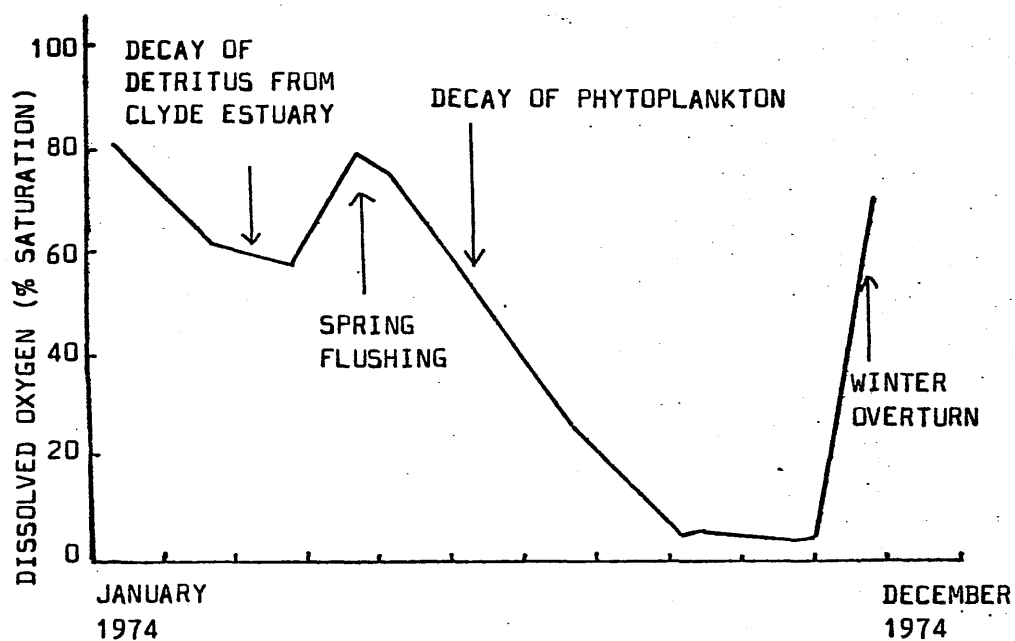


FIGURE 5. Variation of dissolved oxygen in the bottom water of Loch Goil during 1974. (Clyde River Purification Board, 1974a)

channel of 21 miles width between the Mull of Galloway and the Irish coast. No direct evidence is available concerning the relative proportion of Irish Sea to Atlantic water entering the Clyde Sea Area but a large Irish Sea contribution is implied by the data of Topping (1974) and Cambray et al (1975) for trace metal supply to the Clyde Sea (Table 3). Indirect evidence for water exchange derives from the well established north-easterly flow of the Atlantic in this area (Appendix 1), the dominant south westerly winds and the residual northwards flow of the Irish Sea (Proudman, 1948 ; Bowden, 1955 ; Wilson, 1974), all of which will promote exchange of water with the Clyde Sea.

The region supports heavy biological activity including a wide variety of marine flora and fauna. Herring, white fish, salmon and shellfish provide the catch for important fisheries in the area (Natural Environment Research Council, 1974). The firth and sea lochs exhibit an annual spring 'outburst' of phytoplankton followed throughout the summer by 'blooms' of both phytoplankton and zooplankton. The timing and size of the spring diatom outburst has been found to vary considerably from year to year (Marshall, 1974). Both benthic and pelagic organisms are abundant in the firth and sea lochs but are severely restricted or absent in the estuary as a result of the gross pollution prevalent there.

Pollutants added directly to the water of the area by the industrial and domestic activities of the 2.5 million people in the total catchment can be classified into six main types : oxygen consuming materials such as domestic sewage and certain industrial effluents, oil, trace organic materials, toxic metals, thermal pollution and radioactivity. As well as these 'direct' inputs, concentrations of contaminants in rainfall and Irish Sea water entering the area must be considered (Cambray et al, 1975). A summary of some major pollutant inputs is presented in Table 3. At

present the estuary receives the bulk of the pollution burden and concentrations of pollutants have been used to assess the dispersion of estuarine waters into the firth and sea lochs (Clyde River Purification Board, 1973, 1974a). The firth will, however, receive an increasing pollution load with the continuing movement of industrial and population centres to the Ayrshire coast and deep-water sites of the firth and sea lochs.

In summary, the present state of knowledge concerning the hydrography and sediments of the Clyde Sea Area depicts the system as a series of deep water basins with weak tidal action and stable water structure. Surface currents are wind induced, and consequently transient, while deep currents are very weak and of complex origin. Estimates of mixing and residence times for water in the firth and sea lochs are limited in number and tenuously based. The proportion of Irish Sea to Atlantic water entering the region remains undefined. The superficial sediment deposits are well characterised in terms of composition and pollutant concentrations but information concerning the sedimentation rate and stability of the unconsolidated sediment is limited.

Major topics for further investigation therefore concern water circulation and renewal rates and patterns and rates of sediment accumulation. This thesis describes a preliminary investigation of these processes by radiotracer studies with ^{134}Cs , ^{137}Cs , ^{226}Ra and ^{228}Ra in the northern section of the area. The research was performed in conjunction with a complementary investigation of sedimentation rates by ^{210}Pb dating techniques.

1. 3. Radium isotopes in the marine environment.

Radium is element number 88 in the periodic classification of elements and is the heaviest member of group 11a of the periodic table. It has a stable oxidation state of +2 in aqueous solutions and exhibits similar chemical properties to calcium, strontium and barium. All four elements form typically 'ionic' compounds in which the M^{2+} ions have high hydration energies. A systematic variation of physical and chemical properties is observed in the series Ca - Sr - Ba - Ra, the electropositive nature of the metal and ionic character of their compounds increasing from Ca to Ra. This results in a decrease in solubility of the sulphates, nitrates and chlorides down the group (Cotton and Wilkinson, 1968).

Radium exists in a number of isotopic forms, all of which are radioactive and the production and decay modes of the different isotopes are shown in Table 4. While the stable group 11a analogs of radium occur in minerals such as dolomite ($\text{Ca CO}_3 \cdot \text{Mg CO}_3$), carnallite ($\text{Mg Cl}_2 \cdot \text{K Cl} \cdot 6 \text{ H}_2\text{O}$) and barytes (Ba SO_4), radium originates naturally only by radioactive decay of its uranium and thorium precursors. In consequence, the geochemistry of radium is inherently associated with those of the other members of the three natural decay series supported by the long-lived primordial nuclides ^{232}Th , ^{235}U and ^{238}U (Figure 6). Radium was discovered in 1898 by the Curies and despite its low concentrations, ^{226}Ra was one of the first radionuclides to be analysed in marine materials (Strutt, 1906; Joly, 1908a, 1908b; Eve, 1907, 1909) as a result of the ease of collection and radioassay of the 'radium emanation' (^{222}Rn). Even in these early measurements, Joly observed that ^{226}Ra concentrations are higher in near-shore than open ocean surface water and that it is concentrated

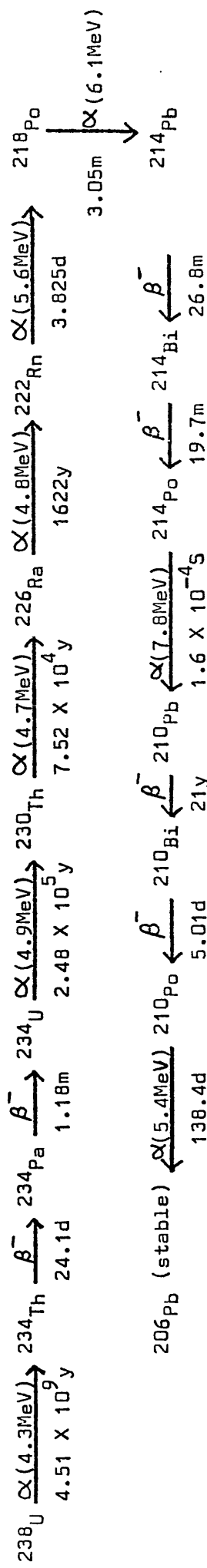
ISOTOPES OF RADIUM *

Isotopes	Principal decay Mode	Half-life	Source.
^{223}Ra	α	11.4d	(^{235}U natural series)
^{224}Ra	α	3.64d	(^{232}Th natural series)
^{225}Ra	β^-	14.8d	(^{229}Th man-made daughter)
^{226}Ra	α	1622y	(^{238}U natural series)
^{227}Ra	β^-	41m	(^{226}Ra man-made (n, γ))
^{228}Ra	β^-	5.77y	(^{232}Th natural series)

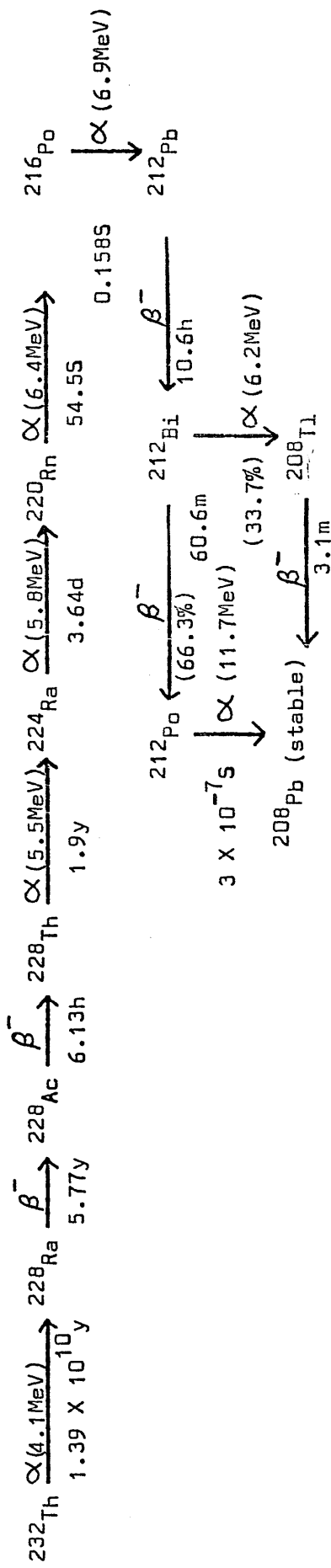
* Radium isotopes of atomic weights 212, 213, 214, 215, 216, 217, 219, 220, 221, 222 and 229 are also known to exist (Friedlander et al, 1964; Lederer et al, 1967; Heath, 1974) but all have half-lives of less than 1 hour and are not encountered in the marine environment.

TABLE 4. Isotopes of radium found in natural waters (Johnson, 1971).

(a) ^{238}U series:



(b) ^{232}Th series:



(c) ^{235}U series:

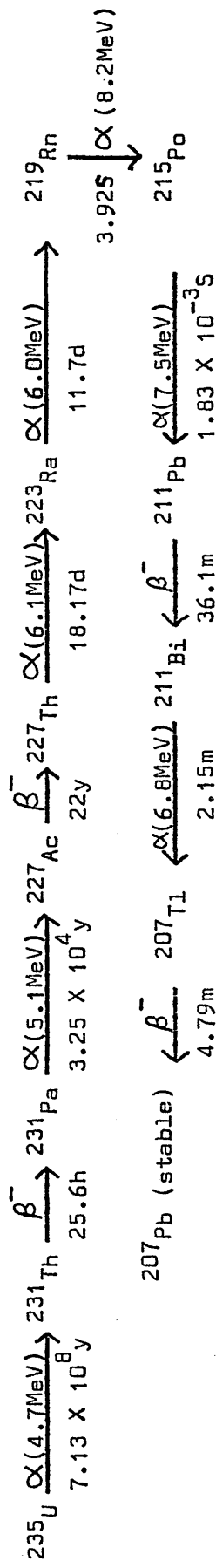


FIGURE 6. The natural decay series (only major decay modes shown).

in sediments, particularly red clay. Despite the significance of these observations, no satisfactory description of the marine geochemistry of radium could be formulated until techniques were developed for the isolation and measurement of the other members of the natural decay series. The geochemistry of the natural decay series constitutes a diverse and complex branch of science and only those developments which pertain directly to radium will be discussed here. General aspects of the subject were reviewed by Burton (1965), Thomson and Walton (1972) and Goldberg (1974). The first major developments in an understanding of the marine geochemistry of ^{226}Ra were the observations by Evans et al (1938a, 1938b) that concentrations of this isotope increase with depth in the oceans and by Pettersson et al (1930, 1937, 1939) that in the oceans, a radioactive disequilibrium exists within the natural decay series. It was demonstrated that, in sea water, ^{226}Ra is depleted in concentration by a factor of about six relative to ^{238}U and that ^{232}Th is greatly depleted compared to ^{238}U relative to their concentrations in continental rocks.

Pettersson concluded that while uranium is soluble in sea water, thorium has low solubility and is rapidly incorporated into sediments, giving an enrichment in sediments and depletion in sea water of thorium, and its daughters, relative to uranium. Pettersson further proposed a theoretical distribution of ^{226}Ra in an undisturbed sediment involving three sections:

(1) Growth to secular equilibrium with ^{230}Th in accordance with the equation

$$A_d = A_p (1 - e^{-\lambda_d t}) \quad (1)$$

where A_d = activity of daughter nuclide at time t ,

A_p = activity of parent nuclide,

and λ_d = decay constant of daughter nuclide.

(Friedlander, Kennedy and Miller, 1964).

(2) Decrease in supported ^{226}Ra concentration in accordance with decay of the unsupported ^{230}Th .

(3) Decrease in concentration of ^{230}Th , ^{226}Ra , and ^{234}U with the ^{238}U half-life after decay of all unsupported ^{230}Th .

The decay of the unsupported ^{230}Th thus provides an absolute method for determining the age of a particular layer of sediment. Subsequent work by Piggott and Urry (1941) on sediment cores confirmed the general trends of ^{226}Ra concentrations predicted by Pettersson and led to the proposal by Urry (1948) that the easily measured ^{226}Ra could be used as an indicator of ^{230}Th concentration in geochronological studies. This assumes firstly that ^{226}Ra is in equilibrium with ^{230}Th and secondly that either the ^{230}Th concentration in the sediment at the time of deposition or the rate of deposition remains constant over the period concerned. Later measurements of ^{226}Ra distribution in sediments, in particular those from the Swedish Deep Sea Expedition, revealed a more complex situation with the general trends of the theoretical model being followed but with a complex series of secondary maxima and minima also observed, giving rise to erratic profiles (Pettersson, 1951 ; Kroll, 1953, 1954, 1955). It was therefore concluded that ^{226}Ra could not in general be used in geochronological studies although recently Koide et al (1976) have suggested that under certain conditions, ^{226}Ra can provide a reliable indicator of sedimentation rate. Pettersson (1951) proposed that while variations in sedimentation rate may be responsible for some of the deviations in ^{226}Ra profiles, radium mobility within the sediment is also an important factor. Evidence that ^{226}Ra tends to accumulate in the authigenic mineral phillipsite confirmed the concept of radium mobility in sediments (Arrhenius and Goldberg, 1955 ; Arrhenius et al, 1957).

Koczy (1954, 1958) extended Pettersson's model for radium distribution in sediments to the concept that upwards migration of radium occurs, followed by leaching into the bottom waters of the oceans. Furthermore he proposed that this mechanism provides the major source of radium to the world's oceans and in a later publication (Koczy, 1965) suggested that rivers supply less than 5% of oceanic ^{226}Ra . He advocated that the observed ^{226}Ra profiles in ocean water result from upwards mixing by vertical eddy diffusion accompanied by decay of the ^{226}Ra and proposed that ^{226}Ra concentration variations could be used to study this process. The general equation describing the spatial distribution of concentration, C , of some species is:

$$\frac{\delta C}{\delta t} = \frac{\delta}{\delta x} \left(K_x \frac{\delta C}{\delta x} \right) + \frac{\delta}{\delta y} \left(K_y \frac{\delta C}{\delta y} \right) + \frac{\delta}{\delta z} \left(K_z \frac{\delta C}{\delta z} \right) \quad (2)$$

$$= u \frac{\delta C}{\delta x} - v \frac{\delta C}{\delta y} - w \frac{\delta C}{\delta z} + R$$

Where OX , OY and OZ are rectangular axes with OX and OY in a horizontal plane and OZ in the vertical. u , v and w are the components of the advective velocity of the water parallel to these axes and K_x , K_y and K_z are the respective coefficients of eddy diffusion. R is the rate of in-situ production or loss (Sverdrup et al, 1942). To simplify this equation, Koczy assumed a stationary distribution, no vertical advection and diffusion occurring in the vertical direction only. In-situ production and loss were considered only in terms of radioactive decay ie. $R = -\lambda C$, where λ is the decay constant. This generates the result:

$$C = C_0 e^{-\beta z} \quad (3)$$

$$\text{such that } \beta = \sqrt{\frac{\lambda}{K_z}} \quad (4)$$

where C_0 = concentration at some level

and C = concentration at a second level at vertical distance z from the first.

Koczy further proposed that where advection and not diffusion is the mechanism of vertical mixing then the distribution is described by:

$$v = \frac{1}{\lambda z} \ln \frac{C}{C_0} \quad (5)$$

and that the amount of radium given off from the sediment is:

$$Q = - \left(Kz \frac{\delta C}{\delta z} \right)_{z=0} \quad (6)$$

This relationship gave a value for Q of $1.2 - 1.8 \times 10^{-14} \text{ g } ^{226}\text{Ra cm}^{-2} \text{ y}^{-1}$ when applied to Koczy's results.

With the advent in the 1950's of commercially available, high stability, low background nuclear counting equipment and the consequent enhanced research interest in marine radioactivity in geochronological and water movement studies it became apparent that the basic model proposed by Koczy could not adequately explain all aspects of ^{226}Ra distribution in the oceans. In particular the large depletion of ^{226}Ra in surface ocean water is incompatible with simple diffusion and decay considerations. Koczy and Titze (1958) proposed that ^{226}Ra removal from surface water occurs by incorporation into organisms and subsequent sinking to deeper waters upon death of the organism. Partial re-dissolution of the decaying remains thus gives an "internal cycle" of ^{226}Ra in the oceans. The ^{226}Ra content of calcareous plankton as measured by Koczy and Titze was however too low to explain the observed surface depletion without invoking a mixed layer residence time of 1,200 years, a value too large to be compatible with ^{14}C , and later fission product, estimates. Szabo (1967) defined the ^{226}Ra content of mixed plankton samples from the Bahamas as $8.4 \times 10^{-14} \text{ g/g}$ of dried sample relative to concentrations in the ambient water of $4.5 \times 10^{-14} \text{ g/l}^{-1}$. This corresponds to an enrichment factor of about 2,000 where "enrichment factor" is defined

as the ratio of the weight of ^{226}Ra in one kilogram of dried sample to the weight in one kilogram of sea water. On this basis, Szabo calculated a mean residence half-life for ^{226}Ra in the mixed zone as 950 years. Shannon and Cherry (1971), however, subsequently demonstrated a large difference between ^{226}Ra concentrations in phytoplankton and zooplankton. In the Agulhas current, off South Africa, they found particularly high ^{226}Ra concentrations of 7.7×10^{-12} g/g dried sample in phytoplankton corresponding to an enrichment factor of 7,300. Zooplankton in the same area had concentrations of 0.3×10^{-12} g/g dried sample. Postulating that primary production is the mechanism for radium removal, Shannon and Cherry suggested that Phytoplankton concentrations should be used in assessing the rate of radium removal from surface water. This produced a mean biological removal time of ^{226}Ra from surface water of one year in the Agulhas current and 8 years elsewhere. They argued that since Szabo had used a mixed plankton sample, consisting dominantly of zooplankton, his values for biological scavenging were too low and his residence time consequently too high.

With biological effects playing an obvious part in the determination of ^{226}Ra distribution in the oceans, the necessity to normalise ^{226}Ra concentrations against some stable analog became apparent and barium, being chemically very similar to radium, was the obvious choice. However since barium is added to the oceans via river input and is thereafter distributed throughout the aquatic, biological and sedimentary components of the ocean system, its geochemical cycle is in marked contrast to that proposed for ^{226}Ra . Chow and Goldberg (1960) and Turekian and Johnson (1966) proved that oceanic distributions of barium are similar to those of ^{226}Ra in that surface waters are depleted and there is a general increase in concentration with depth.

However insufficient information was available to draw any definite conclusion. More recently, good correlations of barium and ^{226}Ra concentrations have been demonstrated by Wolgemuth and Broecker (1970) and Wolgemuth (1970) who rationalised the observed barium distribution on a simple box model and derived a biological removal rate of barium from surface waters of $4.4 \mu\text{g cm}^{-2} \text{y}^{-1}$. Ku et al (1970) and Edmond (1970), in a consideration of carbonate and silicate scavenging of ^{226}Ra found a strong correlation between ^{226}Ra , barium and silicate concentrations but a poor correlation of ^{226}Ra with alkalinity. From these observations it was concluded that opaline silica is the major scavenger for ^{226}Ra and barium. Li et al (1973) provided further evidence confirming the ^{226}Ra - barium correlation and, summarising data from a number of sources, produced a correlation plot of barium versus ^{226}Ra concentrations in which Antarctic data formed a straight line of gradient 0.714 (corresponding to the ratio of ^{226}Ra concentration to barium concentration) passing through the origin, while data from other areas formed a straight line with the same gradient but offset from the origin. Whether the offset was a real effect or a result of poor inter-laboratory calibration could not be defined. That a good correlation is obtained for all depths is somewhat surprising since ^{226}Ra decay in regions of long residence time should produce deviations. This situation was resolved by Li et al by the proposal that ^{226}Ra decay is balanced by input from sediments. They also used Wolgemuth and Broecker's box model to derive ^{226}Ra fluxes of $1.7 \times 10^{-14} \text{g cm}^{-2} \text{y}^{-1}$ and $4.6 \times 10^{-14} \text{g cm}^{-2} \text{y}^{-1}$ for deep ocean and continental shelf sediments respectively.

Despite these good correlations, the situation is still not totally resolved. For example Bacon and Edmond (1972) demonstrated that although a set of barium profiles showed trends consistent with the

internal cycle model, they could also be explained by vertical advection and diffusion between horizontally advecting water masses without invoking in-situ loss or production. They also derived a value for the cyclic flux of ^{226}Ra of $1.2 \times 10^{-14} \text{ g cm}^{-2} \text{ y}^{-1}$ ie. the same order of magnitude as the estimated flux from sediments. The importance of considering horizontal advection has also been stressed by Chung (1973a, 1973b) in discussion of transient features observed in excess radon profiles. Chung (1974) also reported that the strong ^{226}Ra /barium correlation does not occur in all parts of the oceans and summarised data showing an increase in ^{226}Ra : Ba concentrations with depth, indicating a different input for the two species. The validity of the assumption that rivers play a minor role in the supply of ^{226}Ra to the oceans has recently been questioned by Kuznetsov et al (1973) who proposed that the value of $7 \times 10^{-14} \text{ g l}^{-1}$ used by Koczy for the concentration of ^{226}Ra in river water should be amended to $40 \times 10^{-14} \text{ g l}^{-1}$, thus making river input one of the most important sources of ^{226}Ra to the oceans.

^{226}Ra concentrations in the oceans are, therefore, fairly well defined and, after initial intercalibration problems, agreement between different laboratories is now good (Chung et al, 1974). A summary of mean oceanic concentrations of ^{226}Ra is given in Table 5. The details of the marine geochemistry of ^{226}Ra are, however, complex and input from both sediments and rivers as well as internal biological cycling all appear to be important in determining its distribution in the oceans. Detailed studies of the three dimensional distribution of radium, barium and silicate will be necessary before a rigorous model can be defined in which ^{226}Ra concentrations can unambiguously be used to establish oceanic mixing mechanisms. Probably the most useful model available at present is that proposed by Chung and Craig

Water Body	Typical $[^{226}\text{Ra}]$ (dpm/1000 l)
Atlantic Ocean	85
Pacific Ocean (surface)	85
Pacific Ocean (bottom)	330
Indian Ocean	85
Gulf of California	50 - 120
Santa Barbara Basin	145
Arctic Ocean	90
Loch Lomond, Scotland	60

TABLE 5. Typical ^{226}Ra concentrations in the world's oceans.

(Data derived from : Conlan et al, 1969; Chung and Craig, 1973; Chung, 1973a; Chung, 1973b; Kaufman, et al, 1973).

(1973) in which they apply the equation derived by Craig (1969) for the distribution of a nonconservative radioactive tracer:

$$Kz \frac{\delta^2 C}{\delta z^2} + J = w \frac{\delta C}{\delta z} + \lambda C \quad (7)$$

where J is the in situ production or loss (cf. equation (2)).

This model therefore takes into account advective and diffusive mixing, internal cycling by biological and other mechanisms and radioactive decay.

In recent years, the shorter-lived isotope ^{228}Ra (β^- , $t_{1/2}$ 5.77y) has received attention as a tracer of marine processes. The first measurements of ^{228}Ra concentrations in the oceans were reported by Moore (1969a, 1969b, 1969c). These analyses required the collection and extraction of large volume (1000l) water samples since ^{228}Ra is present in very low concentrations in ocean water (10^{-15} - 10^{-16} g l^{-1}). Moore proposed that the activity ratio $^{228}\text{Ra}/^{226}\text{Ra}$ should provide a useful tracer of processes on a timescale of 3-30 years since this parameter should be free of the problems affecting ^{226}Ra , provided no fractionation of radium isotopes occurs in any removal process. Moore demonstrated that ^{228}Ra is unsupported by its ^{232}Th parent in sea water and is enriched in nearshore relative to mid-ocean surface waters, typical $^{228}\text{Ra}/^{226}\text{Ra}$ activity ratios for these regions being 1.0 and 0.1 respectively. Vertical profiles of $^{228}\text{Ra}/^{226}\text{Ra}$ ratios in deep ocean areas showed a rapid decrease from the surface, reaching near zero levels by middle depths, but with significant amounts in near bottom samples. This bottom water enrichment was more pronounced in the Atlantic than the Pacific and reflected a general tendency to higher ^{228}Ra concentrations in the Atlantic. Based on this observed distribution, Moore proposed that the major source of ^{228}Ra to the world's oceans is diffusion from ^{232}Th -bearing sediments, especially those of the continental shelf. The enhanced enrichment of ^{228}Ra

relative to ^{226}Ra in inshore waters derives from two causes. Firstly ^{228}Ra with its short half-life is generated more rapidly in sediments than the longer-lived ^{226}Ra for an equal activity of their respective thorium parents. Secondly, ^{230}Th , the parent of ^{226}Ra , is produced uniformly throughout the oceans by decay of ^{234}U whereas ^{232}Th , the parent of ^{228}Ra , is a primordial nuclide with no soluble parent and has a short residence time in sea water (Broecker et al, 1973) so that $^{230}\text{Th}/^{232}\text{Th}$ ratios are lower in nearshore and terrigenous sediments. Moore (1972) and Trier et al (1972) successfully applied $^{228}\text{Ra}/^{226}\text{Ra}$ ratios to a study of vertical eddy diffusivity rates in the thermocline and Kaufman et al (1973), in an extensive survey, confirmed the distribution of ^{228}Ra in the world's oceans reported by Moore and applied ^{228}Ra concentrations to studies of both vertical and lateral mixing processes. A summary of the distribution of ^{228}Ra is shown in Table 6.

The $^{228}\text{Ra}/^{226}\text{Ra}$ activity ratio therefore provides an attractive tracer for short-term marine processes, and in particular has considerable potential in investigations of mixing between open ocean and inshore surface water where large variations are observed. Also if the appropriate fluxes from the sediments can be determined, the enrichment of absolute radium concentrations and enhancement of the $^{228}\text{Ra}/^{226}\text{Ra}$ activity ratio could be used to assess the residence time of water in semi-enclosed basins.

The present research involves a preliminary survey of the concentrations of ^{228}Ra and ^{226}Ra in part of the Clyde Sea Area with the aim of defining spatial and temporal variations in both the absolute concentrations and activity ratio of the two isotopes. An evaluation is made of the potential of this information to assess the exchange of water between the Clyde Sea Area and the Atlantic

Water body	Typical [^{228}Ra] (dpm/1000 l)
North Atlantic surface water (open ocean)	25
North Atlantic surface water (nearshore)	120
North Atlantic 3000m	1
North Atlantic 5000m	10
Mediterranean surface water	27
South Pacific surface water	4
Equatorial Pacific surface water	6
North Pacific surface water	7
North Pacific 3000m	<1
North Pacific 4500m	3
Arctic surface water	26
Arctic 2000m	<0.4
Southern ocean surface water	4
Amazon river surface water	12

TABLE 6. Typical ^{228}Ra concentrations in the worlds oceans.

(Data derived from : Moore, 1969b, 1969c, 1972;

Trier et al, 1972; Kaufman et al, 1973).

Ocean/Irish Sea and to identify any areas of long water residence time. Since the activity ratio is used, biological effects are considerably simplified. However in any rigorous attempt to define a radium budget for the area such effects would have to be quantitatively evaluated. Nevertheless the study presents a useful investigation of some aspects of radium geochemistry in a semi-enclosed, polluted water body.

1.4. Radiocaesium in the marine environment.

Artificially produced radionuclides represent potentially dangerous pollutants in the marine environment but at the same time can be extremely valuable tracers in the study of oceanographic processes. Largely as a result of their potentially harmful effects on marine biota and, through the food chain and other exposure pathways, on man, the concentrations of artificial radionuclides in marine materials have been intensively studied virtually since the start of the nuclear era. While nuclear weapons testing provides the largest single input of man-made radionuclides to the marine environment, concentrations considerably in excess of those produced by this mechanism often occur locally in the vicinity of nuclear reactors or fuel-processing plants of the nuclear power industry. Data for the total inventory of man-made radionuclides added to the world's oceans up to the year 1970 and 2000 as estimated by Preston (1974) are presented in Table 7. The effect of enhanced concentrations of man-made radionuclides close to nuclear power production sites is apparent from the data in Tables 8 and 9 which show Food and Agriculture Organisation estimates of artificial radioactivity in marine materials for 1971. Despite the fact therefore that artificial radionuclides constitute only about 0.1% of the total oceanic radioactivity inventory, localised

	YEAR 1970	YEAR 2000
<u>Nuclear Explosions</u>		
Fission products (exclusive of Tritium)	2.6×10^8	$? \times 10^8$
Tritium	10^9	$? \times 10^9$
<u>Reactors and reprocessing of fuel</u>		
Fission and activation products (exclusive of tritium)	3×10^5	3×10^7
Tritium	3×10^5	$? \times 10^8$
Total artificial radioactivity	10^9	10^9
Total natural ^{40}K (>90% of natural marine radioactivity)	5×10^{11}	5×10^{11}

TABLE 7. Total inventory (in Ci) of artificial radionuclides introduced into the world's oceans (Preston, 1974).

Radionuclide	Water	Sediments	Biological Materials			
			Seaweeds	Mollusca	Crustacea	Fish
^3H	$1 - 10^2$					
^{54}Mn	1	$10^3 - 10^4$	10^3			
^{90}Sr	$10^{-1} - 1$	$1 - 10^2$	$1 - 10$	$10^{-1} - 10$	$1 - 10$	$1 - 10$
$^{95}\text{Zr}/^{95}\text{Nb}$	$10^{-1} - 10$	$10^2 - 10^5$	$10^3 - 10^4$			
^{106}Ru	$10^{-2} - 1$	$10^2 - 10^5$	$10 - 10^4$	$10 - 10^2$	$1 - 10^2$	$1 - 10^3$
^{137}Cs	$10^{-1} - 1$	$10 - 10^4$	$1 - 10$	$1 - 10$	$1 - 10$	$1 - 10^2$
^{144}Ce	$10^{-2} - 1$	$10^2 - 10^5$	$10 - 10^4$	$10 - 10^3$	$1 - 10^2$	$1 - 10^2$
^{239}Pu	$10^{-5} - 10^{-3}$	$10^{-1} - 1$	1	10^{-1}		10^{-3}

TABLE 8. Radionuclide concentrations from Global fallout as p Ci l^{-1} for seawater, p Ci kg^{-1} for dry sediments and p Ci kg^{-1} for wet biological material (Food and Agriculture Organisation, 1971).

Radionuclide	Water	Sediments	Biological Materials			
			Seaweeds	Mollusca	Crustacea	Fish
^3H	$10^1 - 10^3$					
^{32}P	$1 - 10$			$10^2 - 10^3$		
^{55}Fe	$10^{-1} - 10$		10^2	$10^2 - 10^3$		
^{60}Co	$10^{-2} - 1$	$10^2 - 10^3$	$10^2 - 10^3$	$10 - 10^3$		
^{65}Zn	$10^{-3} - 1$	10^3	$10^2 - 10^3$	$10^2 - 10^5$		
^{90}Sr	$1 - 10^2$		$10 - 10^2$	$10^2 - 10^3$	10^3	1
$^{95}\text{Sr}/^{95}\text{Nb}$	$1 - 10^3$	$10^5 - 10^7$	$10^4 - 10^6$	$10^4 - 10^6$	$10^3 - 10^4$	
^{106}Ru	$1 - 10^3$	$10^5 - 10^8$	$10^4 - 10^6$	$10^4 - 10^6$	$10^3 - 10^5$	10^3
$^{110\text{m}}\text{Ag}$	$10^{-3} - 10^{-2}$			$10^2 - 10^3$		
^{134}Cs	$1 - 10$	10^3				10^3
^{137}Cs	$1 - 10^2$	$10^2 - 10^4$	10^3	$10^2 - 10^3$		$10^3 - 10^4$
^{144}Ce	$1 - 10^3$	$10^5 - 10^7$	$10^4 - 10^6$			
^{239}Pu		$10^2 - 10^5$	$10^2 - 10^4$			$1 - 10$

TABLE 9. Radionuclide concentrations resulting from the controlled disposal of radioactive wastes from nuclear power production as p Ci l^{-1} for seawater, p Ci kg^{-1} for dry sediments and p Ci kg^{-1} for wet biological material (Food and Agriculture Organisation, 1971).

inputs and complex interactions with the sedimentary and biological cycles can result in locally high concentrations in certain marine materials and so constitute a health hazard to man. Exposure of the population to radioactivity from the controlled discharge of nuclear waste is assessed by "critical pathway analyses" (Preston 1974), the salient features of which are shown in Figure 7.

Two of the fundamental requirements in such an analysis are firstly a detailed knowledge of the mixing and dispersion characteristics of the water receiving the discharge and secondly a knowledge of the general distribution of the radionuclides in marine materials. The distribution of man-made radionuclides has been widely studied and a number of extensive surveys have been reported (Food and Agriculture Organisation, 1971; United Nations, 1972; Mitchell, 1975). The determination of the characteristics of the receiving water body presents a more difficult problem and while conventional oceanographic techniques can be used to study the system, the distribution of the man-made radionuclides themselves can often provide uniquely valuable information on the processes occurring.

A variety of "bomb" and reactor-produced radionuclides have been used to study marine processes (Preston et al, 1972; Preston, 1974) and one of the most useful has been the fission product ^{137}Cs (β^- , $t_{1/2} = 30\text{y}$). The shorter lived activation product ^{134}Cs (β^- , $t_{1/2} = 2.1\text{y}$), produced by an (n, γ) reaction of ^{133}Cs (100% natural abundance; thermal neutron capture cross section = 30 barns), also has considerable potential as a tracer of short-term processes. Stable ^{133}Cs occurs in concentrations of about $2.8 \times 10^{-7} \text{ g l}^{-1}$ and while not strictly conservative in behaviour has a residence time of about 40,000 years in sea water (Broecker, 1974). This is very much

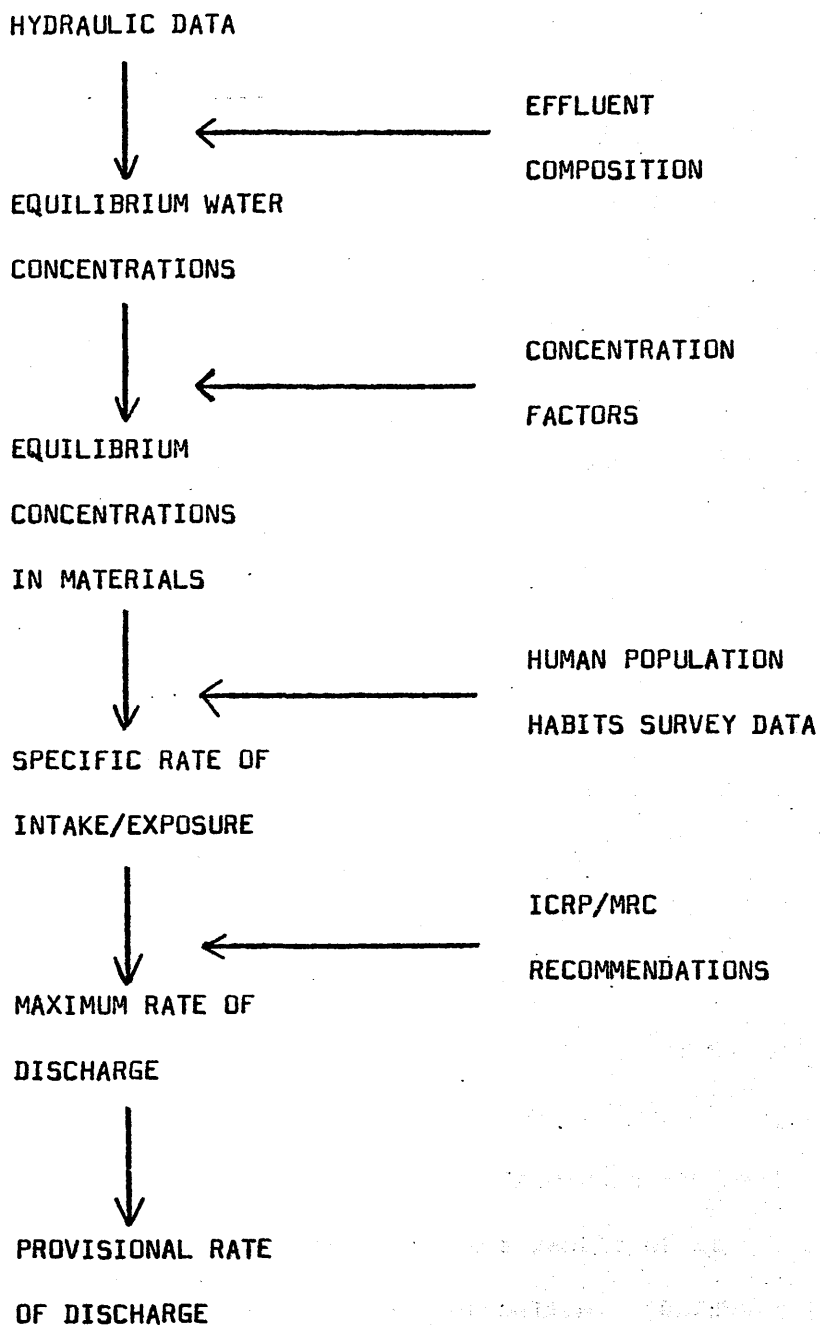


FIGURE 7. Component operations in critical pathway analysis
(Preston, 1974).

longer than the mean lifetimes of both ^{137}Cs and ^{134}Cs so that to a first approximation these isotopes may be treated as being removed from sea water only by radioactive decay. The data in Tables 8 and 9 do, however, show that ^{137}Cs is accumulated to a significant extent in sediments and biological materials and these effects must be considered in any rigorous application of radiocaesium to oceanographic studies.

Atmospheric testing of nuclear weapons reached a maximum level in 1961-62 after which underground testing prevailed, this trend being paralleled by atmospheric concentrations of bomb-produced radionuclides. Most of this fallout radioactivity, including ^{137}Cs was rapidly "rained out" from the atmosphere giving rise to a maximum in concentration of these nuclides in surface sea water in 1962-63. Furthermore sedimentary materials deposited in 1962-63 contained maximum concentrations of bomb-produced radionuclide thus providing a layer of known age in the sediment and consequently a means of determining sedimentation rates (United Nations, 1972; Krishnaswami et al, 1973; Goldberg, 1974). Although bomb-produced ^{137}Cs was incorporated into sediments in this way, its use in sedimentation studies has been subject to some doubt as a result of its possible mobility in the sediment after initial deposition. Goldberg (1974) quoted a diffusion coefficient for ^{137}Cs in sediments of 10^{-9} to $10^{-8} \text{ cm}^2 \text{ sec}^{-1}$ compared to values of 10^{-8} to $10^{-7} \text{ cm}^2 \text{ sec}^{-1}$ for ^{90}Sr and 10^{-11} to $10^{-10} \text{ cm}^2 \text{ sec}^{-1}$ for rare earth nuclides such as ^{144}Ce , ^{147}Pr and ^{155}Eu . He concluded that although the rare earth nuclides, with low diffusivities, could be used to establish reliable geochronologies, ^{137}Cs and ^{90}Sr concentrations would be significantly altered by diffusion, even in sediments accumulating at a rate of several centimeters per year, thus making them unreliable indicators of sedimentation rates. The mobility of ^{137}Cs in sediments has been

considered by a number of workers (Doursma and Gross, 1975; Lietzke et al, 1973; Lerman and Lietzke, 1975) and it has been widely accepted that this provides a barrier to its use in sedimentary studies. A number of workers have, however, found a low mobility of ^{137}Cs in sediments and good age correlations with reliable indicators such as ^{210}Pb (Ritchie et al, 1973; Pennington, 1973; Robbins and Edgington, 1975). Furthermore, Krishnaswami et al (1971) observed that post-depositional diffusion of ^{137}Cs would not change the depth of the peak maximum in the sediment, simply its magnitude. They further suggested that the occurrence of the maximum at greater depths than expected is the result of physical or biological mixing of the sediment. This viewpoint was endorsed by Robbins and Edgington (1975) who demonstrated that ^{137}Cs gave consistent results with ^{210}Pb chronologies if a 2cm surface mixing depth was considered. The validity of ^{137}Cs as an indicator of sedimentation rate is, therefore, subject to uncertainty and may vary with the nature and degree of mixing of the particular sediment concerned. It should also be noted that many of the above-mentioned investigations were applied to fresh water systems, notably the Great Lakes of North America and that extrapolation of results from fresh water to salt water systems may not be valid.

Fallout ^{137}Cs has also been utilised in oceanic vertical mixing processes. Broecker and co-workers reported the successful application of ^{137}Cs in the measurements of vertical diffusion rates in the upper oceans, values obtained being compatible with those from other methods (Rocco and Broecker, 1963 ; Broecker et al, 1966). This conclusion is in marked contrast to earlier work suggesting a much more rapid penetration of both ^{90}Sr and ^{137}Cs into deep waters (Bowen and Sugihara, 1960; Miyake et al, 1962). This discrepancy probably arises as a result of association of ^{137}Cs with settling particulate matter giving a more rapid removal to deeper water than would be obtained by

simple vertical mixing. The association of ^{137}Cs with settling particulates is indicated in the data of Bowen et al (1974) and Noshkin and Bowen (1972) who found a reduction of the $^{137}\text{Cs}/^{90}\text{Sr}$ activity in surface sea water relative to that in precipitation. They also found both isotopes to be present in deep ocean sediments but with an enhanced $^{137}\text{Cs}/^{90}\text{Sr}$ ratio, again suggesting a stronger association of the ^{137}Cs with some form of settling particulate matter.

While bomb-produced radionuclides have provided useful tracers on a worldwide basis, those produced by nuclear reactors and fuel-processing plants have been applied successfully to investigations of more limited areas, particularly near-shore waters and estuaries (Osterberg et al, 1966; Lowton et al, 1966). This type of study is particularly suited to investigations of water dispersal and movement since the effluent is added in known amounts at a "point source" giving a precise "labelling" of the water. ^{137}Cs and ^{134}Cs present a particularly useful pair of radio-isotopes in this context since they constitute a large fraction of the low-level effluent discharged into coastal waters, have relatively conservative behaviour and provide a tracer, in the form of the $^{134}\text{Cs}/^{137}\text{Cs}$ activity ratio, which should be independent of all removal processes except radioactive decay thus providing an ideal "clock" for assessing rates of short term processes. Mitchell (1975) listed 21 sites in the United Kingdom contributing significant discharges of radioactivity to coastal waters in 1972/73. The locations of these sites are shown in Figure 8 and their outputs are listed in Table 10. From the discharge data it is apparent that the fuel-reprocessing plant at Windscale is the largest single source of radioactivity to coastal waters in the United Kingdom and in fact discharges more radioactivity than the combined total of all other sites in the country. The relatively large amounts of ^{137}Cs and ^{134}Cs

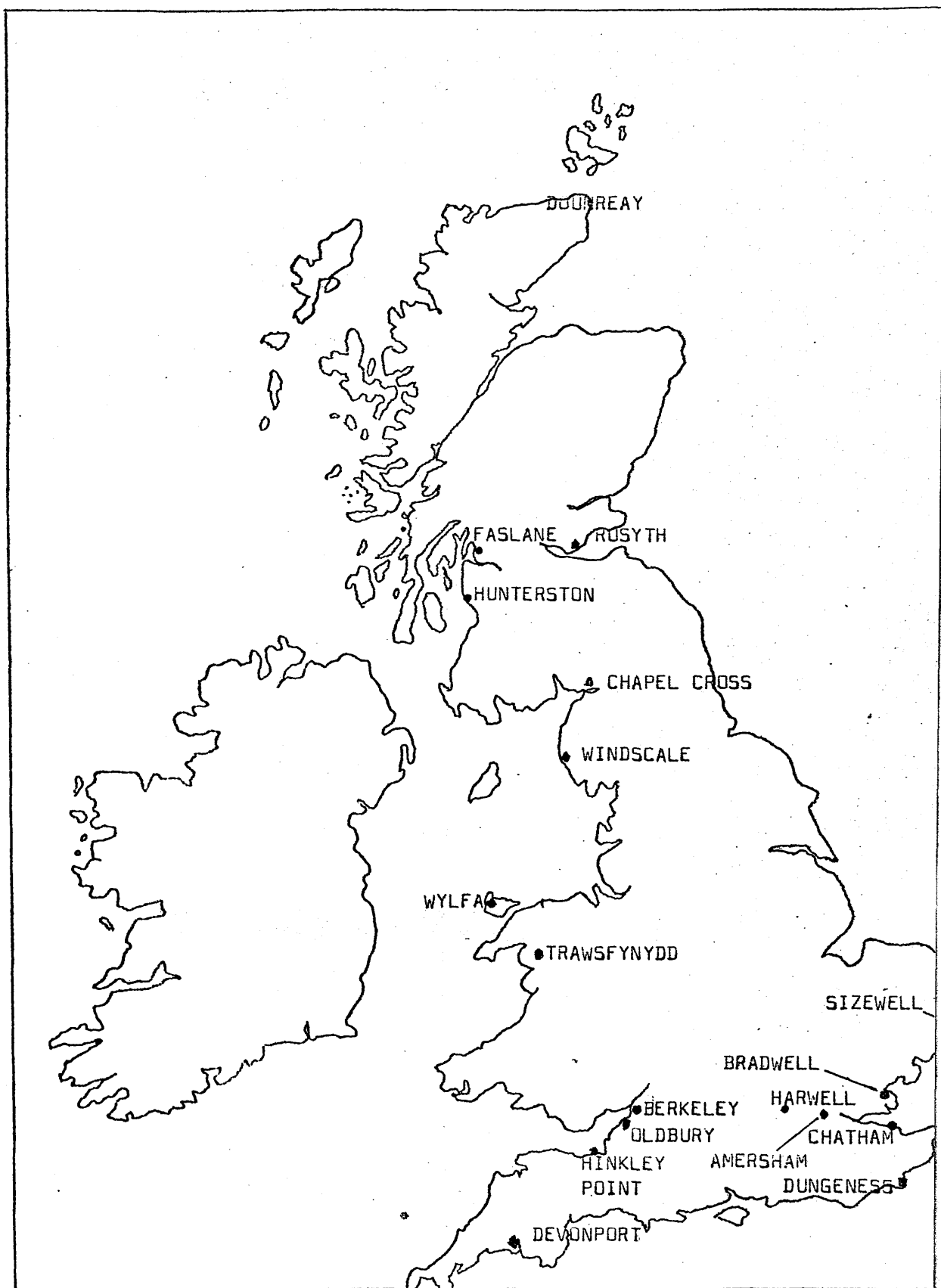


FIGURE 8. Locations of sites discharging liquid radioactive waste to surface and coastal waters during 1972/73 (cf table 10).

SITE	RADIOACTIVITY	AUTHORISED DISCHARGE (Ci y ⁻¹)	PERCENTAGE UTILIZED
Windscale	Total beta	300,000	45
	Total alpha	6,000	73
Springfields	Total beta	12,000	12
	Total alpha	360	6
Chapelcross	Total activity *	700	1
	Tritium	150	7
Winfrith	Total activity	30,000	4
Harwell	Total activity *	240	32
	Tritium	240	28
Dounreay	Total activity	240	11
Amersham	Total activity *	72	40
	Tritium	400	52
Berkeley	Total activity *	200	11
	Tritium	1,500	9
Bradwell	Total activity	200	43
	Tritium	1,500	15
Dungeness	Total activity *	200	13
	Tritium	2,000	2
Hinkley Point	Total activity *	200	65
	Tritium	2,000	2
Oldbury	Total activity *	100	5
	Tritium	2,000	<1
Sizewell	Total activity *	200	7
	Tritium	3,000	4
Trawsfynydd	Total activity *	40	60
	Tritium	2,000	4
Wylfa	Total activity *	65	<1
	Tritium	4,000	4

CONTINUED/...

SITE	RADIOACTIVITY	AUTHORISED DISCHARGE (Ci y ⁻¹)	PERCENTAGE UTILIZED
Hunterston	Total activity *	65	14
	Tritium	4,000	5
Chatham	Total activity *	20	< 1
	Tritium	20	< 1
Devonport	Total activity *	4	< 1
	Tritium	10	< 1
Faslane	Total activity *	1	< 1
Rosyth	Total activity	30	< 1
Aldermaston	Total activity	156	10

* Excluding Tritium.

TABLE 10. Major discharges of liquid radioactive waste to surface and coastal waters during 1972/73 (Mitchell, 1975).

discharged have consequently provided extremely useful water movement tracers in the Irish Sea and Atlantic ocean. For example, Wilson (1975) applied continuity conditions to water and salt in the St. George's Channel and, combining these with observed ^{137}Cs distributions, derived values for the mean advective and diffusive movements of water in the area. His results verified the net northwards flow of water in the Irish Sea but indicated a smaller flow rate than had previously been reported.

Mitchell (1975) reported mean ^{137}Cs and ^{134}Cs concentrations in the Irish Sea and North Channel for the period 1972/73 and these data are shown in Table 11, the locations of sampling sites being given in Figure 9. He also reported concentrations of Windscale-derived radionuclides in biological and sedimentary materials as listed in Tables 12 and 13. The low enrichment factors for radiocaesium in sediment and biological materials verify its relatively conservative behaviour.

In a report on the dispersal of ^{137}Cs from the Windscale effluent into the Irish Sea and Atlantic Ocean, Jefferies et al (1973) revealed a fairly uniform dilution in the northern Irish Sea followed by a dominant flow through the North Channel continuing as a semi-entrained northwards surface flow round the Scottish coast (Figure 10). The decay of ^{134}Cs relative to ^{137}Cs provides a measure of the travel time of the water.

The Windscale discharge, and in particular the isotope pair $^{137}\text{Cs} - ^{134}\text{Cs}$, therefore provides an excellent tracer for study of water exchange and mixing patterns in the general Irish Sea/North Atlantic system, including the Clyde Sea Area. While Windscale is the largest source of radiocaesium to the Clyde Sea Area, contributions are also received from Chapelcross, Hunterston, Faslane and from

Position number *	Location	^{134}Cs (dpm l ⁻¹)	^{137}Cs (dpm l ⁻¹)	$^{134}\text{Cs}/^{137}\text{Cs}$ Activity Ratio
1	Seascale	165.0 (28.6 - 462)	880.0 (149.6 - 2860)	0.188
2	North Irish Sea	5.7 (3.3 - 12.8)	44.0 (19.6 - 94.6)	0.130
3	Mid North Channel	5.3 (1.5 - 9.7)	39.6 (16.1 - 70.4)	0.133
4	Mull of Kintyre	4.0 (0.7 - 7.3)	28.6 (9.7 - 50.6)	0.138
5	Islay	2.6 (0.4 - 6.6)	20.2 (5.5 - 48.4)	0.130
6	Inistrahull ground	0.4 (0 - 1.5)	4.0 (0.4 - 17.4)	0.100

* See Figure 9 (p48)

TABLE 11. Mean ^{134}Cs and ^{137}Cs concentrations in sea water from the Irish Sea and its north western approaches 1972/73 (Range shown in brackets). (Mitchell, 1975).

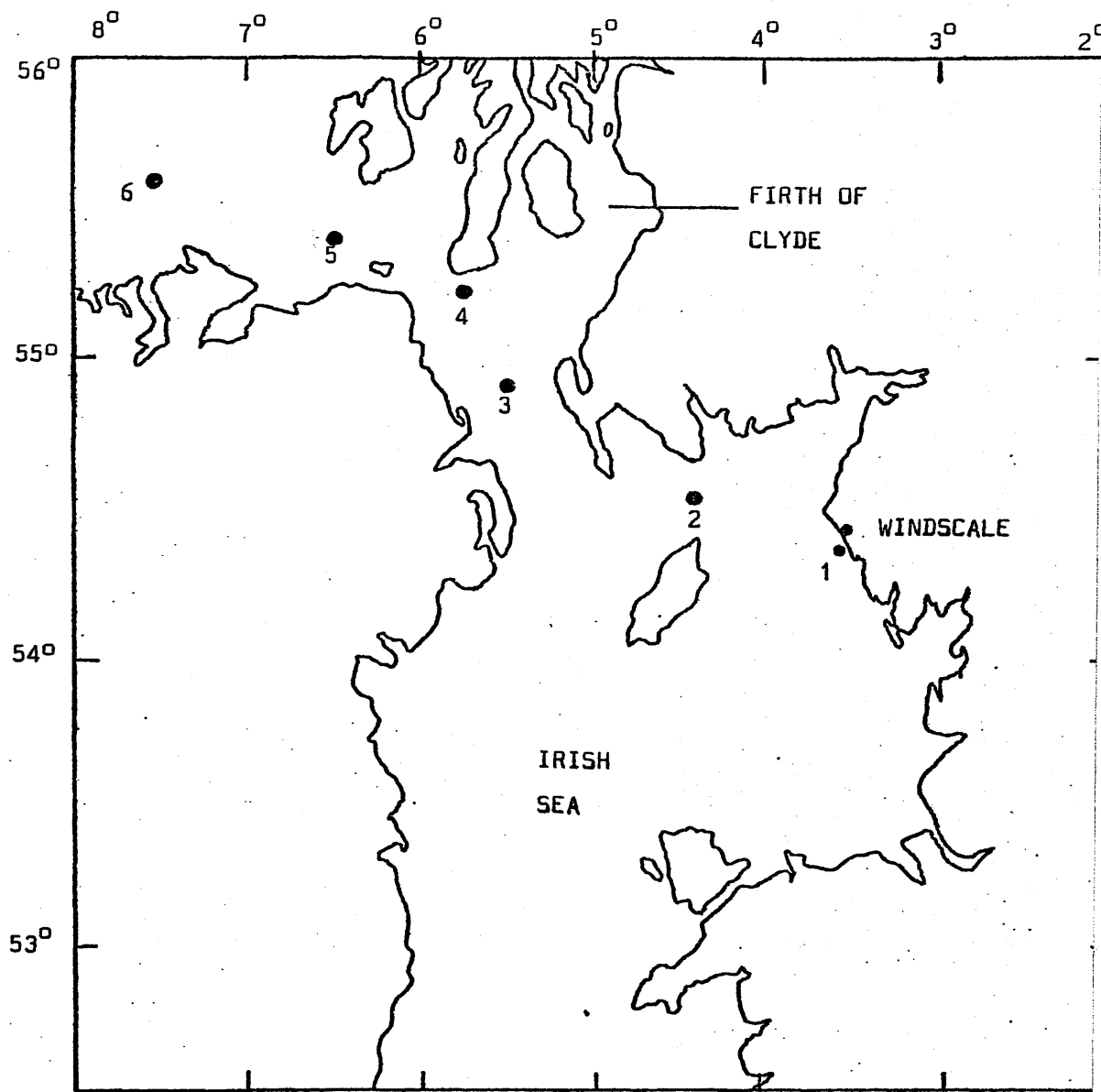


FIGURE 9. MAFF. sampling positions for caesium analyses (Table 11)
(Mitchell, 1975).

Species	Sampling Area.	Concentration of radioactivity (dpm/g of wet sample)				
		^{106}Ru	^{134}Cs	^{137}Cs	^{90}Sr	$^{239/240}\text{Pu}$
Plaice flesh	North Irish Sea	0.22	0.66	5.3	0.09	0.02
	Windscale discharge area	2.2	3.08	17.6	0.22	0.07
Dab flesh	Windscale discharge area	5.3	3.52	22.0	0.35	0.11
Skate (edible parts)	Windscale discharge area	6.4	3.74	24.2		
Herring (edible parts)	North Irish Sea		0.44	2.4		
Nephrops (edible parts)	North Irish Sea	0.44	0.44	2.9		
Mussel flesh	Windscale discharge area	396.0	0.88	10.8		
Crab	Windscale discharge area	21.3		3.5		
Queen flesh	North Irish Sea.	24.2		1.1		

TABLE 12. Radioactivity in fish and shellfish in the Irish Sea, 1972/73.(Mitchell, 1975).

Material and sampling site	Concentration of radioactivity (dpm/g wet sample for seaweeds; dpm/g dry sample for silt and sand)					
	Total beta	$^{95}\text{Sr}/^{95}\text{Nb}$	^{106}Ru	^{134}Cs	^{137}Cs	^{144}Ce
<u>Porphyra</u>						
Labrax Bay	15.6	0.22	1.5		0.22	
Port William	20.9	0.88	7.5		0.22	
Garlieston	20.2	1.98	8.4		0.66	0.2
Kirkcudbright	18.0		3.5		0.44	
<u>Fucus</u>						
<u>vesiculosus</u>						
Port William	70.4	1.76	0.88	0.22	1.98	0.22
Garlieston	93.6	5.06	3.3	0.66	3.52	0.44
Rascarrel Bay	106.6	6.66	4.98	0.66	4.0	1.55
Heysham	124.3	3.55	4.0	1.33	7.3	0.67
<u>Fucus</u>						
<u>serratus</u>						
Millisle	28.9	1.11	0.44		1.1	
<u>Silt</u>						
Garlieston	310.8	14.2	55.5	2.4	15.3	26.6
<u>Sand</u>						
Heysham	266.4	4.0	18.2	2.4	20.9	14.2
Fleetwood.	51.1		0.67	0.67	3.6	1.1

TABLE 13. Radioactivity in seaweed and foreshore materials around the Irish Sea and western Scotland, 1972/73. (Mitchell, 1975)

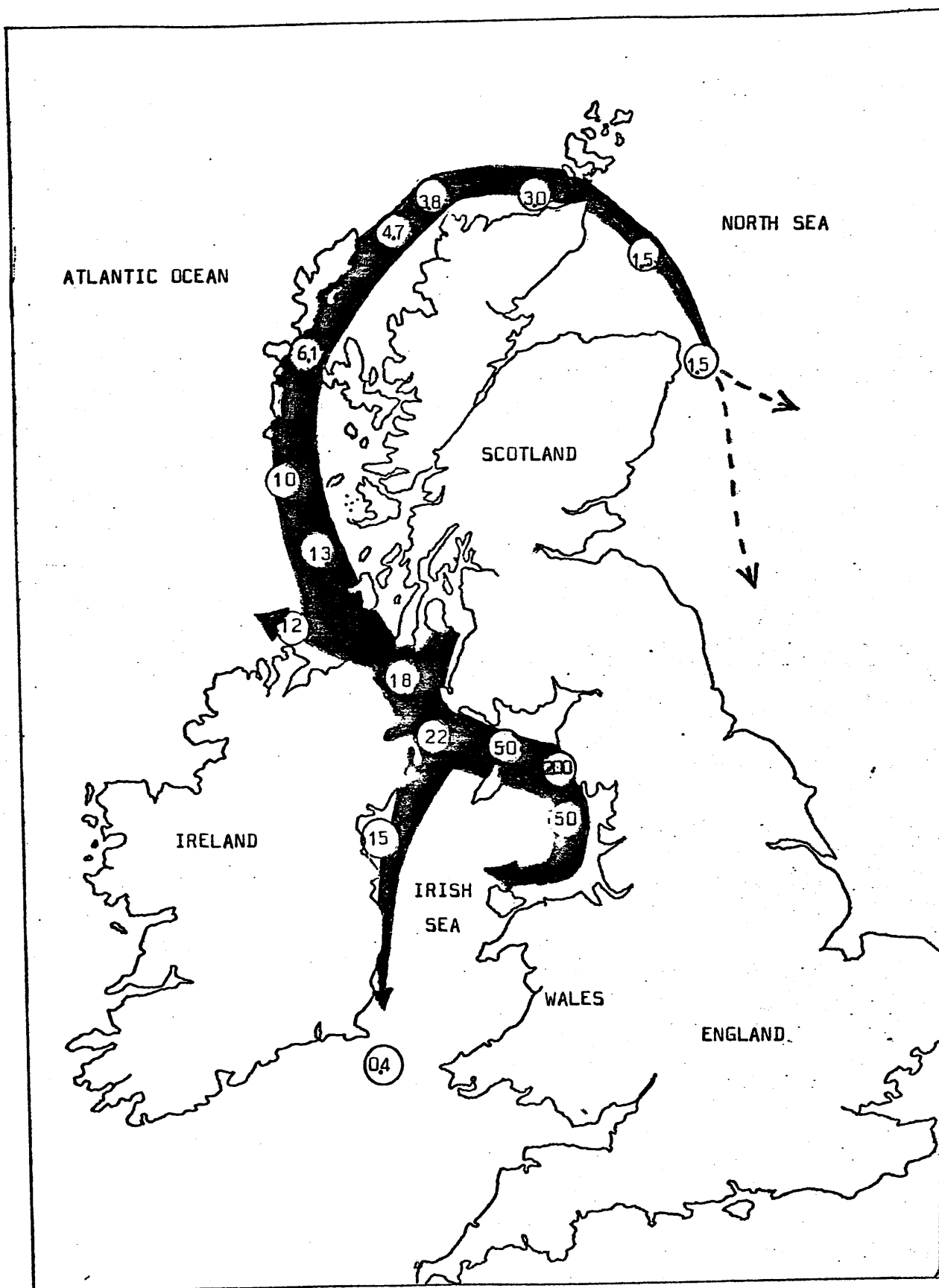


FIGURE 10. Concentrations of ^{137}Cs in British Isles coastal sea water (pCi l^{-1}). (Jefferies et al 1973).

atmospheric fallout but these are small in comparison to the Windscale contribution. This report describes an initial survey of concentrations of radiocaesium in the Clyde Sea Area and an application of the data obtained to water mixing and sedimentation studies in the area.

conducted in terms of direct analysis of the samples.
from 200 samples. 225

10-10-68

CHAPTER 2

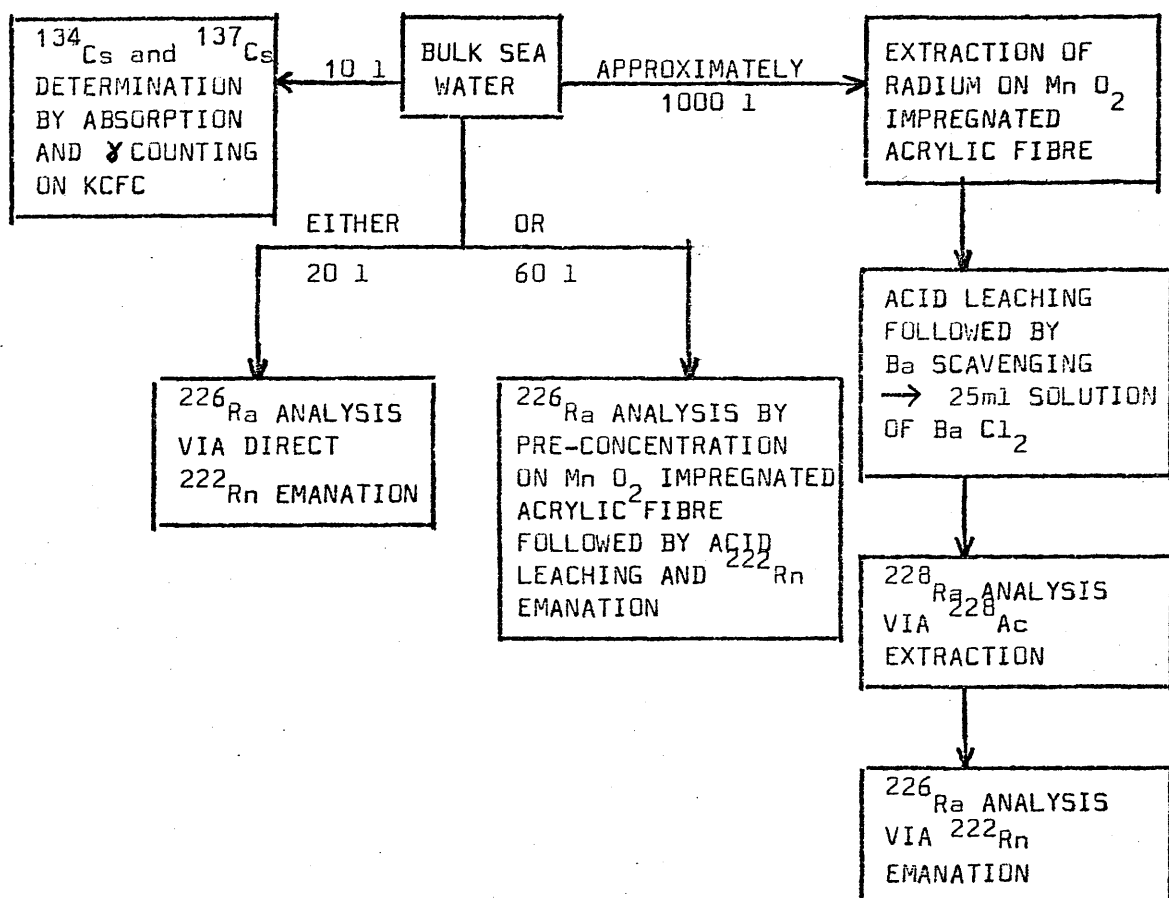
EXPERIMENTAL

2.1. General aspects of analytical procedures.

The techniques described in later sections relate mainly to the analysis of ^{134}Cs , ^{137}Cs , ^{226}Ra and ^{228}Ra in sea water and sediment samples and a flow chart summarising the procedures involved is shown in Figure 11. Water samples, from depths of up to 80m, are collected by pumping through 1 inch P.V.C. tubing while sediment samples are recovered by both a standard gravity corer and a Craib corer, specially designed to retain surface sediment intact. Caesium isotopes are analysed by ion exchange extraction onto potassium hexacyanocobalt (II) ferrate (II) (KCFC) from 10l water samples followed by in-situ analysis of the ion exchange column by γ -spectroscopy. ^{226}Ra analyses were initially performed by preconcentration from 60l water samples onto manganese dioxide supported on acrylic fibre followed by analysis via emanation and α -counting of the ^{222}Rn daughter. This method was discontinued in favour of direct analysis of sea water by ^{222}Rn -emanation from 20l samples. ^{228}Ra concentrations are determined by preconcentration of $^{228}\text{Ra}/^{226}\text{Ra}$ from about 1000l of sea water onto manganese dioxide-impregnated acrylic fibre. ^{228}Ra activity is measured by solvent extraction and β^- counting of its daughter ^{228}Ac , the observed activity being converted into an absolute concentration via the $^{228}\text{Ra}/^{226}\text{Ra}$ activity ratio. Total dissolution of sediment samples is effected by successive acid digestions with intermediate leaching of soluble materials into hydrochloric acid. Analytical procedures applied to sediments are analogous to those for water.

Quantities of materials being analysed are as little as 10^{-14} g

(a) Water



(b) Sediment

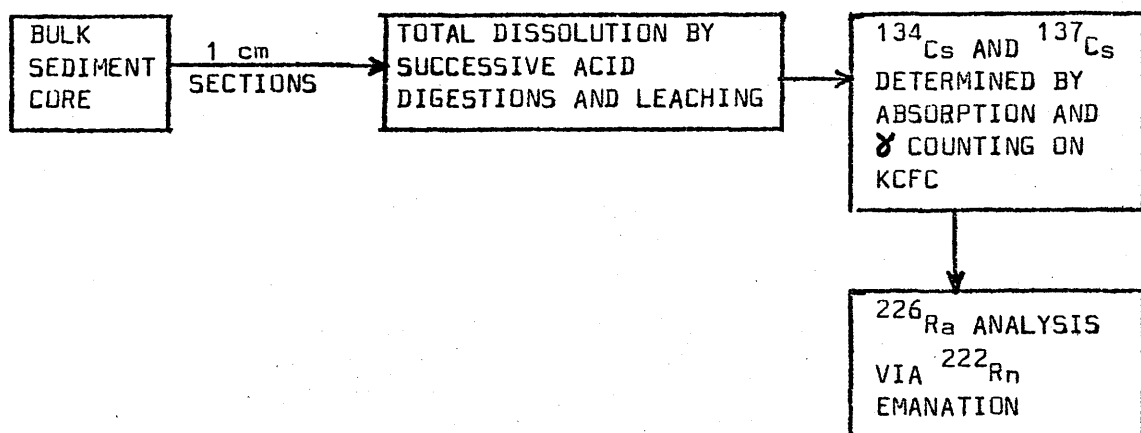


FIGURE 11. Summary of experimental techniques.

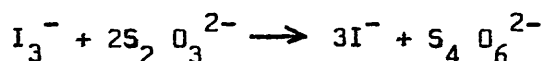
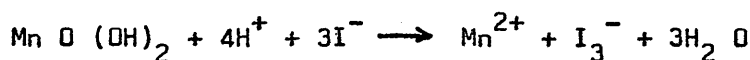
so that contamination and sample loss by adsorption represent major threats to the accuracy of analysis. The following general precautions are observed to overcome these problems. Wherever possible, Analar or equivalent grade chemicals are used and blank runs performed on all processes to assess the degree of contamination. Glassware is cleaned by a sequence of rinsing, washing and steeping in detergent solution, rinsing, steeping in Decon solution for 24 hours, rinsing and finally oven drying. Samples being stored are contained in stoppered vessels to avoid atmospheric contamination. Finally, all high-level radioactivity is, as far as possible, excluded from the laboratory and counting area where low-level analyses are performed.

2.2. Hydrographic data.

Hydrographic data in the form of salinity, temperature and dissolved oxygen content of the water were provided, whenever possible, by the Clyde River Purification Board when radium or radiocaesium analyses of sea water were performed. For a limited number of samples, pH of the water was also recorded. Subsurface samples for these measurements were collected by means of National Institute of Oceanography sample bottles suspended at suitable depths on a hydro-wire and closed by release of brass "messengers". The salinity and temperature profiles thus recorded defined the main features of water structure, indicating suitable depths for radium and caesium sampling. Surface samples were simply collected by means of a plastic bucket attached to a rope.

Salinities and temperatures were measured by a direct reading conductance salinometer/resistance thermometer, the error associated with the salinity measurement being defined as 0.01‰. Dissolved oxygen measurements were performed by the "Winkler Technique" in which a concentrated solution of manganous chloride and excess sodium hydroxide solution, containing potassium iodide, are added to the water

sample being analysed, giving a precipitate of manganese hydroxide. The sample bottle is kept stoppered at all times, except when adding reagents, to avoid dissolution of atmospheric oxygen. The dissolved oxygen in the sample reacts quantitatively with the manganese hydroxide and the oxidised species is dissolved by addition of hydrochloric acid, a stoichiometric amount of iodide ion being liberated in the process. The liberated iodine is titrated with standard thiosulphate solution, using starch indicator, to give a measure of the dissolved oxygen content of the water. The overall reaction sequence involved may be considered as:



(Riley, 1965).

The error on the measurement was defined as 2% of the observed value. Measurement of pH, on a limited number of samples, was performed by direct reading from a combined electrode pH meter.

2.3. ^{226}Ra analytical and nuclear counting techniques.

^{226}Ra analyses were performed on a variety of samples but in all cases the sample, in solution form, was analysed by extraction and α -counting of the gaseous daughter product ^{222}Rn (α , $t_{1/2} = 3.83\text{d}$). Sample pretreatments are described later in appropriate sections. The following method applies to all samples with varying flushing times being used for different sample volumes.

^{226}Ra analyses are performed using the vacuum line system shown in Figure 12. The sample solution is transferred to the equilibration vessel and an initial extraction carried out to remove all ^{222}Rn present, after which the equilibration vessel is sealed and the date and time noted. This initial ^{222}Rn stripping is performed by the same method

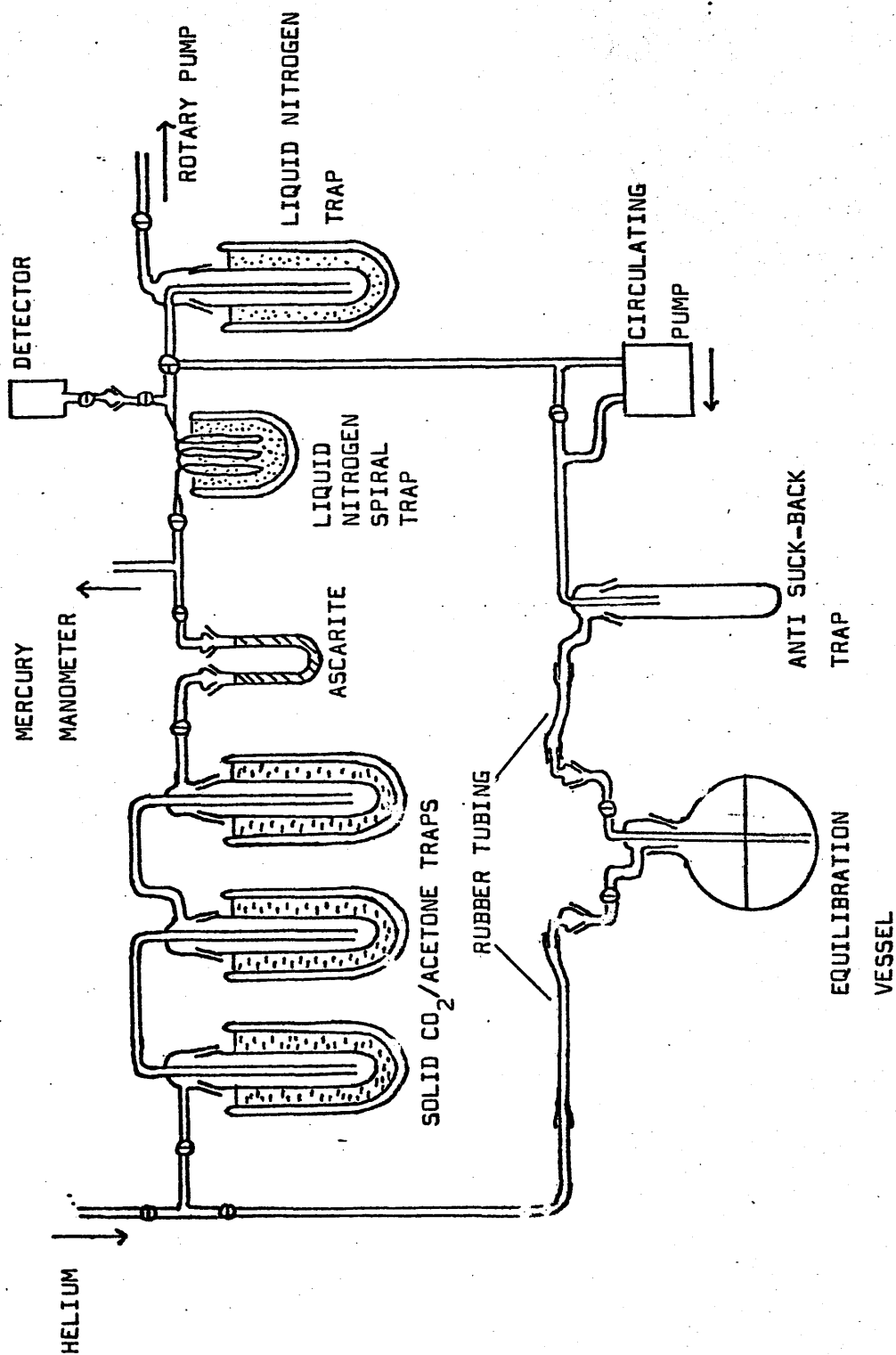


FIGURE 12. ^{222}Rn emanation system.

as a normal ^{222}Rn analysis, as described later, except that the emanated ^{222}Rn is not collected at the end of the procedure. The sealed sample is stored for an appropriate time, during which the ^{222}Rn activity grows towards secular equilibrium with the ^{226}Ra in accordance with the equation

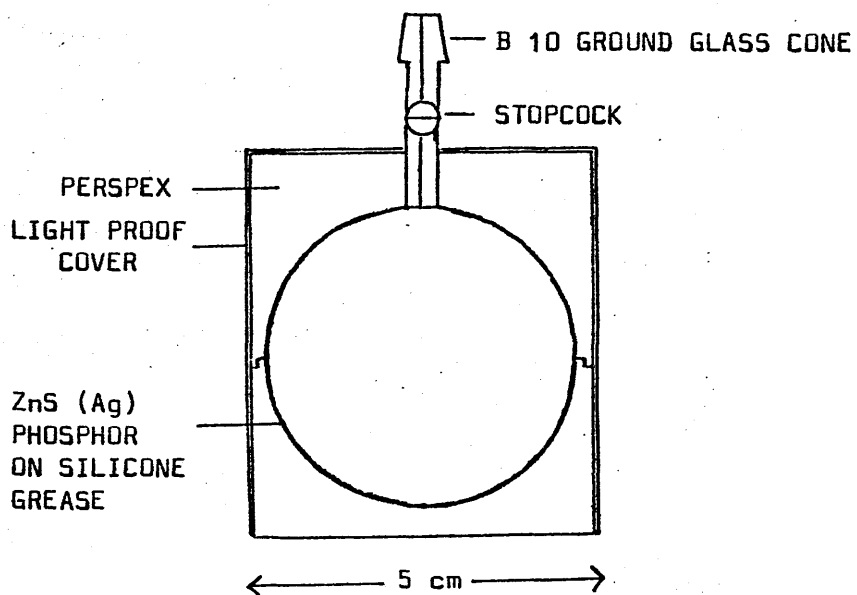
$$A_d = A_p (1 - e^{-\lambda_d t})$$

as defined in section 1.3 (p.23) so that after any fixed grow-in time, the degree of equilibrium between the ^{226}Ra and ^{222}Rn can be defined. In general, samples are stored for greater than 12 days (88.7% equilibrium) prior to analysis. After this time, the sealed equilibration vessel is attached to the vacuum line as shown but without the liquid nitrogen trap. The system is evacuated, the detector sealed and the line twice successively filled to one atmosphere pressure with helium then evacuated to remove contaminants from the helium inlet system. The line is again filled to one atmosphere with helium, closed off to the helium supply and the equilibration vessel is opened to the rest of the system. The circulating pump is used to cycle the helium, and emanated ^{222}Rn , round the system and the liquid nitrogen trap is filled to freeze down the ^{222}Rn in the spiral trap. A flow rate of 4 l min^{-1} is used for all samples. Water vapour is removed by the solid CO_2 /acetone traps and CO_2 , if present, by the Ascarite trap. Samples of volumes 100ml, 500ml and 20l are routinely analysed with flushing times for total extraction of ^{222}Rn being 30, 45 and 120 minutes respectively. Upon completion of the flushing process, the equilibration vessel is again sealed, the time noted and, with the liquid nitrogen trap still in position, the spiral trap is isolated from the rest of the line and evacuated. The detector is then opened to the spiral trap, the combined detector/spiral trap system isolated from the rest of the system and the liquid nitrogen trap removed, vapourisation of the ^{222}Rn being accelerated by warming the spiral trap with a hot air blower.

The ^{222}Rn gas, distributed between the detector (volume approximately 50ml) and the spiral trap (volume approximately 10ml) is forced into the detector by opening the spiral trap to the vacuum line containing one atmosphere pressure of helium. Immediately after the initial "pulse" of helium enters the trap, the detector is sealed, giving virtually quantitative recovery of the ^{222}Rn . The sample is then stored for further analysis after grow-in of a new "crop" of ^{222}Rn and the detector removed for radioactivity measurement on the collected gas.

The construction of the detector is based on a design by Ferrante et al (1964) which was a development from prototype scintillation chambers produced by Damon and Hyde (1952) and Lucas (1957). It consists of two tightly fitting perspex hemispheres of total internal volume about 50ml as shown in Figure 13. All surfaces of the detector are highly polished and the inner walls are lined with a thin smear of silicone grease to which is applied a uniform covering of 2n S (Ag) phosphor (5 mg cm^{-2}). A light-tight, white cover and seal is applied to the outer walls of the detector, with the exception of the bottom face. The capillary-bore gas inlet is connected to a stopcock/B10 ground glass cone system as shown. Seven such detectors were manufactured in the laboratory and two purchased commercially. Determination of the radioactivity of the sample is effected by placing the detector on the face of a photomultiplier as shown in Figure 13. Silicone fluid is used to provide a good light path between the detector and the photomultiplier. α -particles striking the 2n S (Ag) phosphor produce a light pulse which is converted to an electrical impulse and amplified by the photomultiplier before transmission as a voltage pulse to a scaler. In fact each ^{222}Rn decay gives rise to two further α -emitting

(a)



(b)

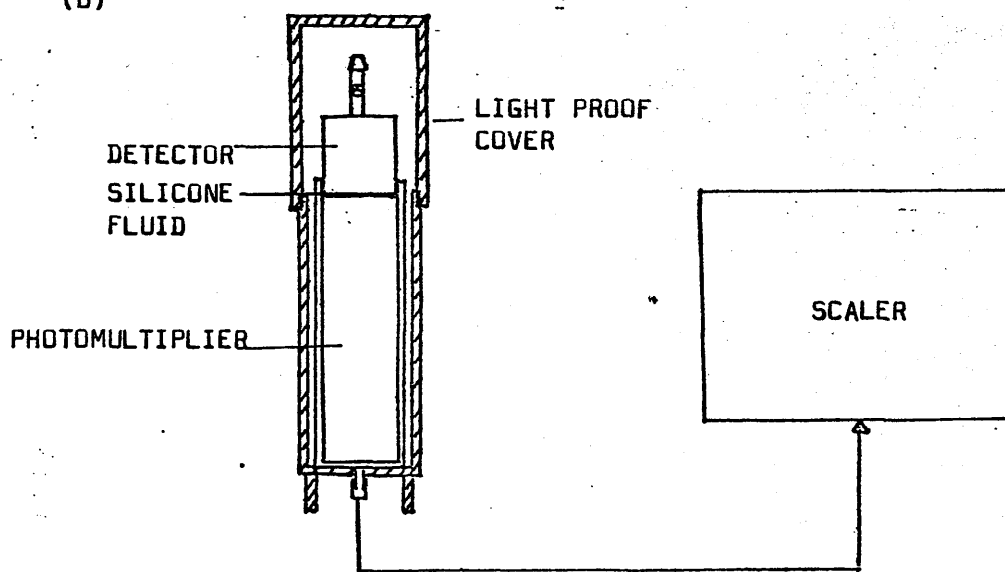


FIGURE 13. (a) Section through ^{222}Rn detector

(b) ^{222}Rn detector/photomultiplier assembly.

species, namely ^{218}Po and ^{214}Po which rapidly grow in to secular equilibrium with the parent ^{222}Rn . Thus at equilibrium, three α -decay events are recorded for each ^{222}Rn decay. To simplify calculations therefore, the detectors are left for at least five hours after filling before counting is commenced, thus ensuring equilibrium between ^{222}Rn , ^{218}Po and ^{214}Po . Counting times range from 3 to 24 hours and for the longer counts, correction for decay during counting is performed by the method of Hoffman and Van Camerik (1967) which defines a correction factor based on the ratio of the count time to the half life. Three scaler/photomultiplier systems are used, two having working voltages of 1000V, the other 1150 volts. A typical plateau is shown in Figure 14. Background count rates vary with the detector in the range 0.1 - 0.4 cpm, no shielding being required to produce these low values since the thin layer of 2n S (Ag) used is not sensitive to β^- , γ or meson background radiation. The efficiency for collection and counting of ^{222}Rn (based on three α decays per ^{222}Rn disintegration) was determined by analysis of a standardised ^{226}Ra solution obtained from the National Bureau of Standards and was found to vary from 50% to 80% depending on the particular detector/scaler system used. Backgrounds and efficiencies for the detectors are shown in Table 14. The observed radioactivity was characterised by observations of grow-in of daughter activity and decay of ^{222}Rn activity, typical plots obtained for these processes being shown in Figures 15 and 16 respectively. System blanks varied with the sample being analysed and are defined in later sections. Counting errors are in the range 1% to 2% where the standard deviation σ on a count rate c is defined as

$$\sigma = \frac{\sqrt{N}}{t}$$

where N is the number of counts collected in time t .

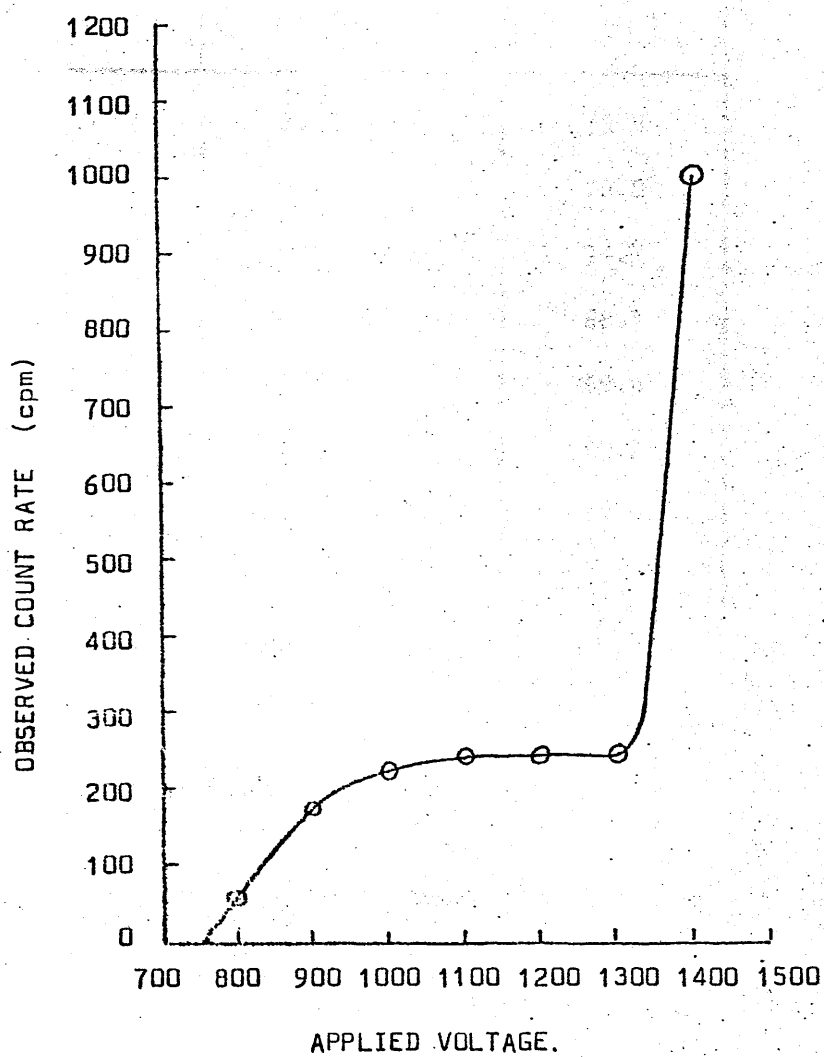


FIGURE 14. ^{222}Rn detector plateau.

Detector	Background (cpm)	Efficiency (%)
1*	0.38	76.8
2*	0.2	78.0
3	0.1	74.2
4	0.1	68.1
5	0.1	69.4
6	0.1	70.2
7	< 0.1	49.9
8	< 0.1	52.1
9	< 0.1	50.3

* commercially manufactured

TABLE 14. ^{222}Rn detector backgrounds and efficiencies.

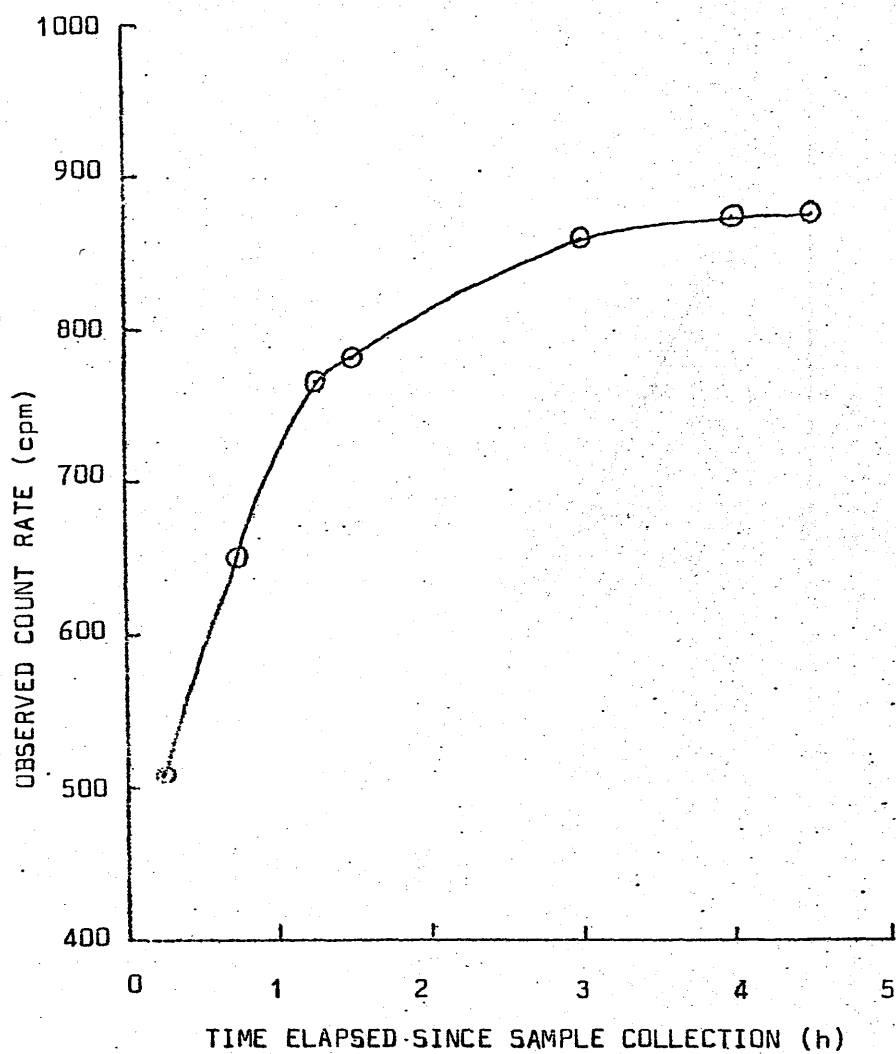


FIGURE 15. Graph of grow in of ^{222}Rn daughter activity.

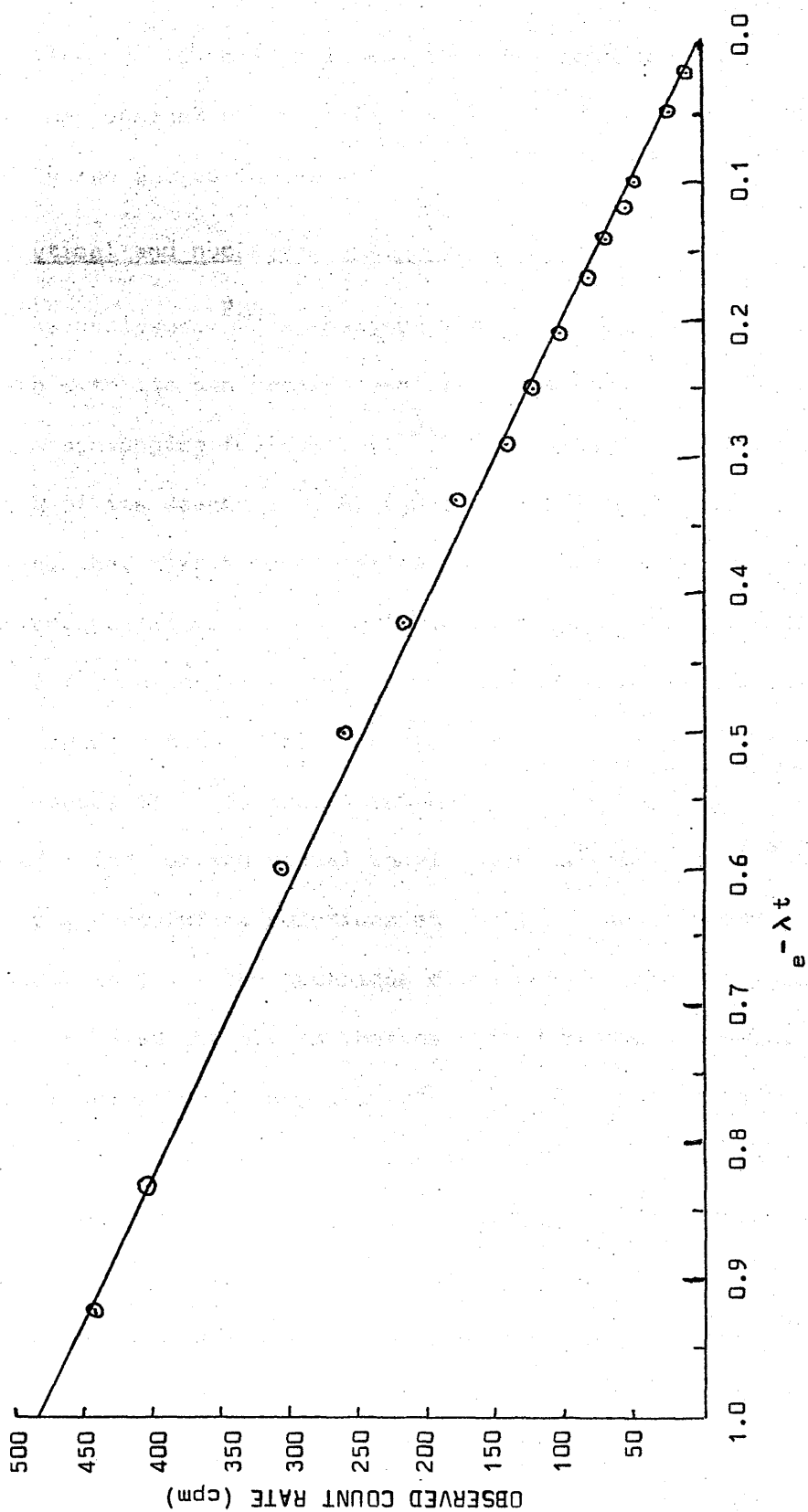


FIGURE 16. Graph of decay of ^{222}Rn .

Replicate analyses on individual samples defined an overall error of 6 % on the measurement where the standard deviation σ is defined as

$$\sigma = \sqrt{\frac{\sum (x - \bar{x})^2}{n-1}}$$

where x is the value obtained in an individual measurement and \bar{x} is the mean of n observations.

Since the overall error is so much larger than the counting error, the former must be regarded as the effective error on any measurement and will be the value quoted on results.

2.4. ^{228}Ra analytical and nuclear counting techniques.

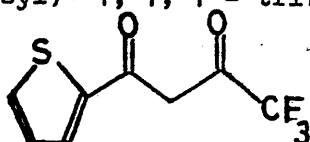
As for ^{226}Ra analyses, ^{228}Ra analyses are performed on a variety of samples, each with its own pretreatment requirements. The following method of barium scavenging followed by ^{228}Ra analysis by extraction and β^- counting of its daughter ^{228}Ac (β^- ; $t_{1/2} = 6.13\text{h}$) applies to all samples after they have been converted to a suitable solution form. The barium scavenging process has a variable chemical efficiency and in fact the $^{228}\text{Ra}/^{226}\text{Ra}$ activity ratio of samples is measured here, the absolute ^{228}Ra concentration being obtained by comparison with the more easily measured absolute ^{226}Ra concentration.

As detailed later for individual sample types, samples for ^{228}Ra analysis are first prepared as solutions at pH 1, having volumes ranging from 100ml to 1l. The technique developed for the analysis of these solutions is based largely on that described by Moore (1969b) for ^{228}Ra analysis of sea water. One gram of Ba Cl_2 dissolved in 50ml of distilled water is added to the sample and Ba SO_4 is precipitated to scavenge the radium from solution by the addition of excess concentrated $\text{Na}_2 \text{SO}_4$ solution over a period of thirty minutes. The sample is stirred continuously during the precipitation and stirring is maintained for a further thirty minutes on completion of this stage. The precipitate is then allowed to settle for a period of at least six hours after which

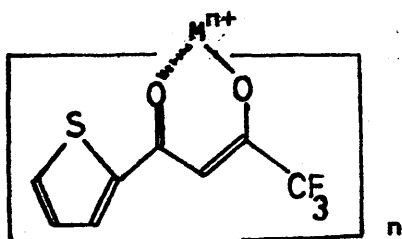
most of the supernatant liquid is poured off, in some cases being discarded and in others being used for further analyses as described later. The Ba SO_4 is separated from the remaining supernatant liquid by centrifugation and is washed with distilled water then hot 6N hydrochloric acid, leaving a pure white powder. For ^{228}Ra analysis, it is necessary to have the sample in a water-soluble form and this is achieved by conversion of the carrier to Ba Cl_2 via a carbonate fusion and acid digestion of the resultant Ba CO_3 . The dried Ba SO_4 is mixed with an excess (about 2g each) of Na_2CO_3 and K_2CO_3 in a platinum crucible which is then heated to 1000°C and maintained at this temperature until the contents of the crucible are totally molten (generally about 20 minutes). The crucible is then allowed to cool slowly and the solidified flux is removed, crushed and thoroughly washed with distilled water to remove soluble potassium and sodium salts, leaving an insoluble residue of Ba CO_3 . This residue is dissolved in dilute hydrochloric acid and the solution taken to dryness, leaving a crystalline deposit of Ba Cl_2 . Total conversion of the original Ba SO_4 to Ba Cl_2 is generally achieved by one such fusion but if any sulphate remains, a second fusion is performed. The Ba Cl_2 is purified by washing with a 5% (V/V) solution of diethyl ether in cold concentrated hydrochloric acid. This step, utilising the decreasing solubility of chlorides on moving down group 11a of the periodic table removes strontium and calcium salts while leaving the barium and radium. Particular care was found necessary in this stage to ensure removal of all ^{90}Sr present since its daughter ^{90}Y interferes in the analysis process for ^{228}Ra . The purified Ba Cl_2 is dissolved in 20ml distilled water and the pH of the solution is adjusted to one for storage prior to analysis.

^{228}Ra analysis and preliminary "clean-up" of the solution are

performed by a combined chelation reaction/solvent extraction procedure using 3- (2- thenoyl)- 1, 1, 1 - trifluoroacetone (TTA):



This species forms chelation compounds of the type



with metal ions in which the equilibrium between the chelated and non-chelated form of the metal is governed by the hydrogen ion concentration of the solution and the stability of the metal/TTA complex. Different metal ions are therefore complexed at different pH values and, by solvent extraction of the complexed species into an organic phase, this process provides a means for selective separation of cations from aqueous solution in accordance with the series:

pH	1	2	3	4	5	6	7	8	9	10
Metal ion	Th Po Bi		Tl(11) Pb		Ac			Tl(1)		

(Katz and Seaborg, 1951, Poskanzer and Foreman, 1961)

Two "clean-up" TTA extractions are performed on the Ba Cl₂ solution before ²²⁸Ra analysis. The first is carried out at pH2 to remove any ²²⁸Th in the solution. This was found necessary since ²²⁴Ra daughter products, notably ²¹²Pb (β^- , $t_{1/2}$ = 10.6h), were encountered as contaminants in early samples. By removing any ²²⁸Th present and storing the solution at pH 1 thereafter for 36 days or more, this problem was overcome through total decay of all ²²⁴Ra plus daughters. The second "clean-up" extraction is carried out at pH 6.5, the pH used in the extraction of ²²⁸Ac, since the first extraction of most samples at this pH produces a scarlet or orange colloidal precipitate, rendering the organic phase unsuitable for preparation of a source for

counting. The nature of this precipitate is undefined but it is probably the product of a reaction of the TTA with some contaminant metal ion producing an insoluble complex and is rarely encountered in subsequent extractions.

^{228}Ra analysis of the purified solution is achieved by storing the solution at pH 1 for greater than 62 hours so that secular equilibrium is established between ^{228}Ra and its daughter ^{228}Ac . The solution is stored in a 30ml stoppering centrifuge tube and, for at least six hours before analysis, is purged with nitrogen to remove ^{222}Rn plus daughters. The pH of the solution is then accurately adjusted to 6.5, at which actinium is strongly complexed with TTA but radium remains uncomplexed. 1ml of 0.25M TTA in benzene is added to the solution which is then shaken vigorously for one minute. Subsequent separation of the organic layer, containing the complexed ^{228}Ac , from the aqueous layer is facilitated by centrifugation. The organic phase is transferred, by means of a Pasteur pipette, to a tapered 10ml centrifuge tube and the extraction is repeated three times, the pH of the solution being maintained at 6.5 by addition of one drop of 0.1M sodium hydroxide solution if necessary. Upon completion of the fourth extraction, the time is noted and the solution is washed with 1ml of benzene to remove any traces of TTA. The benzene washings are added to the combined organic extracts and the total solution is centrifuged to separate any traces of aqueous solution which are returned to the sample. The latter is adjusted to pH 1, thoroughly washed with benzene and stored for further analysis after grow-in of a new crop of ^{228}Ac . The TTA extract is prepared, as quickly as possible, for nuclear counting by dropwise addition to the central depression of a one-inch, stainless-steel, "dimple" planchet heated to about 90°C by contact, at its outer edges, with a metal ring positioned on a hotplate. This system produces a thermal gradient across the planchet,

assisting with localisation of the evaporating drop near the centre of the planchet thus producing reproducible source geometry. After evaporation of all the benzene, the planchet is taken to red heat in a bunsen flame, fixing the actinium as a thin layer of the metal oxide on the surface of the planchet which, when cooled, is ready for β^- counting to determine the ^{228}Ac activity.

β^- counting is performed on an ICN Tracerlab AC-1 Omni/guard Geiger counter; a schematic diagram of which is shown in Figure 17. The detector is a one inch counter surrounded at the sides and top by a guard counter, the two being linked by anticoincidence circuitry to ensure a low background. The background is further reduced by 4-inch lead shielding in all directions round the counter. A flow gas of helium containing 0.85% isobutane and 0.00135% butadiene is used, preventing discharge and giving quenching of U.V. radiation produced in the detector. The detector has an ultra-thin (approximately $150\mu\text{g cm}^{-2}$) window composed of Mono-Mol resin, giving detection efficiencies only slightly less than those of windowless flow counters. The sample planchet is positioned at the counter face by an automatic planchet changer. Working voltages for the detector and guard were found to be 950V and 1425V respectively and typical plateaux are shown in Figure 18. The detector background was characterised as $0.39 + 0.05$ cpm and a histogram of backgrounds observed over a 3 year period is shown in Figure 19. Blank runs gave count rates of less than 0.2 cpm above background.

Standard ^{228}Ra solutions for efficiency determination were not commercially available and were prepared from vintage ^{232}Th as follows. $\text{Th}(\text{NO}_3)_4$ prepared in 1908 was obtained from the Radiochemical Centre Amersham, along with a standardised ^{228}Th solution. The vintage ^{232}Th has all of its decay series, including ^{228}Ra , in secular

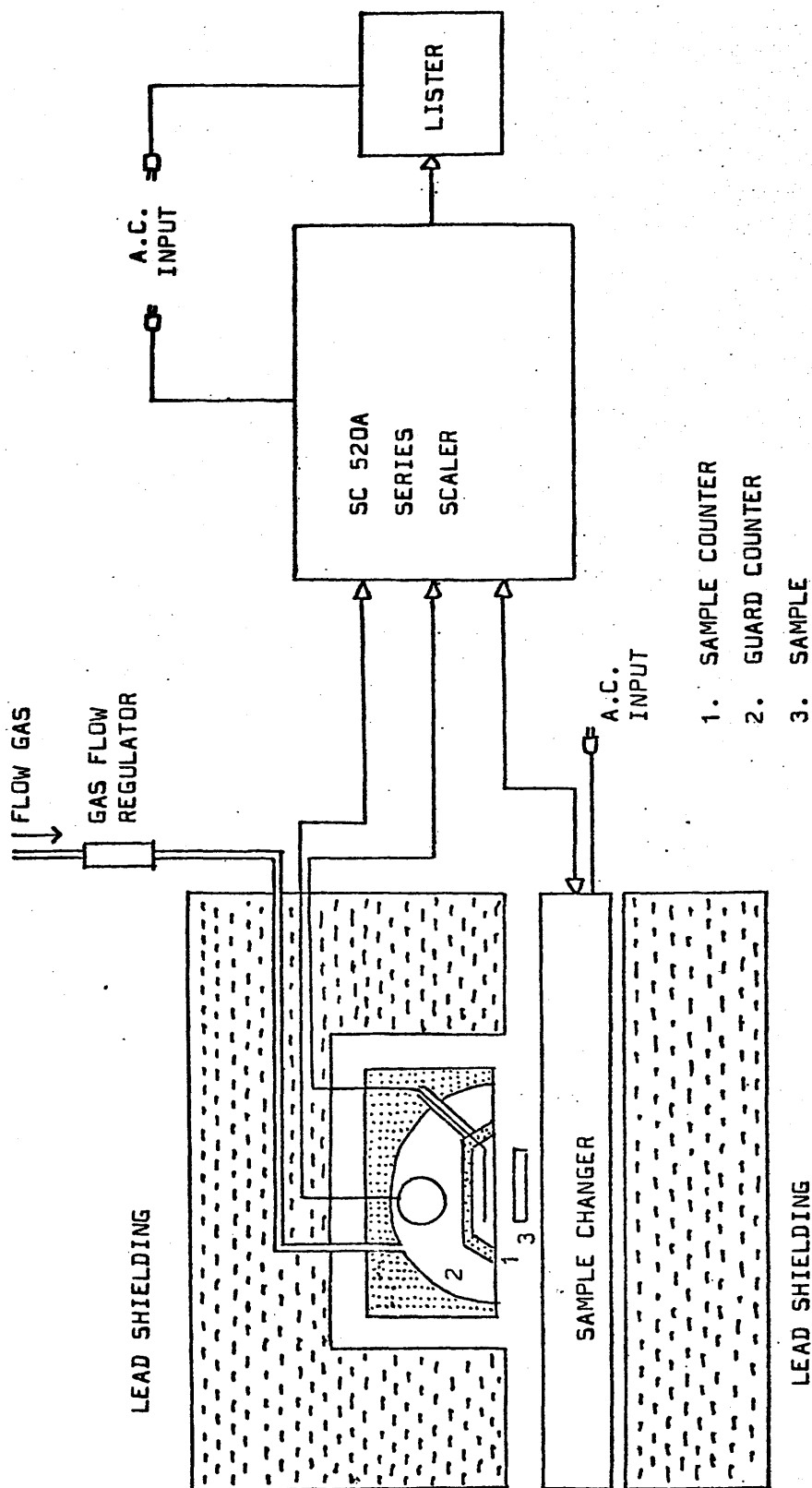


FIGURE 17. Schematic diagram of Tracerlab counter.

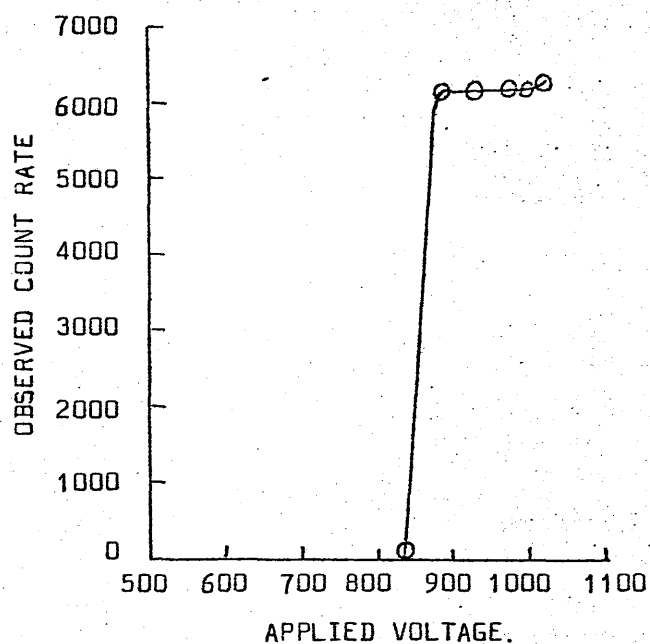
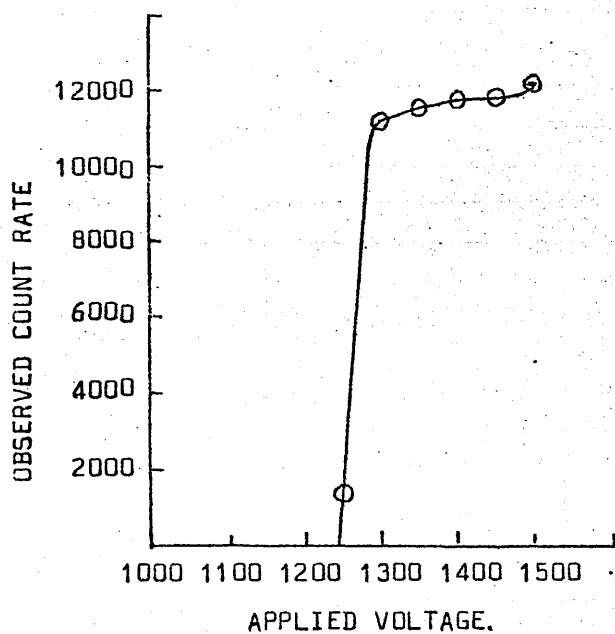
(a) DETECTOR(b) GUARD

FIGURE 18. Tracerlab detector and counter guard plateaux.

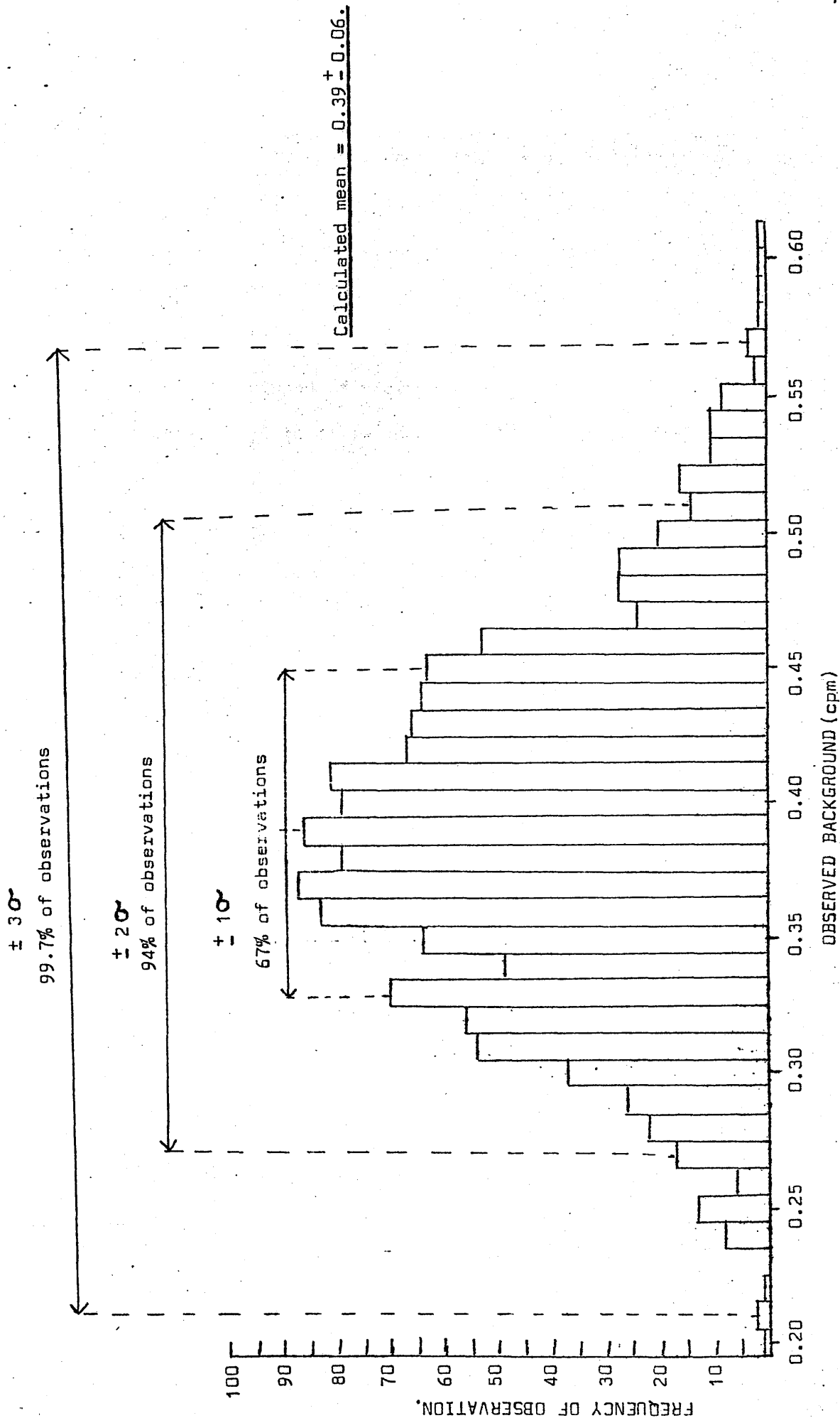
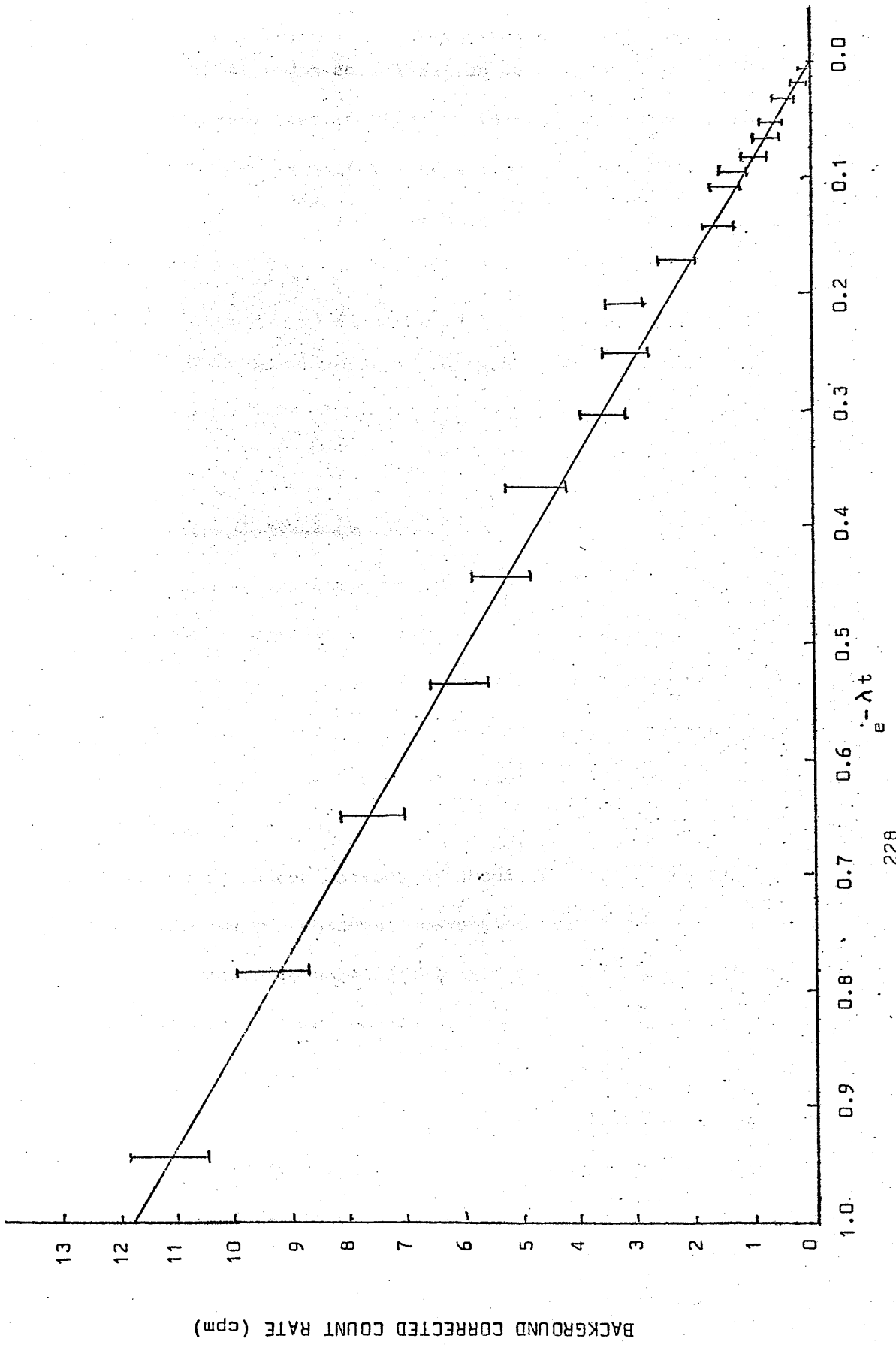


FIGURE 19. Histogram of backgrounds recorded on Tracerlab detector (100min counts) from 1972-1976.

equilibrium and a solution was prepared to give an activity of approximately 30 dpm per 20ml for ^{232}Th plus daughters. Ba Cl_2 carrier was added to give a concentration equivalent to 1g of Ba Cl_2 per 20ml of solution. The absolute activity was determined by TTA extraction of thorium and α -spectrometric comparison with standard ^{228}Th solutions, the methods used being based on those described in detail by Thomson (1972). 20ml aliquots of the standardised solution were stripped of thorium by repeated TTA extractions at pH 2 and, after 36 days to allow decay of ^{224}Ra plus daughters, these solutions were used as ^{228}Ra standards. The decay of the extracted species in analyses of the standards was characterised as ^{228}Ac by observation of the decay and a typical plot of count rate versus $e^{-\lambda t}$ is shown in Figure 20. The mean efficiency of extraction and counting was found to be 32% and replicate analyses defined an error of 8% associated with the measurement. This is large in comparison to the error associated with counting which was found to be in the range 1 to 2% and the overall error defined by the replicate analyses is the value quoted for results.

Samples were counted for 500 minutes, a correction for decay during counting being applied as described by Hoffman and Van Camerick (1967). Small amounts of ^{90}Y (β^- , $t_{1/2} = 63\text{h}$) were detected as a contaminant (generally less than 0.3 cpm ^{90}Y relative to sample count rates of 8 to 12 cpm) and were corrected for by a second observation of the sample activity after 62 hours when decay of ^{228}Ac is complete. A residual count rate was measured after 630 hours and a correction applied where necessary. A computer program in Fortran 1V was written to facilitate these calculations and a specimen calculation along with the program is presented in appendix 3.

The above procedure defines the ^{228}Ra concentration of the Ba Cl_2

FIGURE 20. Graph of decay of ^{228}Ac

solution and upon completion of the ^{228}Ra analysis, the sample is made up to a volume of about 100ml with distilled water and is transferred to a 250ml radon-equilibration vessel for ^{226}Ra analysis as previously described (section 2.3). This is necessary since the scavenging procedure has a variable efficiency between 30 and 70%. However fractionation of ^{228}Ra relative to ^{226}Ra is assumed negligible in the process so that the $^{228}\text{Ra}/^{226}\text{Ra}$ activity ratio of the Ba Cl_2 solution is equal to that of the original sample. By combining the activity ratio obtained in this way with a separate measurement of the ^{226}Ra concentration of the sample, the absolute ^{228}Ra activity is defined.

2.5. ^{226}Ra analysis of water samples.

^{226}Ra analyses of sea water samples were performed by two methods. The first employed a pre-concentration of ^{226}Ra from 60l of sea water by adsorption on finely dispersed manganese dioxide supported on base-treated acrylic fibre. The second method involved direct analysis by ^{222}Rn emanation from 20l samples of sea water.

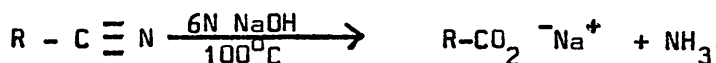
(a) Pre-concentration method.

^{226}Ra occurs in concentrations of about $10^{-14} \text{ g l}^{-1}$ in sea water and its extraction by conventional scavenging techniques such as Ba SO_4 precipitation is generally unsatisfactory, requiring chemical operations on large volume (20l or more) samples and having a variable efficiency. However recent work by Krishnaswami et al (1972) and by Moore and Reid (1973) has demonstrated that a number of trace metals, including radium, can be rapidly and efficiently extracted from sea water by adsorption onto finely dispersed ferric oxide or manganese dioxide supported on base-treated acrylic fibre. Moore and Reid reported that the manganese dioxide impregnated fibre is particularly effective in scavenging

radium and quoted an uptake of greater than 90% of the radium from sea water samples during a single pass through a column of the fibre. Enrichment factors for radium of 10,000 to 30,000 were defined for the manganese impregnated fibre where "enrichment factor" is defined as "the ratio of the concentration of radium in 1 kg of fibre after exposure to sea water to the concentration of radium in 1 kg of sea water". The variation in observed enrichment was a result of varied exposure times and rate of water flow through the fibre. Blank ^{226}Ra concentrations in 100g of fibre were defined as 0.12 dpm.

The manganese dioxide impregnated fibre therefore presents a highly efficient technique for the quantitative removal of radium from sea water and a method involving this material for the determination of ^{226}Ra concentrations in surface and shallow waters was developed in the present research as described below.

The fibre is prepared from Monsanto Chemical's "Acrilan" (3.0 denier, B-16 tow) which is treated with boiling 6N NaOH solution until it assumes an intense red/orange colour as a result of the base catalysed hydrolysis of some of the cyano groups:



Prolonged exposure of the fibre to the hydroxide solution gives excessive conversion to the soluble sodium salt and consequent dissolution of the fibre and so must be avoided. The fibre, thus converted to a cation exchange form, is cooled, wrung dry and added to a 6N solution of Mn Cl_2 at 30 to 40°C, the solution being maintained at pH 1 to 2 by addition of hydrochloric acid to avoid precipitation of $\text{Mn}(\text{OH})_2$. The fibre is soaked in this way for about 20 minutes to ensure total penetration of the manganese after which it is wrung dry and then is teased out to a fluffy texture. Immersion in 6N NaOH solution at room temperature produces a very fine precipitate of $\text{Mn}(\text{OH})_2$ dispersed

throughout the fibre which is then wrung dry and is again teased out. On exposure to air, the $\text{Mn}(\text{OH})_2$ is spontaneously oxidised to MnO_2 , the fibre assuming a dark brown/black colour in the process. The fibre is then thoroughly washed in distilled water to remove any loose MnO_2 and is finally wrung dry, weighed and stored in polythene bags prior to use. This technique gave a loading of about 0.7g of MnO_2 per gram of fibre. The nature of the fibre and the possible mechanism for uptake of radium are discussed in Appendix 2.

Extraction of radium from 60l of sea water by the fibre was carried out on board ship and the extraction system used is shown in Figure 21. Water from the required depth is raised by pumping through 1 inch inside-diameter P.V.C. tubing, fitted with a 1mm filter, and 60l is measured into the calibrated plastic container after filtering through glass wool. The water is cycled through 75g of manganese dioxide impregnated fibre for 30 minutes at a flow rate of about 10l min^{-1} , giving a total of about five passes through the fibre. The excess water is then pumped away and the fibre transferred to a polythene bag for return to the laboratory.

After return to the laboratory, the fibre is leached in 500ml of boiling 6N hydrochloric acid, converting the MnO_2 to soluble Mn Cl_2 . When the fibre is bleached pure white and the solution assumes a clear yellow/green colour, the fibre is removed, drained and washed with distilled water. The combined drainings and washings are added to the acid leachings and the total solution is boiled down to about 500ml volume after which it is allowed to cool and is then filtered into a 1l equilibration vessel for ^{222}Rn emanation analysis as described in section 2. 3.

The potential advantages of this technique include ease of sample transportation, high count rates as a result of extraction of ^{226}Ra

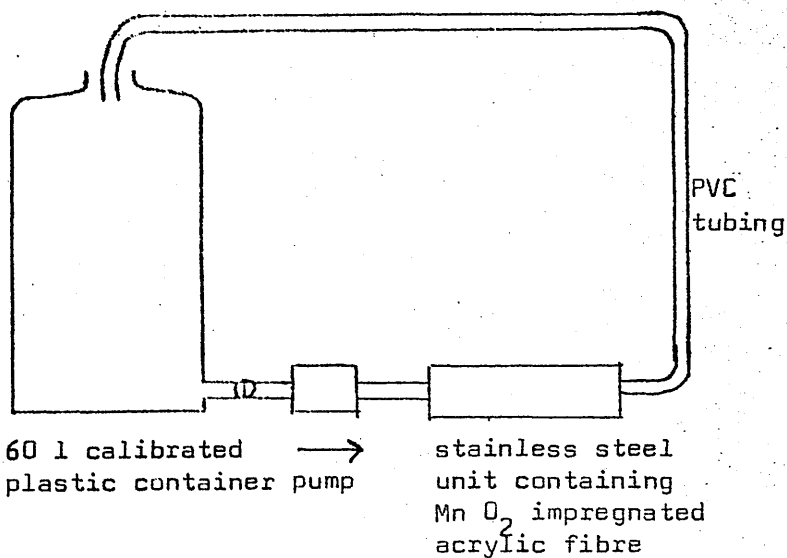
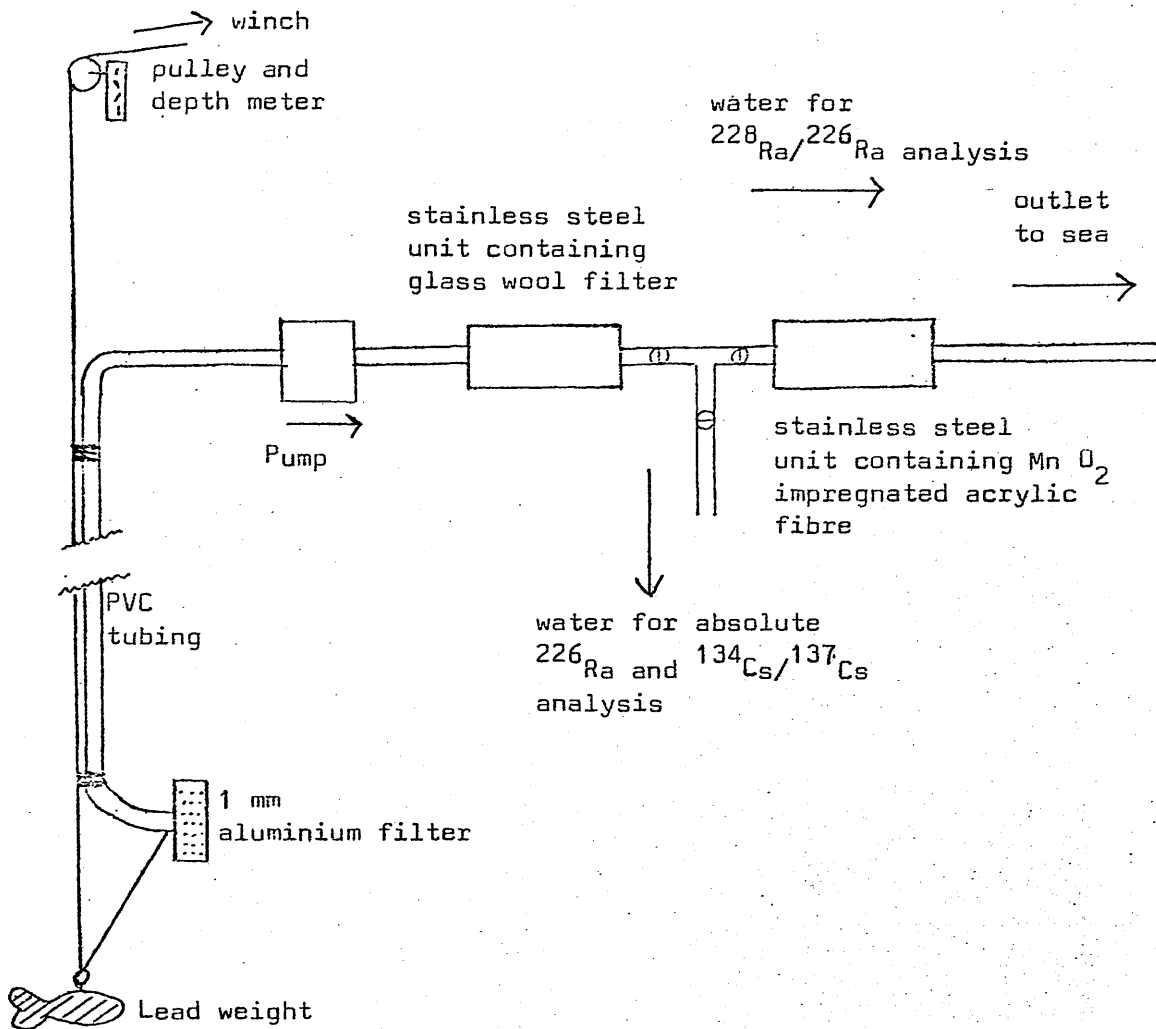


FIGURE 21. Shipboard sampling systems.

from large volume solutions and low blanks. The method as developed was only partially successful in exploiting these advantages. While laboratory experiments demonstrated that a single slow pass of a ^{226}Ra solution through 75g of manganese dioxide-impregnated fibre removed more than 95% of the ^{226}Ra , extractions of 60l standard solutions, as used in the shipboard extraction, indicated an overall mean efficiency for extraction and counting of ^{226}Ra of 34%, corresponding to an extraction efficiency of 50% (Table 15). Replicate analyses defined an error of 10% associated with the method and blank ^{226}Ra concentrations per 100g of fibre were found to be 0.2 cpm. Thus while this technique does have advantages in terms of ease of sample transport and low blanks, the low extraction efficiency and large error detract from its use. It was therefore decided to complete the latter stages of the sampling program by the more conventional technique of ^{226}Ra analysis by direct emanation of ^{222}Rn from 20l samples of sea water.

(b) Direct emanation method.

20l samples for analysis by this method are collected by the sampling system described in section 2.5a and are returned to the laboratory in 25l plastic containers. On return to the laboratory, the samples are filtered and acidified to pH1 before transfer to 20l equilibration vessels. ^{226}Ra analyses are performed as described in section 2.3., a two hour flushing time being found necessary to give reproducible results. Blank count rates varied between 2 and 4 cpm, depending on the particular equilibration vessel and replicate analysis showed the error to be 8%.

Sample	Observed ^{226}Ra count rate (cpm)	Combined counting/extraction efficiency (%)	Extraction efficiency (%)
Mn O ₂ fibre extract from 60 l distilled water	2.2		
Mn O ₂ fibre extract from 60 l distilled water + 23.2 dpm ^{226}Ra spike	10.5	36	53
Mn O ₂ fibre extract from 60 l distilled water + 23.2 dpm ^{226}Ra spike	10.0	34	50
Mn O ₂ fibre extract from 60 l distilled water + 23.2 dpm ^{226}Ra spike	9.4	31	46
Mn O ₂ fibre extract from 60 l distilled water + 23.2 dpm ^{226}Ra spike	9.4	31	46
Mn O ₂ fibre extract from 60 l distilled water + 23.2 dpm ^{226}Ra spike	11.3	39	57
Mn O ₂ fibre extract from 60 l distilled water + 46.4 dpm ^{226}Ra spike	19.8	38	56

TABLE 15. Calibration data for extraction of ^{226}Ra from 60 l standard solutions using manganese dioxide impregnated fibre.

2.6. ^{228}Ra analysis of water samples.

^{228}Ra concentrations in sea water are determined via the $^{228}\text{Ra}/^{226}\text{Ra}$ activity ratio by a non-quantitative extraction of radium from large volumes of sea water onto manganese dioxide impregnated acrylic fibre (Section 2.5 (a); Appendix 2). The absolute ^{228}Ra concentration is derived from the ratio by a separate determination of the absolute ^{226}Ra concentration of the water as described in section 2.5.

Water from the required depth is raised through 1 inch diameter reinforced P.V.C. tubing, as described in section 2.5 (a), and is pumped through 250g of manganese dioxide impregnated acrylic fibre contained in a stainless steel cylinder as shown in Figure 21. With flow rates around 40 l min^{-1} and pumping periods of 30 minutes a total volume in the order of 1000 l passes through the fibre. On completion of the extraction, the fibre is transferred to a polythene bag for return to the laboratory where it is leached with about 1 l of boiling 6N hydrochloric acid. This converts the Mn O_2 to soluble Mn Cl_2 and the solution is allowed to cool when it assumes a clear yellow/green colour and the fibre is bleached pure white. The fibre is then removed, drained and washed with distilled water and the combined drainings and washings are added to the original acid leachings. The total solution is filtered and the $^{228}\text{Ra}/^{226}\text{Ra}$ activity ratio measured as described in section 2.4.

The efficiency of extraction of radium by this method cannot be defined accurately from the data obtained from sample analyses since the procedure involves scavenging chemistry of variable efficiency. However based on likely values for the concentrations and efficiencies concerned, it is estimated that the extraction efficiency is probably in the range 40 to 80%. It is not possible to define an error associated with the pre-concentration stage since facilities are not

available for replicate analyses of 1000 l water samples. However it is an activity ratio which is being measured and fibre blanks are less than 0.2 cpm for both isotopes relative to typical count rates of around 10 cpm for ^{228}Ac and 40 cpm for ^{222}Rn . Thus assuming no fractionation of the radium isotopes during the extraction, any error introduced in the pre-concentration stage will be small compared to the errors associated with the subsequent ^{228}Ra and ^{226}Ra analytical and nuclear counting procedures as previously described. The combined error from these measurements gives rise to an error of 13% associated with measurement of the $^{228}\text{Ra}/^{226}\text{Ra}$ activity ratio.

2.7. Radium analysis of sediment.

Sediment cores are collected by means of a conventional gravity corer and a Craib corer, the constructions of which are shown in Figure 22. The gravity corer is lowered to within 5m of the sediment surface after which it is allowed to free-fall. The sediment, once, forced into the plastic core liner is retained in position by a metal core catcher. A one way valve allows expulsion of water from the core barrel during the coring process and prevents disturbance of the sediment during its return to the surface. The sediment and core liner are withdrawn from the core barrel, supernatant water removed by a syringe and the sediment frozen in a combined freezer/transporter unit, the design of which is shown in Figure 23. Before freezing, the core is maintained in an upright position to prevent mixing of the sediment. A core barrel of length 90cm is used to collect cores of diameter 6 cm and lengths up to 75 cm. Longer cores can be collected using a longer core barrel and more lead weights. The gravity corer however suffers from the disadvantage that surface layers of sediment are often lost or mixed during the sampling process, a problem overcome

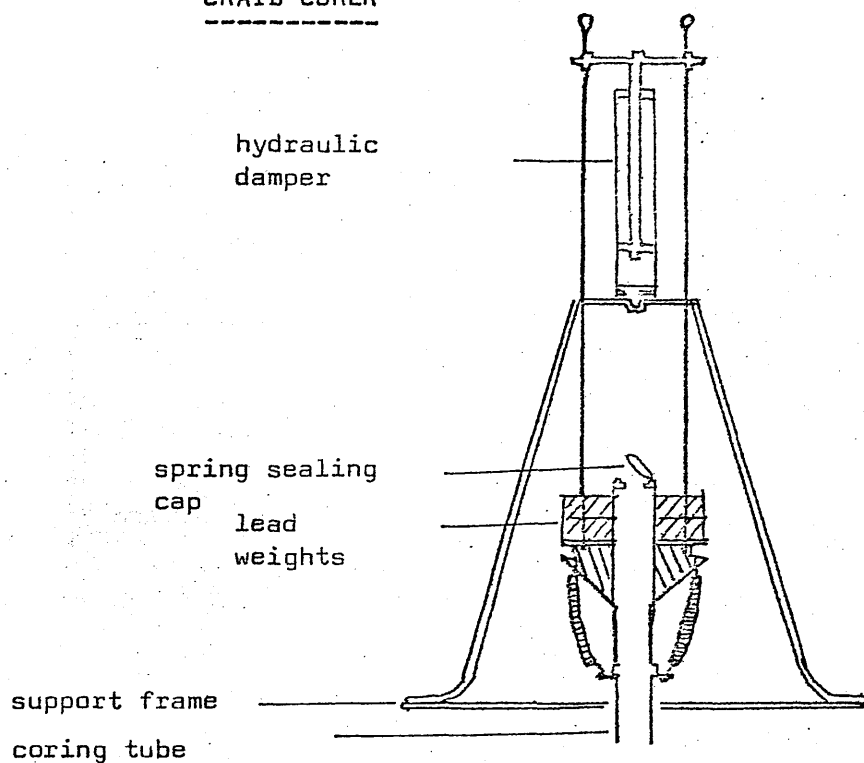
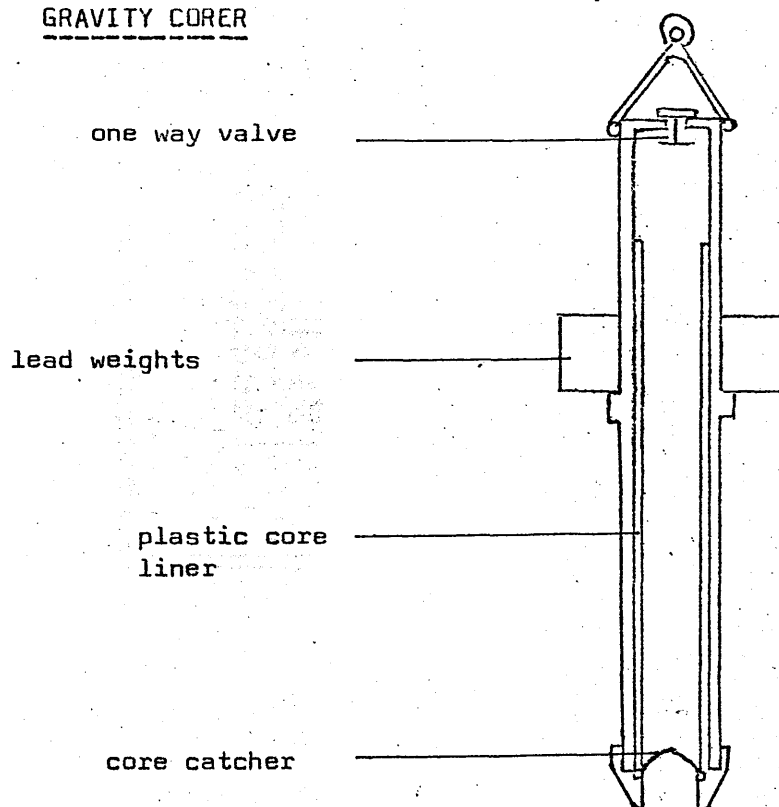
CRAIB CORERGRAVITY CORER

FIGURE 22. Sections of Craib and gravity corers.

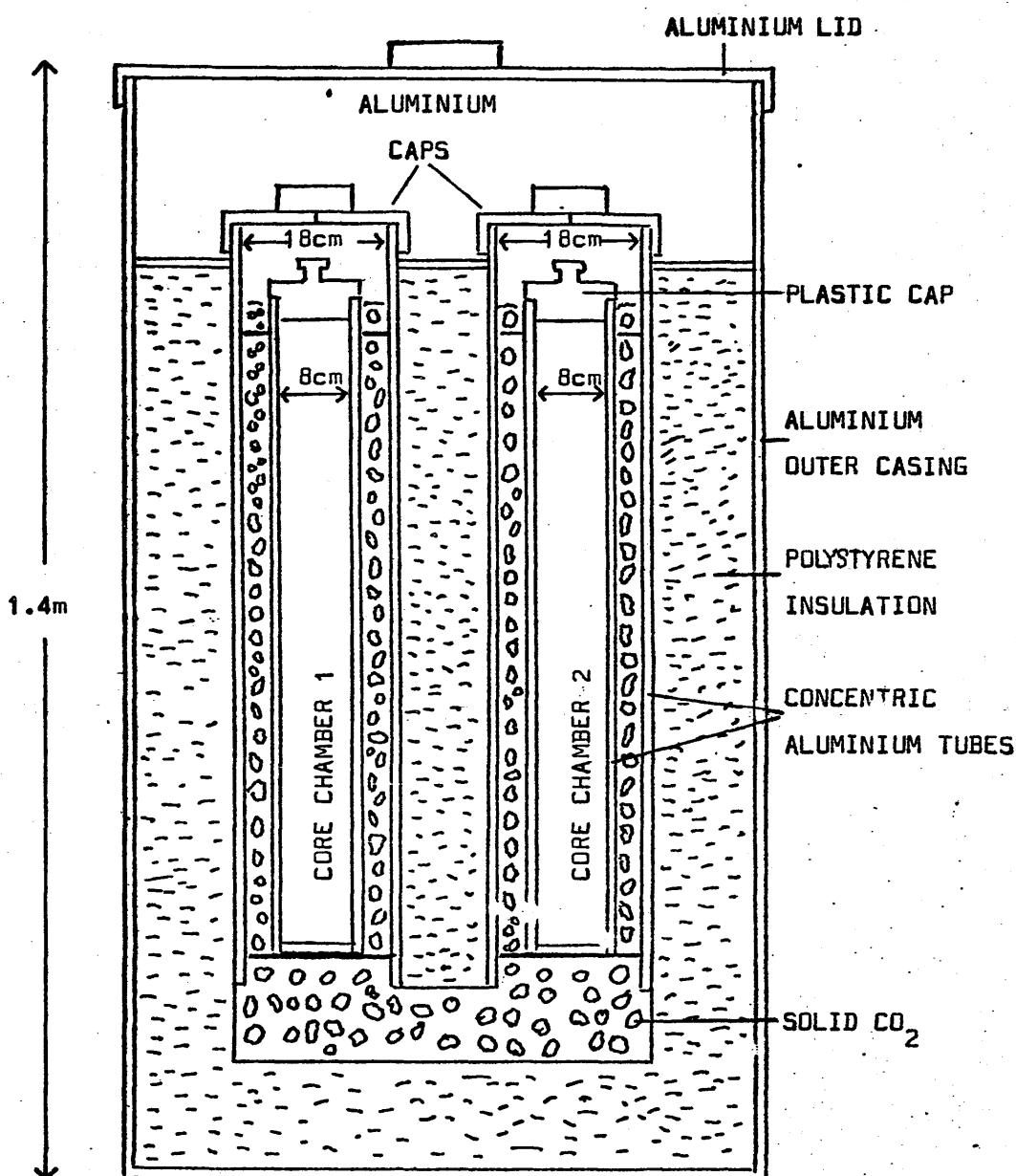


FIGURE 23. Freezer/transporter unit for sediment cores.

by the Craib corer. This device is specially designed for the collection of undisturbed surface sediment cores of diameter 5.7 cm and length 10 to 15 cm. The corer is dropped from about 2 m above the sediment surface, impact of the metal support frame causing release of the weighted plastic coring tube. A very slow penetration of the corer into the sediment is achieved by hydraulic damping and the sediment is retained in the core tube without disturbance by automatic insertion of a rubber ball into the mouth of the tube as it is withdrawn from the sediment. Closure of a spring seal cap prevents disturbance of the sediment as it is raised through the overlying water column (Craib, 1965). Upon recovery, the cores are again maintained in a vertical position and supernatant water withdrawn by syringe. A smaller version of the unit described for gravity cores is used for freezing and transportation of Craib cores.

On return to the laboratory, the frozen cores are stored in a deep freeze unit until required for analysis when they are cut into 1 cm sections by means of a band-saw. Craib cores are extruded from the core tube before cutting since this is an intrinsic part of the corer and is re-used. The extrusion is effected by partially melting the outer parts of the core by sealing in polythene and immersion for several minutes in boiling water. A tightly fitting piston lubricated with silicone grease is then used to extrude the sediment from the core tube. Gravity cores, in contrast, are simply cut in the disposable core liner. The weights of individual sections are recorded after which they are oven-dried for at least 24 hours and are then reweighed.

Material for analysis is selectively taken from the central regions

of the sediment sections since the outer edges may be contaminated by sediment from other depths due to smearing through frictional contact with the core liner during coring. Typical sample weights used are in the range 5 to 8 g of dry sediment and total dissolution is effected by a method based on that described in detail by Thomson (1972), all operations in the dissolution procedure being performed using Teflon apparatus. A summary of the dissolution procedure is given in Figure 24.

10 ml of distilled water followed by 50 ml of 50% (V/V) concentrated hydrochloric acid/concentrated nitric acid are added to the powdered sediment in a Teflon beaker. The vigorous reaction which ensues is observed closely to prevent 'bubbling over' of the reactants and when the reaction becomes subdued the mixture is taken to dryness by heating on a hotplate. The dry residue is leached for 3 hours at 80°C with 25 ml 6N hydrochloric acid after which the solution is allowed to cool and the acid leachings separated from the residue by filtration. A second such acid leaching is carried out and the two sets of acid leachings combined and stored while the residue, consisting largely of obdurate silicate materials, is further degraded by a hydrofluoric acid digestion. 25 ml of 40% hydrofluoric acid is added to the residue and the mixture taken to dryness, causing breakdown of the silicate minerals present. The dry residue is leached, as before, with 25 ml 6N hydrochloric acid, the leachings being combined with those obtained previously. The remaining solid material is taken to dryness with 25 ml perchloric acid. Soluble materials are again leached into 25ml 6N hydrochloric acid, as above, while the residue is dried and weighed. The residual material generally consists of a fine black powder, of high carbon content, comprising less than 0.1% by weight of the original sample and this is regarded as insignificant. If however

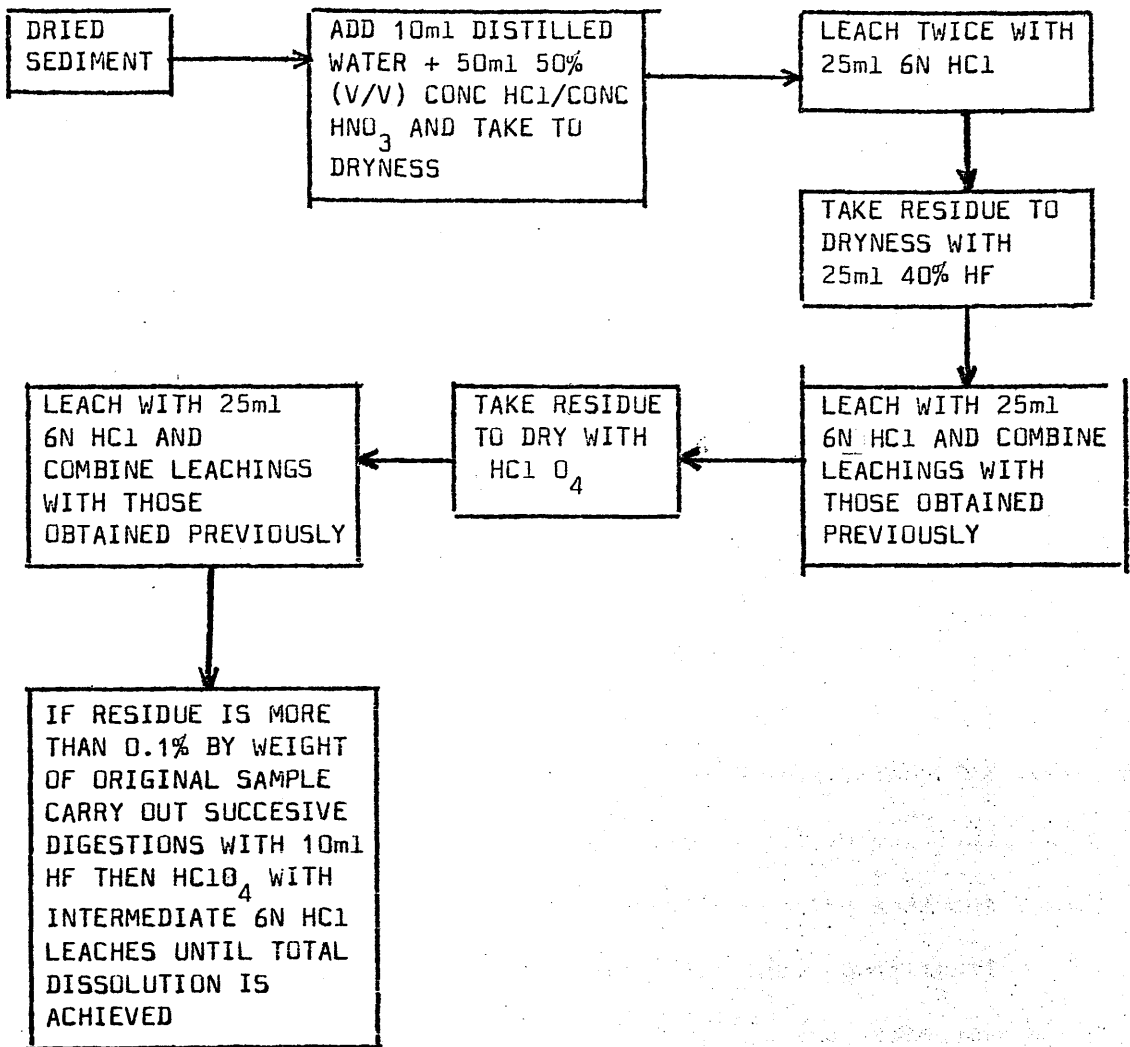


FIGURE 24. Summary of dissolution procedure for sediment samples.

more than 0.1% of the original sample remains then the residue is taken to dryness with 10 ml aliquots of hydrofluoric acid, then perchloric acid, followed by further leaching with 6N hydrochloric acid, this process being repeated until less than 0.1% of the original sample remains.

The combined acid leachings, representing total dissolution of the sample, are transferred to a 1 l radon-equilibration vessel for ^{226}Ra analysis as described in section 2.3. following which most samples are used for $^{134}\text{Cs}/^{137}\text{Cs}$ analysis while a small number are analysed for ^{228}Ra as described in section 2.4.

The above method of total dissolution of sediment was adopted. because the simpler technique of hydrochloric acid/nitric acid digestion followed by hydrochloric acid leaching provides a method for recovery of most of the radium from a sediment sample but leaves about 5% of the ^{226}Ra in the resistant silicate fraction of the sediment (Table 16). The data from this research form part of a wider investigation of the sediment including analyses for ^{210}Pb , ^{14}C and trace metals.. All of these analyses are performed on total sediment so that for comparative purposes (particularly with the ^{210}Pb) it is necessary to derive the total ^{226}Ra concentration in the sediment. Since greater than 99.9% of the sediment is dissolved and material loss during dissolution is carefully avoided, no error is assumed to be introduced in the process and the errors quoted on concentrations are taken as those previously defined in the appropriate analytical and nuclear counting sections.

2.8. Radiocaesium analysis of marine materials.

Radiocaesium measurements are performed on 10 l samples of sea water collected by the pumping system described for ^{226}Ra analyses

LEACHING	^{226}Ra content (dpm)	^{137}Cs content (dpm)
Post HCl digestion	9.0	} 87
Post HCl/HNO ₃ digestion	0.5	
Post HF digestion	0.3	0
Post HCl O ₄ digestion	0.2	0

TABLE 16. ^{226}Ra and ^{137}Cs concentrations in fractional dissolution of sediment from Loch Goil core LGC1 (8.4.75).

(section 2.5.). The samples are filtered and acidified to pH1 prior to analysis by the method described below. The same analytical and counting techniques are used for sediment as for water and the collection and dissolution of these samples is identical to the procedures described for radium analyses (section 2.7.) with, in general, $^{134}\text{Cs}/^{137}\text{Cs}$ measurements following ^{226}Ra analysis of the same sample.

The following method applies to all samples after initial conversion to solution form at pH1 and sample volumes ranging from 200 ml to 10 l. A number of methods are available for analysis of radiocaesium in environmental materials by ion exchange extraction of the caesium followed by γ -spectroscopic analysis (Prout et al, 1965 ; Boni, 1966 ; Kawamura et al, 1971 ; Wilson, 1974 ; Baker, 1975) and the method used in the present research is a development of that described in Prout et al (1965). The technique involves quantitative uptake of caesium by ion exchange displacement of potassium from potassium hexacyanocobalt (II) ferrate (II) (KCFC) followed by in-situ assay of radiocaesium by γ -spectroscopic analysis of the ion exchange column. This particular technique was adopted because it is simple, rapid, inexpensive and has a high specificity for caesium.

KCFC is prepared by the addition of one volume of $0.5\text{M K}_4\text{Fe}(\text{CN})_6$ solution to 2.4 volumes of $0.3\text{ M Co}(\text{NO}_3)_2$ solution over a period of thirty minutes, the reaction being performed at room temperature and with vigorous stirring of the solution. This produces a green precipitate of KCFC:



The precipitate is collected by filtration and oven dried at 90°C for at least 12 hours until a black, hard solid is produced which is then

crushed with a mortar and pestle and dry sieved to 30-80 mesh. Rigorous removal of fines is effected by repeated washings of the KCFC with distilled water and the purified KCFC thus produced is again oven dried at 90°C for at least 12 hours. Yields of purified KCFC are generally about 20% and the material is stored under distilled water prior to use. This step along with the oven drying of the purified KCFC is important to ensure mechanical stability of the material during the extraction process.

Aqueous solutions at pH1 for radiocaesium analysis are initially purified by passing through a 5 cm X 1 cm column of 50 - 100 mesh Bio-Rad Chelex 100 chelating resin in the calcium form to remove interfering radionuclides such as ^{60}Co and ^{65}Zn (Boni, 1966). The sample is thereafter passed through a 5 cm X 1 cm column of KCFC (about 5 g dry weight) contained in P.V.C. tubing, the KCFC being retained in position by a cotton wool plug. Sample volumes range from 200 ml to 10 l and while gravity flow is used for small volume samples, a water pump is required to enhance flow rates for large volume samples. A diagram of the system used for extraction of 10 l samples is shown in Figure 25. Extraction efficiency is constant for flow rates in the range 0.1 to 2 l h^{-1} . After extraction, the ion exchange column is dried at 90°C and is then sealed by insertion of a rubber stopper in each end of the P.V.C. tubing which is then trimmed and sealed with parafilm and cellotape, the top end of the ion exchange column being labelled. The sample is thus prepared as a cylindrical sealed source for γ - spectroscopic analysis.

γ - counting is performed on a 3 inch Na I (Tl) detector coupled with a 1024 channel analyser operated on a 4 X 256 channel mode giving a storage facility for up to four spectra. A low background

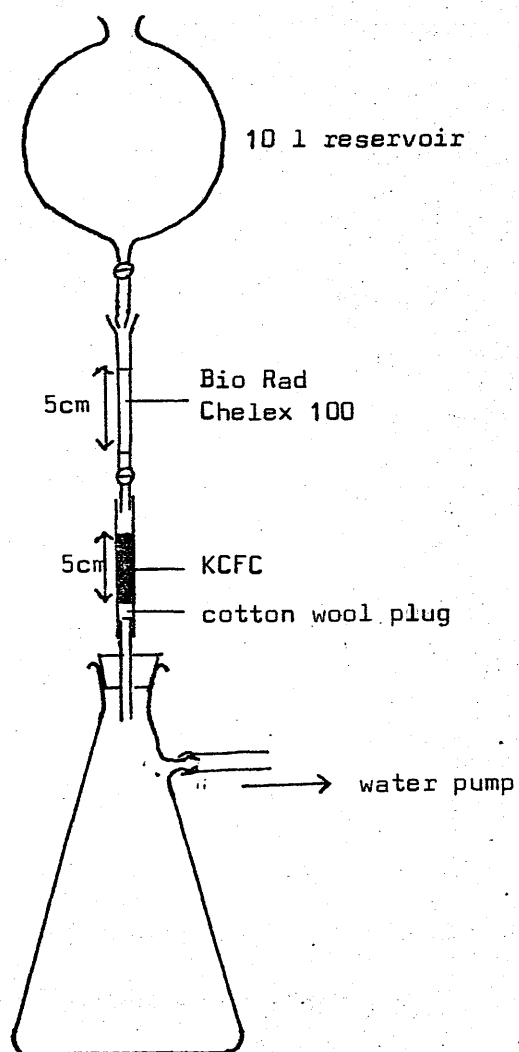


FIGURE 25. Caesium extraction system for 10 l water samples.

is attained by a 4 inch lead shield lined with cadmium. The decay modes of ^{134}Cs and ^{137}Cs are shown in Table 17. The photopeaks produced by the 0.66 Me V and 0.80 Me V γ emissions associated with ^{137}Cs and ^{134}Cs decay respectively are used in the analysis of the two isotopes. The maximum of the ^{137}Cs photopeak is arbitrarily located at channel 111 and all samples are calibrated to this position by a ^{137}Cs reference source before counting. Resolution of the ^{137}Cs photopeak of 9.3% (F.W.H.M.) is maintained during the normal 800 minute counting period by a temperature-compensated main amplifier in which a thermistor senses temperature changes in the detector/photomultiplier assembly and controls the amplifier gain to compensate for signal drift as a function of temperature.

This resolution allows separation of the 0.66 Me V ^{137}Cs photopeak from the 0.80 Me V ^{134}Cs photopeak as can be seen from Figure 26 which shows typical spectra produced from ^{137}Cs and ^{134}Cs reference sources along with a typical sample spectrum produced by analysis of 10 l of Clyde Sea water. The lower energy combined ^{134}Cs photopeak partially overlaps the 0.66 Me V ^{137}Cs photopeak and a correction is made for this in calculations via the ratio of the Compton plus ^{134}Cs counts in the ^{137}Cs photopeak region to the number in the 0.80 Me V ^{134}Cs photopeak. This ratio has a fixed value of 1.45.

Mean background count rates in the 0.66 Me V ^{137}Cs and 0.80 Me V ^{134}Cs photopeak regions are 13.5 cpm and 7.8 cpm respectively while the mean KCFC blank contribution to both regions is the same at 0.3 cpm. Rigorous definition of source geometry is necessary to obtain reproducible results due to localisation of the extracted caesium in the upper sections of the ion exchange column. Analyses of individual 1 cm sections from KCFC columns used for the extraction of 10 l of sea water show that all of the caesium is localised in

^{137}Cs ($t_{1/2} = 30.0\text{y}$) + $^{137\text{m}}\text{Ba}$ ($t_{1/2} = 2.55\text{ min}$)

Decay mode	Energy (MeV)	Intensity (%)
β^-	0.514	93.5
β^-	1.176	6.5
γ	0.6616	93.5

^{134}Cs ($t_{1/2} = 2.05\text{y}$)

Decay mode	Energy (MeV)	Intensity (%)
β^-	0.662	71.0
β^-	0.410	1.0
β^-	0.089	38.0
γ	0.4753	1.5
γ	0.5631	1.8
γ	0.5692	14.0
γ	0.6046	98.0
γ	0.7958	88.0
γ	0.8018	1.9
γ	1.0384	1.1
γ	1.1677	1.9
γ	1.3650	3.4

TABLE 17. Decay schemes for ^{134}Cs and ^{137}Cs (Lederer et al, 1967).

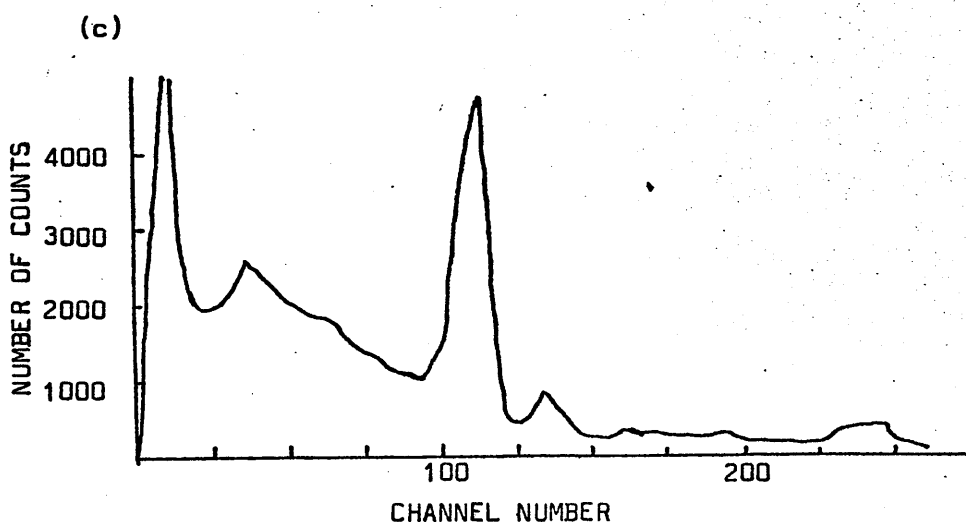
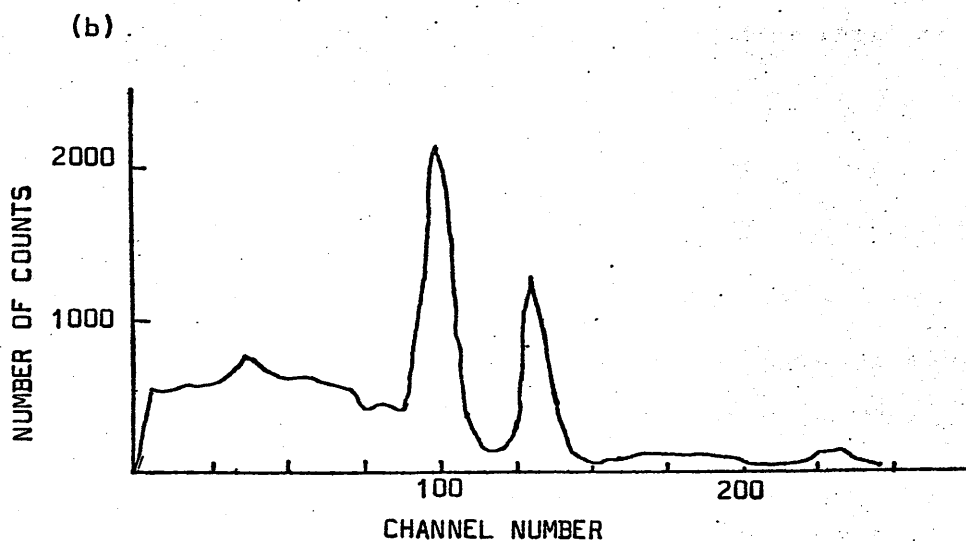
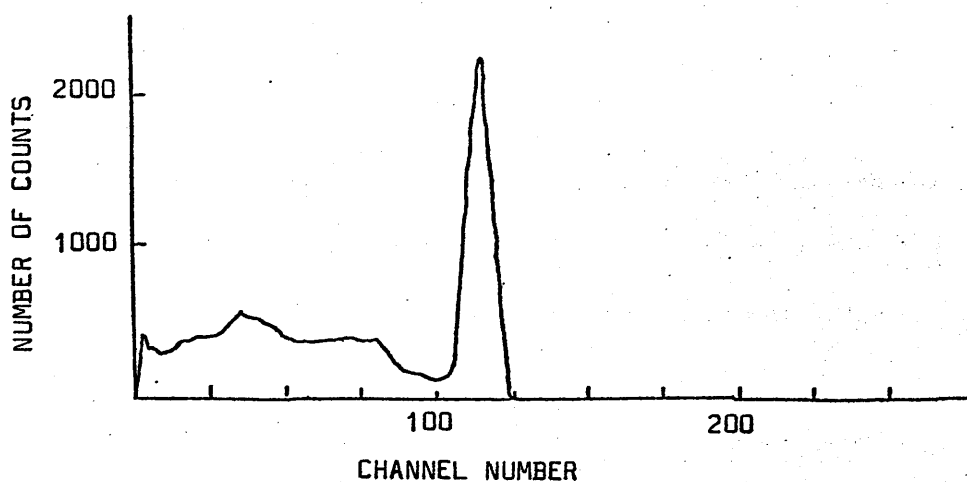


FIGURE 26. Typical spectra. (a) ^{137}Cs reference source (1 min count) (b) ^{134}Cs reference source (1 min count) (c) $^{134}\text{Cs}/^{137}\text{Cs}$ extracted from 10 l of Clyde estuary water (800 min count of KCFC column).

the top 1 cm of the column. During counting the source geometry is therefore defined by locating the column in a fixed position in a perspex holder attached to the detector face such that the top 2 cm of the KCFC column overlap the central 2 cm of the detector (i.e. the region of highest detection efficiency coupled with lowest rate of change of efficiency across the detector).

Combined extraction and detection efficiencies were determined using ^{134}Cs and ^{137}Cs standard solutions obtained from the Radiochemical Centre, Amersham. Figure 27 shows the best fitting straight line defined by computer regression analysis of data obtained from a series of 5 l replicate sea water samples containing increasing amounts of ^{137}Cs spike. The data define the efficiency for extraction and detection of ^{137}Cs as 5.57% and also demonstrate a good linear correlation of observed count rate with ^{137}Cs concentration of the original sample over the entire range of sample activities encountered. Analysis of ^{134}Cs standard solutions defined the efficiency for extraction and detection of ^{134}Cs as 4.77%. Assuming an equal extraction efficiency for both ^{134}Cs and ^{137}Cs these relative values for detection efficiency are in good agreement with theoretically calculated values and imply 100% extraction of Cs

Replicate analyses of 10 l sea water samples defined the error associated with measurement of ^{137}Cs concentration, ^{134}Cs concentration and $^{134}\text{Cs}/^{137}\text{Cs}$ activity ratio to be 2.7%, 3.4% and 2.8% respectively relative to typical counting errors of 0.8%, 2.9% and 2.8% for an individual sample. The observation that the error on the ratio as derived from the replicate analyses is the same as that from counting errors only on an individual sample indicates that no systematic errors are being introduced in the extraction and detection of both ^{137}Cs and ^{134}Cs . The errors of the ^{134}Cs and ^{137}Cs concentrations as defined by replicate analyses being

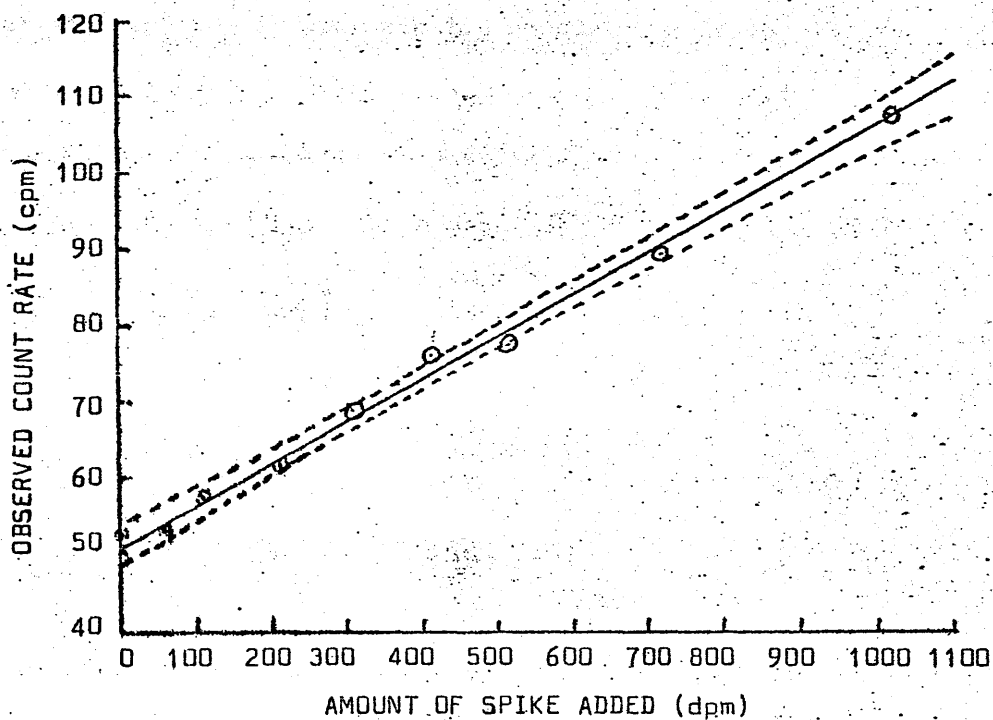


FIGURE 27. Regression analysis plot for data obtained from analysis of ^{137}Cs spiked 5 l sea water samples.

larger than the counting only errors is therefore probably due to a non-homogenous distribution of the radiocaesium across the KCFC column. This would produce variations in the vertical distance of the radiocaesium from the detector face and since there is an inverse square relationship between detection efficiency and height of the source above the detector this would introduce a significant random error on the measurement of absolute concentrations. Assuming no fractionation of ^{134}Cs relative to ^{137}Cs it would not, however, introduce a larger error to the measured activity ratio.

Two minor contamination problems are encountered in the analytical procedure. Firstly a short-lived contaminant in the ^{137}Cs photopeak region of the spectrum is sporadically encountered if samples are counted immediately after extraction. The identity of the contaminant is not defined but it may well be ^{222}Rn daughters with γ emission in this energy range such as ^{214}Bi . This effect is simply overcome by storing samples for at least 15 days between extraction and counting. The second problem involves samples having a very low ^{134}Cs concentration, where a systematic trend towards anomalously high $^{134}\text{Cs}/^{137}\text{Cs}$ activity ratio is observed. Although the error associated with such measurements is generally large enough to render the change in ratio insignificant, the systematic nature of the anomaly and the fact that it is observed by other workers (Baker, 1976) indicate that it is probably a real effect. The cause of this anomaly is undefined but it is again probably the result of some minor contamination during the extraction process, the contaminant activity being insignificant except when ^{134}Cs activities tend towards background levels.

A specimen calculation for determination of radiocaesium concentrations and a computer program in Fortran 1V for its execution are given in Appendix 3.

CHAPTER 3

RESULTS

The results of radium and caesium analyses performed and hydrographic data supplied by the Clyde River Purification Board are presented in Tables 18-57, 1 σ errors being quoted for the radium and caesium measurements. A wide range of salinity values is observed as a result of freshwater input and this can give rise to variations in radium and caesium concentrations simply as a result of dilution. In order to show up such effects, most of the radium and caesium concentrations are presented firstly as a straightforward concentration and secondly arbitrarily normalised to 35‰ salinity. Graphical representations of vertical profiles and maps showing the locations of sampling sites are given in Figures 28-59. For ease of comparison, 2 σ error bars are plotted on radium and caesium profiles. Caesium concentrations in sea water are given in units of dpm l⁻¹ while units of dpm/1000 l are used to give whole number values for radium concentrations. A number of different units are encountered in the literature for these concentrations, depending on the particular application, and the following factors may be applied for inter-conversion:

$$1 \text{ p Ci} = 2.22 \text{ dpm}$$

$$1 \text{ dpm } ^{134}\text{Cs} = 3.4247 \times 10^{-16} \text{ g}$$

$$1 \text{ dpm } ^{137}\text{Cs} = 5.2140 \times 10^{-15} \text{ g}$$

$$1 \text{ dpm } ^{226}\text{Ra} = 4.6150 \times 10^{-13} \text{ g}$$

$$1 \text{ dpm } ^{228}\text{Ra} = 1.6563 \times 10^{-15} \text{ g}$$

SAMPLES R1 - R3

Date : 11.12.73.

General location : estuary (Figure 28)

Sample	Location	Depth (m)	S(%)	D.O. (mg l ⁻¹)	[²²⁶ Ra] (dpm/1000l)	²²⁸ Ra/ ²²⁶ Ra activity ratio
R1	Broomielaw	2	0.0	11.7	119 ± 12	0.4 ± 0.1
R2	Kelvinhaugh	2	0.6	10.9	165 ± 17	0.3 ± 0.1
R3	Renfrew	2	2.4	0.0	104 ± 10	0.4 ± 0.1

TABLE 18. Radium samples from Clyde estuary; 11.12.73.

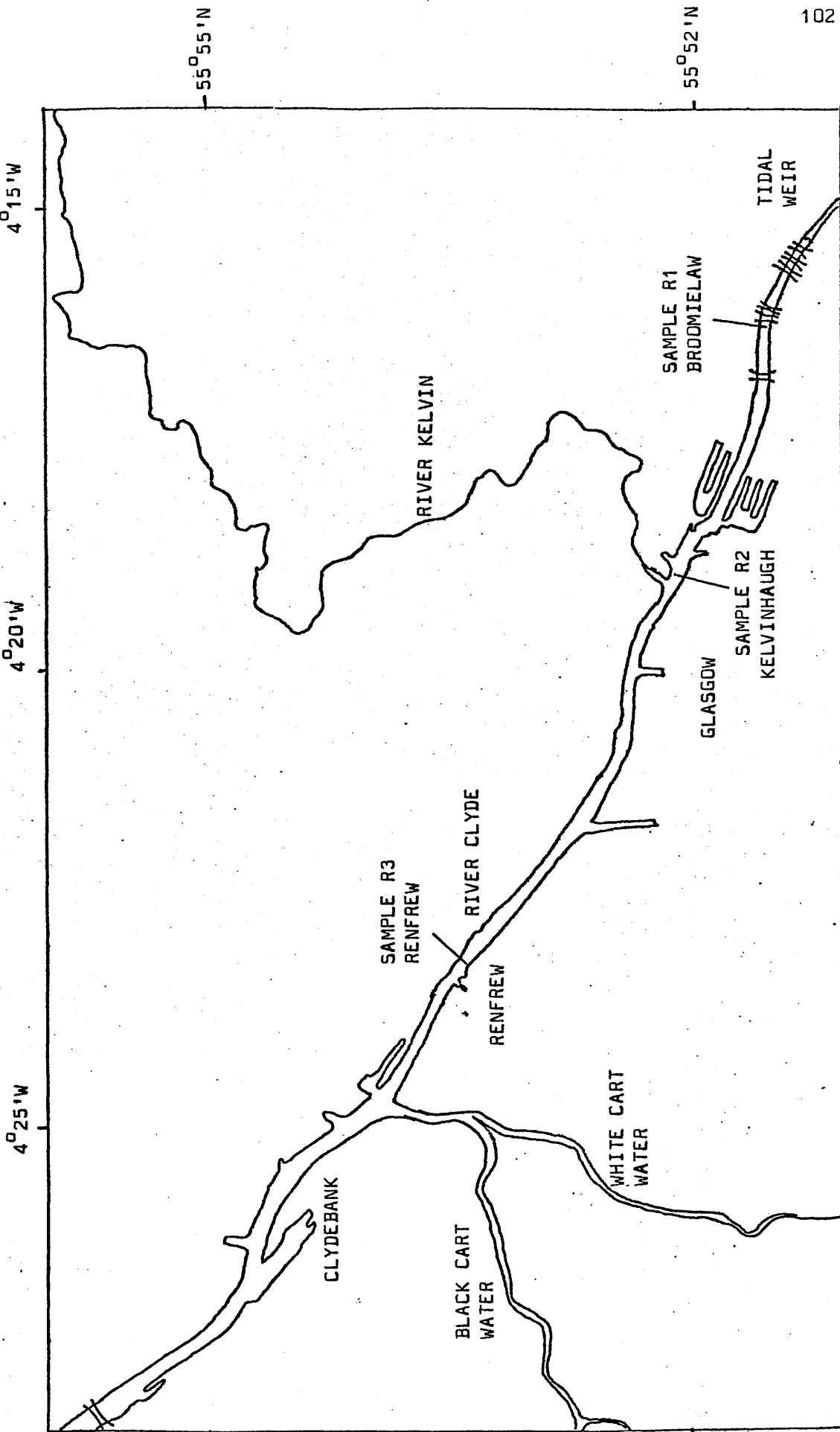


FIG. 20 Location of sampling sites for samples R1 - R3 (scale 1 : 63,360).

SAMPLES R4 - R6

Date : 14.1.74

Location : Gareloch; Station 1 (4° 48'W, 56° 02'N). (Figure 29)

Sample	Depth (m)	S (‰)	D.O. (mg l ⁻¹)	[²²⁶ Ra] (dpm/1000 l)	²²⁸ Ra/ ²²⁶ Ra activity ratio
R4	1	14.5	9.8	30 ± 5	0.5 ± 0.1
R5	15	27.5	8.9	34 ± 5	1.2 ± 0.2
R6	30	29.5	7.5	49 ± 5	1.0 ± 0.2

TABLE 19. Radium samples from Gareloch; 14.1.74

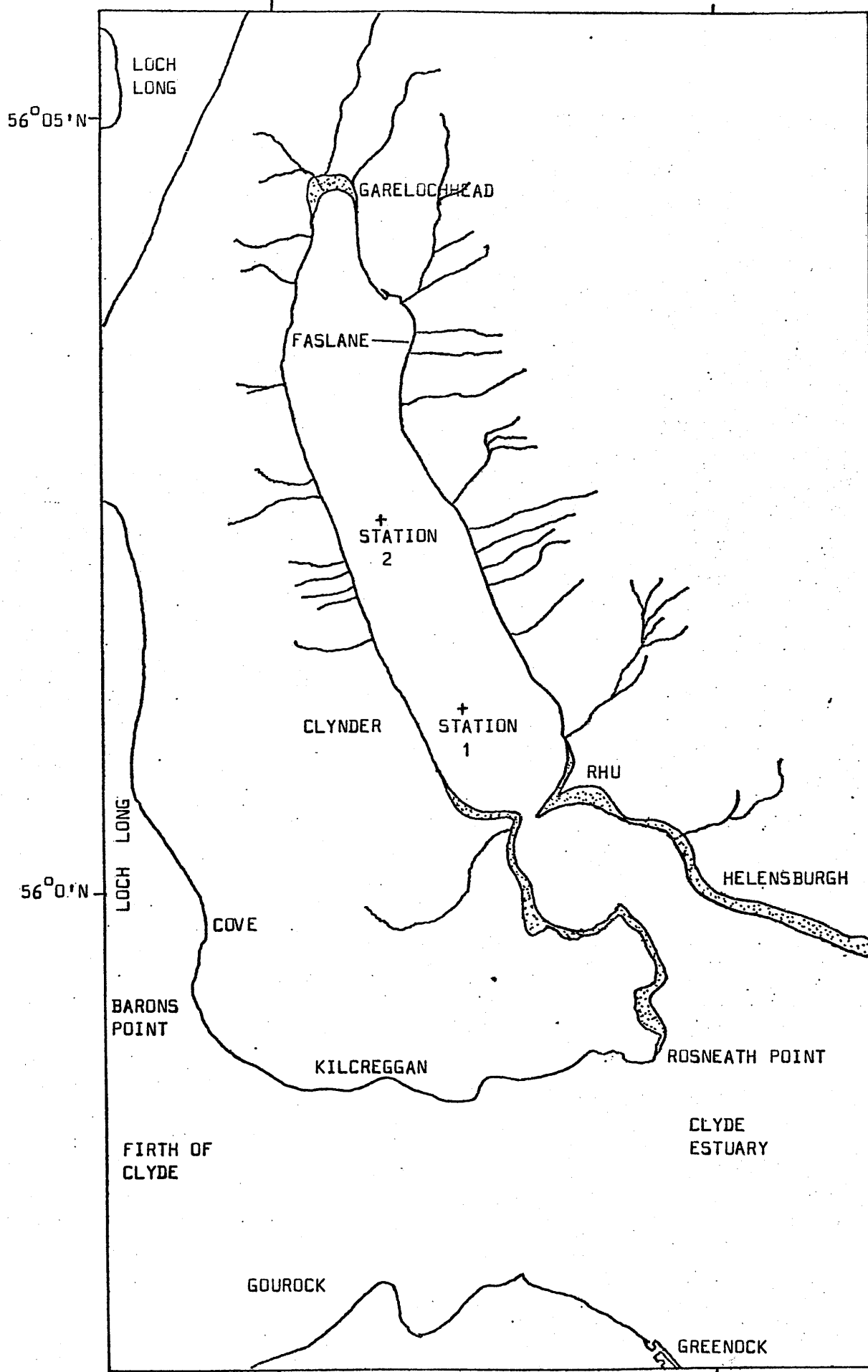


FIGURE 29. Gareloch sampling stations. (scale 1 : 63,360)

SAMPLES R7 - R9

Date : 21.1.74

General location : River Clyde (freshwater). (Figure 30)

Sample	Location	Depth (m)	[^{226}Ra] (dpm/1000 l)	$^{228}\text{Ra}/^{226}\text{Ra}$ activity ratio
R7	Glasgow Green	1	94 ± 9	0.5 ± 0.1
R8	Daldowie	1	115 ± 12	$0.5. \pm 0.1.$
R9	Hazelbank	1	85 ± 9	$1.3. \pm 0.2.$

TABLE 20. Radium samples from River Clyde; 21.1.74.

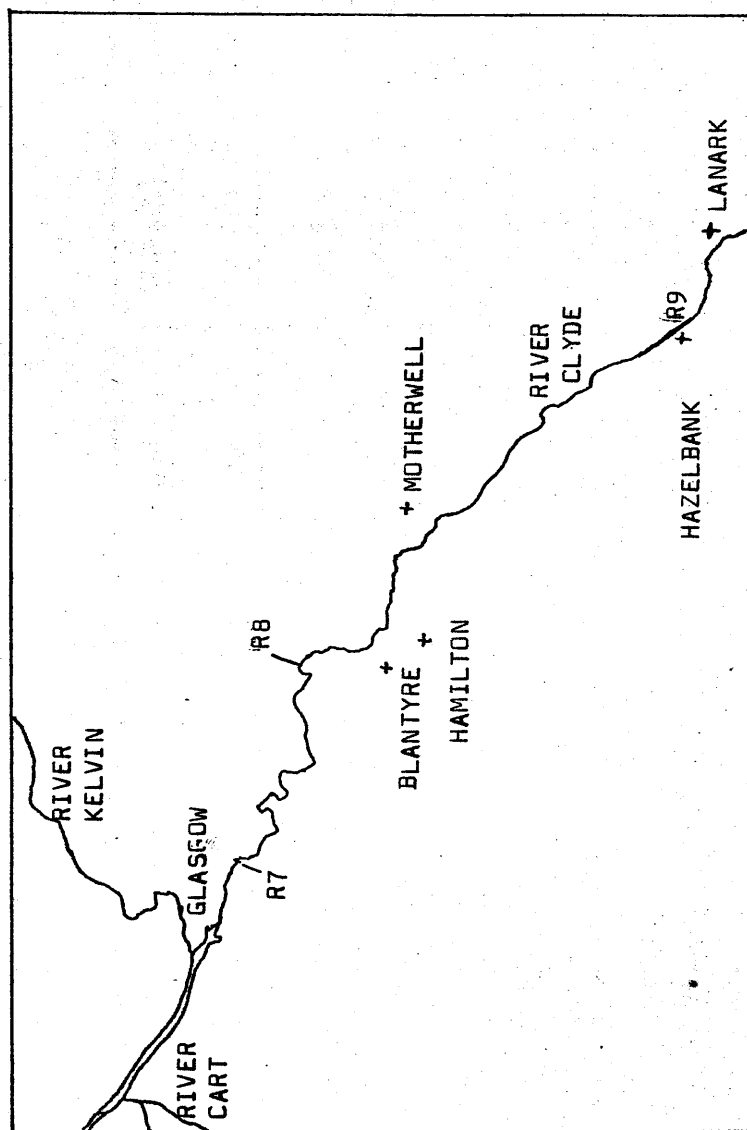


FIGURE 30. Sampling sites for freshwater river samples 21.1.74, R7 - R9.

SAMPLES R10 - R13

Date : 26.2.74.

General location : estuary/River Leven. (Figure 31)

Sample	Location	Depth (m)	S(%)	D.O. (mg l ⁻¹)	[²²⁶ Ra] (dpm/1000 l)	²²⁸ Ra/ ²²⁶ Ra activity ratio
R10	Dumbarton	4	12.9	5.8	30 ± 5	1.0 ± 0.1
R11	River Leven	1	0.01	10.2	41 ± 5	2.0 ± 0.3
R12	Bowling	5	14.4	5.8	114 ± 11	1.0 ± 0.1
R13	Clydebank	2	7.5	3.1	117 ± 12	1.0 ± 0.1

TABLE 21. Radium samples from Clyde estuary/River Leven; 26.2.74.

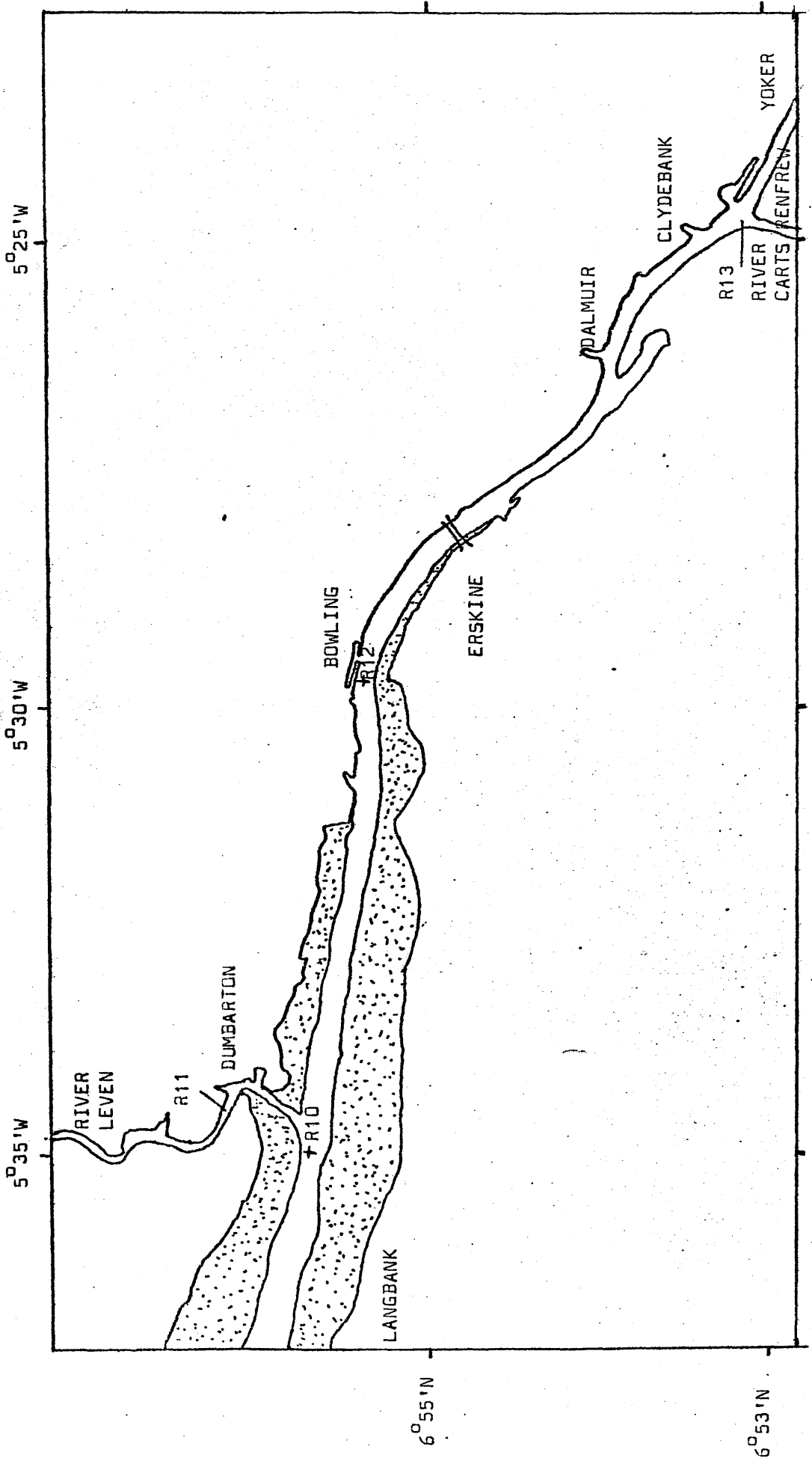


FIGURE 31. Location of sampling sites for samples R10 - R13; estuary 26.7.74. (Scale 1:63360)

SAMPLES R14 - R19

Date : 9.4.74

General location : estuary. (Figure 32)

Sample	Location	Depth (m)	S(‰)	T (°C)	D.O. (mg l ⁻¹)	[²²⁶ Ra] (dpm/1000 l)	²²⁶ Ra normalised to 35‰ salinity (dpm/1000 l)	²²⁸ Ra/ ²²⁶ Ra activity ratio
R14	Buoy D41	1	30.25	9.4	7.2	66 ± 7	76 ± 8	1.5 ± 0.2
R15	Buoy D41	8	31.75	8.9	7.4	71 ± 7	78 ± 8	1.8 ± 0.2
R16	Kilcreggan	25	32.30	7.2	7.4	57 ± 6	62 ± 6	1.1 ± 0.1
R17	Kilcreggan	3	31.30	8.2	8.8	79 ± 8	88 ± 9	1.9 ± 0.2
R18	Buoy D41	8	32.00	7.4	8.8	90 ± 9	98 ± 10	1.4 ± 0.2
R19	Buoy D41	1	30.50	9.2	9.0	90 ± 9	103 ± 10	1.7 ± 0.2

TABLE 22. Radium samples from Clyde estuary; 9.4.74.

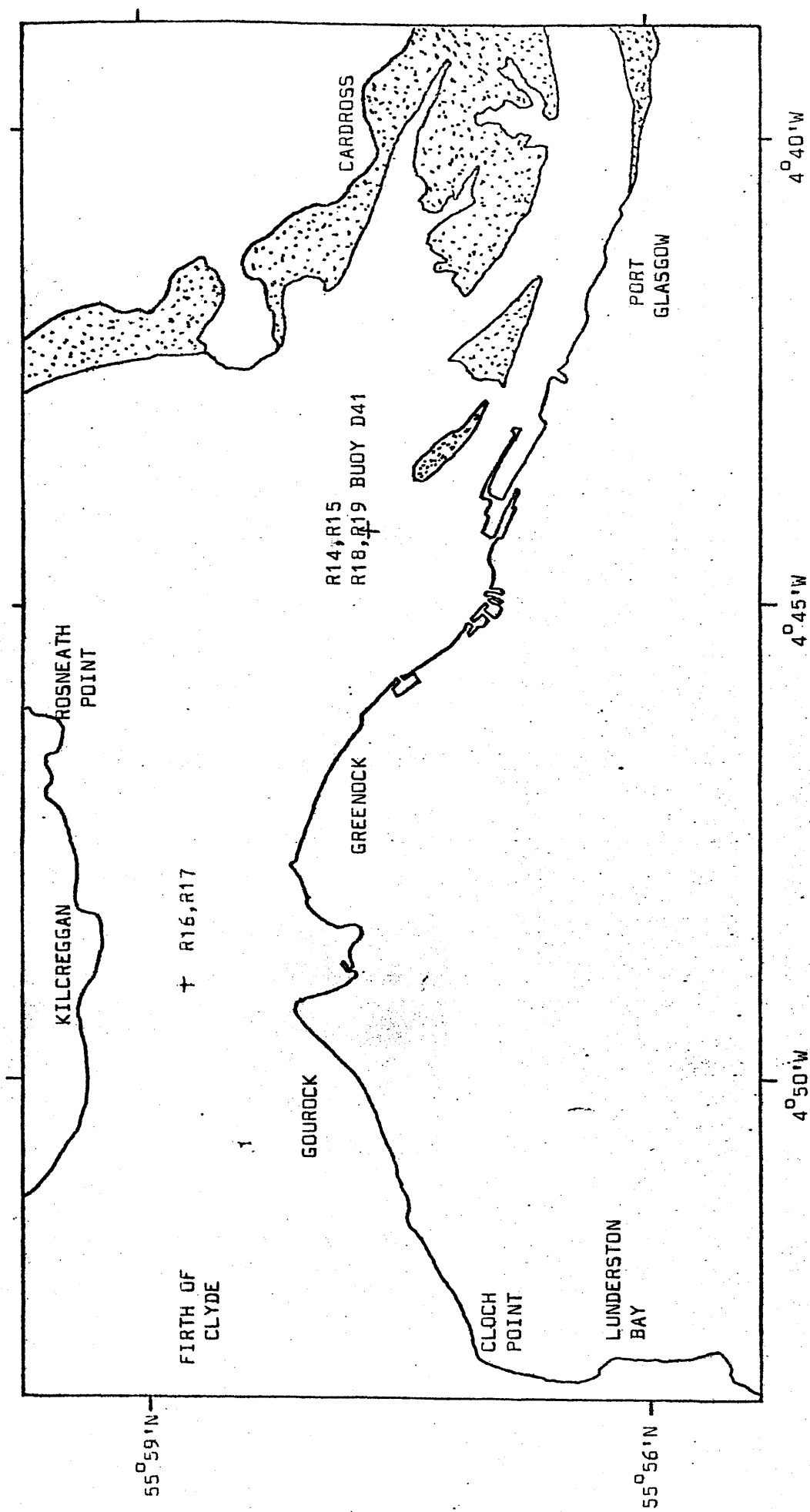


FIGURE 32. Location of sampling sites for samples R14 - R19; Clyde estuary 9.4.74 (scale 1:63360)

SAMPLES R20 - R25

Date : 8.5.74

Location : Loch Goil; Station 1 ($4^{\circ}53'W$, $56^{\circ}8'N$) (Figure 33)Hydrographic data:

Depth (m)	S(‰)	T(°C)	D.O. (mg l ⁻¹)
0	31.50	10.0	10.1
10	31.50	9.7	9.5
20	31.70	9.1	6.6
30	31.70	8.5	7.1
40	31.80	8.6	7.2
50	32.02	8.0	7.4
60	32.02	8.0	7.2
70	32.05	7.8	7.1

Radium data:

Sample	Depth (m)	[²²⁶ Ra] dpm/1000 l)	[²²⁶ Ra] normalised to 35‰ salinity (dpm/1000 l)	²²⁸ Ra/ ²²⁶ Ra activity ratio
R20	5	133 ± 13	148 ± 15	1.3 ± 0.2
R21	20	116 ± 12	128 ± 13	1.5 ± 0.2
R22	40	99 ± 10	109 ± 11	1.6 ± 0.2
R23	50	91 ± 9	100 ± 10	1.7 ± 0.2
R24	60	100 ± 10	110 ± 11	1.5 ± 0.2
R25	70	90 ± 9	98 ± 10	1.3 ± 0.2

TABLE 23. Radium samples from Loch Goil; 8.5.74.

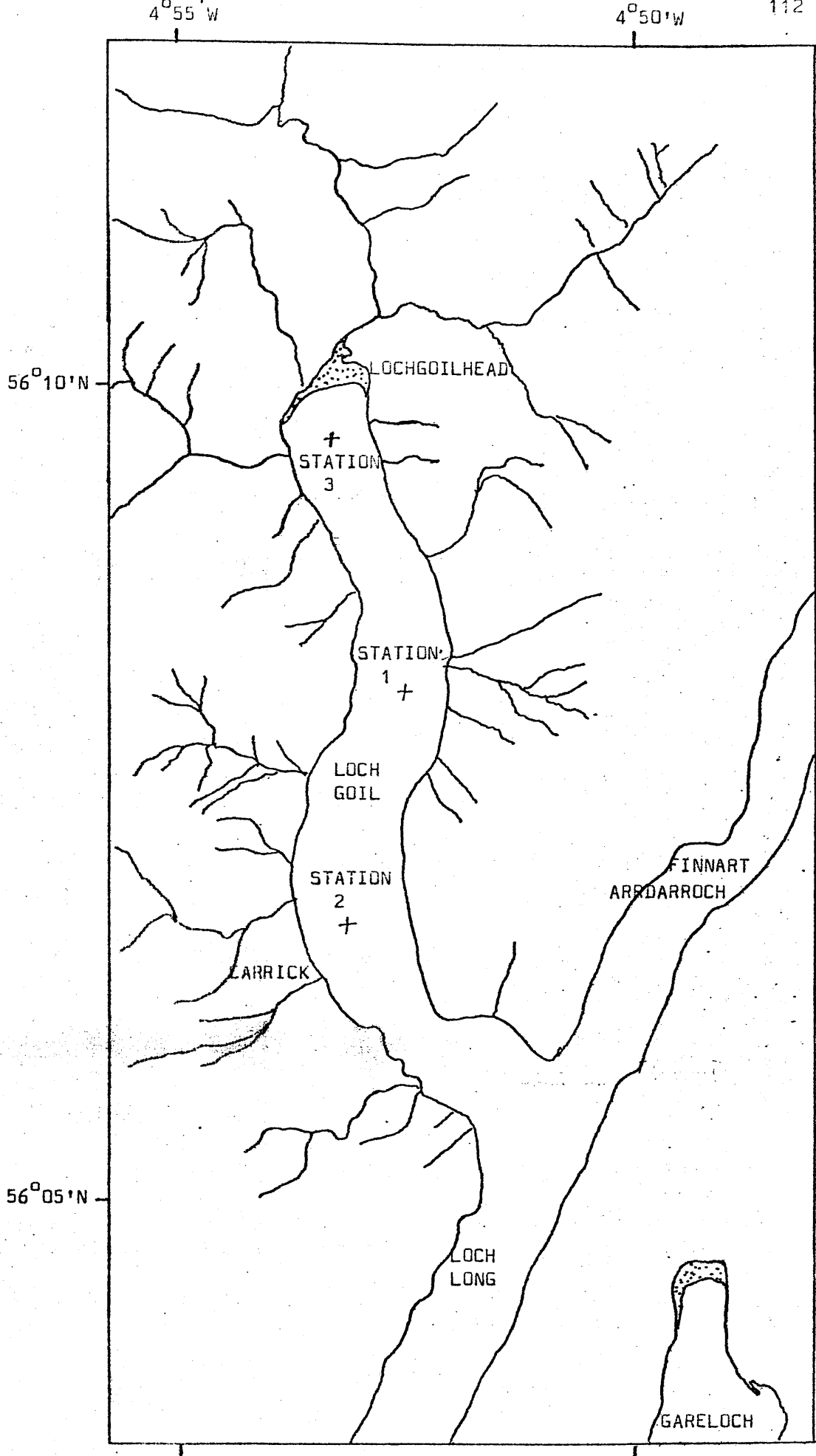


FIGURE 33. Loch Goil sampling stations (scale 1: 63,360)

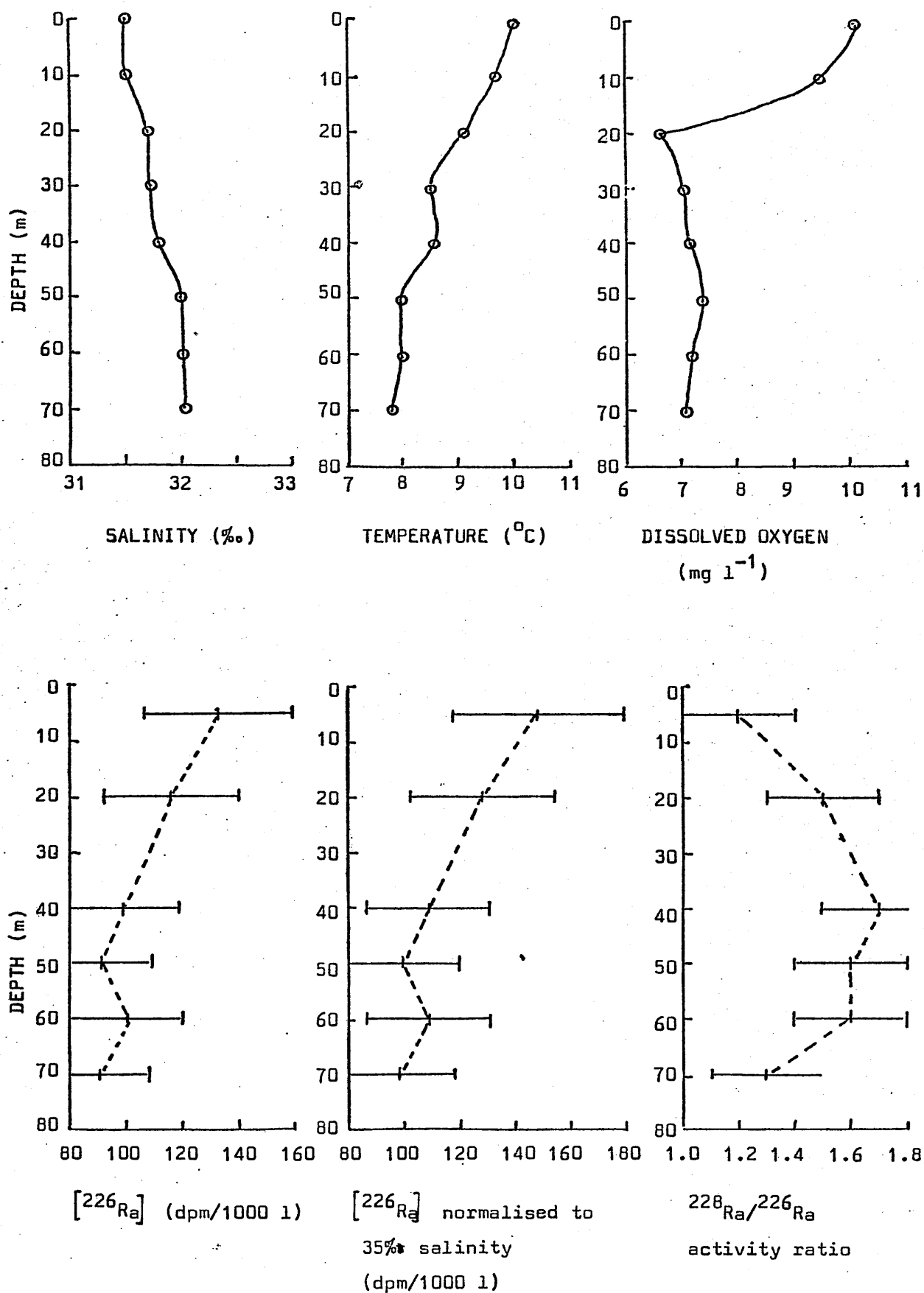


FIGURE 34. Hydrographic and radium profiles for Loch Goil ;
station 1 ; 8.5.74.

SAMPLES R26 - R28

Date : 11.6.74

Location : Skelmorlie Bank ($4^{\circ} 56.2'W$, $55^{\circ}52.3'N$) (Figure 35)Hydrographic data:

Depth (m)	S(‰)	T($^{\circ}C$)	p.H.
0	31.1	10.2	8.2
7	31.6	10.2	8.0
17	31.8	9.7	8.0
24	32.0	9.4	8.0

Radium data:

Sample	Depth (m)	$[^{226}Ra]$ (dpm/1000 l)	$[^{226}Ra]$ normalised to 35‰ salinity (dpm/1000 l)	$^{228}Ra/^{226}Ra$ activity ratio
R26	1	112 ± 11	126 ± 13	1.5
R27	12	80 ± 8	89 ± 9	1.4
R28	24	104 ± 10	114 ± 11	1.6

TABLE 24. Radium samples from firth (Skelmorlie); 11.6.74

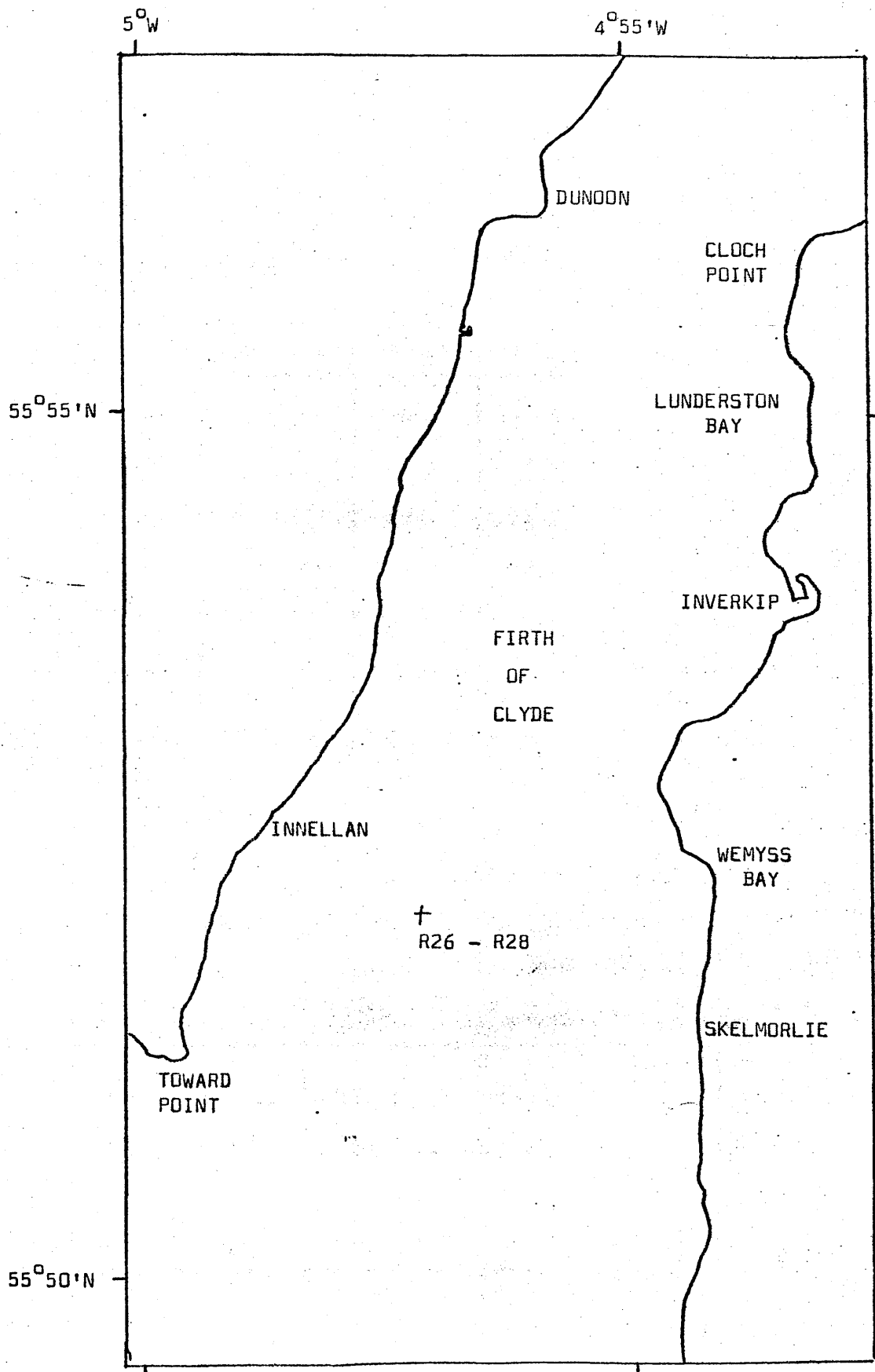


FIGURE 35. Location of sampling site for samples R26 - R28;
Firth of Clyde 11.6.74 (scale 1:63360).

SAMPLES R29 - R32

Date : 20.6.74

Location : Gareloch, station 1 (Figure 29)

Hydrographic data:

Depth (m)	S(‰)	T(°C)	pH
0	30.0	13.6	8.2
5	30.5	14.8	8.0
12	30.5	13.5	8.0
19	31.0	12.8	8.0
26	31.2	12.2	8.0
33	31.3	12.2	8.0

Radium data:

Sample	Depth (m)	$[^{226}\text{Ra}]$ (dpm/1000 l)	$[^{226}\text{Ra}]$ normalised to 35‰ salinity (dpm/1000 l)	$^{228}\text{Ra}/^{226}\text{Ra}$ activity ratio
R29	Surface	111 ± 11	130 ± 13	1.3 ± 0.2
R30	10	125 ± 13	143 ± 14	1.5 ± 0.2
R31	20	135 ± 13	152 ± 15	1.8 ± 0.2
R32	26	105 ± 11	117 ± 12	1.4 ± 0.2

TABLE 25. Radium samples from Gareloch ; 20.6.74.

SAMPLES R33 - R38 : C1

Date : 18.7.74.

Location : Loch Goil, station 1 (Figure 33)

Hydrographic data;

Depth (m)	S(‰)	T(°C)	D.O. (mg l ⁻¹)	pH
0	29.8	14.1	9.2	8.2
10	31.2	13.1	6.8	8.0
20	31.2	12.5	6.4	8.0
30	31.1	11.5	5.2	7.8
40	31.3	10.6	3.9	7.8
50	31.4	10.1	3.9	7.7

Radium data:

Sample	Depth (m)	[²²⁶ Ra] (dpm/1000 l)	[²²⁶ Ra] normalised to 35‰ salinity (dpm/1000 l)	²²⁸ Ra/ ²²⁶ Ra activity ratio
R33	Surface	153 ± 15	180 ± 18	2.0 ± 0.3
R34	10	143 ± 14	160 ± 16	1.9 ± 0.2
R35	20	145 ± 15	163 ± 16	1.5 ± 0.2
R36	30	115 ± 12	129 ± 13	1.3 ± 0.2
R37	40	145 ± 15	162 ± 16	1.7 ± 0.2
R38	65	116 ± 12	129 ± 13	1.3 ± 0.2

Caesium data:

Sample	Depth (m)	[¹³⁷ Cs] (dpm l ⁻¹)	[¹³⁷ Cs] normalised to salinity 35‰ (dpm l ⁻¹)	¹³⁴ Cs/ ¹³⁷ Cs activity ratio
C1	20	42.0 ± 1.1	47.1 ± 1.3	0.12 ± 0.01

TABLE 26. Radium and caesium samples from Loch Goil ; 18.7.74.

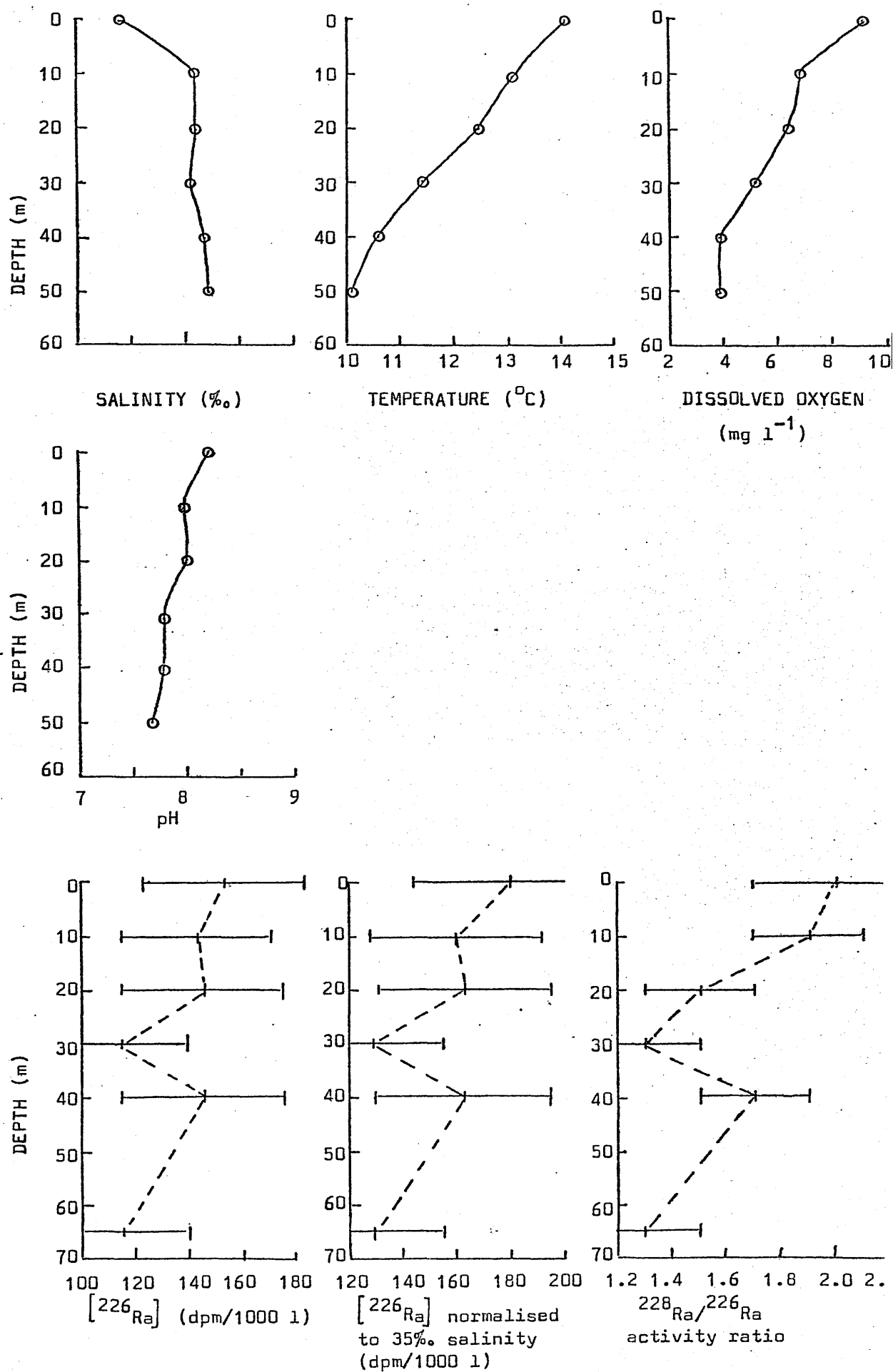


FIGURE 36. Hydrographic and radium profiles for Loch Gail; station 1; 18.7.74.

SAMPLES C2 - C15

Date : 30.7.74.

General location : firth (Troon - Brodick - Greenock) (Figure 37)

Sample	Depth (m)	S (‰)	$[^{137}\text{Cs}]$ (dpm l ⁻¹)	$[^{137}\text{Cs}]$ normalised to 35‰ salinity (dpm l ⁻¹)	$^{134}\text{Cs}/^{137}\text{Cs}$ activity ratio
C2	3	32.70	40.8 ± 1.1	43.7 ± 1.2	0.13 ± 0.01
C3	3	32.66	44.1 ± 1.2	47.3 ± 1.3	0.13 ± 0.01
C4	3	32.80	43.0 ± 1.2	45.9 ± 1.2	0.13 ± 0.01
C5	3	32.86	42.2 ± 1.1	44.9 ± 1.2	0.11 ± 0.01
C6	30	33.01	43.9 ± 1.2	46.5 ± 1.3	0.12 ± 0.01
C7	3	32.86	41.2 ± 1.1	43.9 ± 1.2	0.13 ± 0.01
C8	3	32.85	43.8 ± 1.2	46.7 ± 1.3	0.13 ± 0.01
C9	3	32.92	45.9 ± 1.2	48.8 ± 1.3	0.12 ± 0.01
C10	3	32.59	41.7 ± 1.1	44.8 ± 1.2	0.13 ± 0.01
C11	3	32.36	42.5 ± 1.1	46.0 ± 1.2	0.09 ± 0.01
C12	3	32.07	38.6 ± 1.0	42.1 ± 1.1	0.12 ± 0.01
C13	3	32.21	40.7 ± 1.1	44.2 ± 1.2	0.12 ± 0.01
C14	3	31.40	40.3 ± 1.1	44.9 ± 1.2	0.12 ± 0.01
C15	3	31.10	38.7 ± 1.0	43.6 ± 1.2	0.12 ± 0.01

TABLE 27. Caesium samples from firth; 30.7.74.

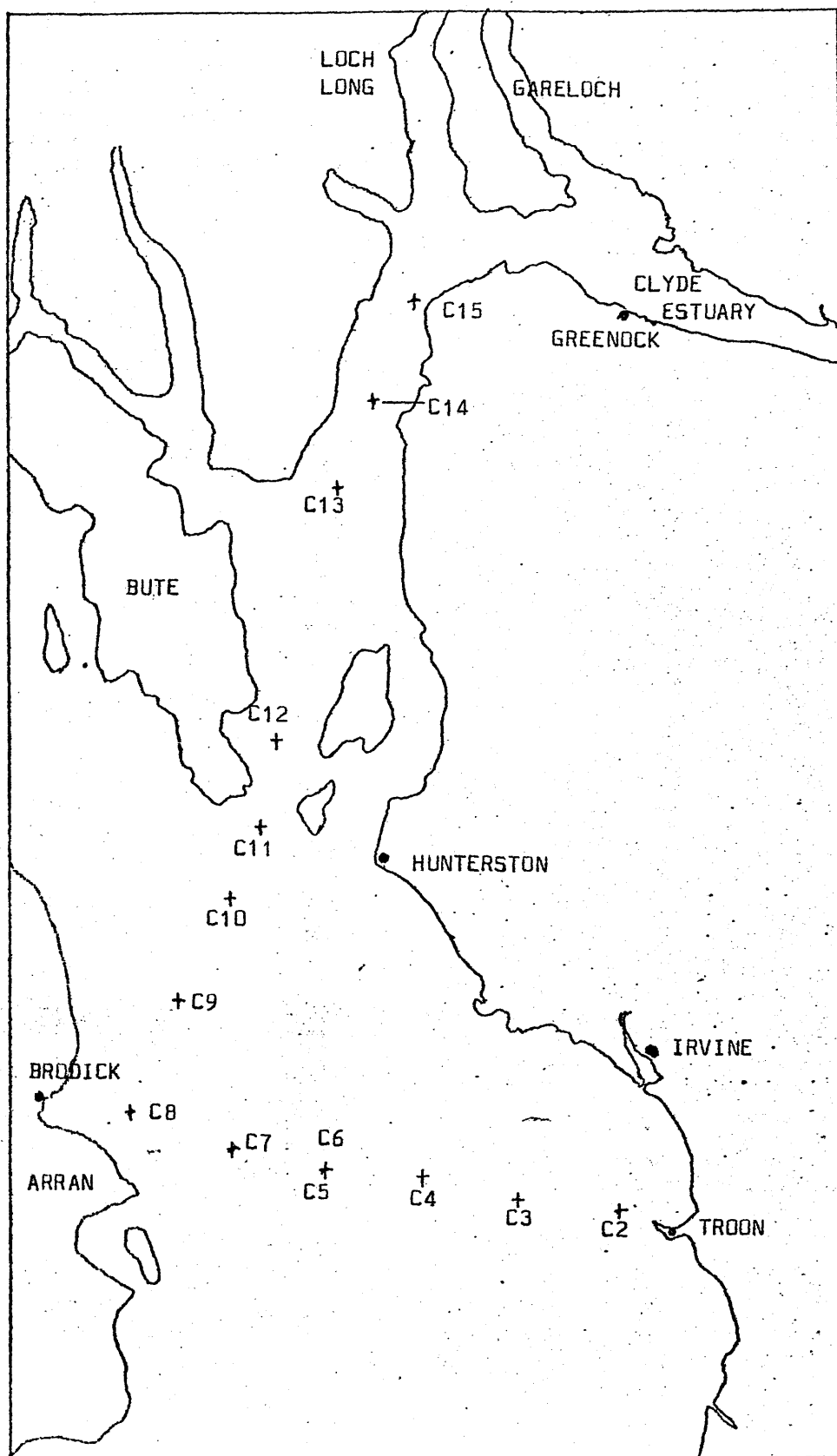


FIGURE 37. Location of sampling sites for samples C2-C15 ;
Firth of Clyde ; 30.7.74.

SAMPLES R39 - R43; C16 - C19

Date : 10.9.74.

Location : Loch Goil, Station 1. (Figure 33)

Hydrographic data:

Depth (m)	S (‰)	T (°C)	D.O. (mg l ⁻¹)
0	24.02	12.5	10.8
3	30.26	13.5	8.1
10	31.58	12.9	5.9
25	32.44	11.7	4.1
50	32.67	9.5	1.8
65	32.70	9.2	1.2
80	32.71	8.9	0.6

Radium data:

Sample	Depth (m)	[²²⁶ Ra] (dpm/1000 l)	[²²⁶ Ra] normalised to 35‰ salinity (dpm/1000 l)	²²⁸ Ra/ ²²⁶ Ra activity ratio
R39	5	113 ± 11	131 ± 13	1.9 ± 0.2
R40	20	121 ± 12	132 ± 13	1.6 ± 0.2
R41	40	103 ± 10	111 ± 11	1.5 ± 0.2
R42	60	103 ± 10	110 ± 11	2.0 ± 0.3
R43	74	101 ± 10	108 ± 11	1.3 ± 0.2

Caesium data:

Sample	Depth (m)	[¹³⁷ Cs] (dpm l ⁻¹)	[¹³⁷ Cs] normalised to 35‰ salinity (dpm l ⁻¹)	¹³⁴ Cs/ ¹³⁷ Cs activity ratio
C16	5	35.8 ± 1.0	41.4 ± 1.1	0.10 ± 0.01
C17	20	43.0 ± 1.2	47.0 ± 1.3	0.10 ± 0.01
C18	40	41.5 ± 1.2	44.6 ± 1.2	0.10 ± 0.01
C19	60	38.7 ± 1.0	41.4 ± 1.1	0.08 ± 0.01

TABLE 28. Radium and Caesium samples from Loch Goil; 10.9.74.

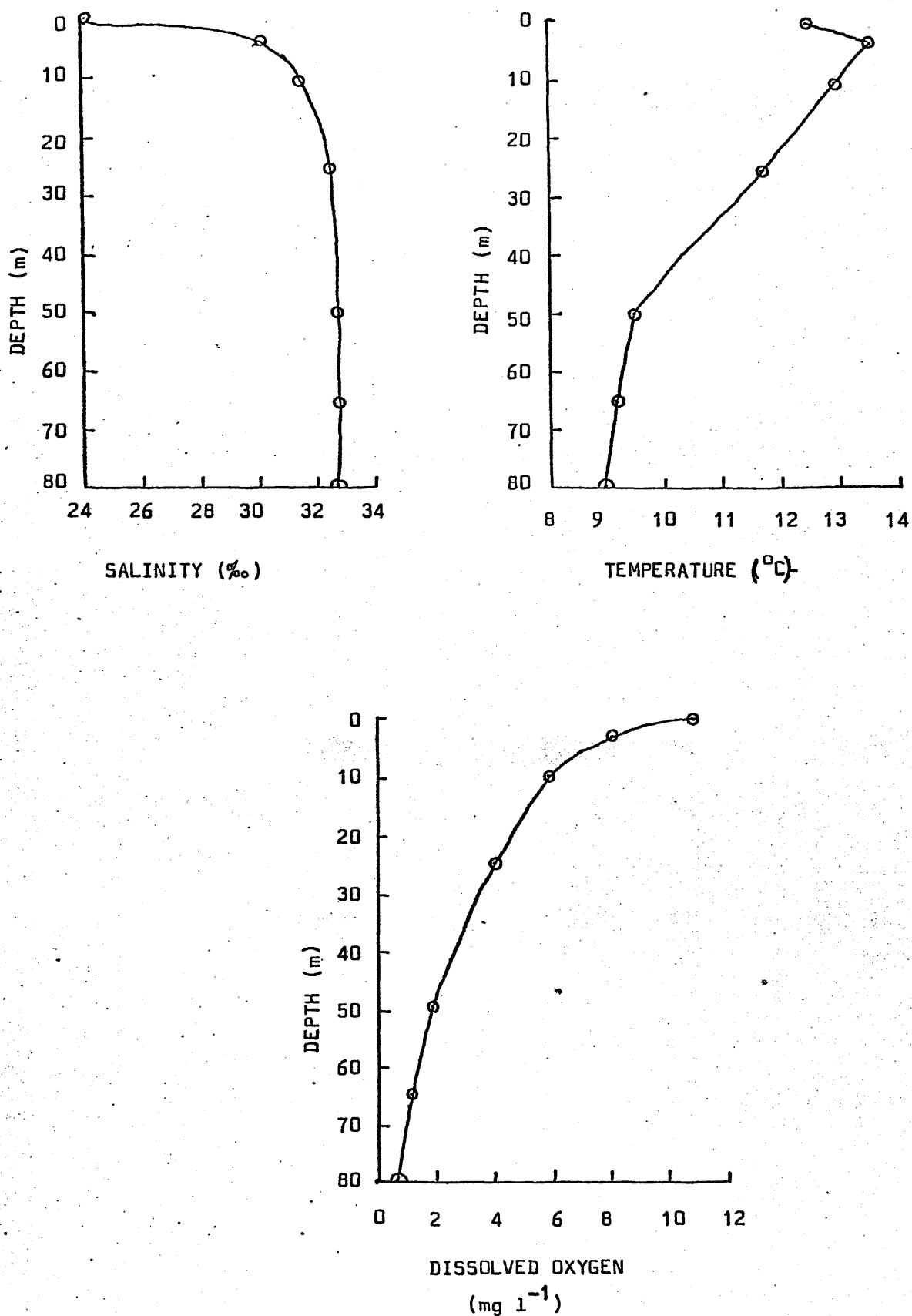


FIGURE 38 (a). Hydrographic profiles for Loch Goil ; station 1 ;
10.9.74.

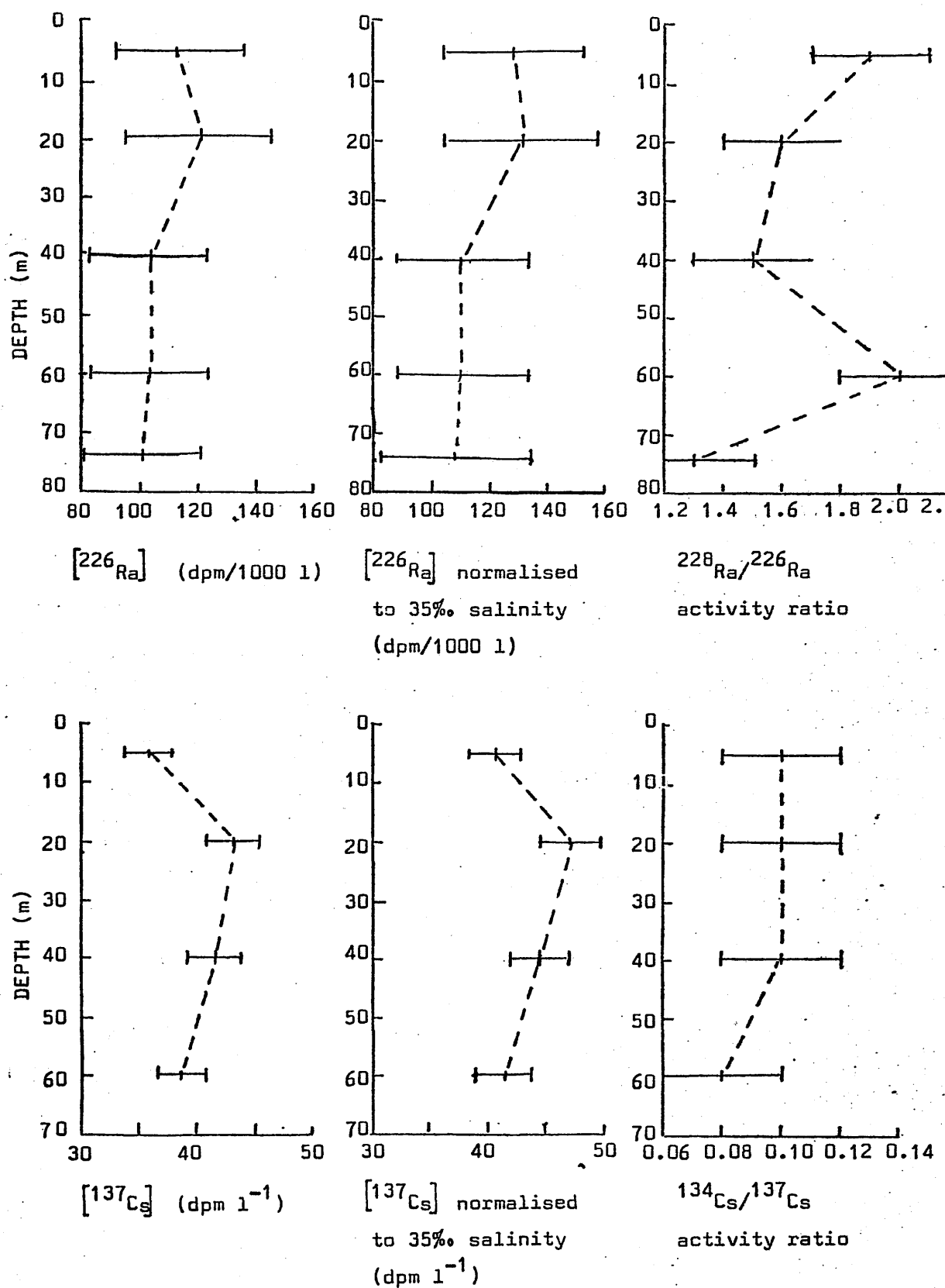


FIGURE 38 (b). Radium and caesium profiles for Loch Gail;
station 1 ; 10.9.74.

SAMPLES R44 - R48

Date : 25.10.74.

Location : Loch Goil, Station 1. (Figure 33)

Hydrographic data:

Depth (m)	S(‰)	T(°C)	D.O. (mg l ⁻¹)	pH
0	32.74	11.4	5.9	7.8
3	32.76	11.6	5.6	7.9
10	32.74	11.4	5.7	7.9
25	32.78	11.4	5.1	7.9
50	32.58	10.6	2.1	7.8
65	32.46	9.8	0.9	7.7
80	32.34	9.6	0.4	7.6

Radium data:

Sample	Depth (m)	[²²⁶ Ra] (dpm/1000 l)	[²²⁶ Ra] normalised to 35‰ salinity (dpm/1000 l)	²²⁸ Ra/ ²²⁶ Ra activity ratio
R44	5	197 ± 20	210 ± 21	1.9
R45	20	123 ± 12	130 ± 13	1.7
R46	40	163 ± 16	175 ± 18	1.1
R47	60	139 ± 14	150 ± 15	1.0
R48	75	180 ± 18	195 ± 20	1.1

TABLE 29. Radium samples from Loch Goil; 25.10.74

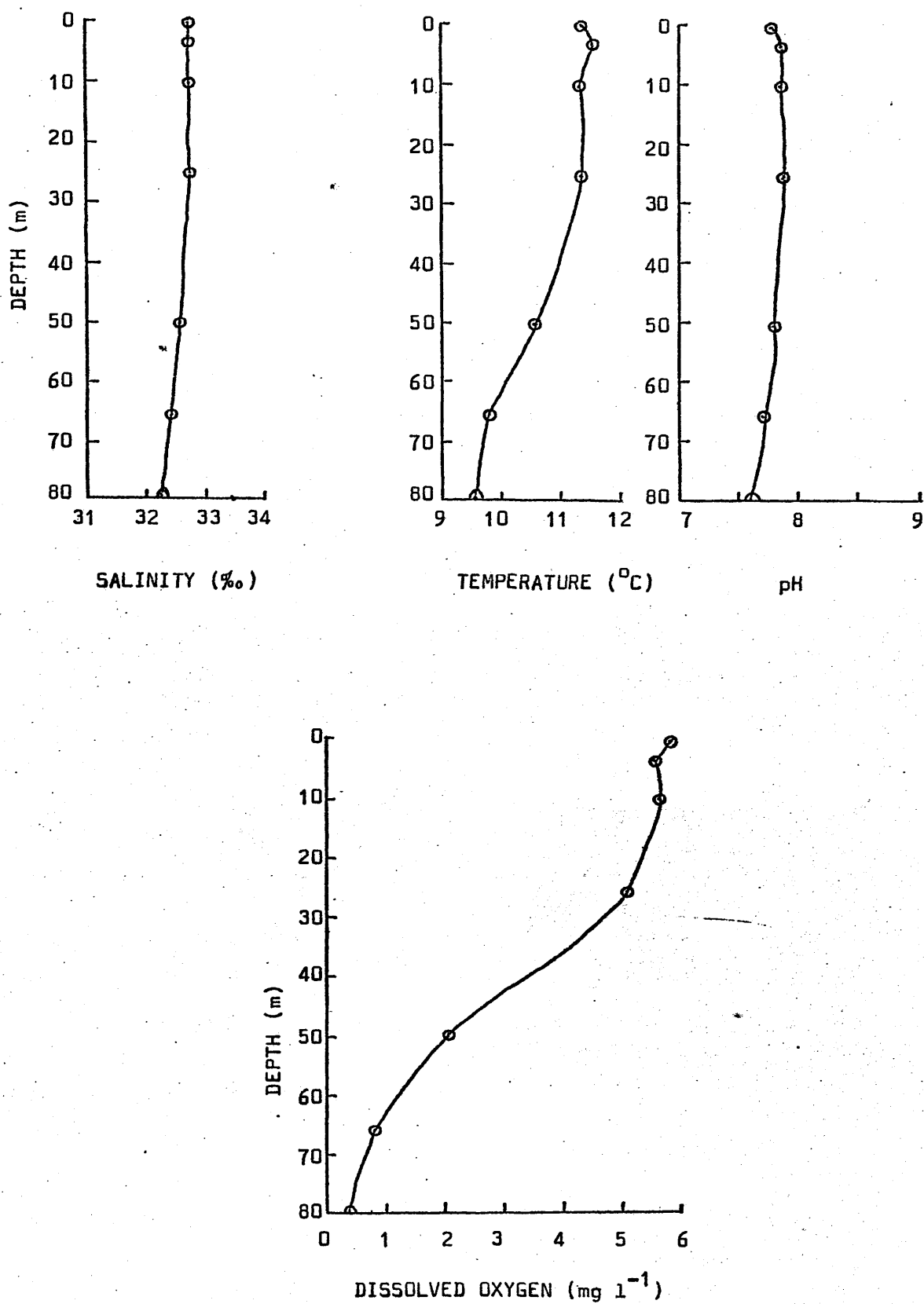
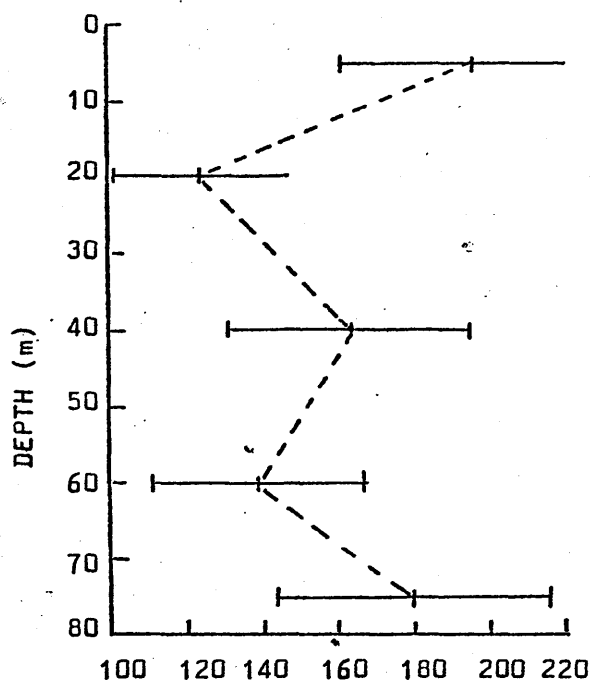
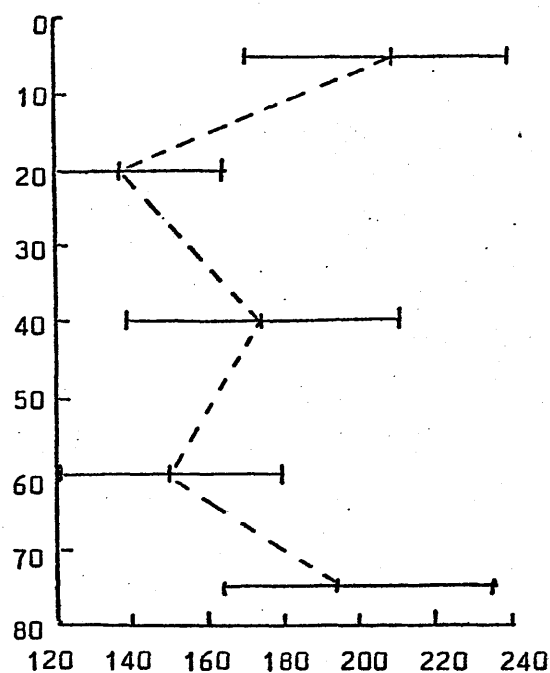


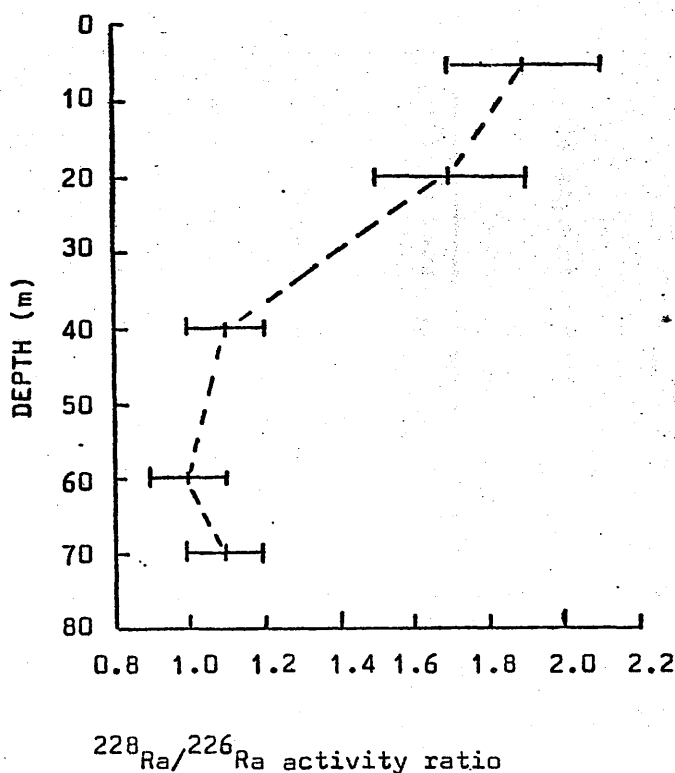
FIGURE 39.(a) Hydrographic profiles for Loch Goil ; station 1 ;
25.10.74.



$[^{226}\text{Ra}]$ (dpm/1000 l)



$[^{226}\text{Ra}]$ normalised to 35‰ salinity (dpm/1000 l)



$^{228}\text{Ra}/^{226}\text{Ra}$ activity ratio

FIGURE 39 (b). Radium profiles for Loch Goil ; station 1 ;
25.10.74.

SAMPLES C20 - C22

Date : 25.2.75.

Location : Firth (Surface water samples collected from the shore) (Figure 40)

Sample	Location	$[^{137}\text{Cs}]$ (dpm l ⁻¹)	$^{134}\text{Cs}/^{137}\text{Cs}$ activity ratio
C20	Gourock	57.2 ± 1.5	0.161 ± 0.009
C21	Hunterston South	62.8 ± 1.7	0.167 ± 0.008
C22	Hunterston North	55.5 ± 1.5	0.155 ± 0.009

TABLE 30. Caesium samples from firth ; 25.2.75.

SAMPLES C23 - C26

Date : 4.3.75.

Location : Estuary/Gareloch/Loch Long (surface water samples collected from the shore) (Figure 40)

Sample	Location	$[^{137}\text{Cs}]$ (dpm l ⁻¹)	$^{134}\text{Cs}/^{137}\text{Cs}$ activity ratio
C23	Helensburgh	49.2 ± 1.3	0.157 ± 0.009
C24	Garelochhead	46.3 ± 1.3	0.161 ± 0.009
C25	Finnart	48.9 ± 1.3	0.17 ± 0.01
C26	Arrochar	44.4 ± 1.2	0.15 ± 0.01

TABLE 31. Caesium samples from Clyde estuary, Gareloch and Loch Long ; 4.3.75.

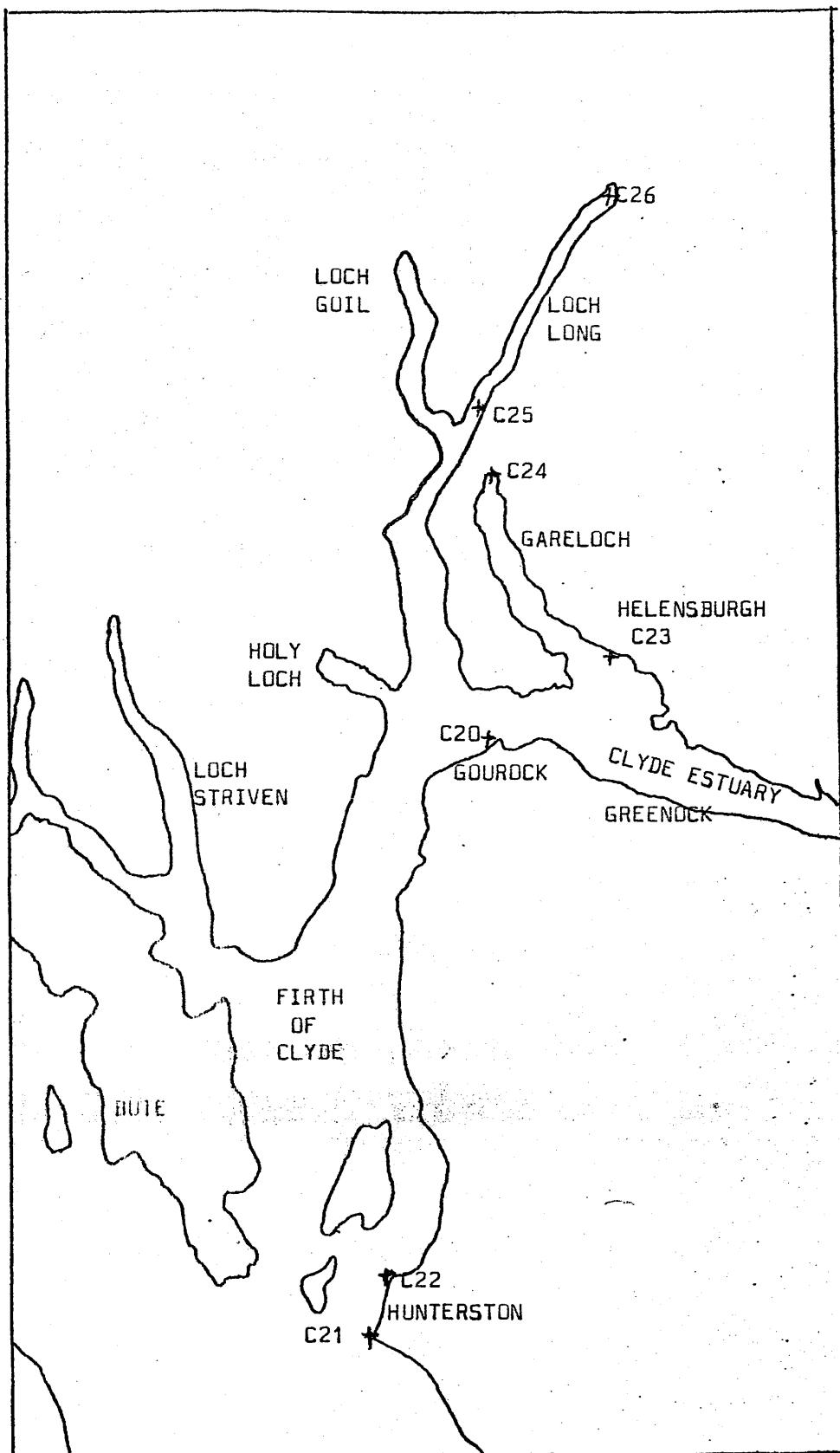


FIGURE 40. Location of sampling sites for samples C20 - C26

SAMPLES R49 - R55 ; C27 - C33.

Date : 8.4.75.

Location : Loch Goil, station 1 (Figure 33)

Hydrographic data:

Depth (m)	S (‰)	T (°C)	D.O. (mg l ⁻¹)
0	32.35.	6.8	8.9
13	32.41	6.6	8.9
28	32.53	6.6	8.8
38	32.44	6.5	8.1
53	32.55	6.5	8.5
68	32.61	6.5	8.1

Radium data:

Sample	Depth (m)	[²²⁶ Ra] (dpm/1000 l)	[²²⁶ Ra] normalised to 35‰ salinity
R49	Surface	119 ± 8	129 ± 9
R50	15	112 ± 8	121 ± 8
R51	30	97 ± 7	104 ± 7
R52	40	112 ± 8	121 ± 8
R53	50	104 ± 7	112 ± 8
R54	60	119 ± 8	128 ± 9
R55	75	107 ± 7	115 ± 8

Caesium data:

Sample	Depth (m)	[¹³⁷ Cs] (dpm l ⁻¹)	[¹³⁷ Cs] normalised to 35‰ salinity (dpm l ⁻¹)	¹³⁴ Cs/ ¹³⁷ Cs activity ratio
C27	Surface	73.9 ± 2.0	80.0 ± 2.2	0.187 ± 0.007
C28	15	76.2 ± 2.1	82.3 ± 2.2	0.182 ± 0.006
C29	30	83.4 ± 2.3	89.7 ± 2.4	0.168 ± 0.005
C30	40	76.0 ± 2.1	82.0 ± 2.2	0.177 ± 0.005
C31	50	77.6 ± 2.1	83.4 ± 2.3	0.167 ± 0.005
C32	60	81.2 ± 2.2	87.2 ± 2.4	0.175 ± 0.005
C33	75	86.9 ± 2.3	93.3 ± 2.5	0.172 ± 0.005

TABLE 32. Radium and caesium samples from Loch Goil ; 8.4.75.

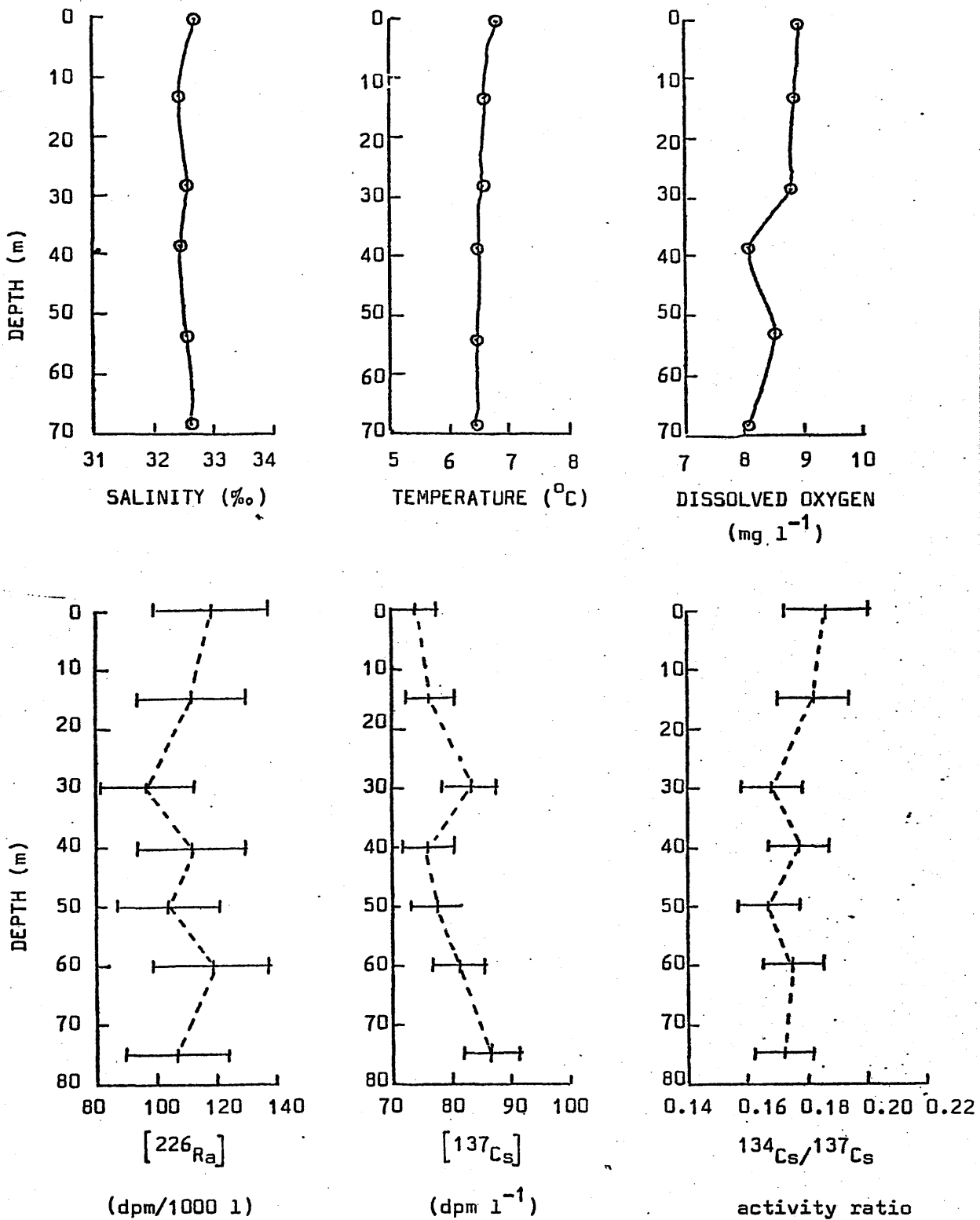


FIGURE 41. Hydrographic, radium and caesium profiles for
Loch Goil ; station 1 ; 8.4.75.

SAMPLES C34 - C38

Date : 8.4.75

Location : Loch Gail, Loch Long, firth (Figure 42)

Sample	Depth (m)	$[^{137}\text{Cs}]$ (dpm l ⁻¹)	$^{134}\text{Cs}/^{137}\text{Cs}$
C34	Surface	76.6 ± 2.1	0.176 ± 0.006
C35	Surface	81.5 ± 2.2	0.170 ± 0.005
C36	Surface	67.5 ± 1.8	0.168 ± 0.006
C37	Surface	104.5 ± 2.8	0.178 ± 0.005
C38	Surface	88.0 ± 2.4	0.182 ± 0.005

TABLE 33. Caesium samples from Loch Gail, Loch Long and firth ;

8.4.75.

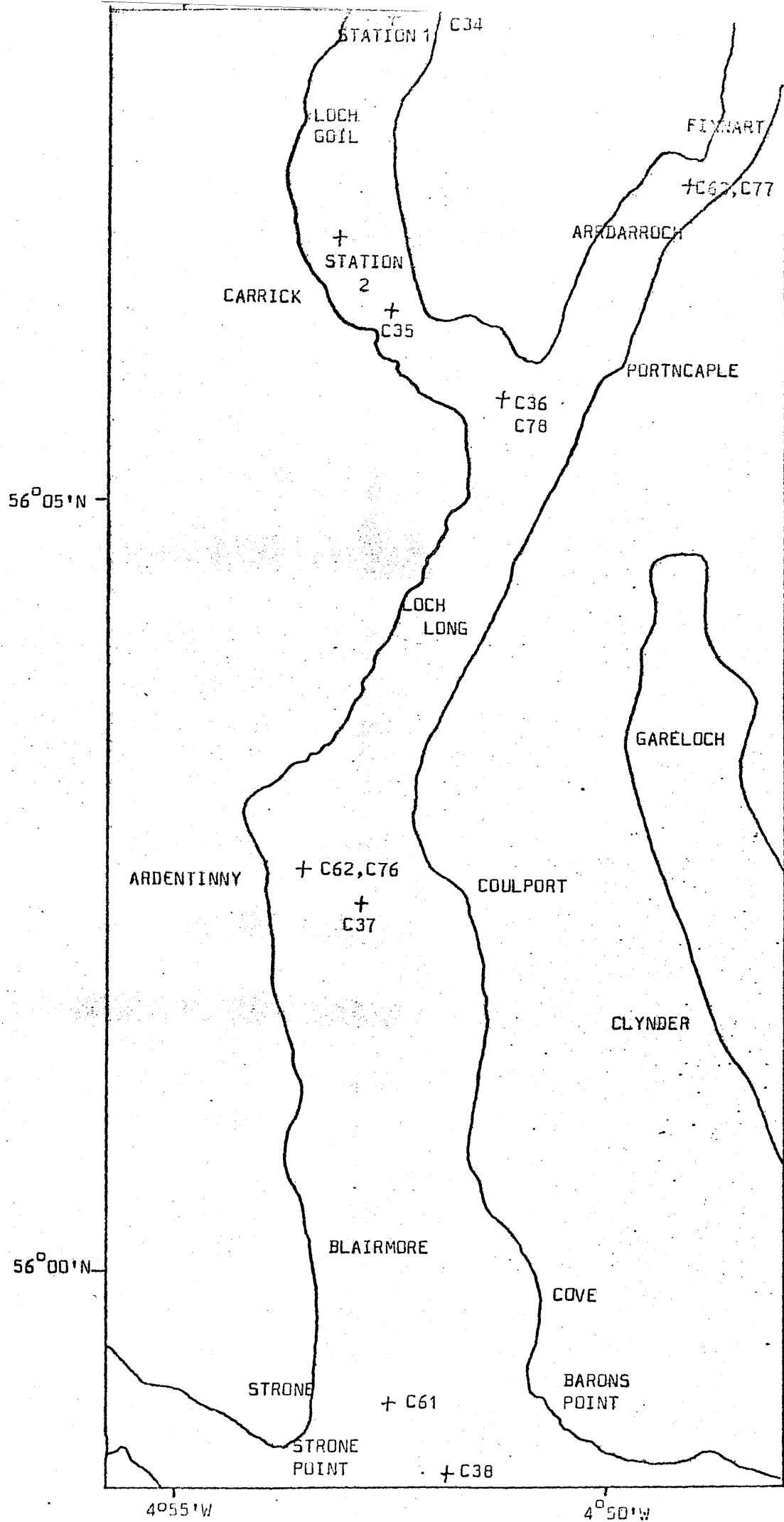


FIGURE 42. Sampling sites in Loch Gail and Loch Long (scale 1:63360)

SAMPLES R56 - R61, C39 - C44

Date : 1.5.75.

Location : estuary (Figure 43)

Sample	Depth (m)	S (‰)	T (°C)	D.O. (mg l ⁻¹)	pH	[²²⁶ Ra] (dpm/1000 l)	²²⁸ Ra/ ²²⁶ Ra activity ratio	[¹³⁷ Cs] (dpm l ⁻¹)	¹³⁴ Cs/ ¹³⁷ Cs activity ratio
R56/C39	2	1.8	12.0	6.1	7.4	65 ± 5	1.9 ± 0.2	2.8 ± 0.1	0.0
R57/C40	2	6.5	11.0	1.8	6.9	77 ± 5	1.3 ± 0.2	14.4 ± 0.3	0.19 ± 0.03
R58/C41	2	8.2	11.5	1.5	7.2	108 ± 8		21.4 ± 0.6	0.16 ± 0.02
R59/C42	2	14.6	11.0	4.5	7.2	119 ± 8	2.0 ± 0.3	45.8 ± 1.2	0.164 ± 0.009
R60/C43	2	21.7	10.0	7.6	7.6	100 ± 7		67.3 ± 1.8	0.175 ± 0.007
R61/C44	2	24.2	10.0	8.4	7.7	160 ± 11		66.8 ± 1.8	0.181 ± 0.007

TABLE 34. Radium and caesium samples from Clyde estuary. 1.5.75.

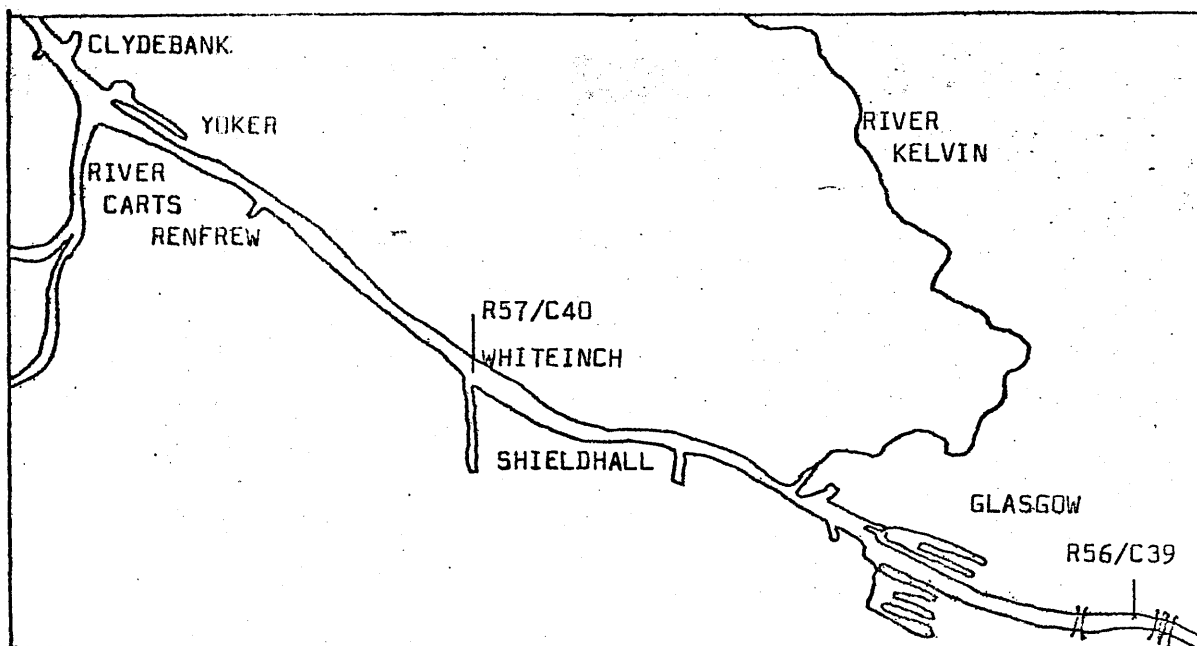
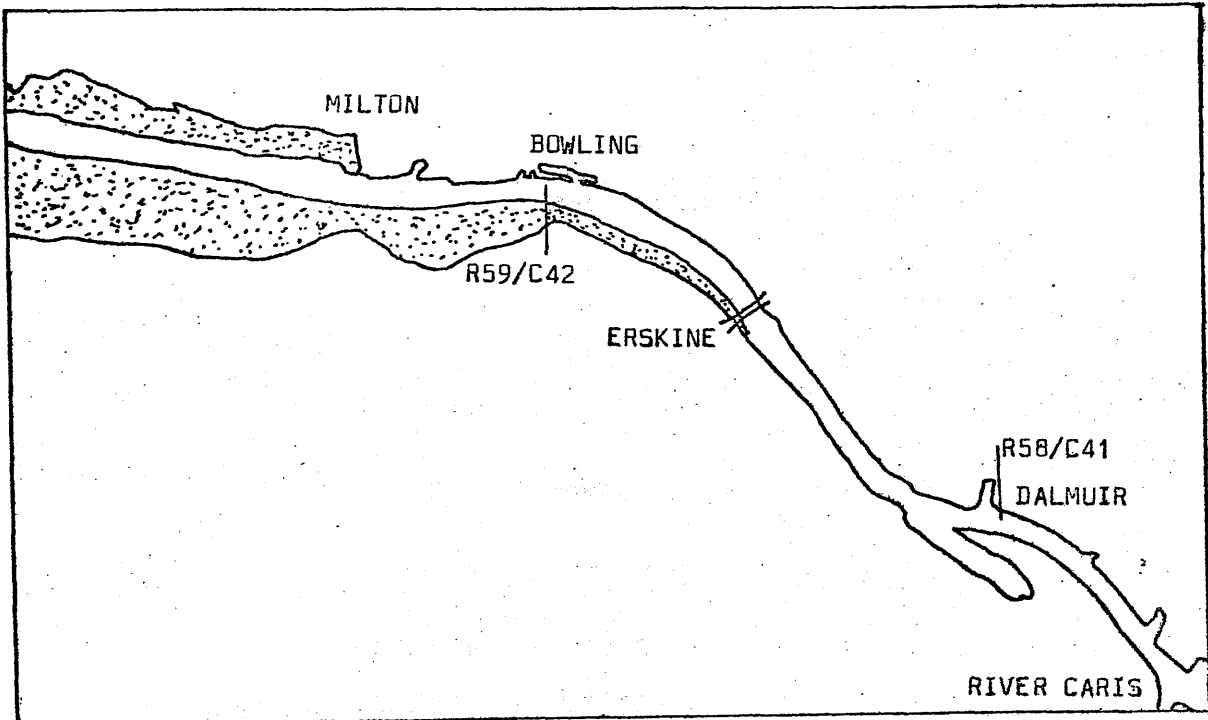
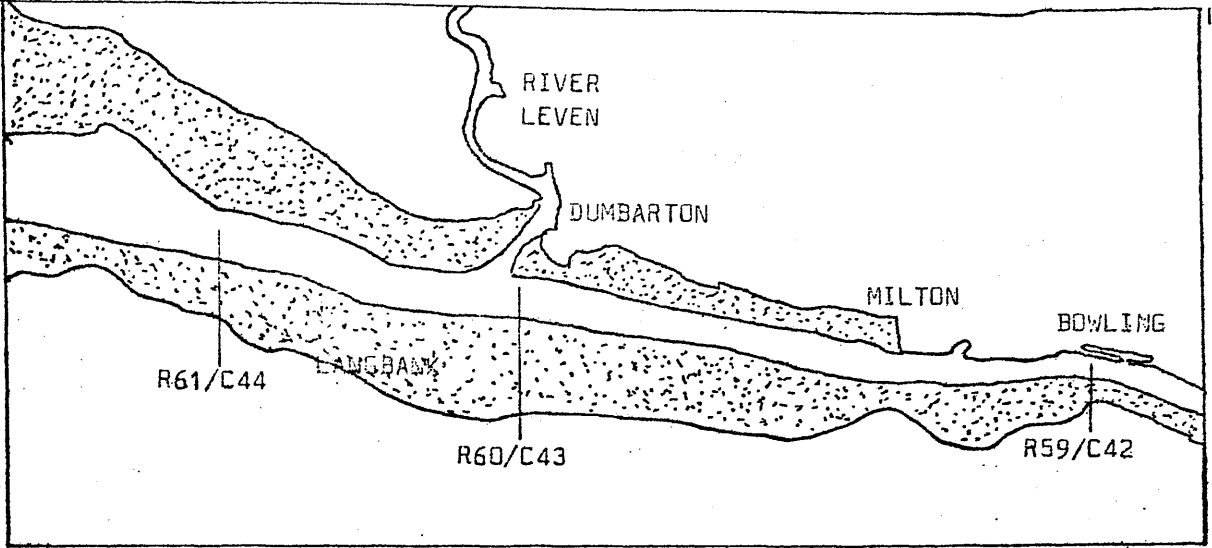


FIGURE 43. Location of samling sites for samples R56 - R61 / C39 - C44;
Clyde estuary 1.5.75 (scale 1:63360)

SAMPLES R62 - R66 ; C45 - C49

Date : 3.6.75.

Location : estuary (Figure 44)

Sample	Depth (m)	S (‰)	T (°C)	D.O. (mg l ⁻¹)	pH	[²²⁶ Ra] (dpm/1000 l)	[¹³⁷ Cs] (dpm l ⁻¹)	¹³⁴ Cs/ ¹³⁷ Cs activity ratio
R62/C45	2		10.6	9.3	7.4	180 ± 13	44.7 ± 1.2	0.19 ± 0.01
R63/C46	2	27.06	10.4	8.3	7.7	173 ± 12	68.6 ± 1.9	0.175 ± 0.007
R64/C47	Surface	30.79	9.4	9.0	7.9	186 ± 13	78.3 ± 2.1	0.180 ± 0.006
R65/C48	6	31.72	9.5	8.8	8.0	186 ± 13	77.6 ± 2.1	0.185 ± 0.007
R66/C49	9	32.88	8.5	8.7	8.3	196 ± 14	88.5 ± 2.4	0.183 ± 0.006

TABLE 35. Radium and caesium samples from Clyde estuary ; 3.6.75.

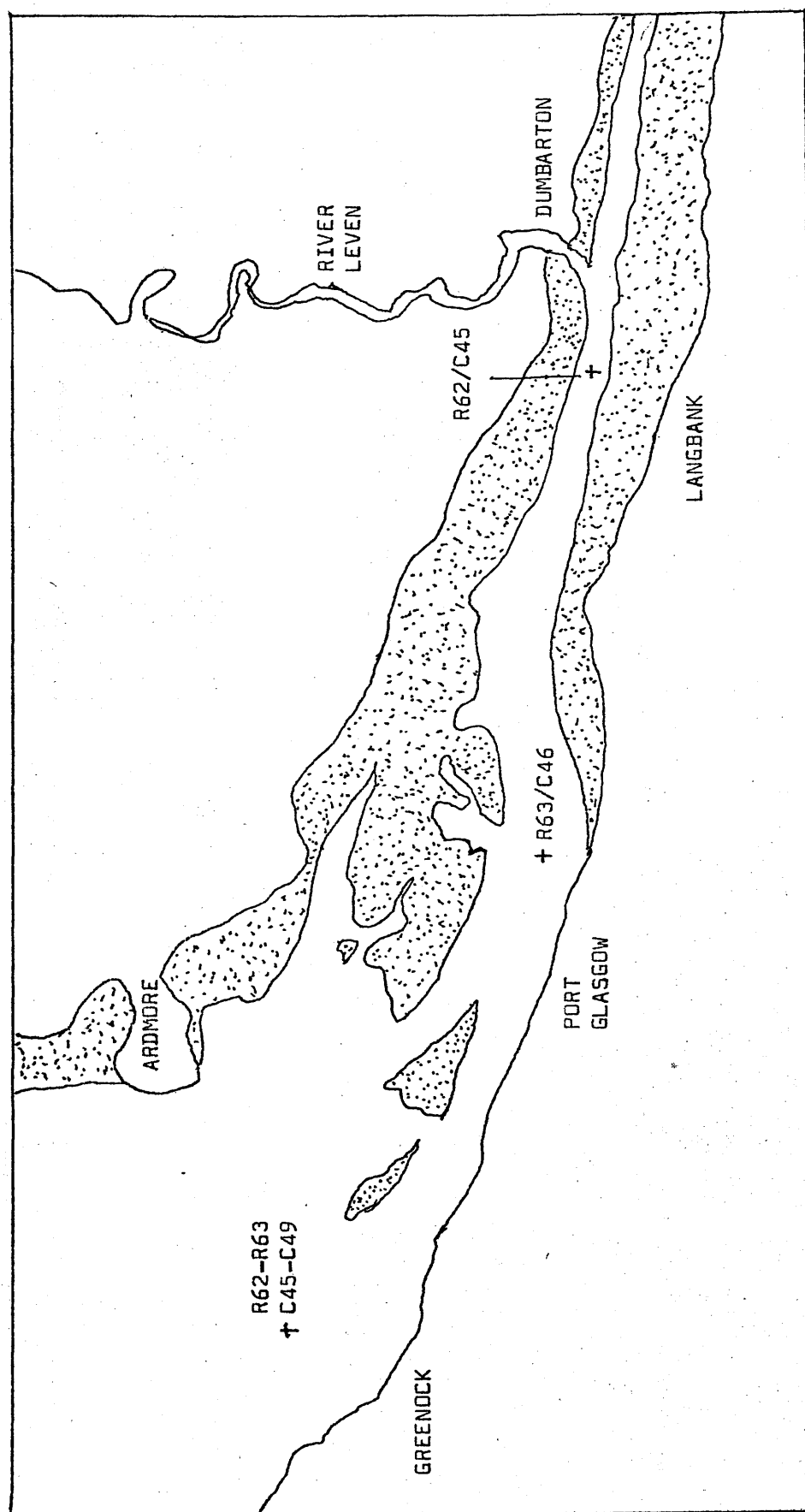


FIGURE 44. Location of sampling sites for samples R62-R66/C45-C49; Clyde estuary, 3.6.75 (scale 1:63360).

SAMPLES C50 - C51

Date : 6.11.75.

Location : Gareloch; station 2 ($5^{\circ}48.8'W$, $56^{\circ}2.3'N$). (Figure 29)Hydrographic data:

Depth (m)	S(‰)	T($^{\circ}C$)	D.O. (mg l^{-1})	p.H.
Surface	29.07	10.8	8.1	7.6
10	29.57	11.1	8.6	7.7
20	30.29	11.3	6.9	7.7
30	31.46	11.9	5.9	7.7
40	31.75	12.0	4.5	7.7

Caesium data:

Sample	Depth	$[^{137}Cs]$ dpm l^{-1}	$[^{137}Cs]$ normalised to 35‰ salinity dpm l^{-1}	$^{134}Cs/^{137}Cs$ activity ratio
C50	20	86.2 ± 2.3	99.6 ± 2.7	0.157 ± 0.004
C51	30	84.3 ± 2.3	93.8 ± 2.5	0.159 ± 0.004

TABLE 36. Caesium samples from Gareloch 6.11.75.

SAMPLES C52 - C60

Date : 14.11.75.

Location : firth (Troon - Brodick - Greenock). (Figure 45)

Sample	Depth (m)	S(‰)	[^{137}Cs] (dpm l $^{-1}$)	[^{137}Cs] normalised to 35‰ salinity (dpm l $^{-1}$)	$^{134}\text{Cs}/^{137}\text{Cs}$ activity ratio
C52	2	32.97	125.4 \pm 3.4	133.1 \pm 3.6	0.155 \pm 0.003
C53	2	32.95	114.4 \pm 3.1	121.5 \pm 3.3	0.162 \pm 0.003
C54	2	32.93	111.7 \pm 3.0	118.7 \pm 3.2	0.158 \pm 0.004
C55	2	32.91	112.9 \pm 3.0	120.1 \pm 3.2	0.162 \pm 0.004
C56	2	32.83	123.5 \pm 3.3	131.7 \pm 3.6	0.162 \pm 0.003
C57	2	32.61	112.1 \pm 3.0	120.3 \pm 3.2	0.155 \pm 0.004
C58	2	32.77	127.4 \pm 3.4	136.1 \pm 3.7	0.155 \pm 0.003
C59	2	32.07	112.2 \pm 3.0	122.5 \pm 3.3	0.170 \pm 0.004
C60	2	30.80	110.0 \pm 3.0	125.0 \pm 3.4	0.159 \pm 0.004

TABLE 37. Caesium samples from firth ; 14.11.75.

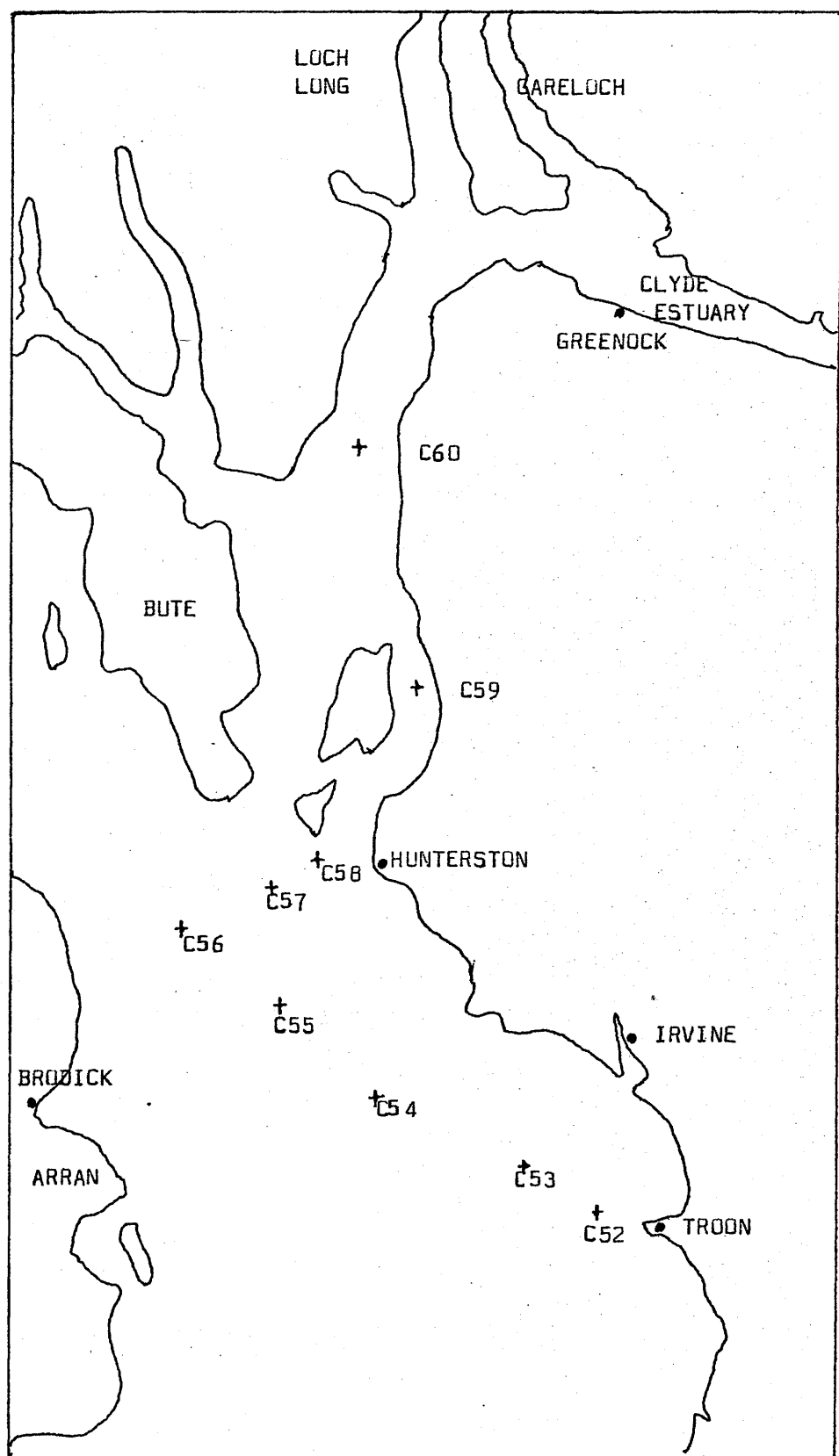


FIGURE 45. Locations of sampling sites for samples C52-C60 ;

Firth of Clyde ; 14.11.75.

SAMPLES C61 - C63

Date : 4.12.75.

Location : Loch Long (Figure 42)

Sample	Location	Depth (m)	S(‰)	D.O. (mg l ⁻¹)	[¹³⁷ Cs] (dpm l ⁻¹)	[¹³⁷ Cs] normalised to 35‰ salinity (dpm l ⁻¹)	¹³⁴ Cs/ ¹³⁷ Cs activity ratio
C61	Barons Point	2	27.43	8.8	103.8 ± 2.8	132.4 ± 3.6	0.158 ± 0.004
C62	Ardentinny	2	30.99	8.1	101.9 ± 2.8	115.0 ± 3.1	0.159 ± 0.004
C63	Ardarroch	2	31.15	7.8	105.2 ± 2.8	118.0 ± 3.2	0.160 ± 0.004

TABLE 38. Caesium samples from Loch Long ; 4.12.75.

SAMPLES C64 - C70

Date 4.12.75.

Location : Loch Goil, station 1. (Figure 33)

Hydrographic data:

Depth (m)	S(‰)	T(°C)	D.O. (mg l ⁻¹)
Surface	31.06	10.9	7.8
10	32.02	11.1	6.7
20	32.75	11.0	6.6
30	32.83	11.0	6.4
40	32.82	10.8	4.8
50	32.86	10.1	3.1
60	32.86	9.8	2.8
70	32.87	-	1.9
80	32.93	-	1.8

Caesium data:

Sample	Depth (m)	[¹³⁷ Cs] (dpm l ⁻¹)	[¹³⁷ Cs] normalised to 35‰ salinity (dpm l ⁻¹)	¹³⁴ Cs/ ¹³⁷ Cs activity ratio
C64	5	103.1 ± 2.8	114.4 ± 3.1	0.170 ± 0.004
C65	20	117.2 ± 3.2	125.3 ± 3.4	0.155 ± 0.004
C66	30	108.8 ± 2.9	116.0 ± 3.2	0.157 ± 0.004
C67	40	91.0 ± 2.5	97.0 ± 2.6	0.156 ± 0.004
C68	50	97.3 ± 2.6	103.6 ± 2.8	0.150 ± 0.004
C69	60	90.6 ± 2.4	96.5 ± 2.6	0.143 ± 0.004
C70	70	91.5 ± 2.5	97.3 ± 2.6	0.151 ± 0.004

TABLE 39. Caesium samples from Loch Goil (1) ; 4.12.75.

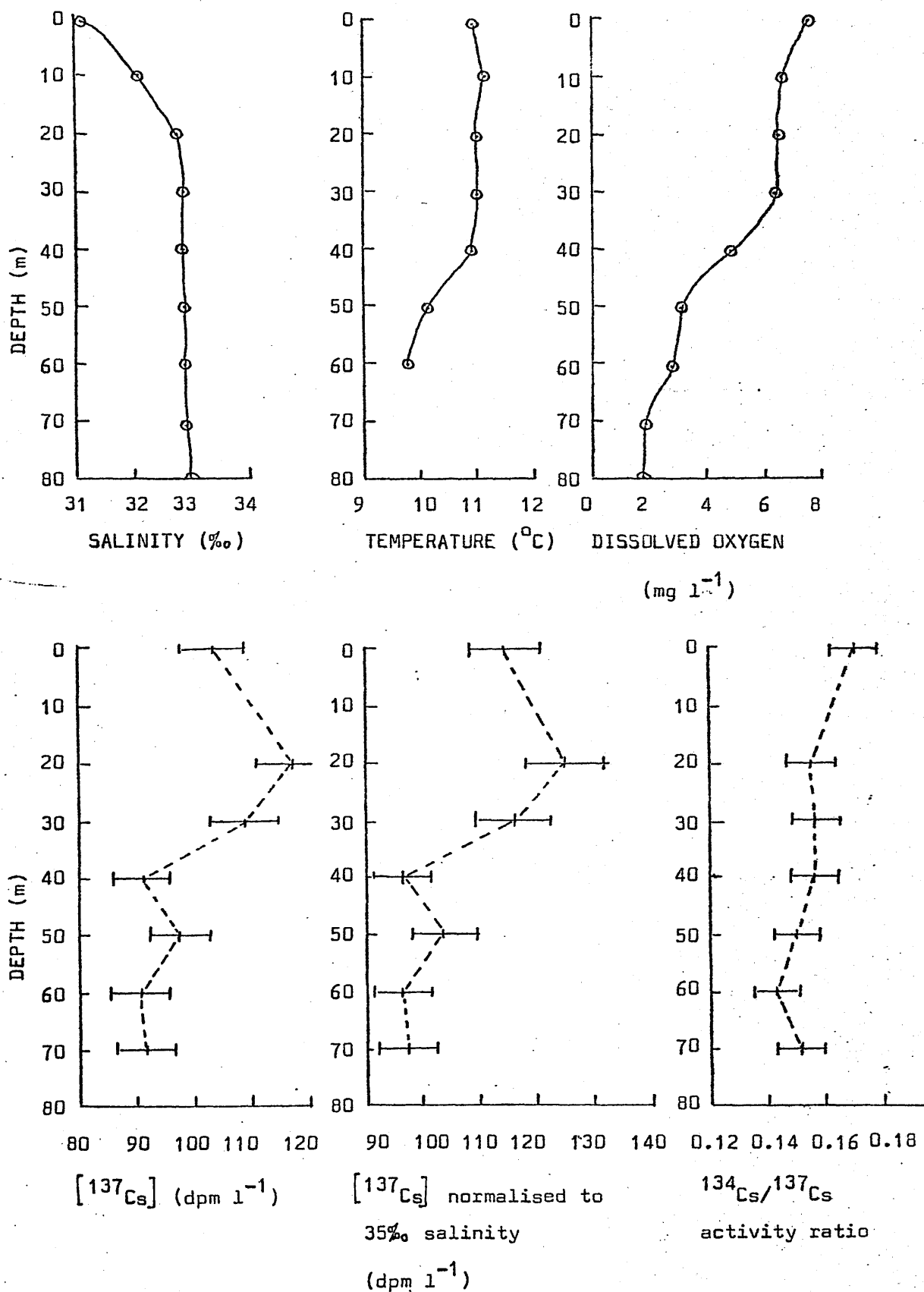


FIGURE 46. Hydrographic and caesium profiles for Loch Gail;
station 1; 4.12.75.

SAMPLES C71 - C75

Date : 4.12.75.

Location : Loch Goil, station 2 ($4^{\circ}53'W$ $56^{\circ}07'N$) (Figure 33)Hydrographic data:

Depth (m)	S(‰)	T($^{\circ}C$)	D.O. (mg l^{-1})
Surface	30.46	10.6	7.8
10	32.03	10.6	7.3
20	32.68	10.9	7.0
30	32.76	10.8	7.0.
40	32.83	7.8	7.9

Caesium data:

Sample	Depth (m)	$[^{137}Cs]$ (dpm l^{-1})	$[^{137}Cs]$ normalised to 35‰ salinity (dpm l^{-1})	$^{134}Cs/^{137}Cs$ activity ratio
C71	5	115.1 ± 3.1	128.9 ± 3.5	0.163 ± 0.003
C72	20	115.3 ± 3.1	123.5 ± 3.3	0.168 ± 0.003
C73	30	112.7 ± 3.0	120.4 ± 3.3	0.156 ± 0.004
C74	40	108.4 ± 2.9	115.6 ± 3.1	0.161 ± 0.004
C75	50	104.0 ± 2.8	110.9 ± 3.0	0.158 ± 0.004

TABLE 40. Caesium samples from Loch Goil (2) ; 4.12.75.

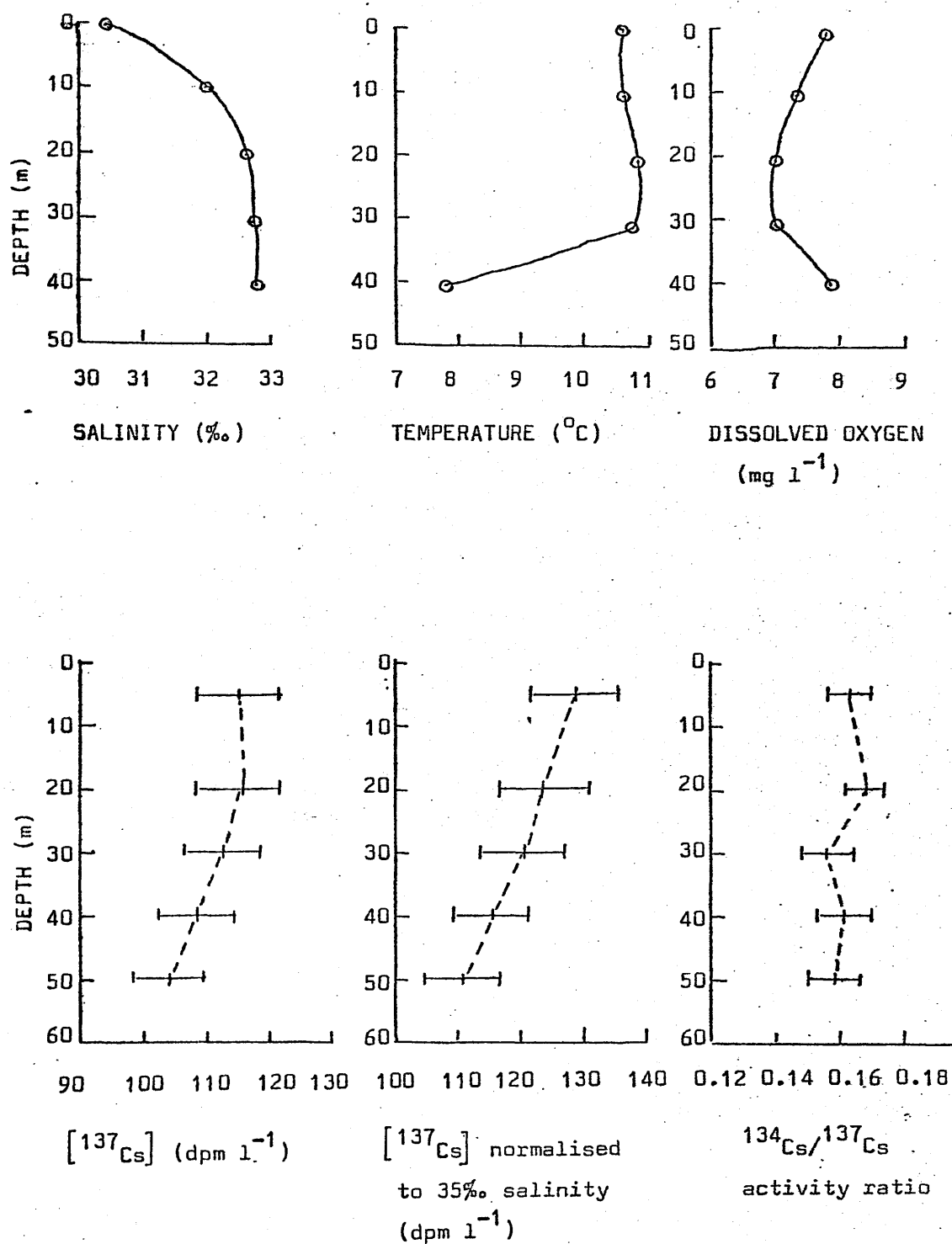


FIGURE 47. Hydrographic and caesium profiles for Loch Goil;
station 2; 4.12.75.

SAMPLES C76 - C78

Date : 8.1.76.

Location : Loch Long (Figure 42)

Sample	Location	Depth (m)	S(‰)	T(°C)	D.O. (mg l ⁻¹)	[¹³⁷ Cs] (dpm l ⁻¹)	[¹³⁷ Cs] normalised to 35‰ salinity (dpm l ⁻¹)	¹³⁴ Cs/ ¹³⁷ Cs activity ratio
C76	Ardentinny	1	28.88	9.35	9.1	109.8 ± 3.0	133.1 ± 3.6	0.157 ± 0.004
C77	Arrdarroch	1	26.75	8.05	9.4	102.9 ± 2.8	134.6 ± 3.6	0.158 ± 0.004
C78	Mouth of Loch Gail	1	26.00	8.30	9.5	103.1 ± 2.8	138.8 ± 3.7	0.152 ± 0.004

TABLE 41. Caesium samples from Loch Long ; 8.1.76.

SAMPLES C79 - C85

Date : 8.1.76.

Location : Loch Goil, station 1 (Figure 33)

Hydrographic data:

Depth (m)	S(‰)	T(°C)	D.O. (mg l ⁻¹)
Surface	25.62	8.50	9.4
10	29.00	8.23	8.6
20	32.30	9.47	7.3
30	32.48	9.60	7.2
40	32.63	9.90	5.6
50	32.64	9.92	4.9
60	32.68	9.82	4.7
70	32.75	9.82	4.3
80	32.75	9.75	3.8

Caesium data:

Sample	Depth (m)	[¹³⁷ Cs] (dpm l ⁻¹)	[¹³⁷ Cs] normalised to 35‰ salinity (dpm l ⁻¹)	¹³⁴ Cs/ ¹³⁷ Cs activity ratio
C79	Surface	83.8 ± 2.3	114.5 ± 3.1	0.152 ± 0.005
C80	10	106.7 ± 2.9	128.8 ± 3.5	0.167 ± 0.004
C81	20	118.2 ± 3.2	128.1 ± 3.5	0.157 ± 0.004
C82	30	113.5 ± 3.1	122.3 ± 3.3	0.162 ± 0.004
C83	40	119.7 ± 3.2	128.4 ± 3.5	0.167 ± 0.004
C84	60	106.5 ± 2.9	114.1 ± 3.1	0.152 ± 0.004
C85	75	101.5 ± 2.7	108.5 ± 2.9	0.153 ± 0.004

TABLE 42. Caesium samples from Loch Goil (1) ; 8.1.76.

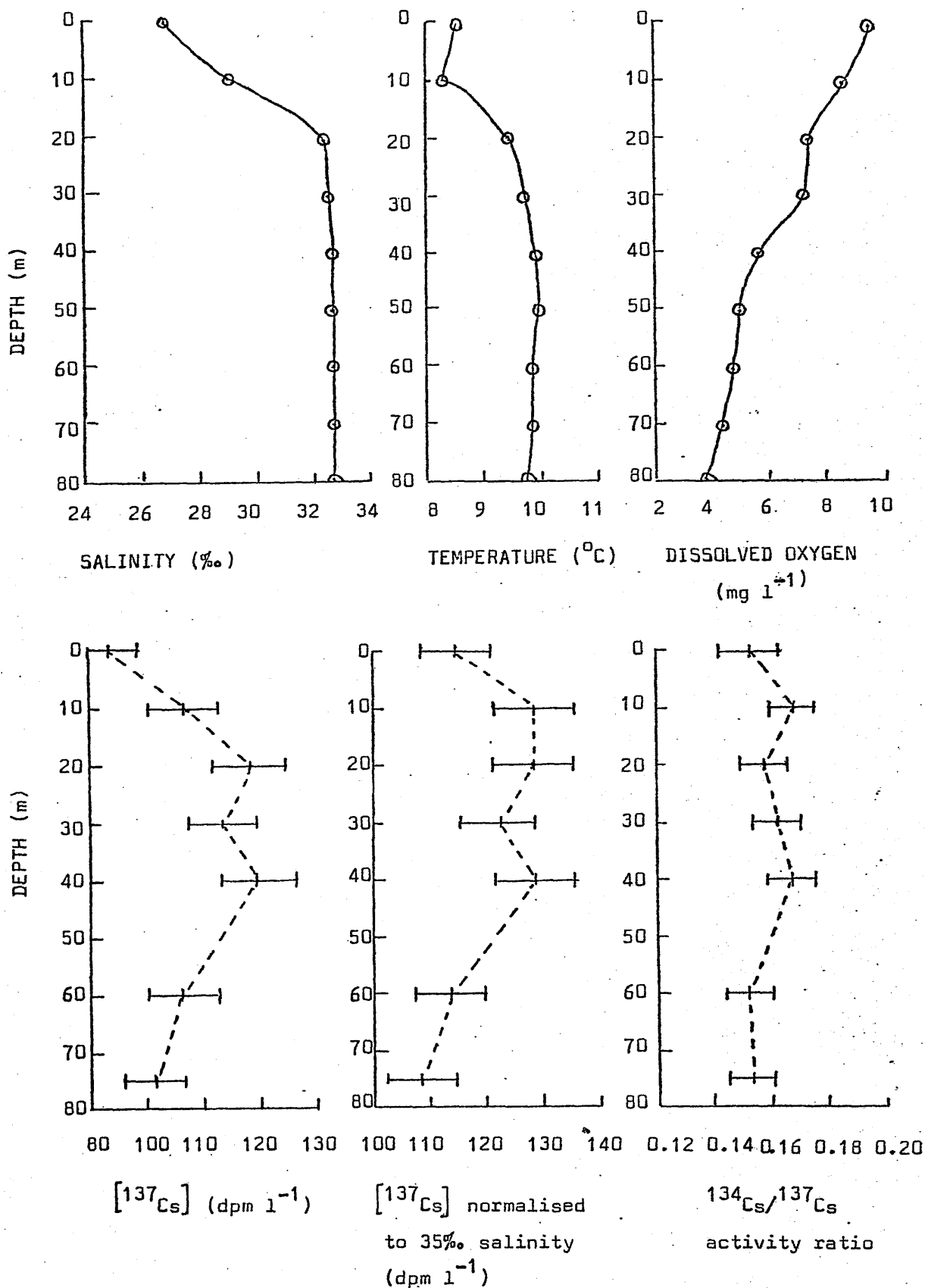


FIGURE 48. Hydrographic and caesium profiles for Loch Goil;
station 1; 8.1.76.

SAMPLES C86 - C91

Date : 8.1.76.

Location : Loch Goil, station 2. (Figure 33)

Hydrographic data:

Depth (m)	S(‰)	T(°C)	D.O. (mg l ⁻¹)
0	26.00	8.10	9.6
10	29.03	8.50	9.1
20	32.32	9.47	7.4
30	32.50	9.60	7.3
40	32.62	9.72	6.3
50	32.93	9.82	5.0

Caesium data:

Sample	Depth (m)	[¹³⁷ Cs] (dpm l ⁻¹)	[¹³⁷ Cs] normalised to 35‰ salinity (dpm l ⁻¹)	¹³⁴ Cs/ ¹³⁷ Cs activity ratio
C86	Surface	102.7 ± 2.8	138.3 ± 3.7	0.158 ± 0.004
C87	10	110.1 ± 3.0	132.7 ± 3.6	0.160 ± 0.004
C88	20	121.1 ± 3.3	131.1 ± 3.5	0.155 ± 0.004
C89	30	117.4 ± 3.2	126.4 ± 3.4	0.160 ± 0.003
C90	40	110.3 ± 3.0	118.3 ± 3.2	0.160 ± 0.004
C91	50	118.6 ± 3.2	126.1 ± 3.4	0.158 ± 0.003

TABLE 43. Caesium samples from Loch Goil (2) : 8.1.76.

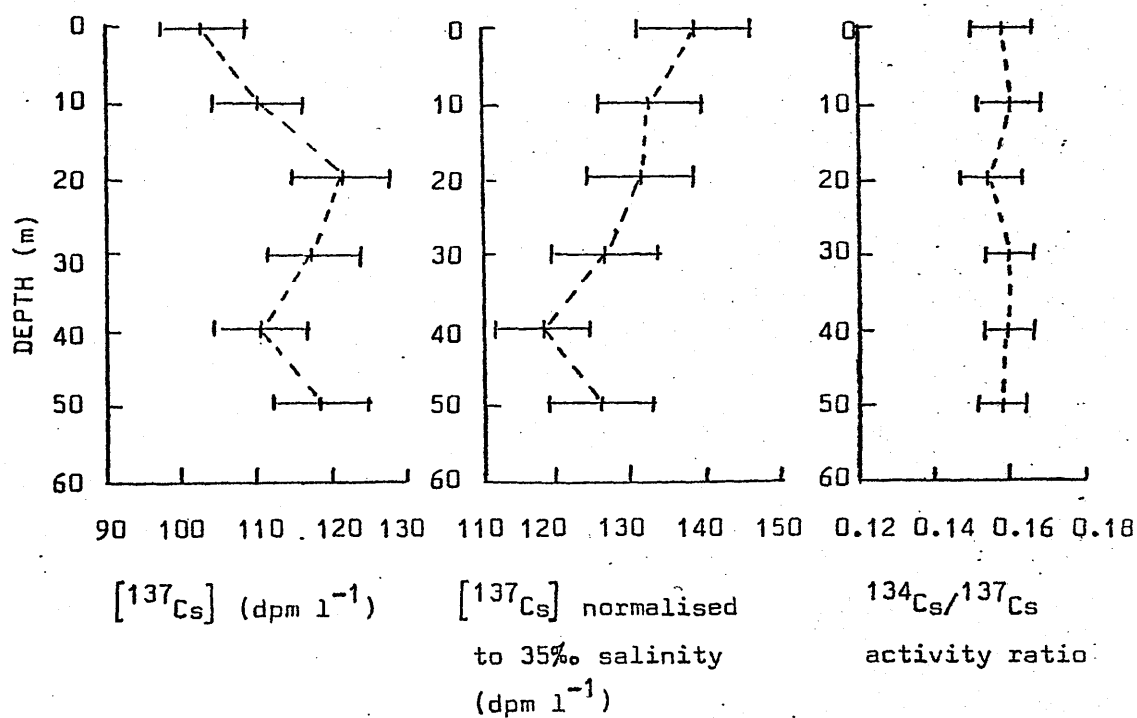
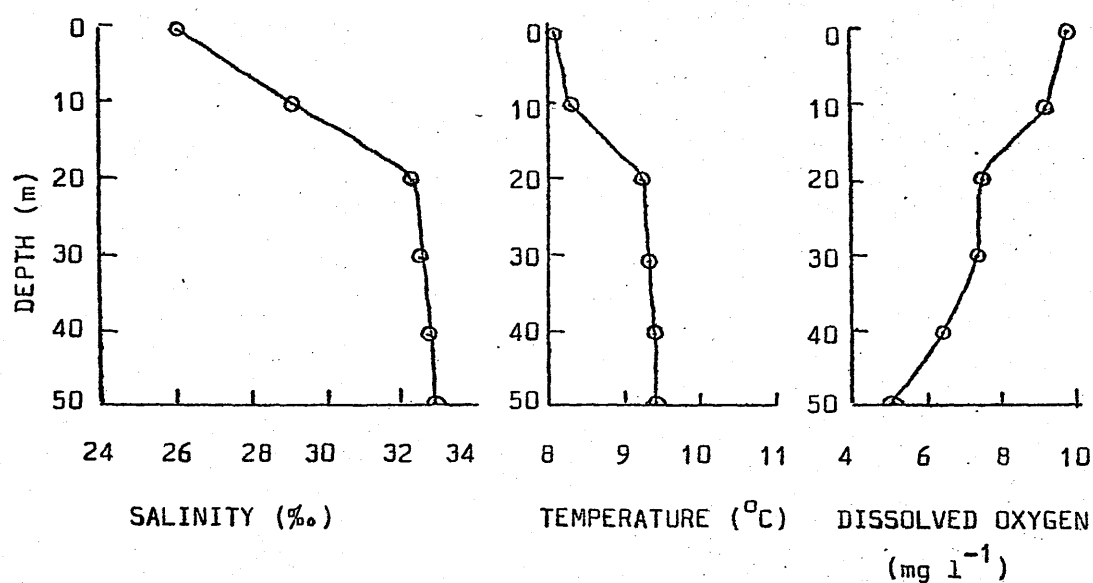


FIGURE 49. Hydrographic and caesium profiles for Loch Goil;
station 2; 8.1.76.

SAMPLES C92 - C99

Date : 4.2.76.

Location : Loch Goil - Loch Long. (Figure 50)

Sample	Location	Depth (m)	S (‰)	T (°C)	D.O. (mg l ⁻¹)	[¹³⁷ Cs] (dpm l ⁻¹)	[¹³⁷ Cs] normalised to 35‰ salinity (dpm l ⁻¹)	¹³⁴ Cs/ ¹³⁷ Cs activity ratio
C92	L.L.1.W	25	31.12	6.5	8.9	112.0 ± 3.0	126.0 ± 3.4	0.153 ± 0.003
C93	L.L.1.E	25	28.36	7.9	7.1	117.2 ± 3.2	144.6 ± 3.9	0.155 ± 0.003
C94	L.L.2.W	25	31.00	6.0	9.2	112.3 ± 3.0	126.8 ± 3.4	0.151 ± 0.003
C95	L.L.2.E	25	32.03	7.5	9.0	114.8 ± 3.1	125.4 ± 3.4	0.156 ± 0.003
C96	L.L.3.W	25	32.06	7.2	9.4	109.8 ± 3.0	119.9 ± 3.2	0.154 ± 0.004
C97	L.L.3.E	25	32.52	7.9	9.1	111.9 ± 3.0	120.4 ± 3.3	0.148 ± 0.003
C98	L. Goil station 1	25	31.94	7.0	9.5	114.3 ± 3.1	125.3 ± 3.4	0.155 ± 0.003
C99	L. Goil station 2	25	31.70	8.0	9.5	96.6 ± 2.7	106.7 ± 2.9	0.155 ± 0.004

TABLE 44. Caesium samples from Loch Goil and Loch Long ; 4.2.76.

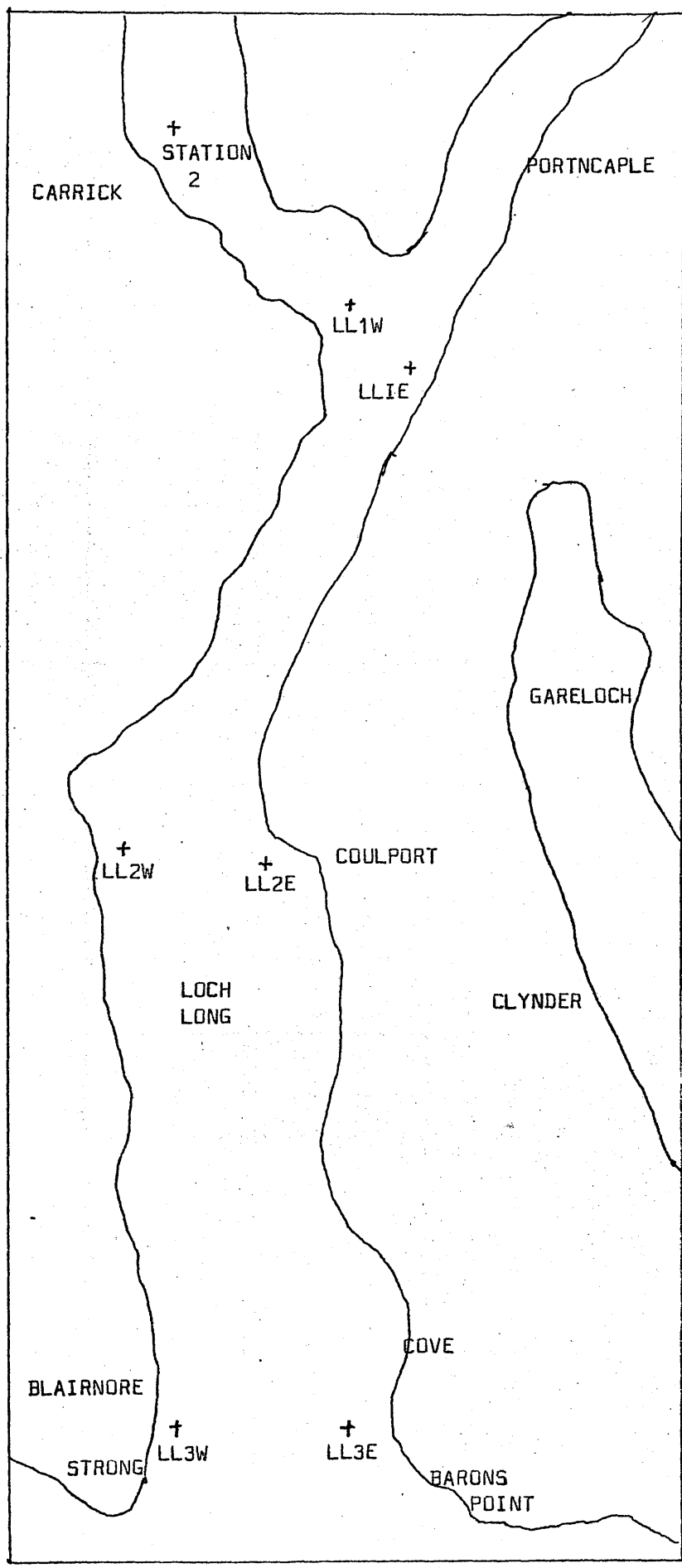


FIGURE 50. Sampling sites in Loch Gail and Loch Long (scale 1:63360).

SAMPLES C100 - C101

Date : 17.2.76.

Location : Loch Fyne. (Figure 51)

Sample	Location	Depth (m)	S (‰)	T (°C)	D.O. (mg l ⁻¹)	[¹³⁷ Cs] (dpm l ⁻¹)	[¹³⁷ Cs] normalised to 35‰ salinity (dpm l ⁻¹)	¹³⁴ Cs/ ¹³⁷ Cs activity ratio
C100	L.F.M.	1	31.22	6.5	9.4	105.3 ± 2.8	118.0 ± 3.2	0.160 ± 0.004
C101	L.F.S.	1	32.67	6.9	9.3	101.1 ± 2.7	108.3 ± 2.9	0.156 ± 0.004

TABLE 45. Caesium samples from Loch Fyne (middle and south basins) ; 17.2.76.

SAMPLES C102 - C106

Date : 17.2.76.

Location : Loch Fyne (North basin) (Figure 51)

Hydrographic data:

Depth (m)	S(‰)	T(°C)	D.O. (mg l ⁻¹)
1	29.88	6.20	9.70
4	31.99	7.58	9.16
7	32.44	7.90	8.92
10	32.59	8.30	8.92
20	32.69	8.30	8.59
30	32.74	8.39	8.41
43	32.84	8.60	8.19
68	32.77	8.00	8.41
93	32.81	8.12	8.38
118	32.85	8.00	8.75
133	32.78	7.92	8.85

Caesium data:

Sample	Depth (m)	[¹³⁷ Cs] (dpm l ⁻¹)	[¹³⁷ Cs] normalised to 35‰ salinity (dpm l ⁻¹)	¹³⁴ Cs/ ¹³⁷ Cs activity ratio
C102	Surface	104.4 ± 2.8	112.3 ± 3.3	0.159 ± 0.004
C103	10	106.9 ± 2.9	114.8 ± 3.1	0.156 ± 0.003
C104	20	110.6 ± 3.0	118.4 ± 3.2	0.153 ± 0.004
C105	30	113.4 ± 3.1	121.2 ± 3.3	0.154 ± 0.004
C106	40	106.1 ± 2.9	113.1 ± 3.1	0.166 ± 0.004

TABLE 46. Caesium samples from Loch Fyne (north basin) ; 17.2.76.

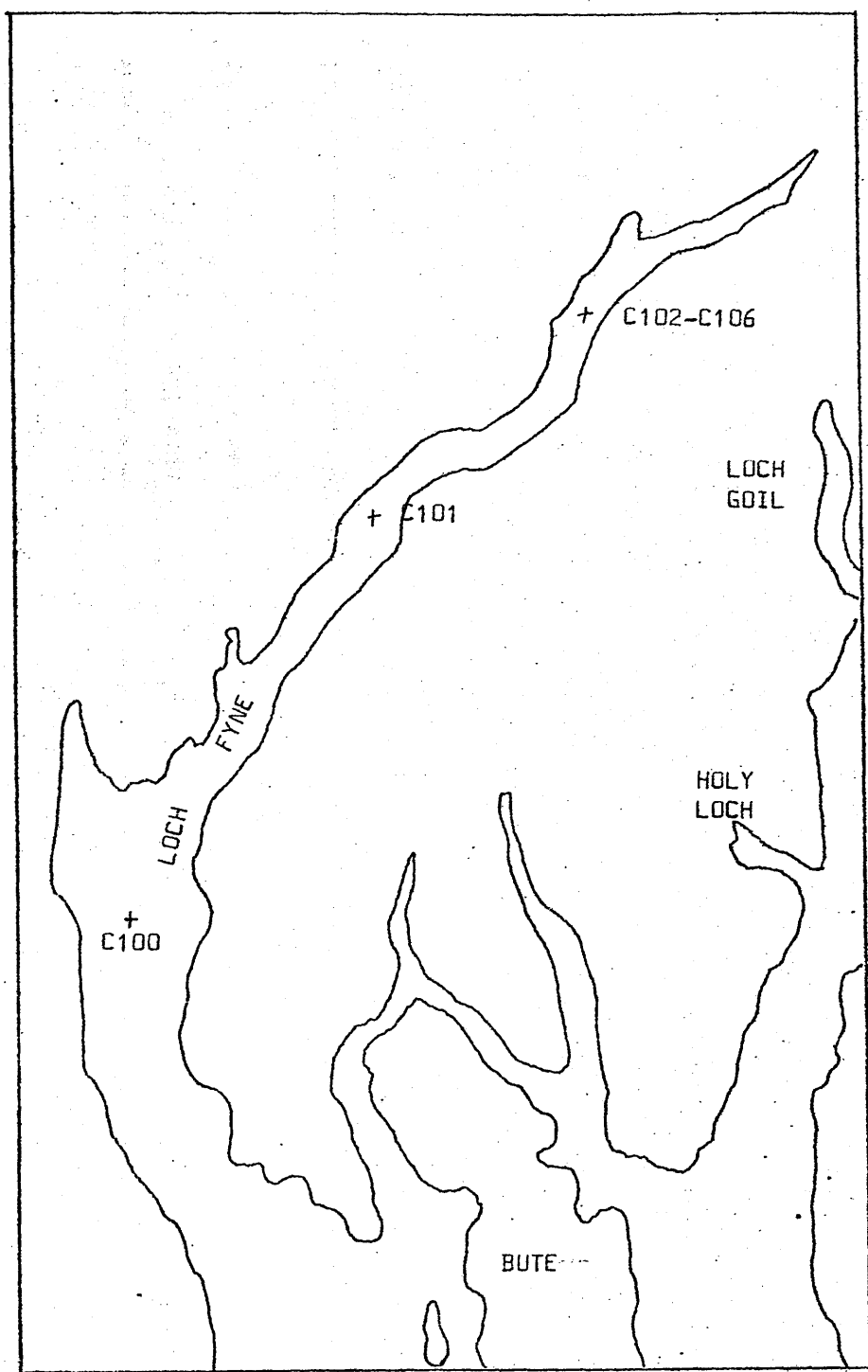


FIGURE 51. Location of sampling sites for samples C100-C106;
Loch Fyne ; 17.2.76.

SAMPLES C107 - C112

Date : 3.3.76.

Location : Loch Long (Figure 50)

Sample	Location	Depth (m)	S (‰)	T (°C)	D.O. (mg l ⁻¹)	[¹³⁷ Cs] (dpm l ⁻¹)	[¹³⁷ Cs] normalised to 35‰ salinity (dpm l ⁻¹)	¹³⁴ Cs/ ¹³⁷ Cs activity ratio
C107	L.L.1.W	2	26.55	6.8	9.0	86.5 ± 2.3	114.0 ± 3.1	0.150 ± 0.004
C108	L.L.1.E	2	28.28	7.4	9.2	81.9 ± 2.2	105.2 ± 2.8	0.150 ± 0.005
C109	L.L.2.W	2	28.36	7.1	9.4	81.9 ± 2.2	101.1 ± 2.7	0.153 ± 0.004
C110	L.L.2.E	2	27.33		9.6	86.3 ± 2.3	110.5 ± 3.0	0.159 ± 0.004
C111	L.L.3.W	2	28.04	7.1	9.5	86.9 ± 2.3	108.5 ± 2.9	0.156 ± 0.004
C112	L.L.3.E	2	27.35		9.5	92.8 ± 2.5	119.8 ± 3.2	0.154 ± 0.004

TABLE 47. Caesium samples from Loch Long ; 3.3.76.

SAMPLES C113 - C120

Date: 3.3.76.

Location : Loch Goil, station 1. (Figure 33)

Hydrographic data:

Depth (m)	S(‰)	T(°C)	D.O. (mg l ⁻¹)
1	-	6.8	9.6
10	30.30	8.5	8.6
20	32.50	9.2	-
30	32.62	8.8	7.7
40	32.67	8.8	7.8
50	32.70	9.0	7.7
60	32.77	8.9	7.8
70	32.77	8.9	7.8
80	32.79	9.2	7.6

Caesium data:

Sample	Depth (m)	[¹³⁷ Cs] (dpm l ⁻¹)	[¹³⁷ Cs] normalised to 35‰ salinity (dpm l ⁻¹)	¹³⁴ Cs/ ¹³⁷ Cs activity ratio
C113	Surface	87.9 ± 2.4	-	0.155 ± 0.005
C114	10	97.0 ± 2.6	104.5 ± 2.8	0.146 ± 0.004
C115	20	106.5 ± 2.9	111.5 ± 3.0	0.146 ± 0.004
C116	30	104.6 ± 2.8	112.2 ± 3.0	0.154 ± 0.004
C117	40	104.9 ± 2.8	112.4 ± 3.0	0.144 ± 0.004
C118	50	97.9 ± 2.6	104.8 ± 2.8	0.161 ± 0.004
C119	60	103.1 ± 2.8	110.1 ± 3.0	0.155 ± 0.004
C120	70	102.7 ± 2.8	109.7 ± 3.0	0.153 ± 0.004

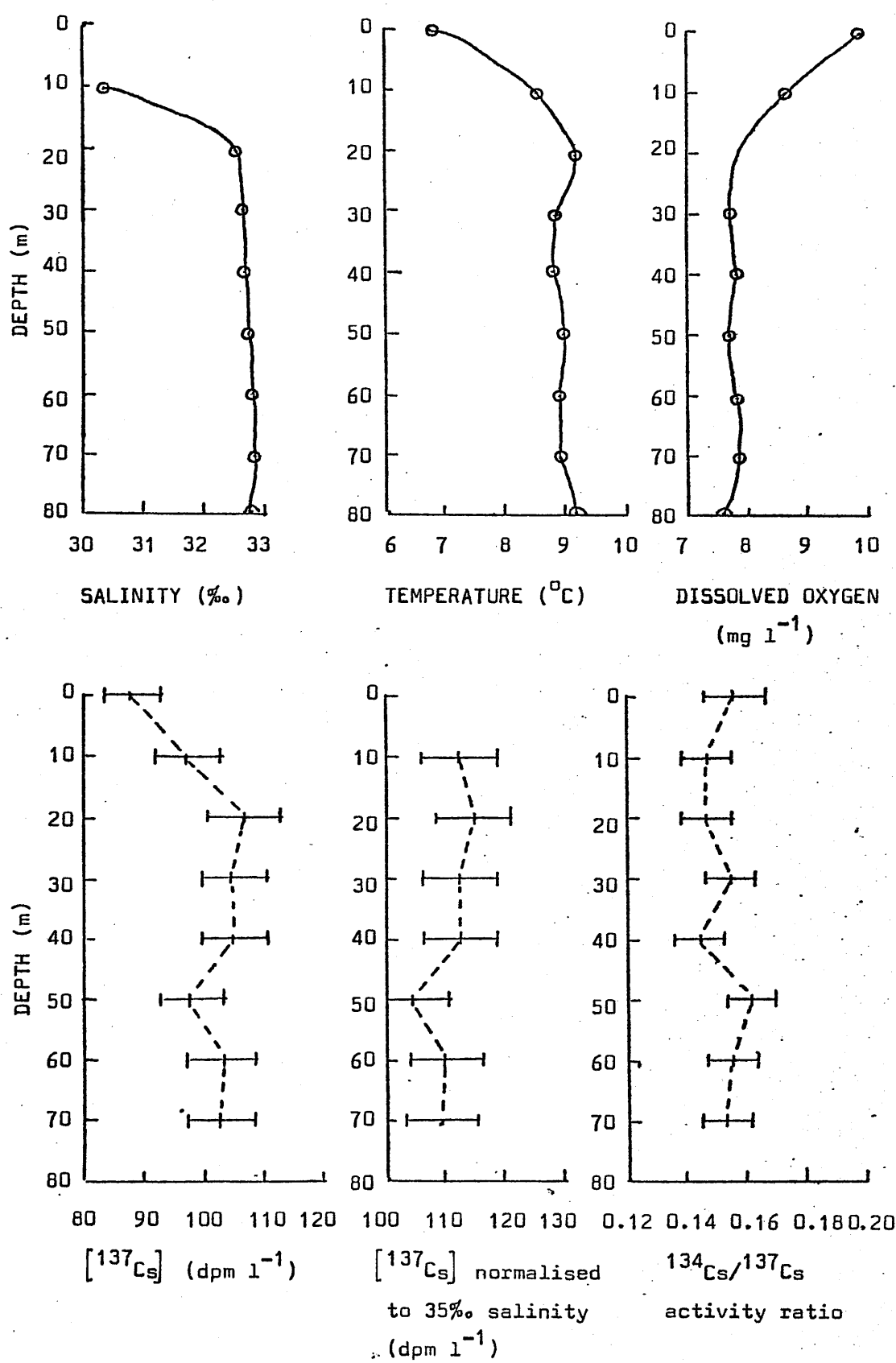


FIGURE 52. Hydrographic and caesium profiles for Loch Gail; station 1; 3.3.76.

SAMPLES C121 - C125

Date : 3.3.76.

Location : Loch Goil, station 2. (Figure 33)

Hydrographic data:

Depth (m)	S(‰)	T(°C)	D.O. (mg l ⁻¹)
1	28.53	8.35	9.4
10	31.27	8.55	8.4
20	32.46	8.50	8.1
30	32.57	8.80	7.9
40	32.59	8.80	7.9

Caesium data:

Sample	Depth (m)	[¹³⁷ Cs] (dpm l ⁻¹)	[¹³⁷ Cs] normalised to 35‰ salinity (dpm l ⁻¹)	¹³⁴ Cs/ ¹³⁷ Cs activity ratio
C121	Surface	86.4 ± 2.3	106.0 ± 2.9	0.156 ± 0.004
C122	10	97.8 ± 2.6	109.5 ± 3.0	0.156 ± 0.004
C123	20	101.5 ± 2.7	109.4 ± 3.0	0.151 ± 0.004
C124	30	98.7 ± 2.7	106.1 ± 2.9	0.158 ± 0.004
C125	40	105.0 ± 2.8	112.8 ± 3.0	0.151 ± 0.004

TABLE 49. Caesium samples from Loch Goil (2), 3.3.76

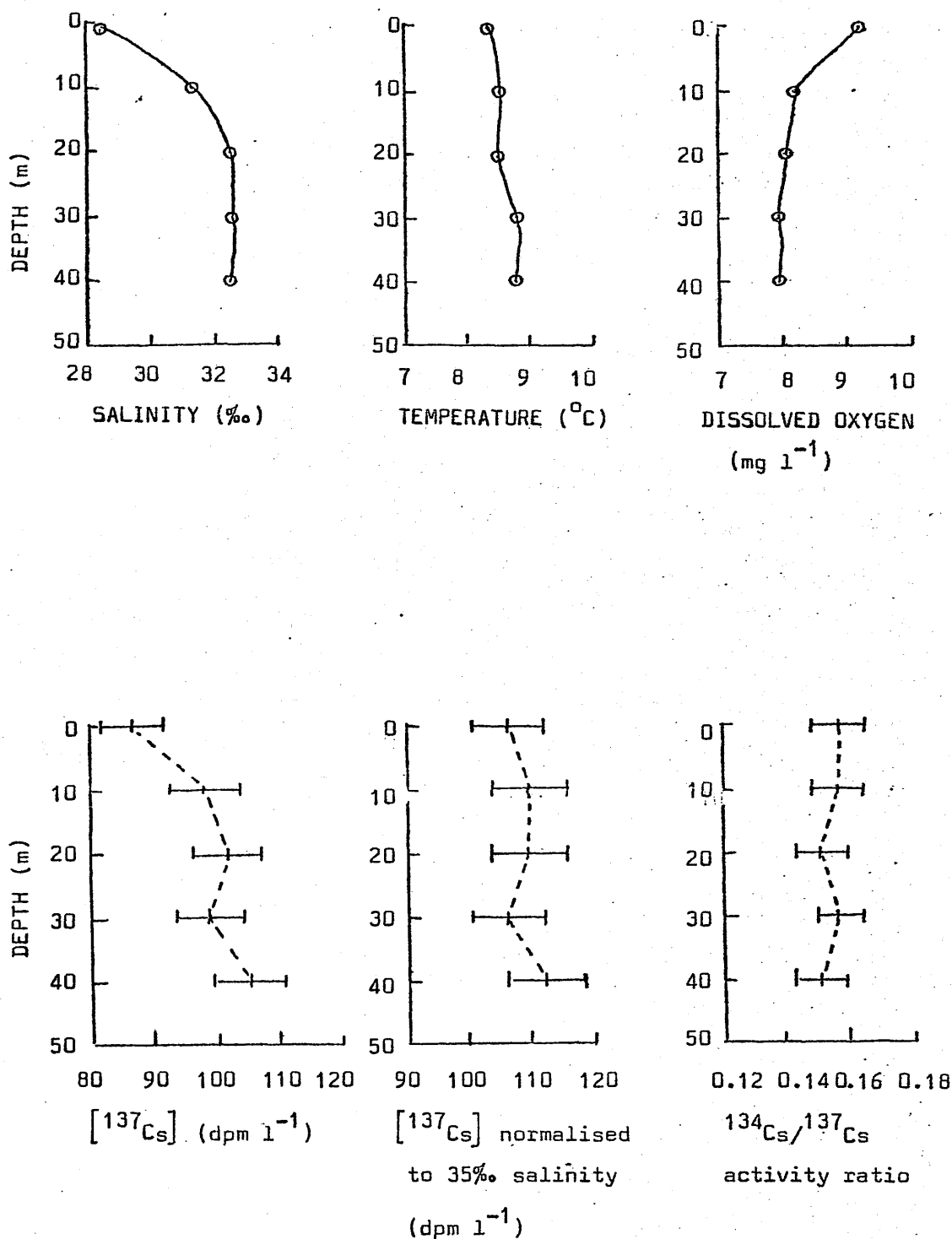


FIGURE 53. Hydrographic and caesium profiles for Loch Goil; station 2; 3.3.76.

SAMPLES C126 - C132

Date : 1.4.76.

Location : Loch Goil, station 1. (Figure 33)

Hydrographic data:

Depth (m)	S(‰)	T(°C)	D.O.(mg l ⁻¹)
Surface	27.33	6.6	11.3
10	30.40	6.9	9.8
20	32.28	7.5	8.5
30	32.62	7.5	8.5
40	32.85	7.8	8.1
50	32.74	7.7	8.2
60	32.75	7.6	8.1
70	32.76	7.6	-

Caesium data:

Sample	Depth (m)	[¹³⁷ Cs] (dpm l ⁻¹)	[¹³⁷ Cs] normalised to 35‰ salinity (dpm l ⁻¹)	¹³⁴ Cs/ ¹³⁷ Cs activity ratio
C126	Surface	75.2 ± 2.0	96.3 ± 2.6	0.145 ± 0.005
C127	10	89.5 ± 2.4	103.0 ± 2.8	0.151 ± 0.004
C128	20	101.2 ± 2.7	109.7 ± 3.0	0.146 ± 0.004
C129	30	95.8 ± 2.6	102.9 ± 2.8	0.154 ± 0.004
C130	40	95.0 ± 2.6	101.2 ± 2.8	0.146 ± 0.004
C131	50	92.7 ± 2.5	99.1 ± 2.7	0.153 ± 0.004
C132	60	93.5 ± 2.5	99.9 ± 2.7	0.147 ± 0.004

TABLE 50. Caesium samples from Loch Goil (1) ; 1.4.76.

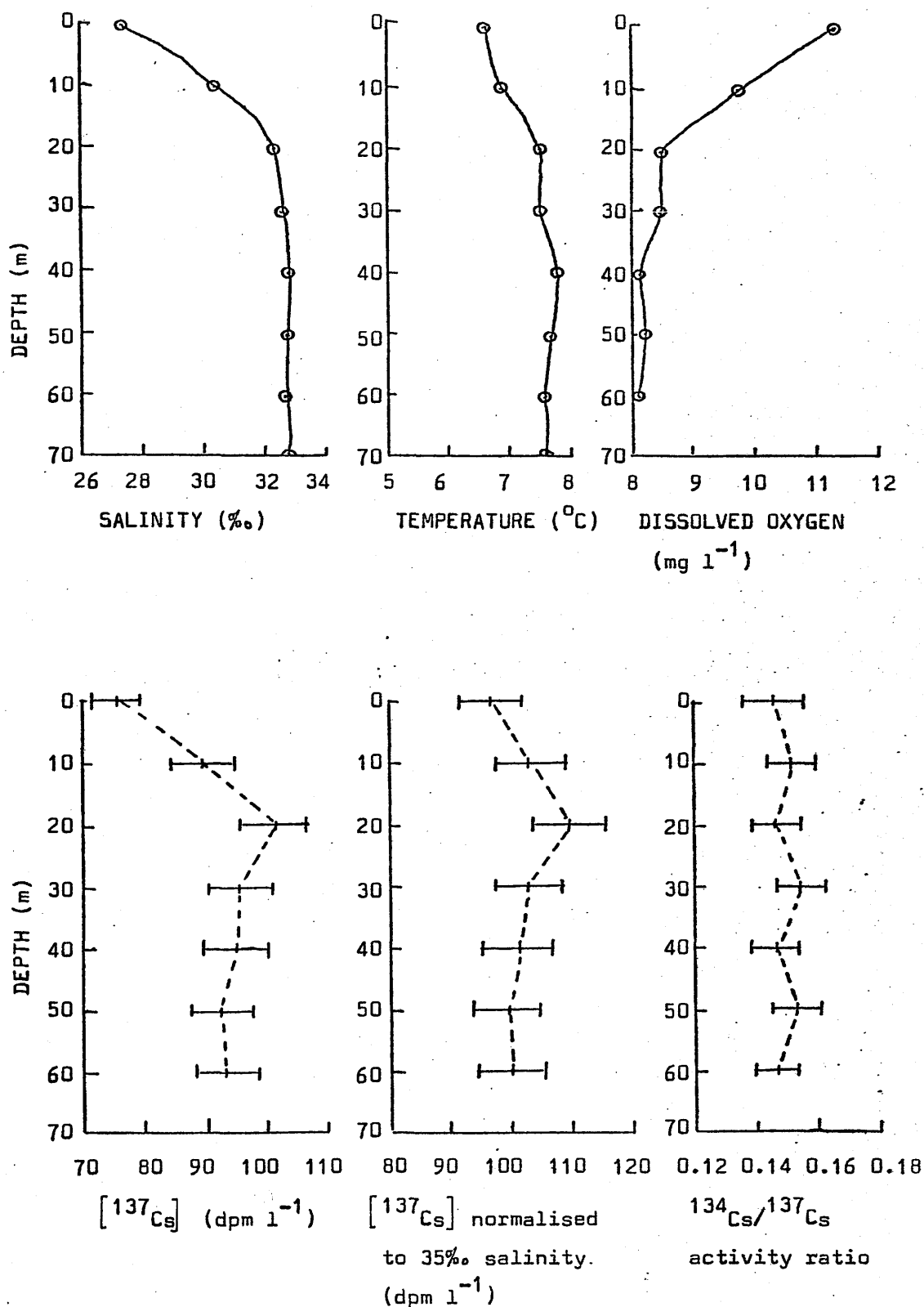


FIGURE 54. Hydrographic and caesium profiles for Loch Goil; station 1; 1.4.76.

SAMPLES C133 - C138

Date : 1.4.76.

Location : Loch Goil, station 2. (Figure 33)

Hydrographic data:

Depth (m)	S(‰)	T(°C)	D.O.(mg l ⁻¹)
Surface	27.15	6.4	10.6
10	30.01	6.8	10.2
20	31.92	7.1	8.7
30	32.33	7.2	8.5
40	32.47	7.6	8.5
50	32.68	7.5	8.4

Caesium data:

Sample	Depth (m)	[¹³⁷ Cs] (dpm l ⁻¹)	[¹³⁷ Cs] normalised to 35‰ salinity (dpm l ⁻¹)	¹³⁴ Cs/ ¹³⁷ Cs activity ratio
C133	Surface	82.5 ± 2.2	106.4 ± 2.9	0.150 ± 0.004
C134	10	82.1 ± 2.2	95.8 ± 2.6	0.154 ± 0.005
C135	20	92.1 ± 2.5	101.0 ± 2.7	0.152 ± 0.004
C136	30	93.1 ± 2.5	100.8 ± 2.7	0.151 ± 0.004
C137	40	99.2 ± 2.7	106.9 ± 2.9	0.145 ± 0.004
C138	50	95.4 ± 2.6	102.2 ± 2.8	0.145 ± 0.004

TABLE 51. Caesium samples from Loch Goil (2) ; 1.4.76.

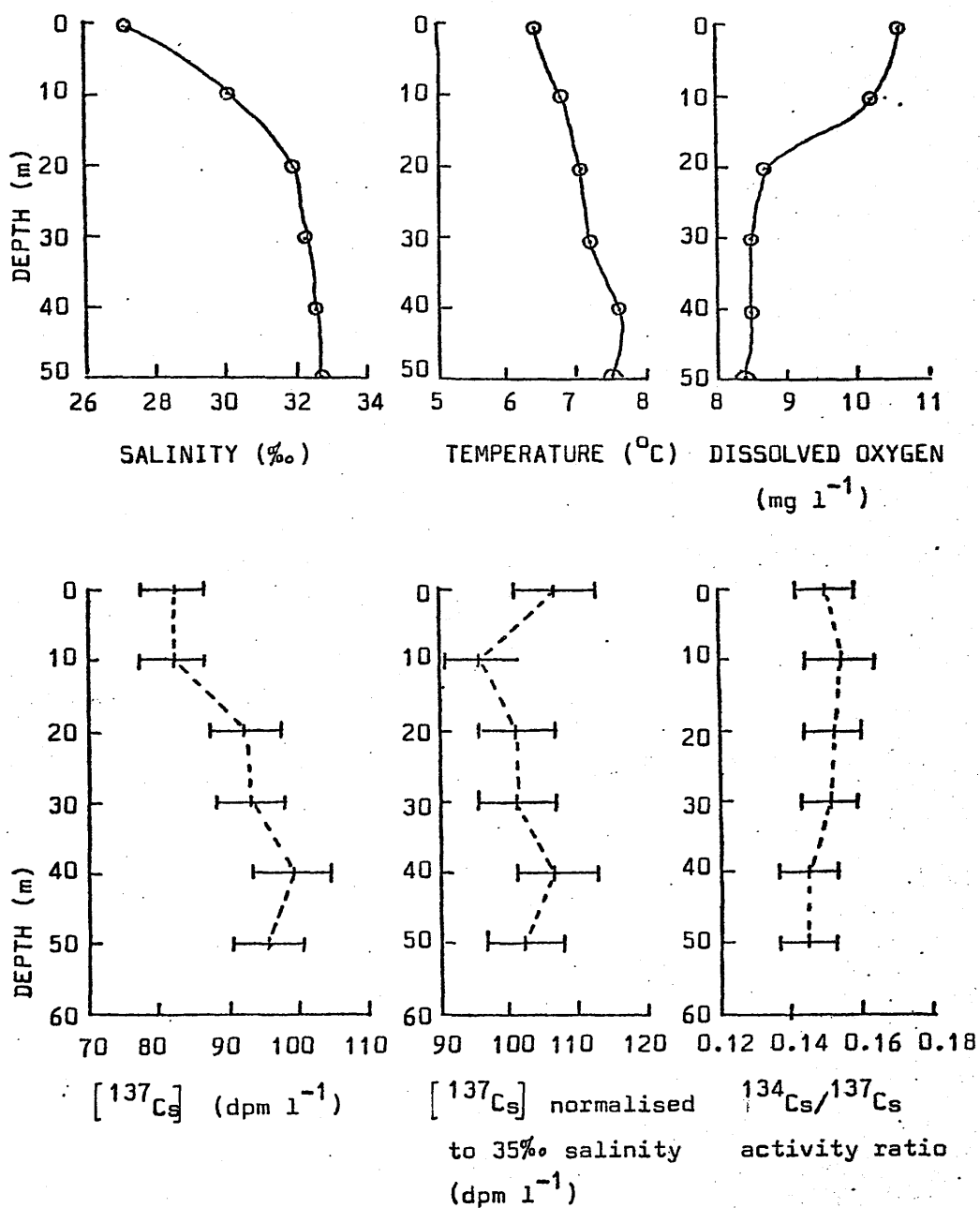


FIGURE 55. Hydrographic and caesium profiles for Loch Gail; station 2; 1.4.76.

SAMPLES C139 - C143

Date : 1.4.76.

Location : Loch Goil; station 3. (Figure 33)

Hydrographic data:

Depth (m)	S(‰)	T°C)	D.O. (mg l ⁻¹)
Surface	25.68	6.2	12.2
10	29.70	6.6	10.0
20	32.25	7.5	8.3
30	32.71	7.9	8.3
40	32.75	7.9	7.4

Caesium data:

Sample	Depth (m)	[¹³⁷ Cs] (dpm l ⁻¹)	[¹³⁷ Cs] normalised to 35‰ salinity (dpm l ⁻¹)	¹³⁴ Cs/ ¹³⁷ Cs activity ratio
C139	Surface	71.9 ± 1.9	98.0 ± 2.6	0.141 ± 0.005
C140	10	81.9 ± 2.2	96.5 ± 2.6	0.143 ± 0.005
C141	20	97.7 ± 2.6	106.0 ± 2.9	0.145 ± 0.004
C142	30	102.0 ± 2.8	109.1 ± 2.9	0.150 ± 0.004
C143	40	98.2 ± 2.7	104.9 ± 2.8	0.151 ± 0.004

TABLE 52. Caesium samples from Loch Goil (3) ; 1.4.76.

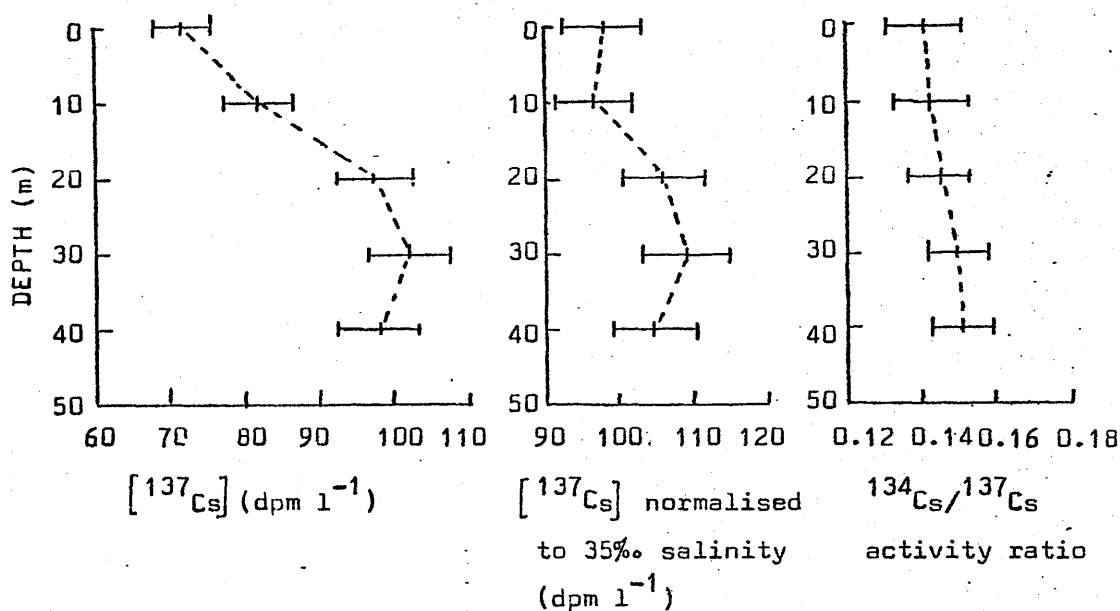
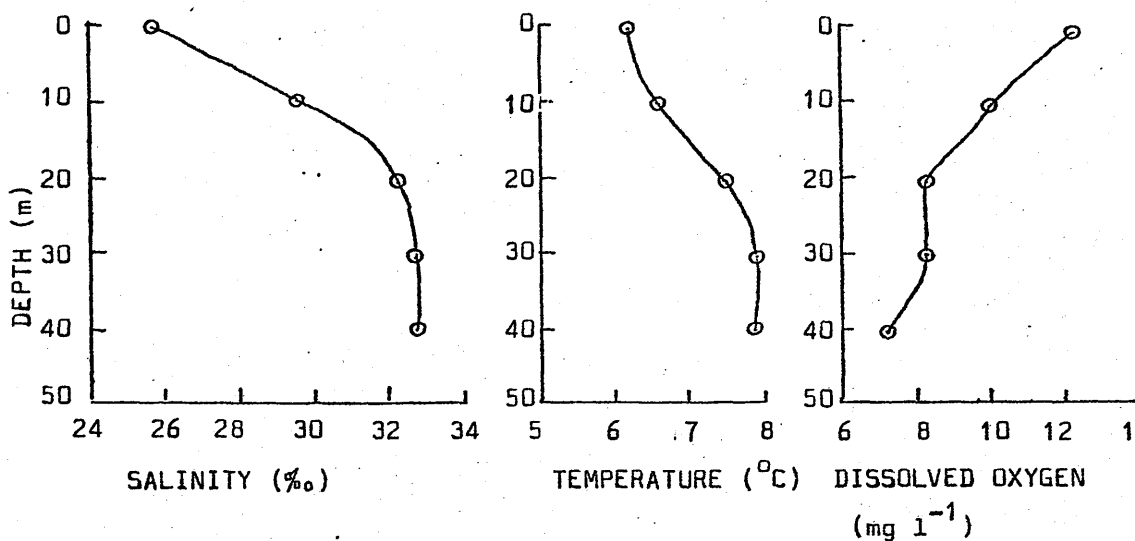


FIGURE 56. Hydrographic and caesium profiles for Loch Goil; station 3; 1.4.76.

SAMPLES C144 - C147

Miscellaneous samples : surface water samples collected from the shore.

Location : Figure 57.

Sample	Location	Date	[^{137}Cs] (dpm l ⁻¹)	$^{134}\text{Cs}/^{137}\text{Cs}$ activity ratio
C144	Staffin	23.3.75	1.8 ± 0.1	0.18 ± 0.04
C145	Carsaig	30.3.75	7.3 ± 0.2	0.17 ± 0.01
C146	Furnace	1.4.75	7.6 ± 0.2	0.157 ± 0.008
C147	Brora	24.4.75	0.6 ± 0.1	0.08 ± 0.05

TABLE 53. Radiocaesium analyses of miscellaneous water samples.

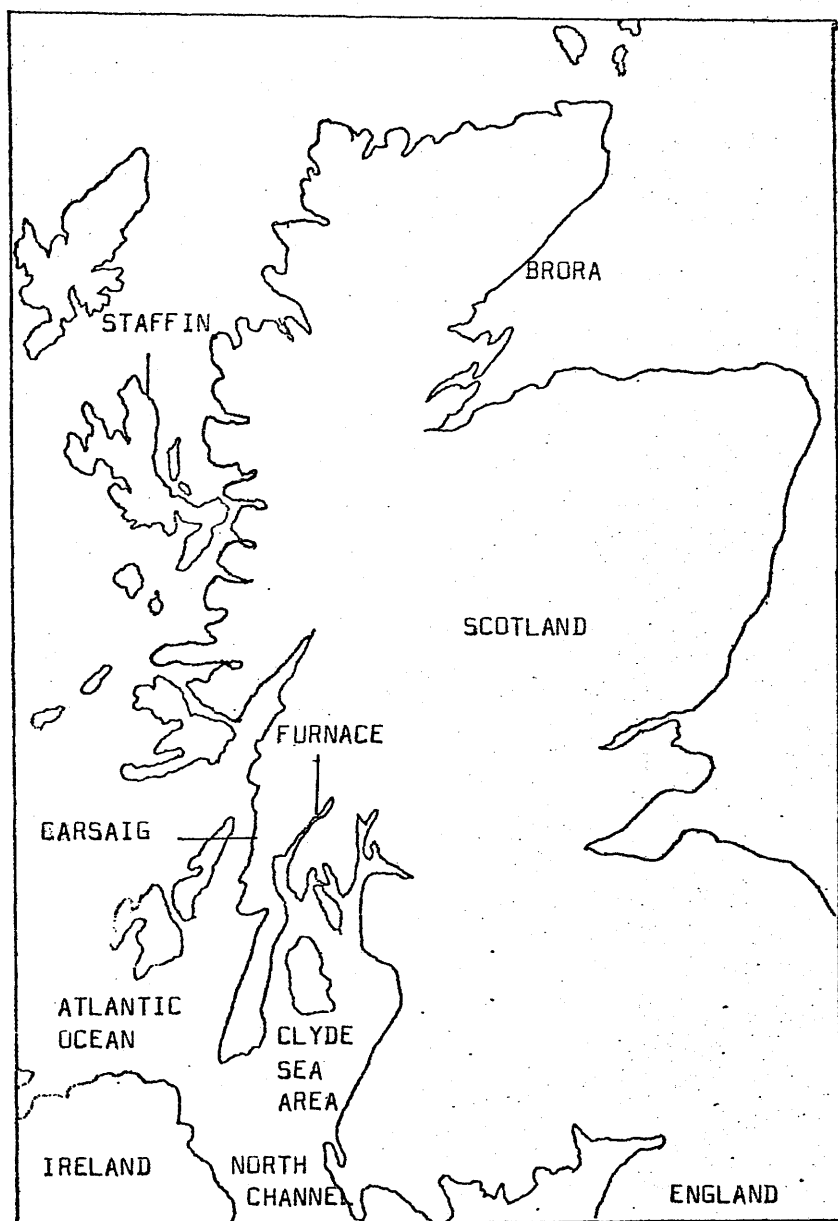


FIGURE 57. Location of sampling sites for miscellaneous caesium samples C144-C147.

SEDIMENT CORES G L G 1, G L G 2

Collection date : 14.1.74.

Location : Gareloch ; station 1. (Figure 29)

Core type: G L G 1 : gravity

G L G 2 : gravity

Core G L G 1:

Depth in core (cm)	Dry/Wet ratio	[^{226}Ra] (dpm/g dry sediment)
0 - 1	0.33	2.7 ± 0.2
1 - 2	0.36	1.6 ± 0.1
2 - 3	0.36	1.4 ± 0.1
7 - 8	0.39	1.3 ± 0.1
11 - 12	0.35	2.0 ± 0.1
23 - 24	0.46	1.0 ± 0.1

Core G L G 2:

Depth in core (cm)	Dry/Wet ratio	[^{226}Ra] (dpm/g dry sediment)
1 - 2	0.36	1.0 ± 0.1

TABLE 54. Radium analyses of sediment cores G L G 1 and G L G 2 collected by gravity corer from Gareloch, station 1, 14.1.74.

SEDIMENT CORE L G C 2

Collection date : 8.4.75.

Location : Loch Goil; station 1. (Figure 33)

Core type : Craib.

Depth in core (cm)	Dry/Wet ratio	[²²⁶ Ra] (dpm/g dry sediment)	²²⁸ Ra/ ²²⁶ Ra activity ratio	[¹³⁷ Cs] (dpm/g dry sediment)	¹³⁴ Cs/ ¹³⁷ Cs activity ratio
0 - 1	0.17	6.9 ± 0.4	1.2 ± 0.3	25.7 ± 0.7	0.13 ± 0.01
1 - 2	0.31	8.6 ± 0.5	0.5 ± 0.2	23.5 ± 0.6	0.13 ± 0.01
2 - 3	0.30	9.2 ± 0.6	-	20.6 ± 0.6	0.07 ± 0.01
3 - 4	0.27	11.1 ± 0.7	-	19.8 ± 0.5	0.10 ± 0.01
4 - 5	0.27	10.6 ± 0.6	-	15.1 ± 0.4	0.0
5 - 6	0.28	5.6 ± 0.3	-	13.8 ± 0.4	0.0
6 - 7	0.30	3.7 ± 0.2	-	8.9 ± 0.2	0.0
7 - 8	0.32	2.7 ± 0.2	-	9.8 ± 0.3	0.0
8 - 9	0.32	2.5 ± 0.2	-	6.7 ± 0.2	0.0
9 - 10	0.32	1.3 ± 0.1	-	6.7 ± 0.2	0.0

TABLE 55. Radium and caesium analyses of sediment core L G C 2 collected by Craib corer from Loch Goil station 1 ; 8.4.75.

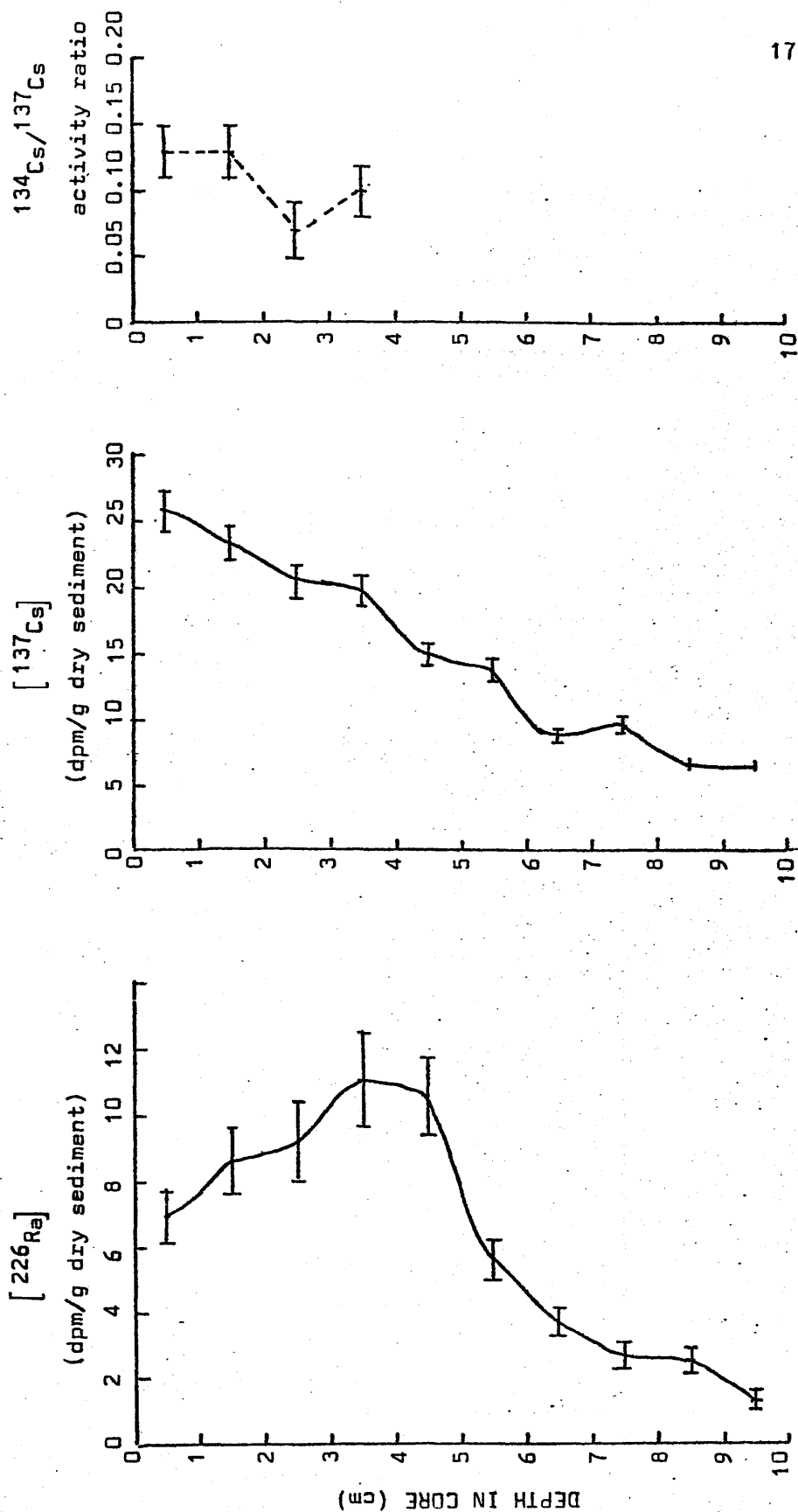


FIGURE 58. Radium and caesium profiles in core L G C 2.

SEDIMENT CORE L G G 5

Collection date : 8.4.75.

Location : Loch Goil ; station 1. (Figure 33)

Core type ; gravity

Depth in core (cm)	Dry/Wet ratio	[^{226}Ra] (dpm/g dry sediment)	[^{137}Cs] (dpm/g dry sediment)	$^{134}\text{Cs}/^{137}\text{Cs}$ activity ratio
2 - 3	0.25	4.0 ± 0.2	7.5 ± 0.2	0.0
15 - 16	0.36	2.7 ± 0.2	0.0	0.0
24 - 25	0.38	2.2 ± 0.1	0.0	0.0

TABLE 56. Radium and Caesium analyses of sediment core L G G 5 collected by gravity corer from Loch Goil, station 1, 8.4.75.

Collection date : 6.11.75.

Location : Gareloch ; station 2. (Figure 29)

Core type : Craib.

Depth in core (cm)	Dry/Wet ratio	[²²⁶ Ra] (dpm/g dry sediment)	[¹³⁷ Cs] (dpm/g dry sediment)	¹³⁴ Cs/ ¹³⁷ Cs activity ratio
0 - 1	0.22	1.5 ± 0.1	58.2 ± 1.6	0.12 ± 0.01
1 - 2	0.29	1.5 ± 0.1	60.8 ± 1.6	0.120 ± 0.009
2 - 3	0.27	1.2 ± 0.1	58.3 ± 1.6	0.162 ± 0.009
3 - 4	0.30	1.0 ± 0.1	45.9 ± 1.2	0.10 ± 0.01
4 - 5	0.33	0.7 ± 0.1	32.2 ± 0.9	0.12 ± 0.01
5 - 6	0.33	1.0 ± 0.1	31.1 ± 0.8	0.06 ± 0.01
6 - 7	0.35	0.7 ± 0.1	29.7 ± 0.8	0.07 ± 0.01
7 - 8	0.35	0.7 ± 0.1	25.0 ± 0.7	0.08 ± 0.02
8 - 9	0.36	—	23.3 ± 0.6	0.05 ± 0.02
9 - 10	0.37	—	22.9 ± 0.6	0.04 ± 0.02

TABLE 57. Radium and Caesium analyses of sediment core G L C 1 collected by Craib corer from Gareloch ; station 2; 6.11.75.

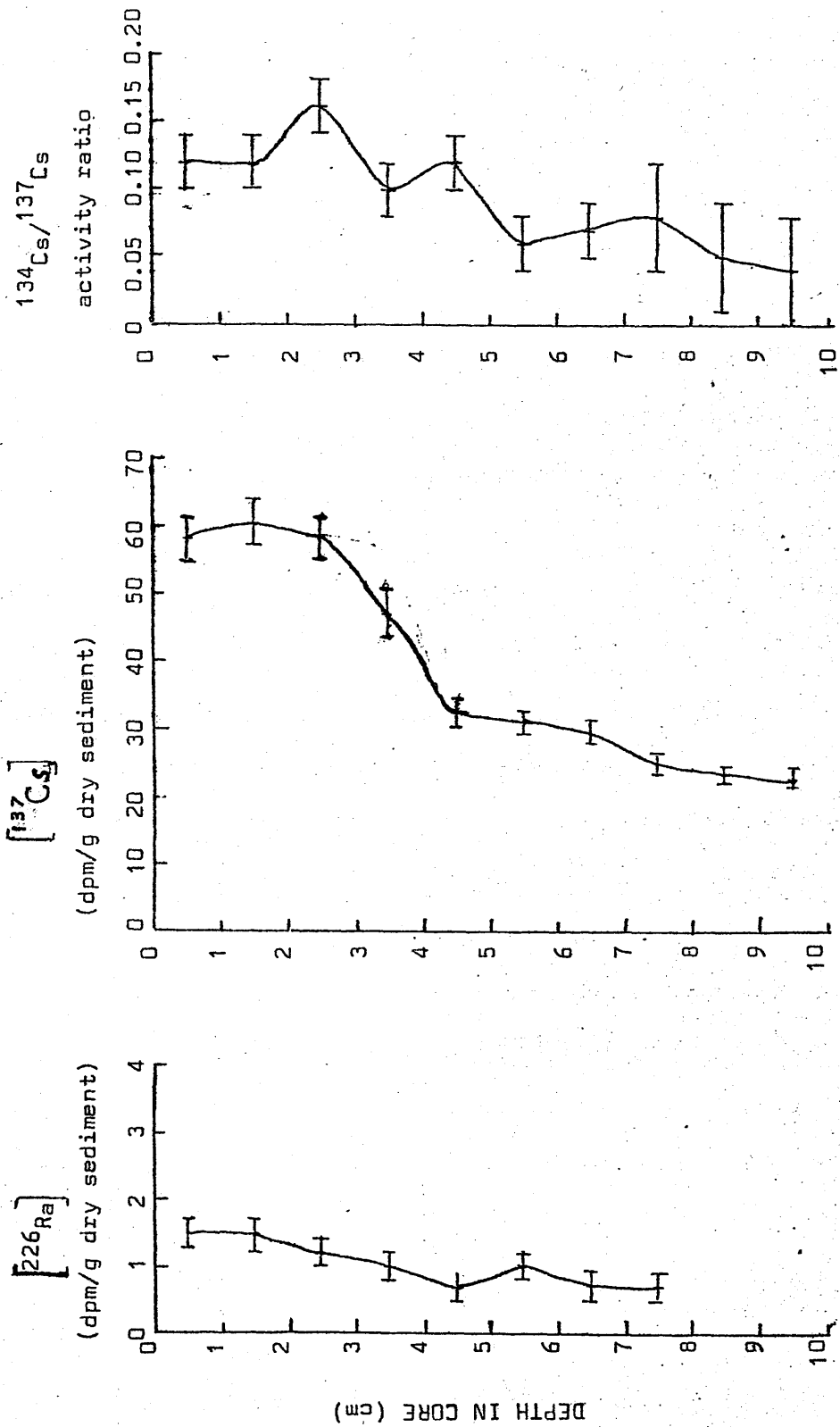


FIGURE 59. Radium and caesium profiles in core GL61.

CHAPTER 4

DISCUSSION AND CONCLUSIONS

The diversity of sample type, collection date and location leads to complexity in interpreting observed data. The following general scheme has been found useful and will be followed in discussion of the results : (1) General aspects of caesium concentrations in Clyde Sea Area water (2) General aspects of radium concentrations in Clyde Sea Area water (3) Water residence time and mixing patterns for Loch Goil (4) Radium and radiocaesium concentrations in Clyde Sea Area Sediments (5) Caesium budget for the Clyde Sea Area (6) Radium budget for the Clyde Sea Area (7) General conclusions.

4.1. General aspects of caesium concentrations in Clyde Sea Area water.

In consideration of the observed caesium data it is useful to approximate the system under study to one in which caesium exhibits conservative behaviour in sea water and has a single dominant input to the area, namely the effluent discharged from the Windscale nuclear fuel reprocessing plant. This approximation is largely justified by the data in Tables 8 to 13 which indicate that the activity discharged from Windscale is several orders of magnitude larger than any other possible input to the area and that the resultant concentration of ^{137}Cs in sea water in the approaches to the Clyde Sea Area are much larger than contemporary atmospheric fallout concentrations for surface sea water (0.1 to 0.2 dpm l^{-1}). Furthermore the concentrations of ^{137}Cs in biological and sedimentary materials indicate a concentration factor relative to water in the order of 10 - 100, verifying a relatively conservative behaviour for caesium. On the basis of this model, it is possible to attempt a correlation of the known variations in the amount

of ^{137}Cs and ^{134}Cs discharged from Windscale with observed concentrations of these nuclides in the Irish Sea and Clyde Sea Area, thus deriving mean water transport times within the coastal system.

The mean output of ^{137}Cs from Windscale during the period 1965 to 1975 is shown in Figure 60 while detailed variations in the relative monthly discharge (normalized to January 1975) are shown in Figure 61 (Howells, 1976). Mean data obtained by the Ministry of Agriculture, Fisheries and Food for sea water concentrations of ^{137}Cs for the St Bees-Seascale area (close to the Windscale discharge point) and for the North Channel are also presented in Figure 61 (Jefferies, 1976). It is apparent from these graphs that the variations of ^{137}Cs concentrations in the Irish Sea, while primarily determined by the Windscale output, undergo major modifications as a result of dilution and mixing, the magnitude of these modifications increasing with distance from the discharge point. The key point for correlation of the three graphs is the large increase in the Windscale output from March to August 1974 which almost certainly relates to the peaks labelled 1 in the Seascale/St Bees and North Channel graphs. This gives a water transit time of about six months from Windscale to the North Channel, this value again being obtained if the peaks labelled 2, 3 and 4 in both diagrams are assumed to be related. Correlation of the data for 1975 and 1976 is less obvious possibly as a result of decreased water transit time or more complex mixing with Atlantic water.

Assuming the Windscale output to be the only major source of radiocaesium to the Clyde Sea Area, it would be expected that Clyde Sea waters would show trends in radiocaesium concentrations and isotope ratio similar to those observed in the North Channel but modified by (a) radioactive decay (b) mixing with previously contaminated water (c) fresh water input (d) incursion of Atlantic water. Matching the observed Clyde Sea Area data with the North Channel figures is complicated

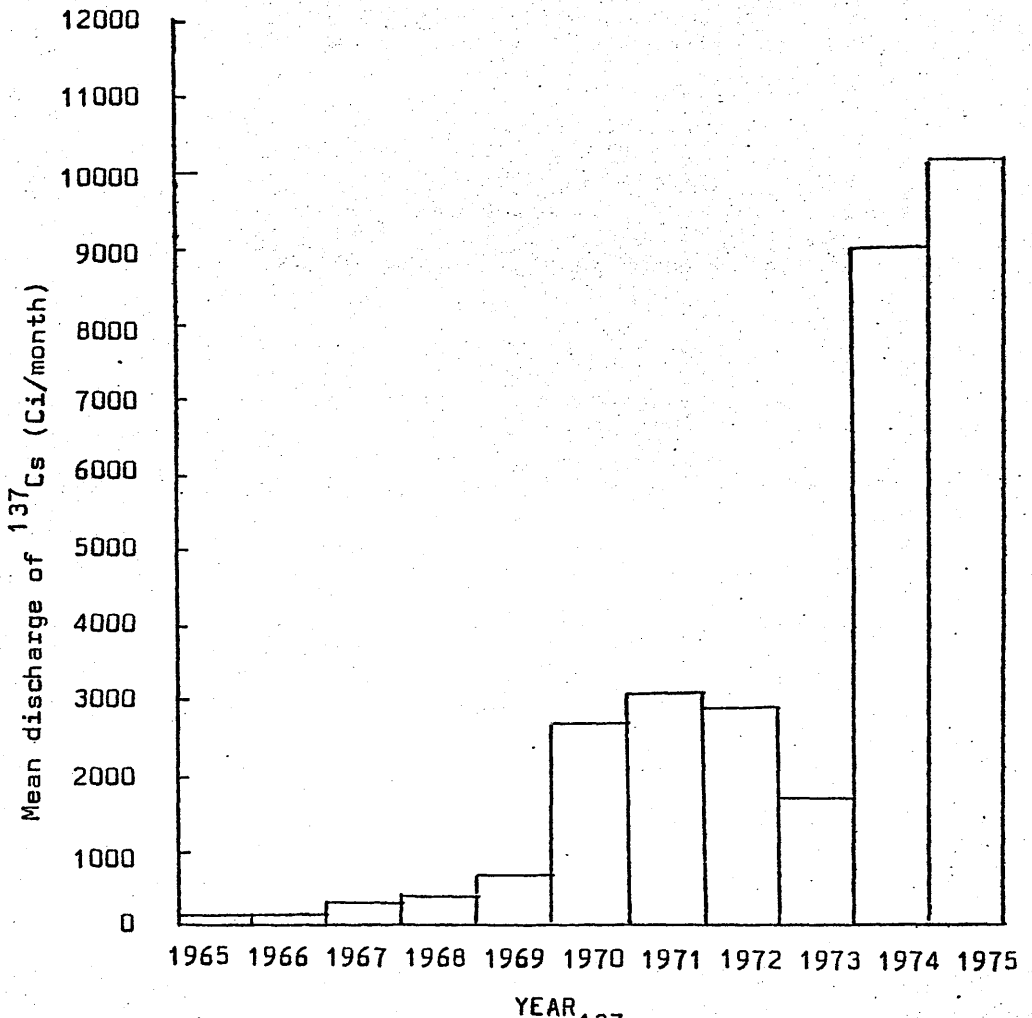


FIGURE 60. Mean discharge of ^{137}Cs from the Windscale nuclear fuel processing plant during the period 1965-1975.

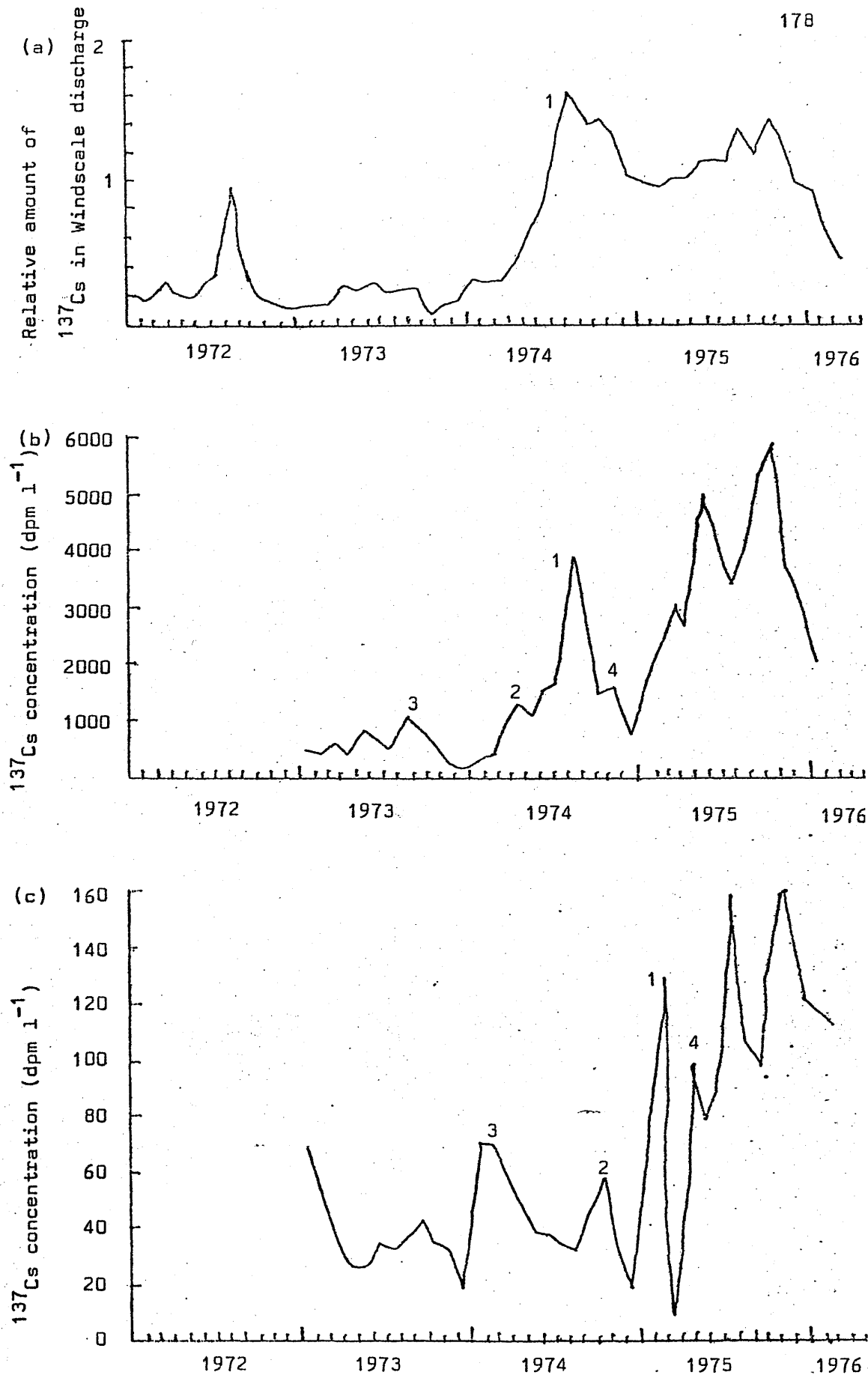


FIGURE 61. (a) Monthly output of ^{137}Cs (normalized to January 1975) from Windscale, 1973 - 1976.
 (b) Mean Seascale - St Bees seawater concentrations of ^{137}Cs 1973 - 1976
 (c) Mean North Channel sea water concentrations of ^{137}Cs 1973 - 1976. (Jefferies, 1976 ; Howells, 1976).

by lack of continuity in the former as a result of occasional non-availability of sampling facilities. The following provisional correlation can, however, be postulated while a more definite relationship awaits establishment through continuing accumulation of data for the Clyde Sea Area.

Vertical profiles of ^{137}Cs concentrations for the Clyde Sea Area show considerable variations, notably as a result of freshwater input, an effect which could mask similarities with North Channel concentrations. This can be overcome by (a) using observed data from a fixed depth (say 20m) not significantly affected by freshwater input or (b) arbitrarily normalizing surface ^{137}Cs concentrations to 35‰ salinity. Graphs showing variations of ^{137}Cs concentrations in surface water of the Clyde Sea Area from 1974 to 1976 as defined by both of these methods are shown in Figure 62 along with the corresponding data for the North Channel. $^{134}\text{Cs}/^{137}\text{Cs}$ activity ratios available for the Windscale discharge, North Channel and Clyde Sea Area are shown in Figure 63. The trends shown in the salinity normalised ^{137}Cs concentration and the 20m concentration graphs are substantially the same so either can be used for comparison with the North Channel data. Despite the limited data available for the Clyde Sea Area, the increase in ^{137}Cs concentration observed between February and May 1975 can, with little ambiguity, be related to the maximum in concentration observed in the North Channel in February 1975. Two arguments support this relationship. Firstly, the ^{137}Cs concentrations of greater than 80 dpm l^{-1} observed in Loch Long and Loch Goil on 8.4.75 (Tables 32 and 33) had on only one occasion been exceeded in the North Channel prior to this date, namely during the February 1975 maximum. Secondly the February 1975 peak has previously been related to the August 1974 maximum in output from Windscale which also corresponded to a maximum in $^{134}\text{Cs}/^{137}\text{Cs}$ activity ratio in the effluent. Since the activity

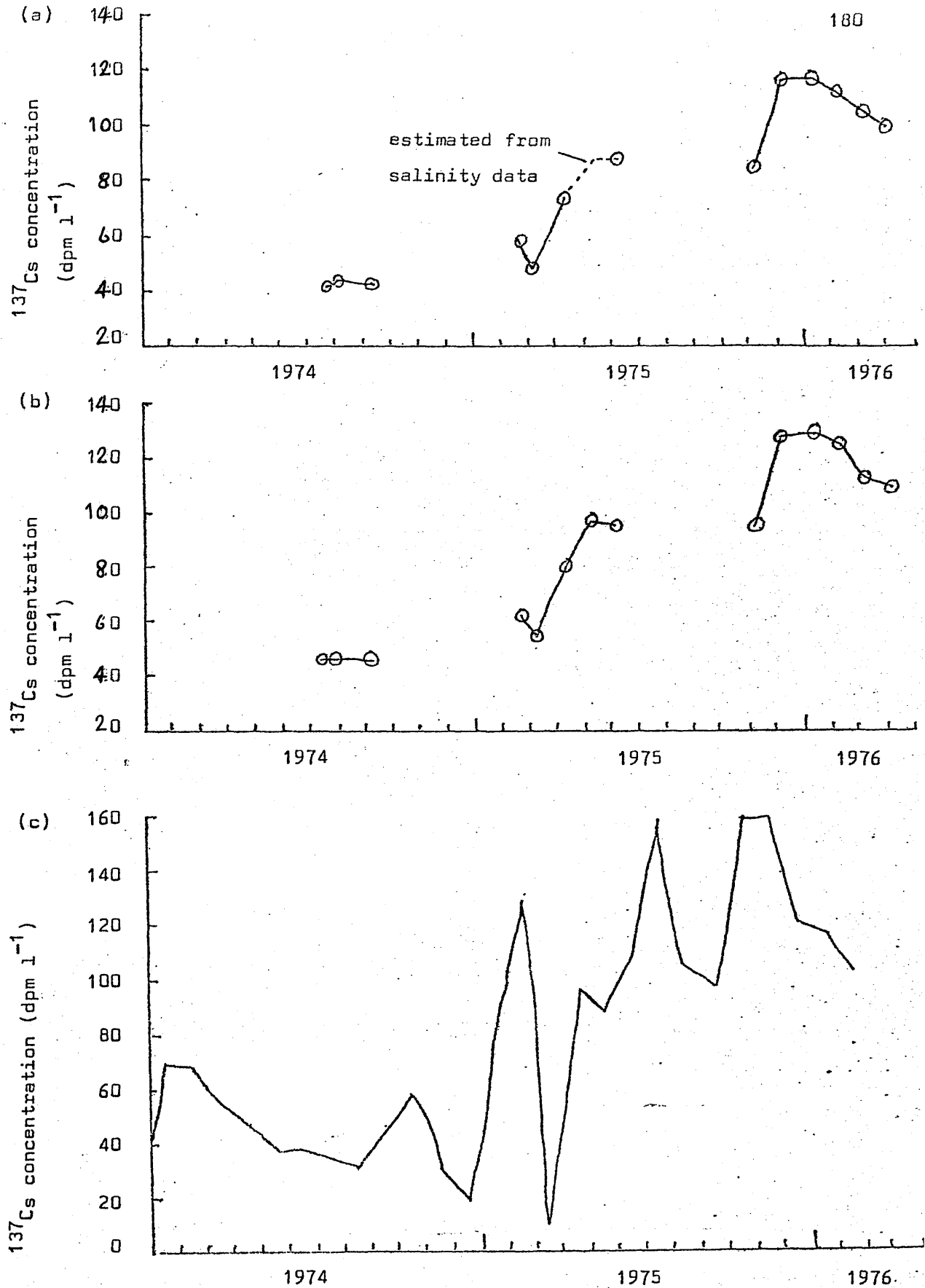


FIGURE 62. ^{137}Cs concentrations in sea water 1974-1976 for (a) Clyde Sea Area (20m) (b) Clyde Sea Area (surface concentrations normalized to 35‰ salinity) (c) North Channel.

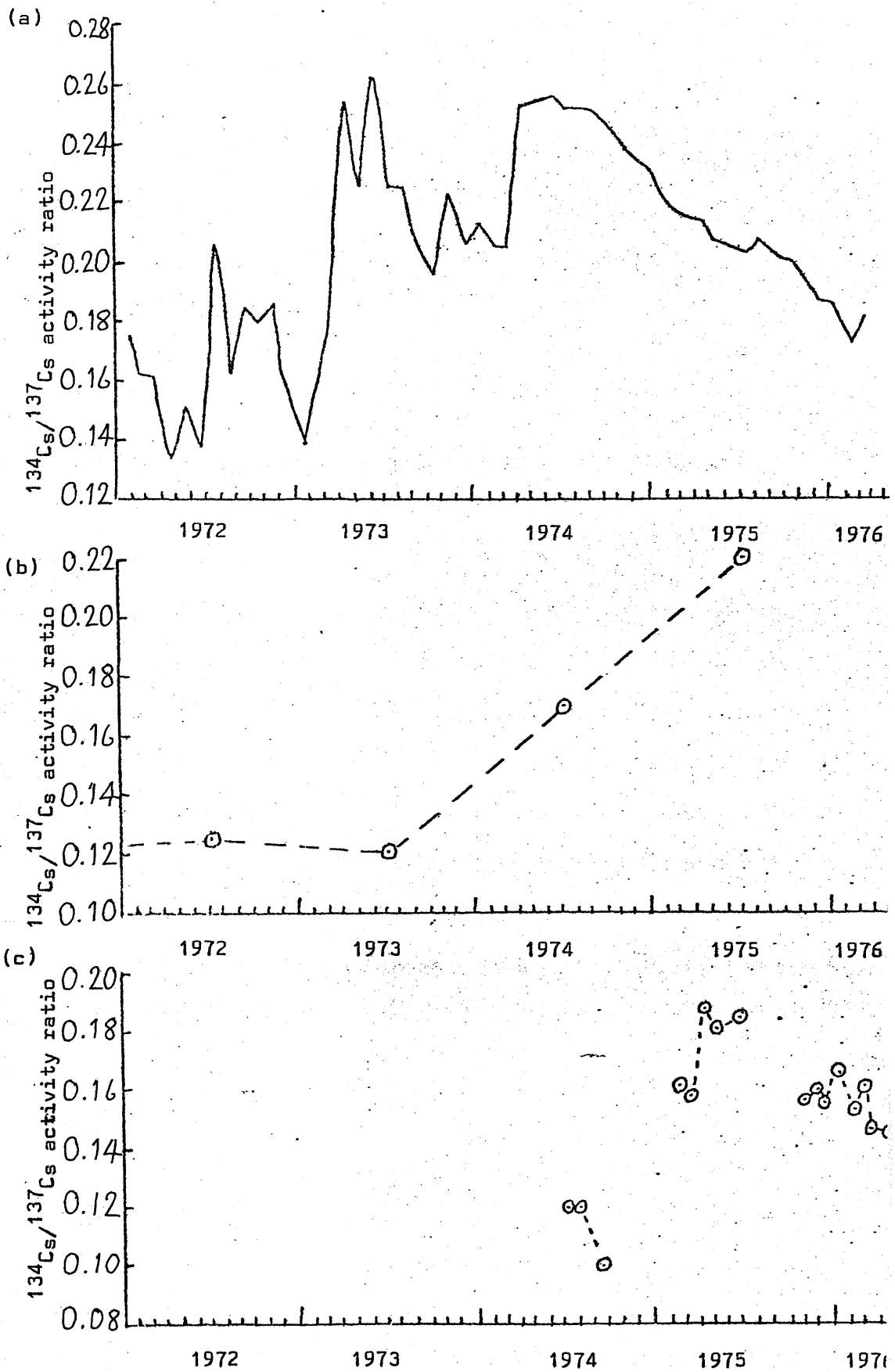


FIGURE 63. $^{134}\text{Cs}/^{137}\text{Cs}$ activity ratio for (a) Windscale effluent
(b) North Channel sea water (c) Clyde Sea Area surface
water.

ratio reached a maximum in April 1975 in the Clyde Sea Area (Figure 63) this further supports the correlation of the May 'peak' in the Clyde with the February maximum in the North Channel. This gives a water transit time of about three months from the North Channel to the Northern section of the Clyde Sea Area, good agreement with this being obtained if the January 1976 Clyde maximum is related to the October - November 1975 maximum in the North Channel.

The above correlation is necessarily non-rigorous as a result of the limited data available but it does indicate that comparison of Clyde Sea Area radiocaesium concentrations with those of the Irish Sea can define water transit times.

Discussion has so far been limited to surface water. The data presented in Tables 27, 35, 36, 44, and 46 however show only small variations in ^{134}Cs and ^{137}Cs concentrations with depth, indicating rapid vertical mixing throughout most of the region (Loch Goil which presents an obvious exception will be considered separately). This homogeneity of vertical distribution is supported by Wilson (1974) who reported no significant variation of ^{137}Cs concentrations with depth in the Irish Sea. Thus the above water transit time of three months derived for surface water is also probably applicable to subsurface water for most of the region.

The use of the radiocaesium observations to derive a water residence time for the Clyde Sea Area is complicated by the fact that water entering from the North Channel mixes to some extent with previously contaminated water, thus altering both the absolute concentration and the $^{134}\text{Cs}/^{137}\text{Cs}$ activity ratio. While a mathematical interpretation of the system could be performed if a steady state situation applied (Thiebaut and Thiebaut 1974 ; Thiebaut 1975), the large variations in rate of input prohibit such a treatment. It is therefore necessary to

apply simplifying approximations to the system in order to estimate a residence time. In the following two attempts, movement of water from the North Channel, during a maximum in ^{137}Cs concentration, into the Clyde Sea Area is approximated to the mixing of large water body of fixed high concentration with a smaller water body of lower but increasing concentration. Since the peaks in caesium concentration are of finite duration relative to the timescale of mixing in the Clyde Sea Area, this approximation will give an upper limit for the residence time.

The first method for estimating the water residence time applies to a situation in which the North Channel water has a markedly higher ^{137}Cs concentration than that of the Clyde Sea Area and involves consideration of the movement of a small volume of water from the North Channel along some undefined path to the Northern section of the Clyde Sea Area. As the water moves through the area mixing may occur with previously contaminated water, Atlantic Ocean water or freshwater and radioactive decay will occur.

Assuming a water travel time within the Clyde Sea Area of

three months:

Let C_1 = initial ^{137}Cs concentration in Clyde Sea Area
 C_2 = initial ^{134}Cs concentration in Clyde Sea Area
 $R_1 = C_2/C_1$
 C_3 = ^{137}Cs concentration in North Channel at peak maximum
 C_4 = ^{134}Cs concentration in North Channel at peak maximum
 $R_2 = C_4/C_3$
 C_5 = ^{137}Cs concentration in Clyde Sea Area at peak maximum
 C_6 = ^{134}Cs concentration in Clyde Sea Area at peak maximum
 $R_3 = C_6/C_5$
 C_7 = ^{137}Cs concentration in Atlantic Ocean surface water

t = water transit time in Clyde Sea Area

λ_1 = decay constant for ^{137}Cs

λ_2 = decay constant for ^{134}Cs

When the water reaches the northern section of the area it could contain ^{134}Cs and ^{137}Cs from (a) incoming water from the North Channel and (b) residual water originally present in the area. A small ^{137}Cs contribution (but no ^{134}Cs) will result from any Atlantic water entering the system.

Considering a unit volume of water at the peak maximum in the Clyde Sea Area:

Let a = proportion of residual 'Clyde' water

b = proportion of incoming North Channel water

d = proportion of incoming Atlantic water

Then

$$\sum ^{137}\text{Cs} = C_5 = aC_1e^{-\lambda_1 t} + bC_3e^{-\lambda_1 t} + dC_7e^{-\lambda_1 t} \quad (1)$$

$$\sum ^{134}\text{Cs} = C_6 = aC_2e^{-\lambda_2 t} + bC_4e^{-\lambda_2 t} \quad (2)$$

$$a + b + d = 1 \quad (3)$$

Substituting $d = 1 - (a+b)$ in (1) gives:

$$C_5 = a(C_1 - C_7)e^{-\lambda_1 t} + b(C_3 - C_7)e^{-\lambda_1 t} + C_7e^{-\lambda_1 t} \quad (4)$$

Evaluation of a , b and d in these simultaneous equation gives the fraction of water replaced within the known transit time. If rapid mixing is assumed then the replacement of water initially present can be regarded as a statistical process in which the rate of removal is proportional to the volume remaining:

$$\text{ie } - \frac{dV}{dt} \propto V$$

$$\text{Thus } V = V_0 e^{-\alpha t}$$

where V_0 is the initial volume present and V is the volume remaining

after some time t . Observation at two distinct times therefore allow evaluation of the constant α , the reciprocal of which represents the mean time that any (infinitely small) volume of water spends in the area ie. the mean residence time.

This model can be applied to the movement of water into the Clyde Sea Area from February to May 1975. A value is required for the ^{134}Cs concentration in the North Channel and the only available estimate is based upon a $^{134}\text{Cs}/^{137}\text{Cs}$ activity ratio of 0.22 - the mean value for the year.

The following data can therefore be applied to the above equations using North Channel values for February 1975 and Clyde Sea Area values for March to May 1975:

$$\begin{aligned} C_1 &= 47 \text{ dpm l}^{-1} & C_2 &= 7.6 \text{ dpm l}^{-1} \\ C_3 &= 128.8 \text{ dpm l}^{-1} & C_4 &= 25.8 \text{ dpm l}^{-1} \\ C_5 &= 79 \text{ dpm l}^{-1} & C_6 &= 13.8 \text{ dpm l}^{-1} \\ C_7 &= 0.2 \text{ dpm l}^{-1} \text{ (assumed value)} \end{aligned}$$

A considerable degree of uncertainty exists in choosing the best values for these variables, giving an inherently large uncertainty in the derived residence time. Thus while results for this and subsequent calculations are given to several decimal places, this is for ease of computational comparison only and is not intended to represent an implied accuracy to this number of significant figures.

Application of the above concentrations gives values:

$$a = 0.529 \quad ; \quad b = 0.426 \quad ; \quad d = 0.045$$

These results therefore indicate that exchange of Clyde Sea Area water is largely with North Channel water and that little additional Atlantic water enters the system. The ratio of new: residual water is 0.471 : 0.529 corresponding to 47.1% replacement of the water within three months. This gives a value for α of 2.547y^{-1}

corresponding to a residence time of 4.7 months. This value is probably too high for two reasons. Firstly the February 1975 peak was very narrow so that if the maximum was missed by even one week in the Clyde Sea Area sampling then the values appropriate for Norch Channel concentrations would be considerably lower. Secondly the above calculation does not take account of freshwater flushing of the area, again giving a larger value for the residence time.

A similar treatment could be applied to the October-November 1975 peak from the North Channel entering the area if a value for the $^{134}\text{Cs}/^{137}\text{Cs}$ activity ratio in the North Channel was available. The mean value for the year cannot be used in this case since it is in fact greater than the value for the effluent corresponding to this peak. Without detailed information on the $^{134}\text{Cs}/^{137}\text{Cs}$ ratio in the North Channel this treatment is therefore of limited value.

A second approach to the evaluation of residence time can be made by considering a steady state exchange of water between the Clyde Sea Area and the North Channel, as follows.

Let V = total volume of Clyde Sea Area

v_0 = the volume of water exchanged per day ($V \gg v_0$)

C_1 = ^{137}Cs concentration in North Channel

C_2 = initial ^{137}Cs concentration in Clyde Sea Area

Two extreme cases can be considered for the behaviour of the incoming water namely complete mixing and no mixing.

If no mixing occurs then after n days, the change in ^{137}Cs concentration in the Clyde Sea Area will be:

$$\Delta [^{137}\text{Cs}] = \frac{v_0}{V} n C_1 - \frac{v_0}{V} n C_2$$

The concentration will therefore be

$$[^{137}\text{Cs}] = C_2 + \frac{v_0}{V} n C_1 - \frac{v_0}{V} n C_2$$

Thus observation of radiocaesium concentrations at two times allows evaluation of the fraction of water replaced in this time interval and so allows evaluation of the residence time.

In the case of complete mixing, the situation is more complex in that water entering the Clyde Sea Area is itself available for exchange back into the North Channel. If the exchange is purely a random process then the probability of water of a particular type

being replaced will be proportioned to the amount present ie. a fixed proportion will be replaced in any given time. Thus the amount of original water being replaced will decrease exponentially while the amount of 'new' water being replaced will increase exponentially.

Thus if v_0 is the total volume being exchanged per day then after t days, the volumes of original and 'new' water being replaced are:

original: $v = v_0 e^{-\beta t}$

new: $v = v_0 (1 - e^{-\beta t})$

where β is a constant.

The total amount of 'original' water replaced is given by:

$$\begin{aligned} v &= v_0 \int_0^t e^{-\beta t} dt \\ &= v_0 \left[-\frac{1}{\beta} e^{-\beta t} \right]_0^t \\ &= \frac{v_0}{\beta} - \frac{v_0}{\beta} e^{-\beta t} \\ &= \frac{v_0}{\beta} (1 - e^{-\beta t}) \end{aligned}$$

This also equals the volume of new water added so that the change in ^{137}Cs concentration is:

$$\Delta [^{137}\text{Cs}] = C_2 - \frac{v_0}{V} \frac{1}{\beta} (1 - e^{-\beta t}) (C_1 - C_2)$$

Since there are two unknowns in this case, three observations of ^{137}Cs concentrations must be made to solve the equation.

The true system of water exchange will lie somewhere between the extremes of no mixing and total mixing which give upper and lower limits respectively when used to calculate the residence time.

This model can be applied by assuming the mean surface water concentrations of ^{137}Cs shown below:

Date	[¹³⁷ Cs] dpm l ⁻¹
4.3.75	47.2
8.4.75	76.2
1.5.75	88 (estimated from salinity data)

and using the values

$$C_1 = 130 \text{ dpm l}^{-1}$$

$$C_2 = 47.2 \text{ dpm l}^{-1}$$

for the initial North Channel and Clyde Sea Area ¹³⁷Cs concentrations.

This gives the simultaneous equations:

$$29 = 47 - \left(\frac{V_0}{V}\right) \frac{1}{\beta} (1 - e^{-35\beta}) 82.8$$

$$40.8 = 47 - \left(\frac{V_0}{V}\right) \frac{1}{\beta} (1 - e^{-58\beta}) 82.8$$

which yield solutions:

$$\beta = 0.0183$$

$$\text{and } \frac{V_0}{V} = 0.00844$$

Assuming a first order process

$$V = V_0 e^{-\alpha t}$$

gives a value for α of 0.00848 d^{-1} corresponding to a residence time of 117.98 days (ie. 0.32 y or 3.9 months).

In the 'no mixing' case, application of the above data generates the two independent equations:

$$76.2 = 47.2 + \frac{V_0}{V} 4550 - \frac{V_0}{V} 1652$$

$$88 = 47.2 + \frac{V_0}{V} 7150 - \frac{V_0}{V} 2737.6$$

both of which give the solution $\frac{V_0}{V} = 0.01$, corresponding to a residence limit of 3.3 months.

The maximum in ¹³⁷Cs concentrations observed in the Clyde Sea Area in January 1976 is not suitable for application of the 'total mixing' model since only two observations are available for the period during which concentrations were increased. The 'no mixing' model can be applied by using the data:

Date	$[^{137}\text{Cs}]$ (dpm l^{-1})
6.11.75	85
4.12.75	117
$C_1 = 160$	$C_2 = 85$

This gives the result $\frac{v_0}{V} = 0.152$, yielding a residence time of 65.1 days (2.14 months).

The residence time for the Clyde Sea Area calculated by these various methods therefore has minimum and maximum limits of 2.1 and 8.2 months respectively. The best estimate is probably that obtained from the 'total mixing' treatment of the May 1975 peak (ie. 3.9 months), although it should be borne in mind that the mean residence time of the water will undoubtedly vary depending upon prevailing conditions.

A residence time of 3.9 months corresponds to a renewal of $1.398 \times 10^8 \text{ m}^3 \text{ day}^{-1}$. This value is considerably in excess of the estimated total freshwater flow and sewage input to the area of $9.46 \times 10^6 \text{ m}^3 \text{ day}^{-1}$ (50% exceedence) and $10^6 \text{ m}^3 \text{ day}^{-1}$ respectively. Thus while the freshwater flow is only a factor of 10 greater than the sewage input, the salt water exchange is a factor of 1000 greater. Assuming a uniform distribution of the sewage throughout the area and applying the residence time of 3.9 months implies a 'standing crop' of $1.18 \times 10^8 \text{ m}^3$ of sewage, diluted by a factor of about 1400 (v/v) from its original concentration. This idealized situation of total dispersion of the sewage will obviously not occur and higher or lower concentrations of sewage will occur depending on local environment.

Beyond these general considerations, a number of sets of samples are worthy of individual consideration and these are discussed below.

Samples C2 - C15 ; C52 - C60. These samples collected from the open Firth (Figures 37 and 45) present the interesting possibility of a localized effect as a result of caesium discharge from Hunterston.

In both sets of samples, values to the south of Hunterston are generally higher than those to the north. There is also a tendency towards higher ^{137}Cs concentrations towards the Ayrshire and Arran coasts with lower values in the central Firth. These effects are illustrated in Figures 64 and 65 which show residual ^{137}Cs concentrations after subtraction of the lowest observed concentration on each date from all other values. These results could therefore be tentatively interpreted as indicating a general southwards dispersion of ^{137}Cs from Hunterston with two dominant flows, one along the Ayrshire coast and the other towards Arran. The available data are again, however, limited and there is no corresponding systematic variation in $^{134}\text{Cs}/^{137}\text{Cs}$ activity ratio. Also the increase in ^{137}Cs concentrations to the south might simply reflect generally increasing concentrations in the area as a result of the increasing output from Windscale. Nevertheless the maximum residual concentrations in each case are considerably outside the error for the measurement and the possibility remains that there is a measurable 'Hunterston effect'. If so, this presents a potentially valuable tracer for this locality especially in consideration of present and planned industrial developments. Any such study would necessarily have to be carried out in close collaboration with the Hunterston reactor authorities as a consequence of the sporadic nature of the discharge of effluent.

Samples C39 - C44

These samples, collected from the upper estuary on 1.5.75, show a fairly good linear correlation between the ^{137}Cs concentration and salinity (Figure 66). A perfect straight line fit is not obtained but given the generally varying concentrations of ^{137}Cs in the area and the highly polluted nature of the estuary, these results are a fairly good indication of conservative behaviour of caesium over the range of conditions encountered in the estuary.

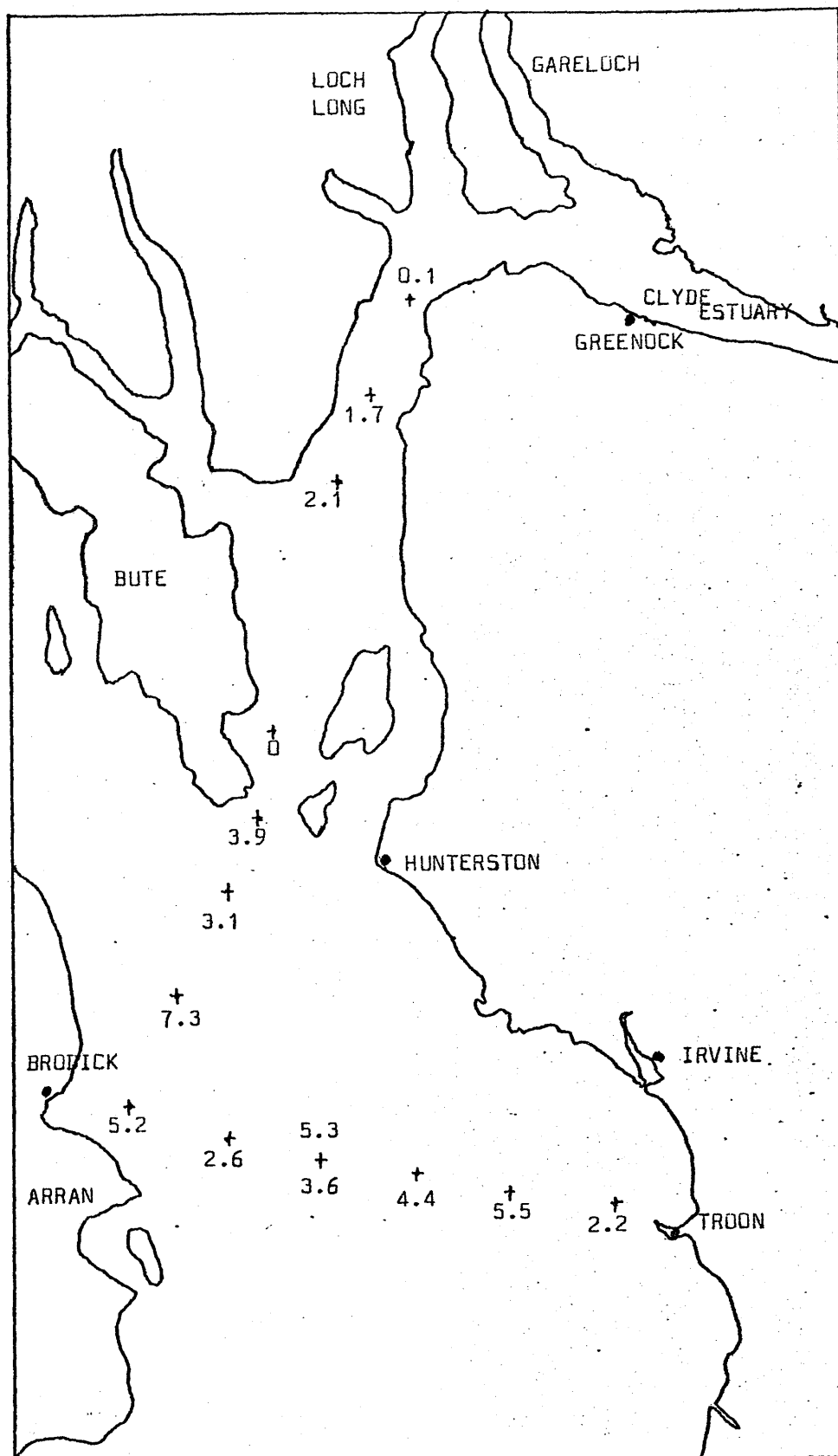


FIGURE 64. Residual ^{137}Cs values for the firth on 30.7.74 after subtraction of the lowest value.

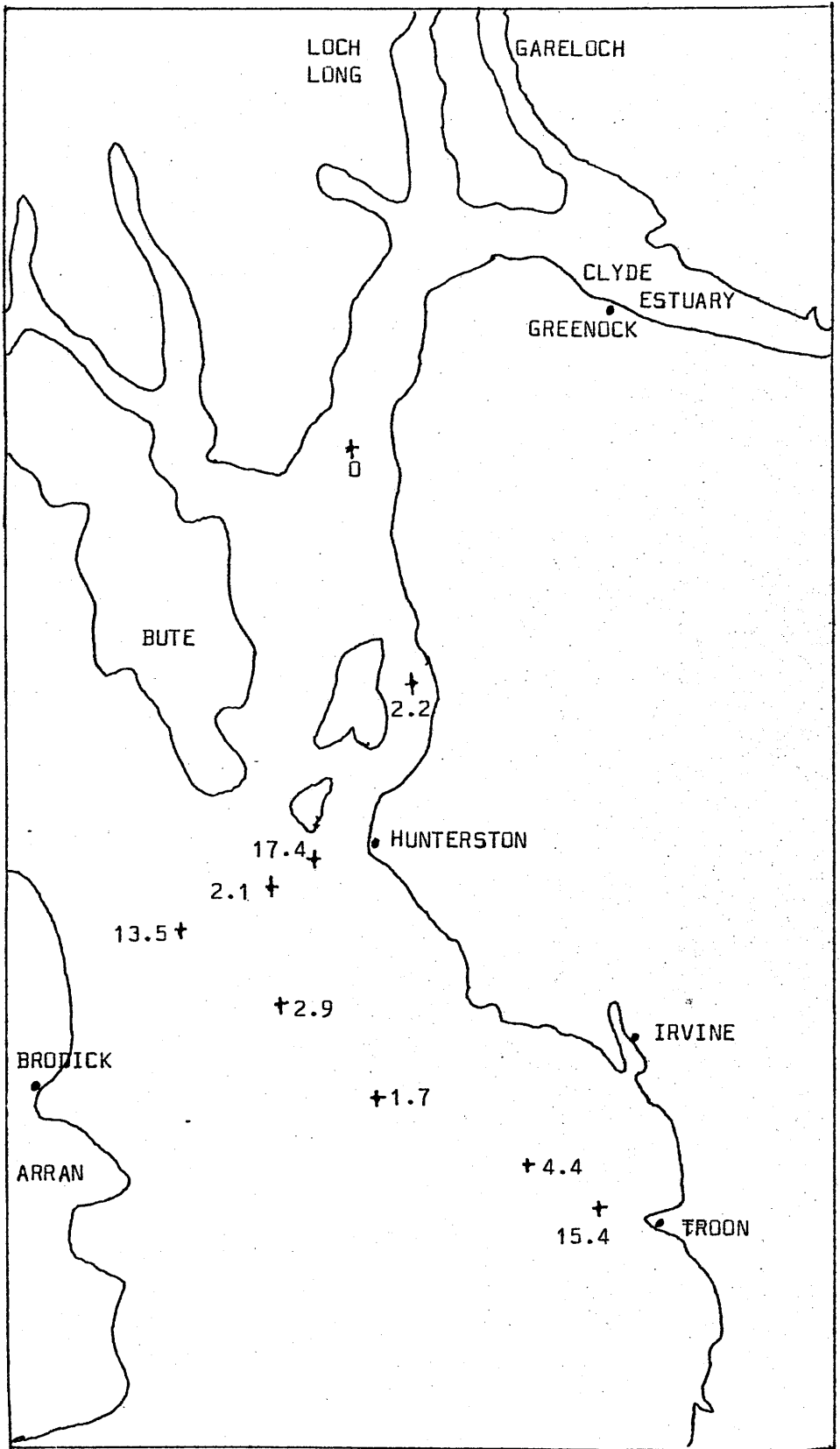


FIGURE 65. Residual ^{137}Cs values for the firth on 14.11.75 after subtraction of the lowest value.

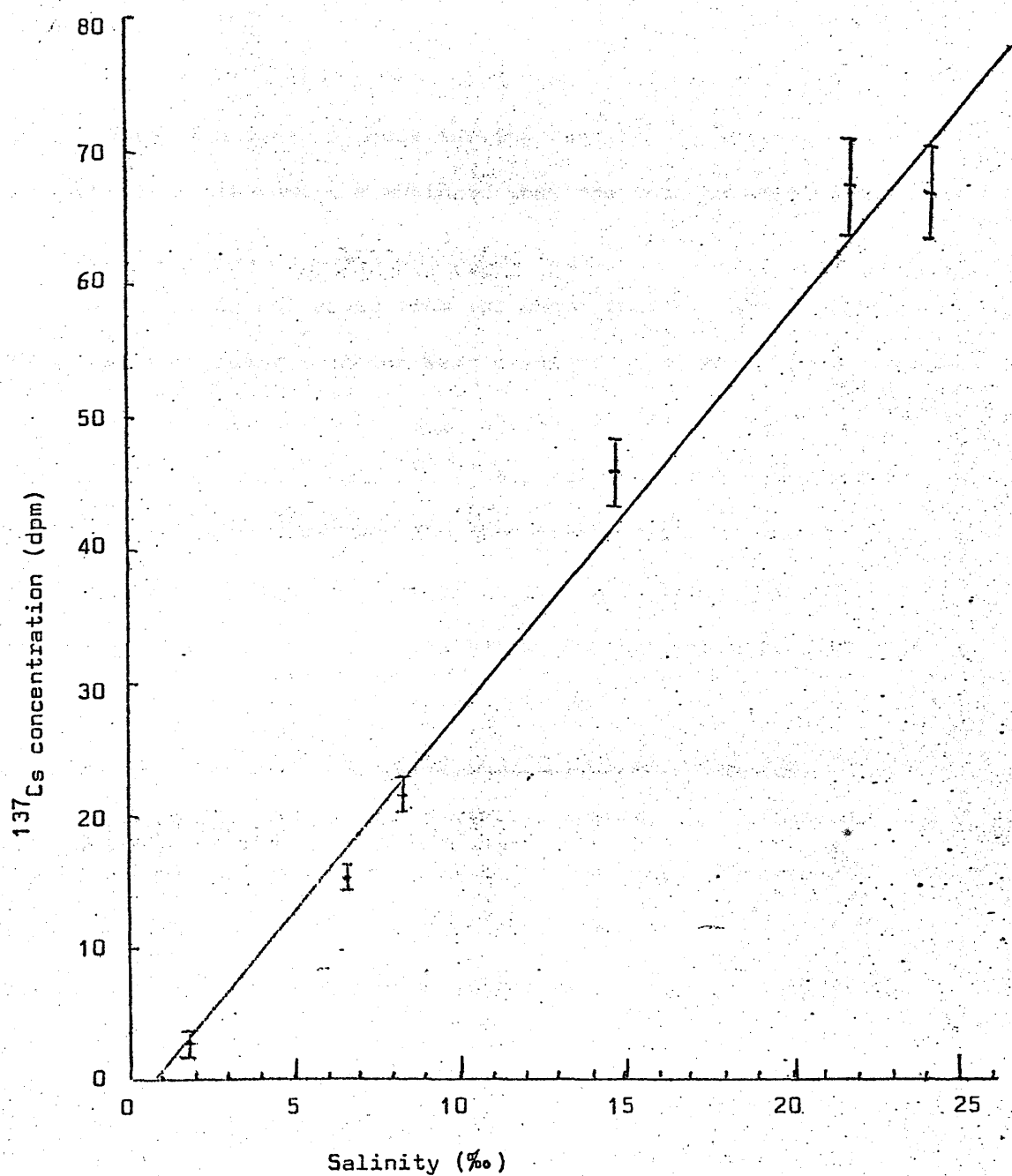


FIGURE 66. Plot of ^{137}Cs concentration versus salinity for samples collected on 1.5.75.

Samples C61 - C63, C76 - C78, C92 - C97 and C107 - C112

These samples for Loch Long indicate no significant variation of ^{137}Cs along the loch or between the east and west sides of the Loch either at the surface or at 25m. Thus Loch Long is indicated to be a well mixed system.

Samples C100 - C106

These samples indicate that Loch Fyne water characteristics are substantially the same as those for the rest of the region, despite its geographical isolation, and indicate that the Loch is well mixed.

Samples C144 - C147

These samples collected from the shore indicate the effects of the Windscale discharge on the West coast of Scotland. The Carsaig and Furnace samples show very good agreement but this is of limited comparative value since salinities were not measured. The sample from Brora shows a ^{137}Cs concentration higher than contemporary fallout levels but this excess cannot be unambiguously assigned to the Windscale discharge since the North Sea receives a considerable input of radionuclides from mainland Europe.

4.2. General aspects of radium concentrations in Clyde Sea Area water.

The complex nature of the marine geochemical and biogeochemical behaviour of radium relative to caesium is apparent by inspection of the radium results. Systematic spatial variations and input and removal processes are not obvious although a definite trend of mean concentrations with time appears to exist. Figure 67 shows the variation of mean ^{226}Ra concentration and $^{228}\text{Ra}/^{226}\text{Ra}$ activity ratio during 1974 and 1975. A wide range of concentrations was observed during the period with very low values of about 40 dpm/1000 l for both ^{228}Ra and ^{226}Ra concentrations in January 1974. Between April and October 1974, ^{226}Ra concentrations rose steadily from 76 to 160 dpm/1000 l while ^{228}Ra concentrations rose from 122 to 224 dpm/1000 l

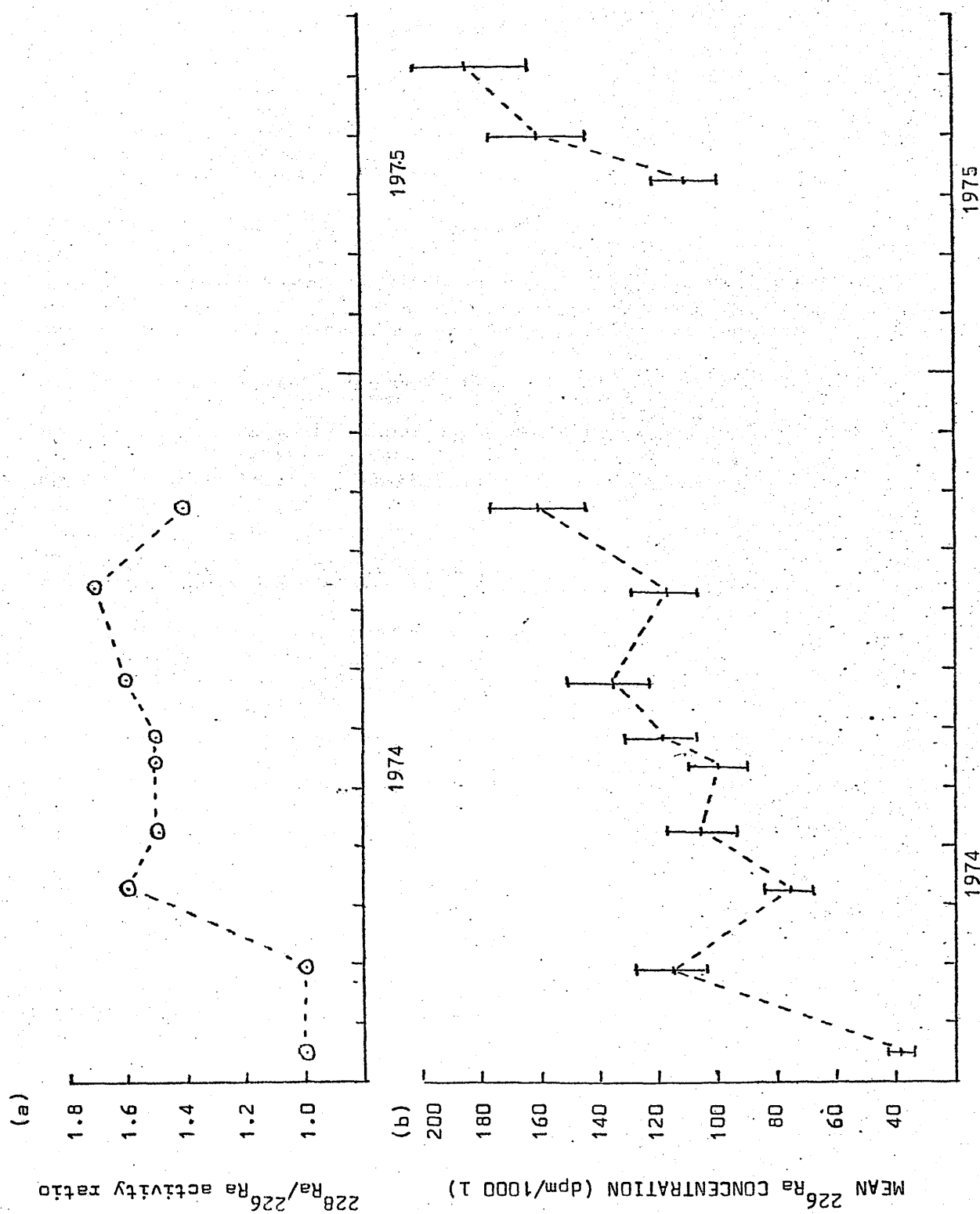


FIGURE 67. Variation of (a) $^{228}\text{Ra}/^{226}\text{Ra}$ activity ratio (b) Mean ^{226}Ra concentration in Clyde Sea Area water during 1974 and 1975.

A large increase in ^{226}Ra concentrations from 110 to 184 dpm/1000 l was again observed during the period April to June 1975. Thus concentrations considerably in excess of the typical Atlantic concentrations of 85 and 25 dpm/1000 l for ^{226}Ra and ^{228}Ra are observed. A number of processes could cause the observed variations in absolute concentration and activity ratio including variable residence time of water in the Clyde Sea Area/Irish Sea, variable river input of radium and biological effects.

The very low values observed in January 1975 can almost certainly be attributed to the prevailing weather conditions at the time, the samples being collected two days after a hurricane (Hurricane Delta) had caused extremely high tides accompanied by large freshwater input due to heavy rainfall. The abnormal conditions are indicated by the depleted salinity values (compare Tables 19, 25 and 36). The low activity ratio would also be compatible with a greater than normal volume of Atlantic water entering the system.

The increase in concentrations during the summers of 1974 and 1975 could indicate a longer residence time in summer than in winter or could be the result of other effects such as biological activity. It is impossible from the radium data alone to identify the cause of the increase but it will be demonstrated later that detailed consideration of radium and caesium concentrations in Loch Goil can at least partially solve this problem. If the increased concentrations are considered as arising from radium diffusion from the sediments then the data for 9.4.74 and 11.6.74 can be used to estimate the radium flux from the sediment. Both sets of samples were collected in the open Firth or estuary and so should be typical of most of the area. The ^{226}Ra enrichment in the 63 days between the two sets of samples was 23 dpm/1000 l which if assumed for the whole Clyde Sea Area gives a

total enrichment of 3.795×10^{12} dpm. This corresponds to an enrichment of 1.7514g from an estimated sediment area of $2.5 \times 10^{13} \text{ cm}^2$ giving a flux of $4 \times 10^{-13} \text{ g } ^{226}\text{Ra cm}^{-2} \text{ y}^{-1}$. A corresponding calculation applied to the ^{228}Ra data for this period gives a flux of $3.29 \times 10^{-17} \text{ g cm}^{-2} \text{ y}^{-1}$. The ^{226}Ra values is somewhat high in comparison to estimates of $1.7 \times 10^{-14} \text{ g } ^{226}\text{Ra cm}^{-2} \text{ y}^{-1}$ (Li et al 1973, Bacon and Edmond, 1972) and $1.2 - 1.8 \times 10^{-14} \text{ g } ^{226}\text{Ra cm}^{-2} \text{ y}^{-1}$ (Koczy 1958) for the flux from deep ocean sediments and $5 \times 10^{-14} \text{ g } ^{226}\text{Ra cm}^{-2} \text{ y}^{-1}$ (Li et al 1973) for the flux from continental shelf sediments.

In theory, this derived flux from the sediments could be used in conjunction with observed enrichments to derive a residence time for the water. However the water entering the Clyde Sea Area is enriched to an unknown extent in the Irish Sea so, without such data, a residence time cannot be estimated. However if the above flux is used with the enrichment relative to Atlantic water then a total residence time for the water in the Clyde Sea Area/Irish Sea can be estimated. This estimate is subject to a very large error since it assumes a mean water depth equal to the mean depth of the Clyde Sea Area, during the total enrichment process, whereas the real system may vary considerably from this. Thus, although absolute values are subject to a very large error, the relative values provide an interesting comparison. Table 58 shows the residence times estimated on this basis for the mean radium data for 1974 and 1975. To compensate for freshwater dilution, a ^{226}Ra concentration of 78 dpm/1000 l has been assumed for Atlantic water. The results indicate a residence time ranging from about 2 months in early 1974 to 8 months by October 1974. Similarly an increase from 3.2 months to 10.5 months is observed between April and June 1975. The values of 2 - 3 months are comparable to the residence time for the Clyde Sea

Date	Mean $[^{226}\text{Ra}]$ (dpm/1000 l)	Estimated residence time. (Months)
26.2.74	116	3.8
9.4.74	76	0
8.5.74	105	2.7
11.6.74	99	2.1
20.6.74	119	4.1
18.7.74	136	5.7
11.9.74	117	3.9
25.10.74	160	8.1
8.4.75	110	3.2
3.6.75	184	10.5

TABLE 58. Estimated combined water residence times for the Clyde Sea Area/Irish Sea based on ^{226}Ra measurements.

Area as previously estimated from the caesium data. Thus if the estimate based on the radium results is correct, it implies that very little Irish Sea water was entering the area in early 1974. This conclusion is in general agreement with Ministry of Agriculture Fisheries and Food estimates of the mean northwards flow of water through the North Channel across a line from Stranraer to Larne as shown in Table 59 (Jefferies, 1975). These data indicate a very weak northwards flow in the period July 1973 - July 1974 with a large increase in July 1974. It is therefore probable that the North Channel water in early 1974 would have contained a much higher proportion of Atlantic water than during the subsequent period. This proposed large Atlantic influence at the start of 1973 is to some extent corroborated by the low $^{228}\text{Ra}/^{226}\text{Ra}$ ratios observed in the Clyde Sea Area during this period.

As with the caesium data, the Loch Goil results will be considered separately and other sets of samples worthy of individual consideration are discussed below.

Samples R10 - R13

These samples show a distinct depletion of ^{226}Ra in the river Leven relative to the Clyde Estuary. Sample R10 which was collected in the estuary just below the entrance of the Leven also show this large dilution. The $^{228}\text{Ra}/^{226}\text{Ra}$ ratio indicates a higher input of ^{228}Ra relative to ^{226}Ra into the Leven than to the estuary. Since the Leven is the only natural outlet for Loch Lomond, the radium concentration might be expected to reflect that of the Loch and the results are generally in good agreement with those obtained by Conlan et al (1969) for Loch Lomond water ranging from 22 to 89 dpm/1000 l and with a mean value of 60 dpm/1000 l.

Period	Estimated flow out of North Channel across Stranraer - Larne line (km ³ day ⁻¹)
October 1971 - May 1972	6.6
May 1972 - July 1973	4.5
July 1973 - July 1974	0.9
July 1974 - November 1974	15.3
November 1974 - July 1975	14.3

TABLE 59. Ministry of Agriculture, Fisheries and Food estimates of northwards flow of water through the North Channel (Jefferies, 1976).

Samples R56 - R66

These samples, collected along the length of the estuary on two separate dates show a relatively good linear correlation of ^{226}Ra concentration with salinity.

In general terms therefore these results show fairly conservative behaviour for radium over the large salinity gradient in the estuary and indicate that this system was stable for at least one month. This in turn indicates that, while river input to the system may be significant, the dominant factor in determining radium concentrations appears to be acting in the 'sea water' part of the system - ie. that part of the area with salinities of 30‰ or greater.

Samples R1 - R3, R7 - R9, R10 - R11, R56

Samples R1 - R3 and R7 - R9 were collected from the upper estuary and freshwater section of the river respectively during a period of high flow rate. The results show a river concentration of ^{226}Ra of 80 - 120 dpm/1000 l. Samples R10 and R11 indicate a ^{226}Ra concentration in the river Leven of 30 - 40 dpm/1000 l. Sample R56, with a ^{226}Ra concentration of 65 dpm/1000 l, is representative of the river input under low flow rate conditions. These values compare favourably with the concentrations of 20 and 70 dpm/1000 l reported by Moore (1967) for the Amazon and Mississippi respectively and with Hammond et al (1975) values of 29 - 64 dpm/1000 l for the Hudson River estuary. The results for the Clyde and Leven are also less than the concentration of 152 dpm/1000 l used by Koczy to estimate the total river supply of

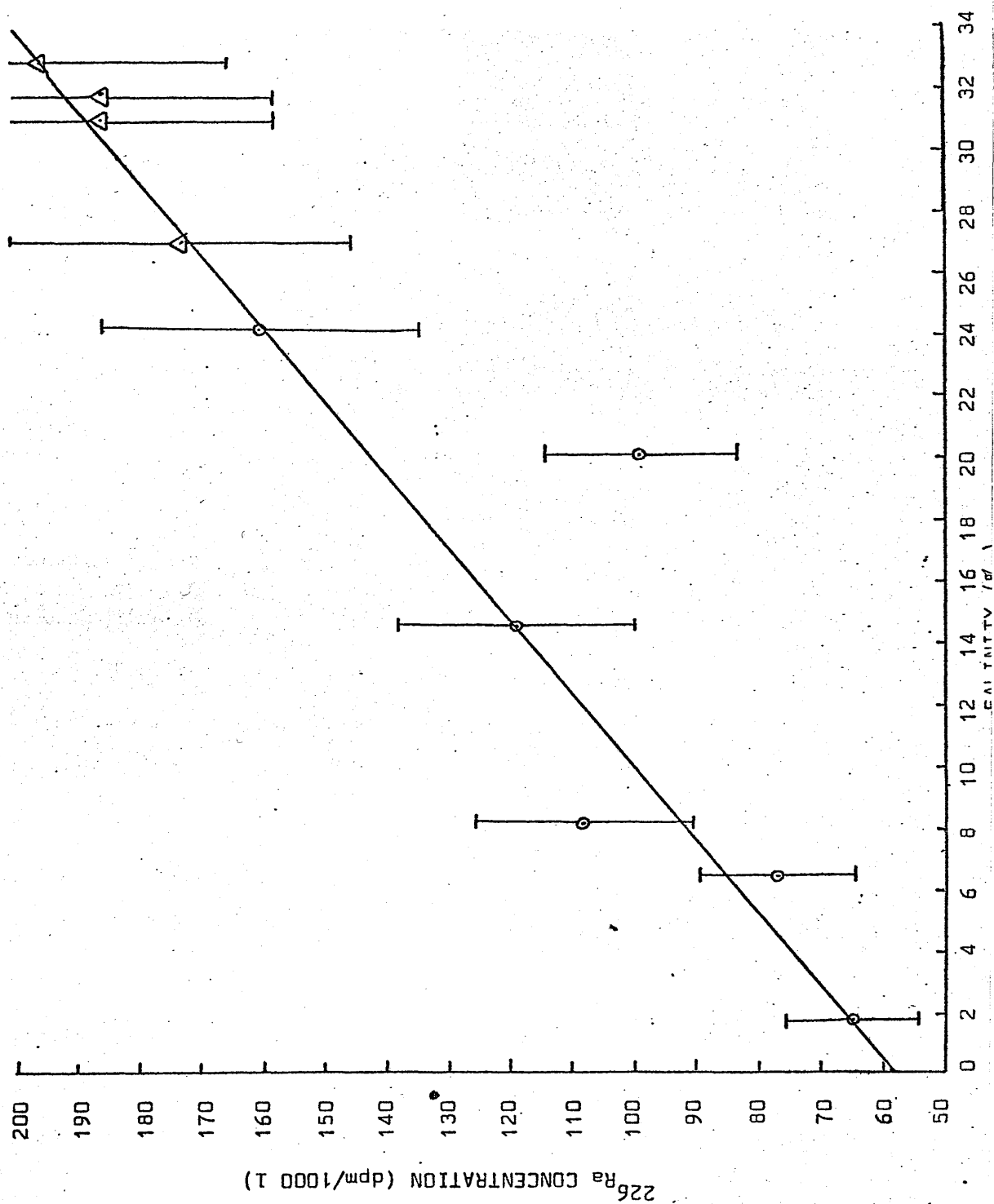


FIGURE 68. Plot of ^{226}Ra concentrations versus salinity for samples collected on 1.5.75 and 3.6.75.

^{226}Ra to the world's oceans and substantiate his calculation of less than 5% of the total oceanic ^{226}Ra inventory being supplied by rivers. This is in contrast to Kuznetsov et al's (1973) conclusion of a much larger river input based on a ^{226}Ra concentration of 867 dpm/1000 l for river water. It should, however, be noted that ^{226}Ra concentration in river water may vary as a function of flow rate and that geological conditions could give rise to varied concentrations in different rivers as suggested by Conlan et al (1969) in explanation of an observed concentration of 266 dpm/1000 l for the river Endrick. Thus while Koczy's original estimate of less than 5% of the ^{226}Ra in the oceans being supplied by rivers has been generally supported by subsequent work, there is still some doubt as to which mean value should be used for ^{226}Ra concentrations in rivers.

4.3. Water circulation and residence time in Loch Goil.

Loch Goil has a maximum depth of 96m but is separated from Loch Long by a sill of depth ranging from 16 to 20m (Figure 2), giving restricted communication with the rest of the Clyde Sea Area. As a result of its semi-enclosed nature, the water properties of the loch can differ markedly from those of water in other parts of the area. As detailed in chapter 1 (pp16 - 17), the annual occurrence of very low dissolved oxygen values in the deep water of the loch suggests a stratification of the water with little vertical mixing. This situation generally exists from mid-summer till early winter when the deep water is rapidly replenished in oxygen. The mechanism of this replenishment and an indication of the reasons for the development of the oxygen depleted state can be derived by consideration of the caesium samples collected between 4.12.75 and 1.4.76.

In order to calculate caesium and salt exchange between surface and deep waters, the volumes of zones in 20m depth increments were calculated from detailed sections drawn to scale and the estimated

volumes are shown below:

Depth zone (m)	km ³	Volume
		l
0 - 20	0.142	1.42×10^{11}
20 - 40	0.0997	9.97×10^{10}
40 - 60	0.0560	5.60×10^{10}
60 - 96	0.0217	2.17×10^{10}

This gives a total volume for the loch of 0.319 km^3 which is in good agreement with the Clyde River Purification Board's value of 0.310 km^3 (Table 1).

Surface water concentrations of radiocaesium in Loch Goil vary rapidly and after salinity correction are generally similar to those in Loch Long. In the following discussion it will therefore be assumed that exchange of surface water is rapid and that the surface zone (0 - 20m) has a very low residence time relative to the deep water (20 - 96m). Comparison of samples from similar depths at station 1 and 2 on any occasion reveals little significant difference. The loch is therefore assumed to be horizontally homogeneous and the data for station 2 are taken as representative of whole loch.

If the distribution of radiocaesium and salinity on 4.12.75 is regarded as an initial state and mixing of different water types present is taken as producing the distribution observed on 8.1.76 then the mechanism and rate of mixing can be deduced as follows. On 4.12.75.

Assuming mean $[^{137}\text{Cs}]$ 0 - 20m = 110 dpm l^{-1}

Then total inventory of ^{137}Cs from 0 to 20m = $1.562 \times 10^{13} \text{ dpm}$

Assuming mean $[^{137}\text{Cs}]$ 20 - 40m = 106 dpm l^{-1}

and mean $[^{137}\text{Cs}]$ 40-96m = 93 dpm l^{-1}

Then total inventory of ^{137}Cs from 20 to 96m = $1.779 \times 10^{13} \text{ dpm}$

On 8.1.76

Assuming mean $[^{137}\text{Cs}]$ 0 - 20m = 106 dpm l^{-1}

Then total inventory of ^{137}Cs from 0 - 20m = 1.505×10^{13} dpm

Assuming mean $[^{137}\text{Cs}]$ 20 - 40m = 117 dpm l^{-1}

mean $[^{137}\text{Cs}]$ 40 - 60m = 113 dpm l^{-1}

and mean $[^{137}\text{Cs}]$ 60 - 96m = 104 dpm l^{-1}

Then total inventory of ^{137}Cs from 20 to 96m = 2.025×10^{13} dpm

The change in total inventory of ^{137}Cs in the 20 to 96m zone is therefore 2.4597×10^{12} dpm.

If mean values of 110 dpm l^{-1} and 95 dpm l^{-1} are assumed for the 0 - 20 and 20 - 96m sections respectively then the observed increase in ^{137}Cs content would require the replacement of 1.6398×10^{11} l of deep water by surface water. Since the 20 - 96m section has a total volume of 1.774×10^{11} l, this implies 92.4% replacement of the deep water. Thus, neglecting density effects and assuming mean salinities of 32.02‰ and 32.8‰ for the surface and deep waters respectively, the resultant salinity of the deep water would be:

$$S = (0.924 \times 32.02 + 0.076 \times 32.8)\text{‰}$$

$$= 32.08\text{‰}$$

However the observed mean salinity of the deep water on 8.1.76 was 32.7‰ indicating that mixing with surface water is probably not the mechanism for deep water renewal. If the water at 20m on 4.12.75 is regarded as the source of the ^{137}Cs increase and its ^{137}Cs concentration and salinity are taken as 117 dpm l^{-1} and 32.75‰ then displacement of 1.118×10^{11} l of deep water would be required, giving a net salinity of 32.77‰. This mechanism is in much better agreement with the observed mean salinity of 32.7‰ on 8.1.76.

Thus from the available data the best estimate of the volume of deep water replaced in the 35 days between the two sets of samples

is 1.118×10^{11} l, corresponding to 3.194×10^9 l day⁻¹ or $36.97 \text{m}^3 \text{sec}^{-1}$

This compares to the fresh water flow in the loch of:

95% exceedence	50% exceedence	5% exceedence
$17.8 \text{m}^3 \text{sec}^{-1}$	$1.7 \text{m}^3 \text{sec}^{-1}$	$0.3 \text{m}^3 \text{sec}^{-1}$

If no mixing is assumed, this result implies total replacement of all deep water in 56 days. If however total mixing is assumed and a fixed amount of water is assumed to exchange per unit time then applying the equation

$$V = V_0 e^{-\alpha t}$$

gives a value of 0.0284 day^{-1} for α corresponding to a mean residence time of water in the loch of 35.2 days.

The $^{134}\text{Cs}/^{137}\text{Cs}$ activity ratio in the deep water increases slightly from 4.12.75 to 8.1.76, in general agreement with the above mechanism. However the most significant aspect of the activity ratio is its relatively homogeneous vertical distribution on both dates. The 2σ value of ± 0.008 corresponds to a time of 2.1 months so that on both dates it can be stated that total vertical mixing of the 20 - 75m section of water occurs in less than 2.1 months. The true mixing time is probably less than this since most of the data points are inside the 2σ error relative to each other.

A similar treatment can be applied to the data for 3.3.76:

Assuming mean $[^{137}\text{Cs}]$ 0 - 20m = 97 dpm l^{-1}

and mean $[^{137}\text{Cs}]$ 20 - 96m = 104 dpm l^{-1}

then a net decrease of 1.80×10^{12} dpm of ^{137}Cs had occurred since 8.1.76.

If surface water is regarded as displacing the deep water then a volume of 1.06×10^{11} l would be required giving a resultant salinity of 30.5‰. whereas the observed mean deep water salinity on 3.3.76 is 32.7‰. Thus replacement of deep water by surface water is again incompatible with conservation of salt considerations. The

deep water on 3.3.76 in fact exhibits a virtually constant ^{137}Cs profile with a mean value of 104 dpm l^{-1} , implying total displacement of the water in this section within the 55 days between observations. The $^{134}\text{Cs}/^{137}\text{Cs}$ activity ratio shows a corresponding uniform decrease verifying this conclusion.

The same treatment can again be applied to the data for 3.3.76 and 1.4.76.

On 1.4.76.

Assuming mean $[^{137}\text{Cs}]_{20-96\text{m}} = 96 \text{ dpm l}^{-1}$

Then the total inventory of ^{137}Cs from 20 to 96m = $1.703 \times 10^{13} \text{ dpm}$ corresponding to a decrease of $1.42 \times 10^{12} \text{ dpm}$ since 3.3.76. If mixing with surface water is assumed to account for the decrease then a displacement of $1.01 \times 10^{11} \text{ l}$ would be required giving a resultant salinity of 31.3‰ whereas the observed mean salinity is 32.7‰. Thus the incompatibility of surface water mixing to give deep water renewal is again apparent.

Again the vertical homogeneity of both the absolute ^{137}Cs concentration and the $^{134}\text{Cs}/^{137}\text{Cs}$ activity ratio imply virtually total replacement of the deep water between the two sampling dates and salinity considerations are again consistent with water from 20m being responsible for the displacement. This would require a minimum water exchange rate of $6.12 \times 10^9 \text{ l day}^{-1}$ corresponding to a maximum mean residence time of 28.5 days.

On the basis of the radiocaesium data it therefore appears that the renewal of Loch Goil deep water is by mixing with water typified by that at 20m with little or no surface contribution. The development of the oxygen depleted state is therefore probably due to the transient existence of some factor inhibiting this exchange. The most probable factor hindering vertical mixing is a strong density gradient or pycnocline and to test this hypothesis, the density

distributions for the Loch Goil sampling dates were estimated. Since the density of sea water varies in a complex manner as a function of salinity, temperature and pressure, its accurate calculation is a subject of much complexity. An approximation is therefore used here in which pressure effects are ignored and the density of the water is derived from chlorinity/temperature/density tables presented by Riley and Skirrow (1975). The relationship between chlorinity and salinity used is:

$$S‰ = 1.80655 Cl‰$$

(Wallace, 1974)

The values derived are shown in Table 60 and plotted in Figure 69.

The density distribution for 4.12.75 shows a strong gradient from 0 to 20m with a lesser, but measurable, gradient from 20 to 60m. In contrast, the profiles for 8.1.76, 3.3.76 and 1.4.76 show very little gradient below 20m but have large gradients from 0 to 20m. This substantiates the previous conclusion that little downwards mixing of the surface water is likely.

It would therefore appear that the limiting factor in the renewal of Loch Goil deep water, and consequently in the maintenance of dissolved oxygen concentrations, is the magnitude of the density gradient below 20m, a strong gradient preventing efficient exchange. This is verified by the density and dissolved oxygen data for 18.7.74 and 10.9.74 where a strong pycnocline below 20m is accompanied by depleted oxygen conditions. The profiles for 25.10.74 show the penetration of higher dissolved oxygen values into the deep water with the removal of the pycnocline. Similarly the profiles for 8.4.75 show virtually no density gradient below 20m and high dissolved oxygen values at all depths.

The circulation of Loch Goil can therefore almost certainly be

8.5.74; Station 1

Depth (m)	Density (g ml ⁻¹)
0	1.0243
10	1.0243
20	1.0245
30	1.0245
40	1.0247
50	1.0249
60	1.0249
70	1.0250

18.7.74; Station 1

Depth (m)	Density (g ml ⁻¹)
0	1.0222
10	1.0233
20	1.0235
30	1.0237
40	1.0240
50	1.0242

10.9.74; Station 1

Depth (m)	Density (g ml ⁻¹)
0	1.0181
3	1.0226
10	1.0238
25	1.0247
50	1.0253
65	1.0253
80	1.0254

25.10.74; Station 1

Depth (m)	Density (g ml ⁻¹)
0	1.0252
3	1.0249
10	1.0252
25	1.0252
50	1.0249
65	1.0250
80	1.0250

8.4.75; Station 1.

Depth (m)	Density (g ml ⁻¹)
0	1.0254
13	1.0254
28	1.0255
38	1.0255
53	1.0256
68	1.0256

4.12.75; Station 1

Depth (m)	Density (g ml ⁻¹)
0	1.0237
10	1.0244
20	1.0250
30	1.0251
40	1.0251
50	1.0253
60	1.0253

TABLE 60. (continued over)

4.12.75 ; Station 2

Depth (m)	Density (gml ⁻¹)
0	1.0232
10	1.0245
20	1.0250
30	1.0250
40	1.0257

8.1.76 ; Station 1

Depth (m)	Density (gml ⁻¹)
0	1.0199
10	1.0225
20	1.0250
30	1.0251
40	1.0251
50	1.0251
60	1.0252
70	1.0252
80	1.0252

8.1.76 ; Station 2

Depth (m)	Density (gml ⁻¹)
0	1.0123
10	1.0225
20	1.0250
30	1.0250
40	1.0251
50	1.0254

3.3.76 ; Station 1

Depth (m)	Density (gml ⁻¹)
10	1.0239
20	1.0251
30	1.0253
40	1.0254
50	1.0253
60	1.0254
70	1.0254
80	1.0253

3.3.76 ; Station 2

Depth (m)	Density (gml ⁻¹)
0	1.0221
10	1.0233
20	1.0252
30	1.0253
40	1.0253

TABLE 60. (continued over)

1.4.76 : Station 1

Depth (m)	Density (gml ⁻¹)
0	1.0214
10	1.0239
20	1.0253
30	1.0255
40	1.0256
50	1.0255
60	1.0255
70	1.0255

1.4.76 : Station 2

Depth (m)	Density (gml ⁻¹)
0	1.0213
10	1.0236
20	1.0250
30	1.0252
40	1.0252
50	1.0256

1.4.76 : Station 3

Depth (m)	Density (gml ⁻¹)
0	1.0199
10	1.0232
20	1.0252
30	1.0255
40	1.0255

TABLE 60. Estimations of density profiles for Loch Goil 1974-1976.

(Based on Chlorinity/temperature/density tables from
Riley and Skirrow, 1975).

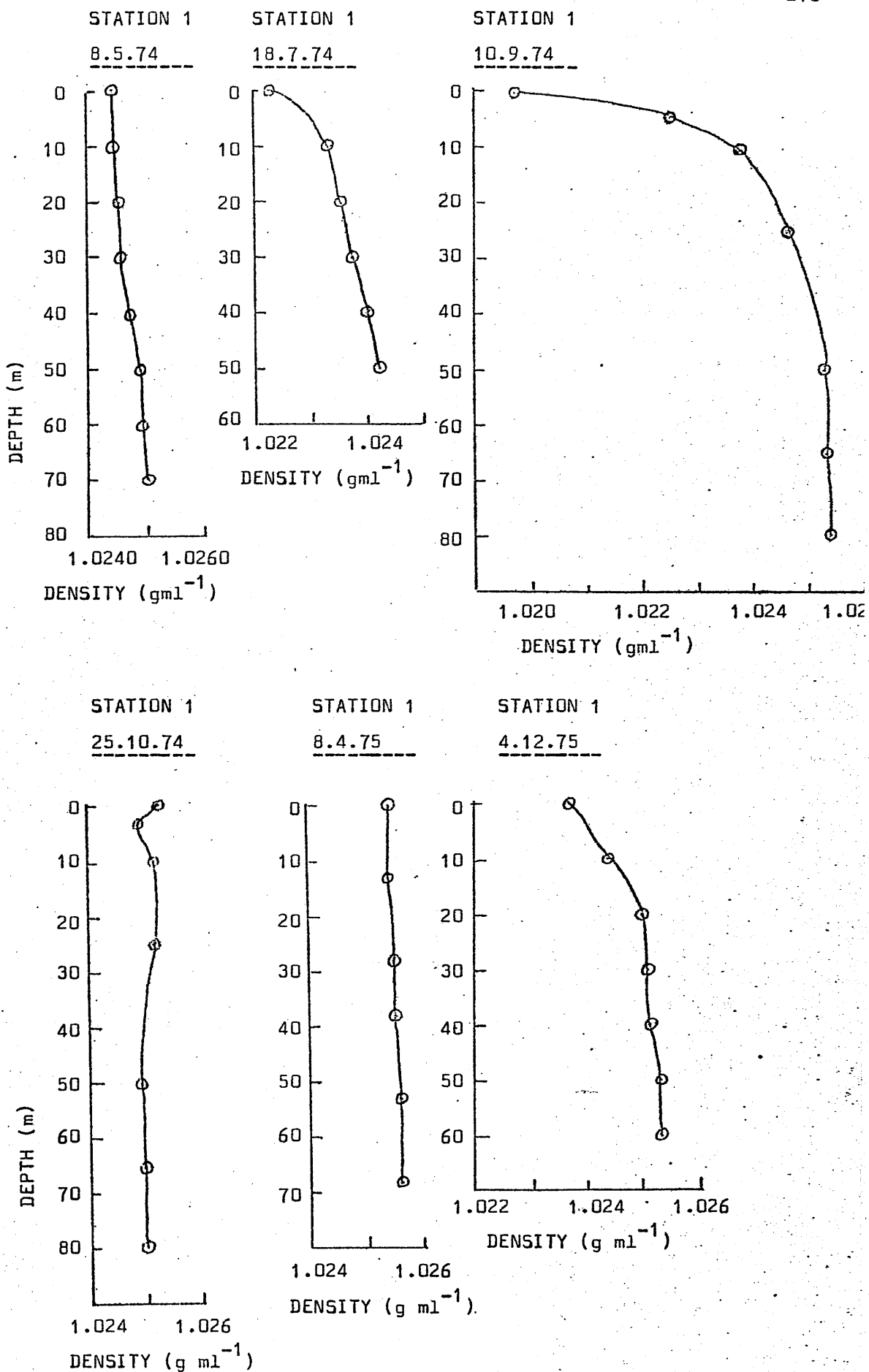


FIGURE 69. (continued over)

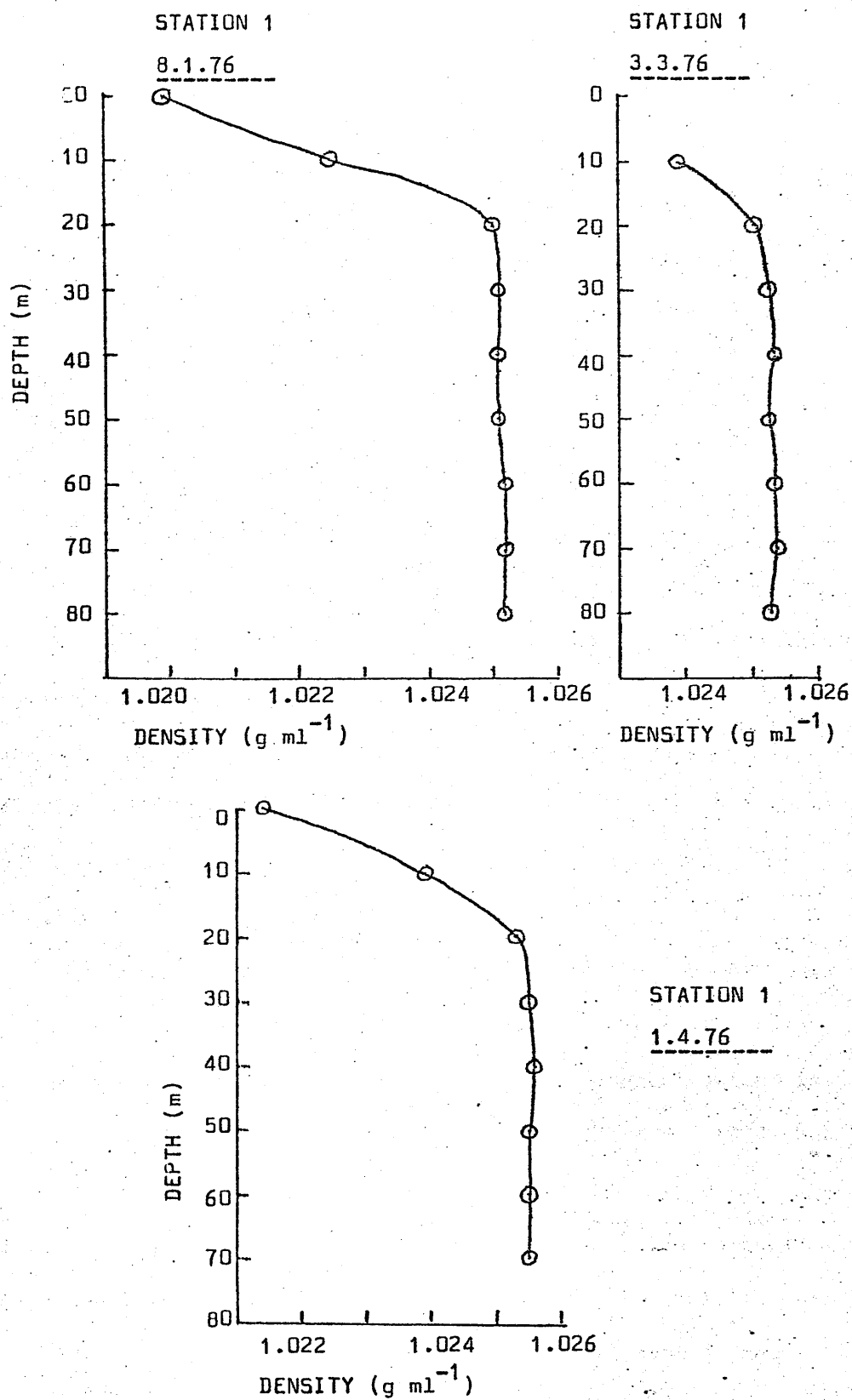


FIGURE 69. Loch Gail density profiles 1974 - 1976.

defined as an 'estuarine' system with a surface outwards flow of low salinity water and a corresponding subsurface inflow of higher salinity water. Interruption of this normal circulation by the extension of a strong pycnoline below 20m prevents renewal of deep water and leads to oxygen depleted conditions as a result of the decay of organic debris. This situation generally arises in late summer due to heating and fresh water input to the surface water at a time when biological activity is high. Under conditions with a small density gradient below 20m, the residence time of the water is probably a month or less but in the converse situation, little renewal of deep water may occur over several months. Even under the 'stratified' condition however the $^{134}\text{Cs}/^{137}\text{Cs}$ activity ratio data indicates that internal mixing within the oxygen depleted water probably occurs in less than 2.1 months.

On the basis of this model, the radium data for Loch Goil during 1974 can now be interpreted and this in turn reveals a valuable indication of the controlling factors of radium concentrations in this environment. The four sets of radium profiles for 1974 when considered in isolation show virtually no systematic trends. The samples for 8.5.74 show a tendency towards higher ^{226}Ra concentrations at the surface with a maximum in the $^{228}\text{Ra}/^{226}\text{Ra}$ profile at about 40m. The absolute ^{226}Ra concentration shows little variation in the 18.7.74 profile but the lower values at 30 and 65m show correspondingly low ratio values. The only notable point in the 10.9.74 profiles is the occurrence of high ratio values at the surface and 60m. The 25.10.74 profiles indicate an erratic ^{226}Ra distribution with a strong tendency to low ratio values at depth.

Thus despite the fact that considerable variations are observed in both ^{226}Ra concentrations and the $^{228}\text{Ra}/^{226}\text{Ra}$ activity ratio, no

interpretative model is obvious. On the basis of the observed oceanic correlation of ^{226}Ra with silicate concentrations, silicate data were obtained from the Clyde River Purification Board (Leatherland, 1976) for this station at the closest available dates to the radium samples. The silicate profiles are shown in Figure 70. While no strong correlation of the individual profiles is observed a systematic trend is apparent if the total inventory of silicate and ^{226}Ra is estimated on the basis of the previously defined 20m depth zones. The estimated total inventories are shown in Table 61 and plotted in Figure 71. The plot of total ^{226}Ra versus total silicate is also shown in Figure 71, revealing a strong linear correlation. It is therefore reasonable to assume that the concentrations of ^{226}Ra and silicate are dominantly controlled by some common factor - almost certainly the intermittent blooms and subsequent death, sinking and decay of siliceous plankton. The general increasing trend in both ^{226}Ra and silicate concentrations during the summer reflects the increasing amount of decaying siliceous material in the loch and the large increase observed on 25.10.74 probably marks the end of the plankton blooms with the onset of winter conditions.

The gradient of the ^{226}Ra versus silicate graph must represent the ratio of ^{226}Ra to silicate in the plankton thus giving an estimate of the enrichment factor for ^{226}Ra . The gradient of $10^{10} \text{ dpm } ^{226}\text{Ra} / 1.4 \times 10^6 \text{ M silicate}$ corresponds to a ratio of $3.4 \times 10^{-11} \text{ g } ^{226}\text{Ra} / \text{g silicate}$, giving an enrichment factor of 6.2×10^5 for ^{226}Ra relative to an assumed water concentration of $1.2 \times 10^{-4} \text{ dpm g}^{-1}$. Since the plankton is only partially composed of silicate, this figure cannot be regarded as representative of the whole organism. However if silicate is assumed to compose 10% by weight of plankton then the

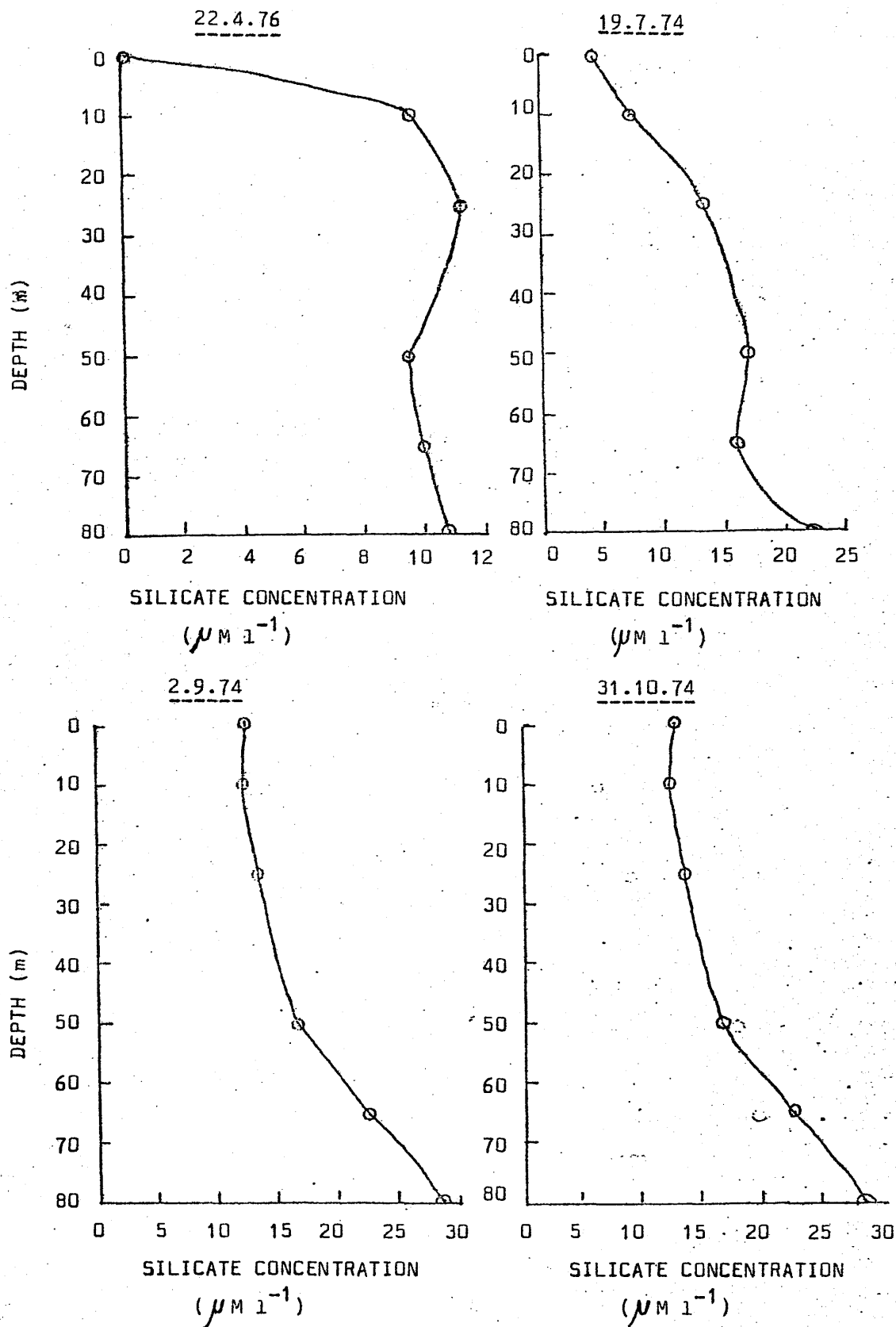


FIGURE 70. Silicate profiles for Loch Goil station 1 during 1974
(Leatherland, 1976).

DATE	TOTAL INVENTORY OF ^{226}Ra (dpm)	TOTAL INVENTORY OF SILICATE (M)
8.5.74	3.58×10^{10}	2.7×10^6
18.7.74	4.30×10^{10}	3.6×10^6
10.9.74	3.57×10^{10}	3.0×10^6
25.10.74	4.93×10^{10}	4.6×10^6

TABLE 61. Estimated total inventories of ^{226}Ra and silicate for Loch Goil during 1974.

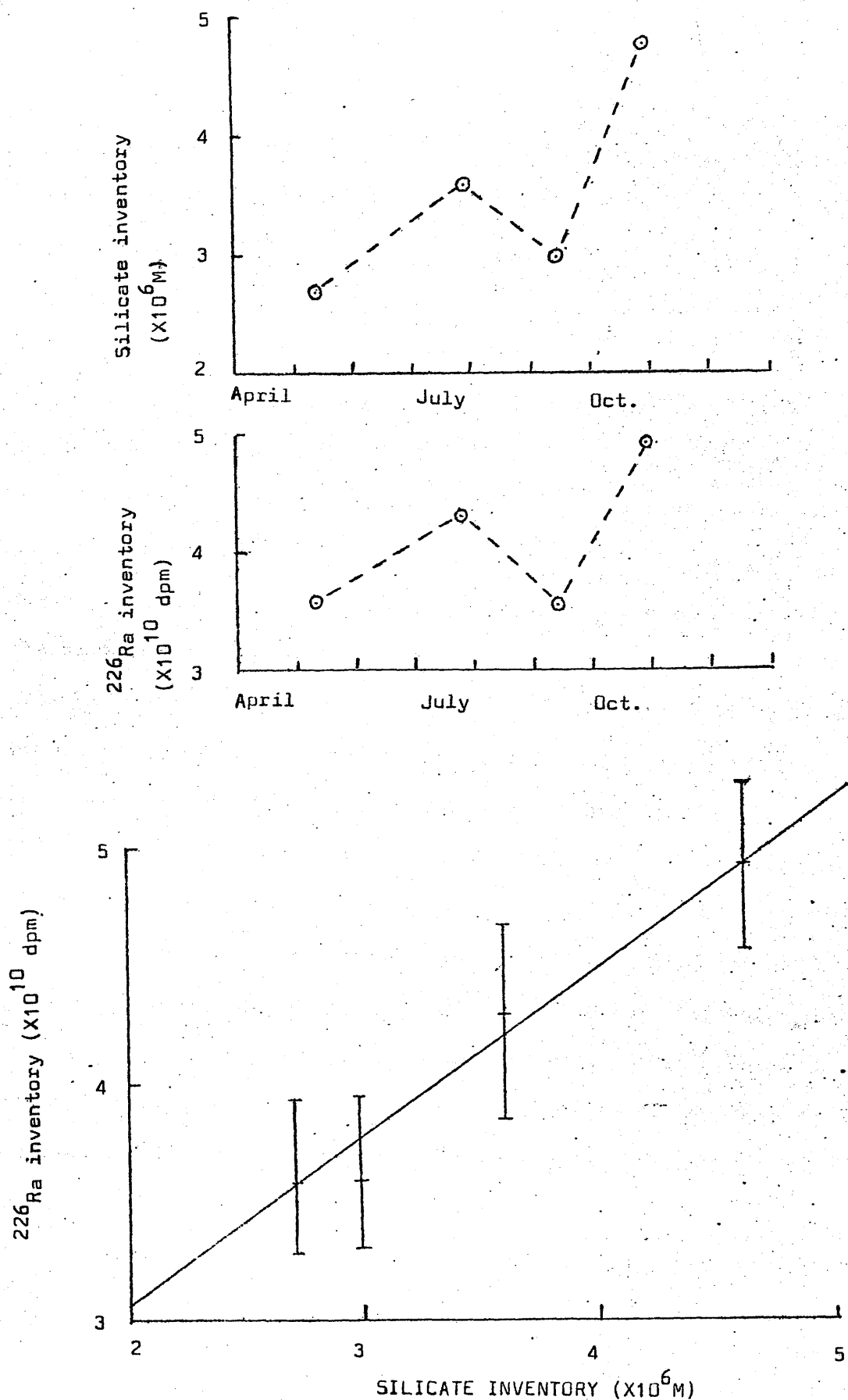


FIGURE 71. (a) Total silicate inventory for Loch Goil during 1974.
 (b) Total ^{226}Ra inventory for Loch Goil during 1974.
 (c) Plot of total ^{226}Ra inventory versus total silicate inventory for Loch Goil during 1974.

^{226}Ra concentration and enrichment factor become 3.4×10^{-12} g/g silicate and 6.2×10^4 respectively. These conclusions are in good agreement with Shannon and Cherry (1971) who reported ^{226}Ra concentrations of 1.0×10^{-12} to 7.7×10^{-12} g $^{226}\text{Ra/g}$ of dry phytoplankton corresponding to an enrichment factor of 7.3×10^4 (wet weight). As reported by Shannon and Cherry, this result is also in good agreement with the figure of about 2×10^{-12} g $^{226}\text{Ra/g}$ dry phytoplankton obtained by Föyn et al, Koczy and Titze (1959) and Cerrai et al.

A further interesting aspect of the Loch Goil radium data is that during the 'stratified' condition of the loch, there is a net scavenging of radium from the rapidly exchanging surface water to the deep waters. $^{228}\text{Ra}/^{226}\text{Ra}$ activity ratios in Clyde Sea Area water at the start of 1974 were low so that any radium taken into the biological cycle at the start of the year and returned to the deep water at a later date could give a deep water depression of the $^{228}\text{Ra}/^{226}\text{Ra}$ relative to surface water. This situation was observed on 25.10.74 and to a lesser extent on 10.9.74. Since this process will be directly related to the dissolution of siliceous plankton which in turn is indirectly related to the oxygen consumption in the deep waters, the graphs of $^{228}\text{Ra}/^{226}\text{Ra}$ ratio versus silicate, $^{228}\text{Ra}/^{226}\text{Ra}$ ratio versus dissolved oxygen and silicate versus dissolved oxygen were plotted and are shown in Figures 72, 73 and 74 respectively. The silicate versus $^{228}\text{Ra}/^{226}\text{Ra}$ graphs show an increasing tendency towards linearity from 8.5.74 to 10.9.74 followed by a large deviation from linearity on 25.10.74 and this trend is in fact similar to that observed in the other two sets of graphs. This may indicate a maximum effect of biological cycling observed on 10.9.74 with a disruption of the system by 25.10.74 as a result of the incursion

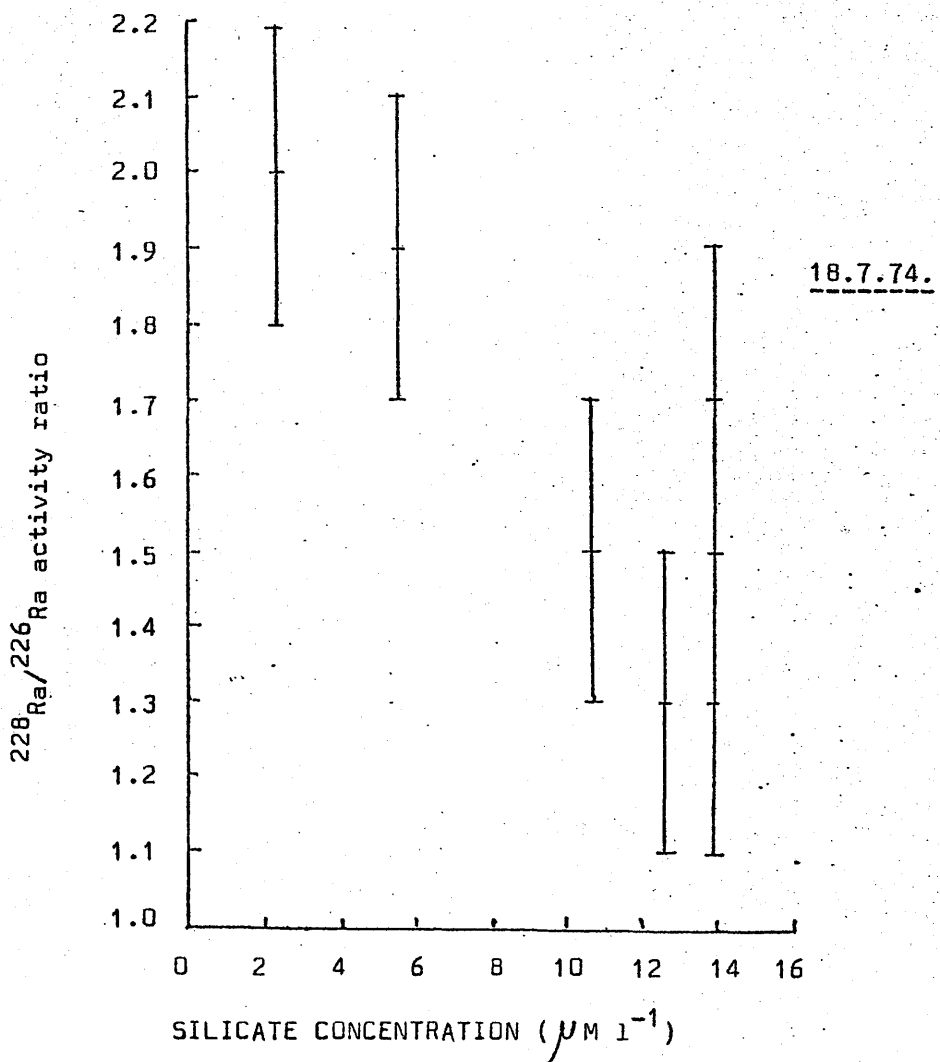
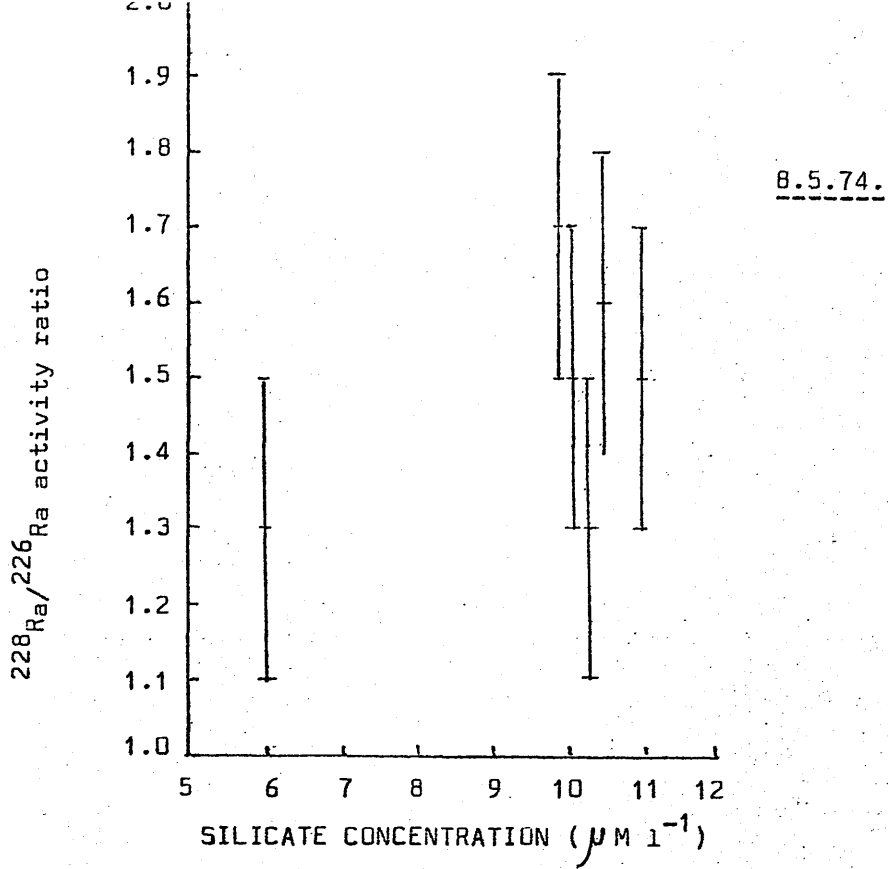


FIGURE 72. (continued over.)

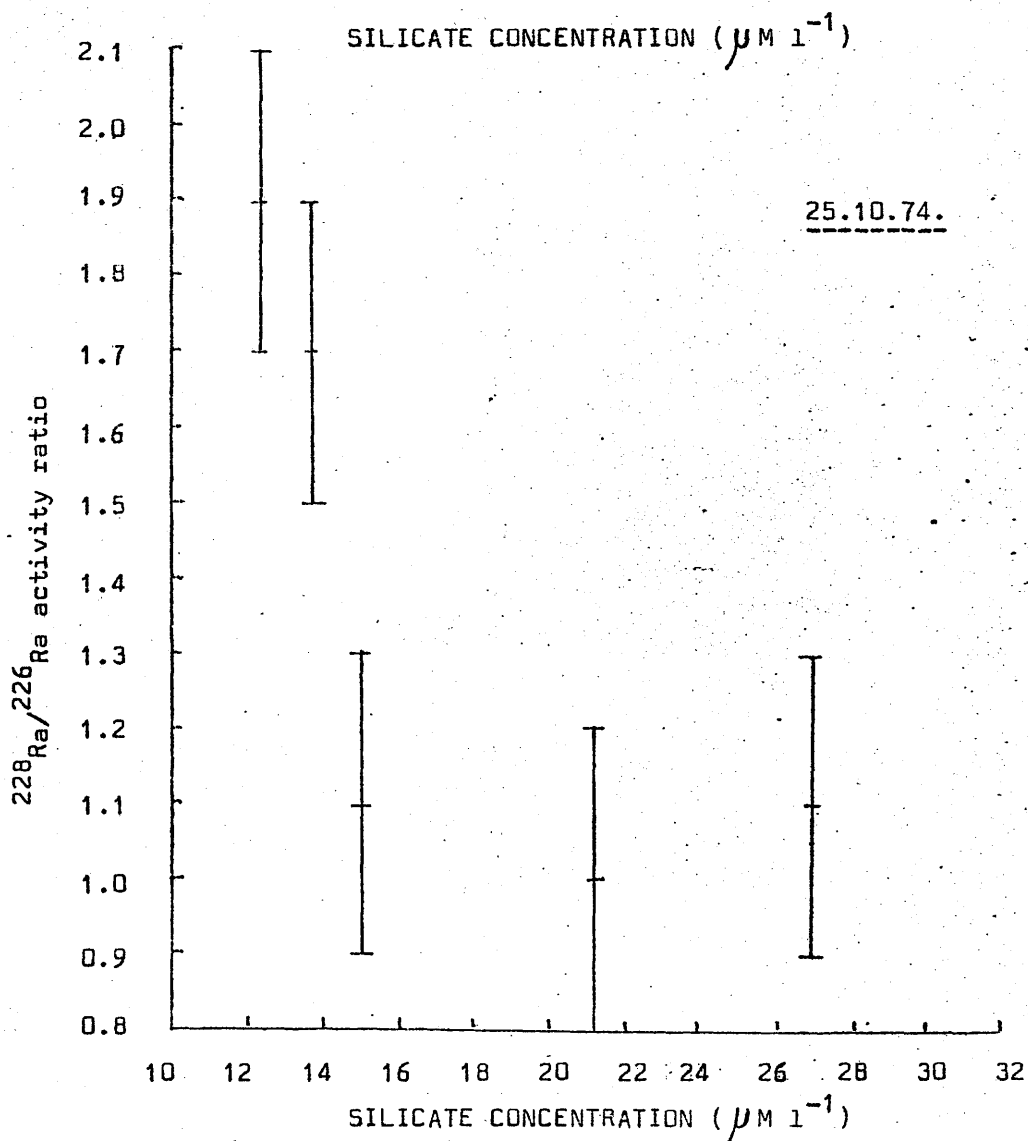
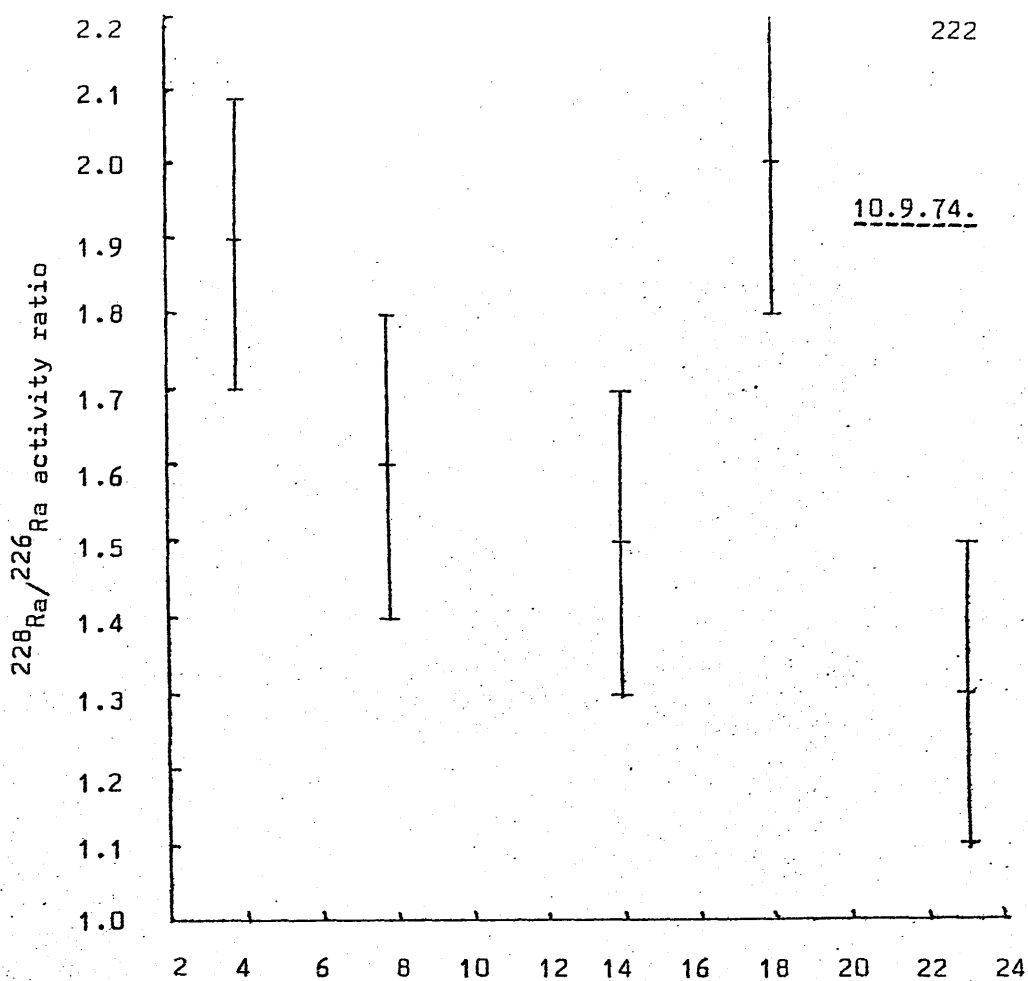


FIGURE 72. $^{228}\text{Ra}/^{226}\text{Ra}$ activity ratio versus silicate concentration for Loch Goil during 1974.

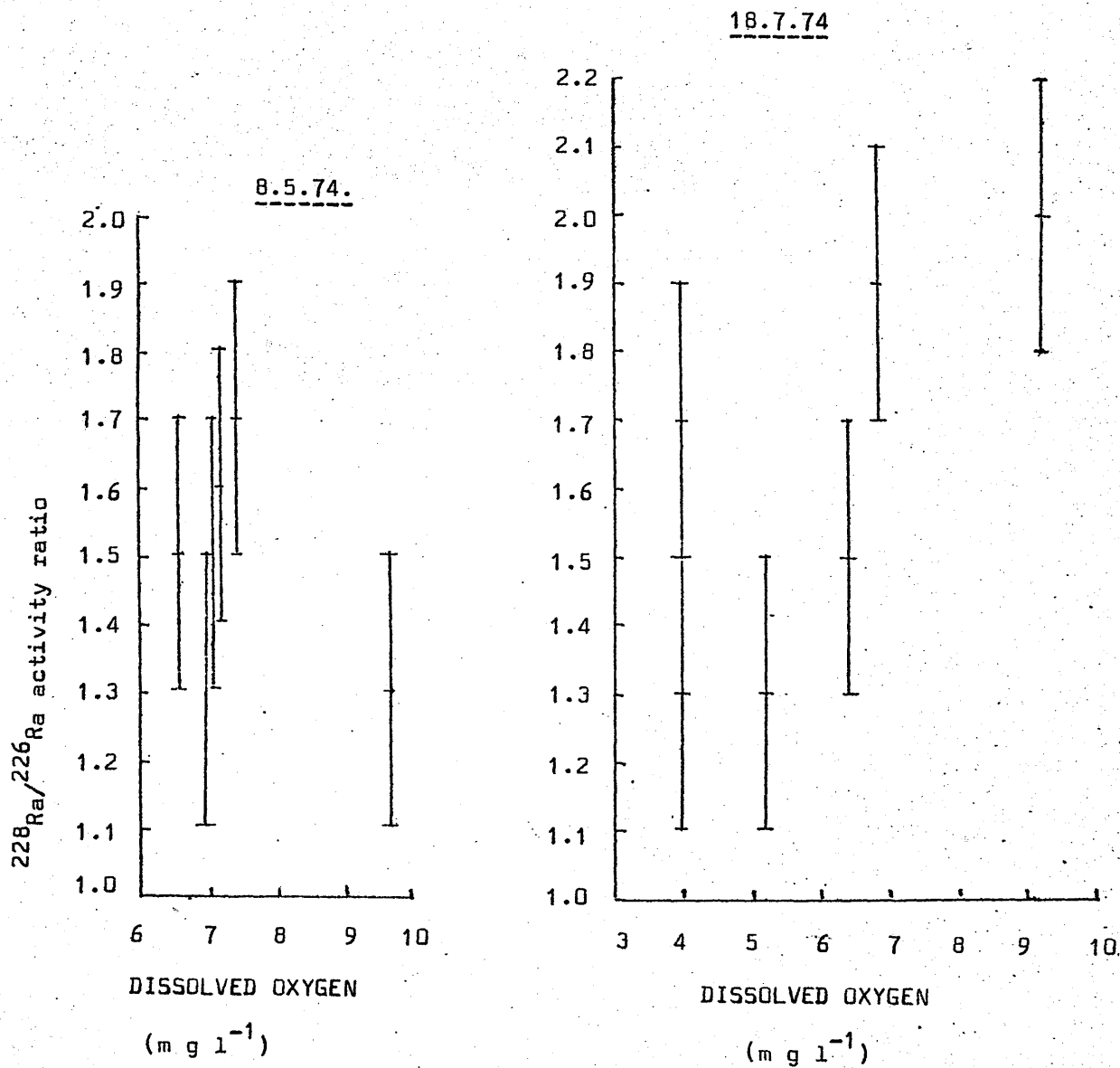


FIGURE 73. (Continued over.)

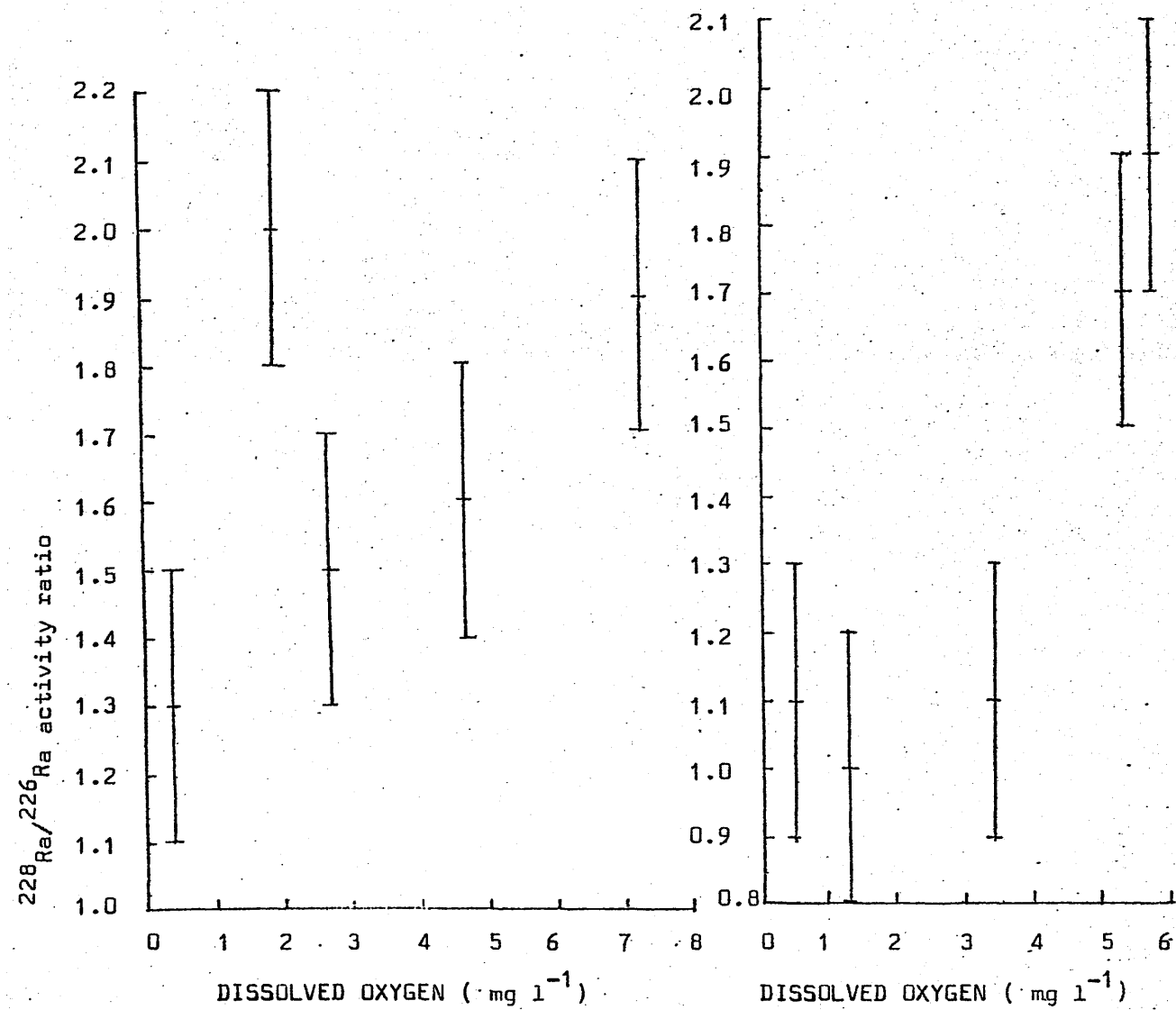


FIGURE 73. ²²⁸Ra/²²⁶Ra activity ratio versus dissolved oxygen for Loch Goil during 1974.

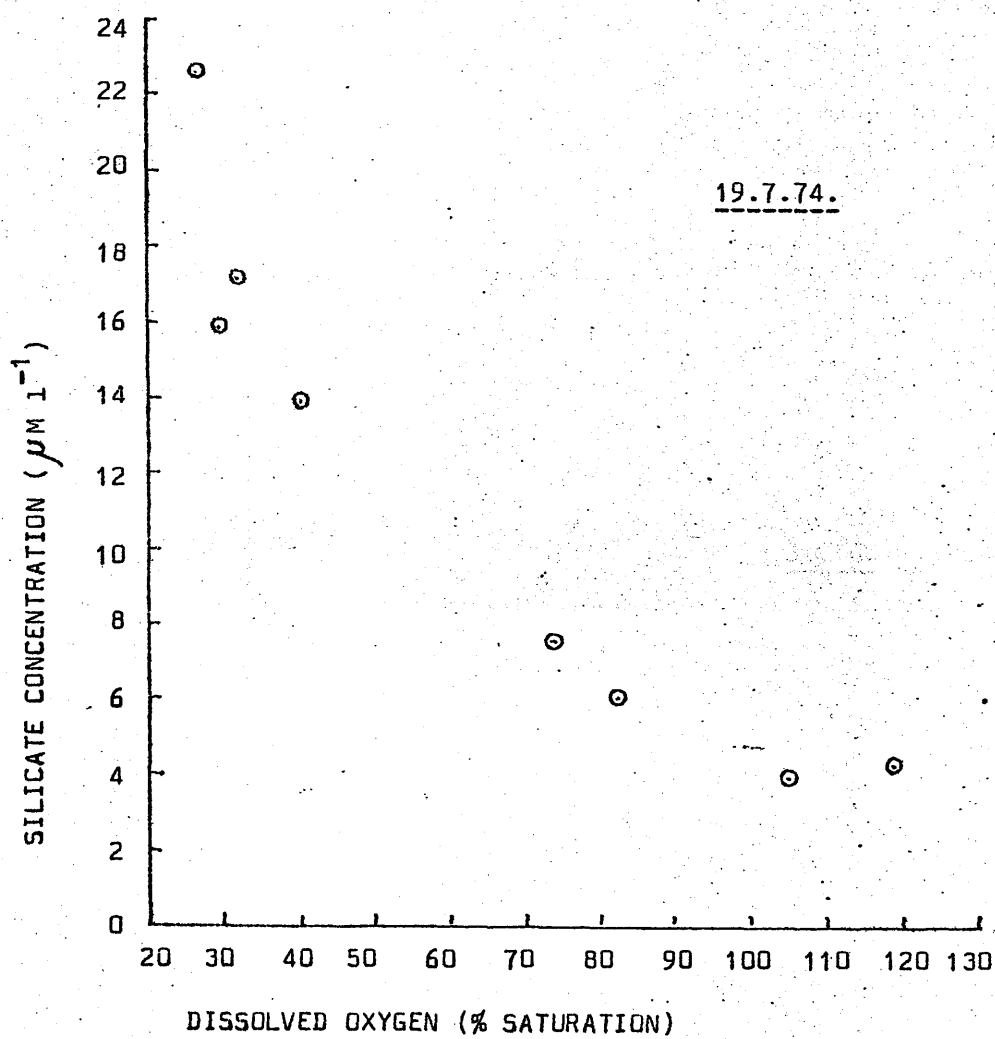
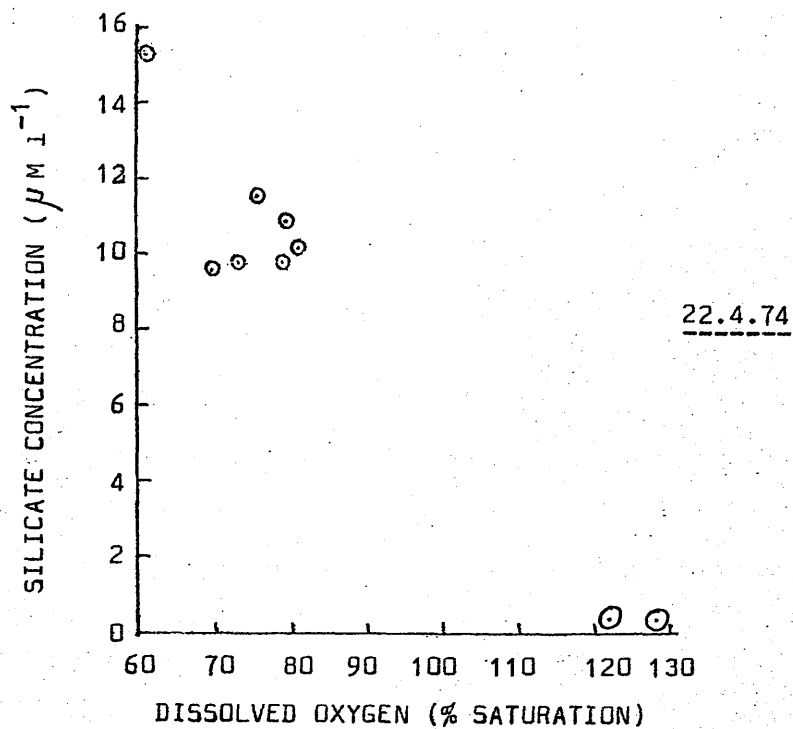


FIGURE 74. (continued over.)

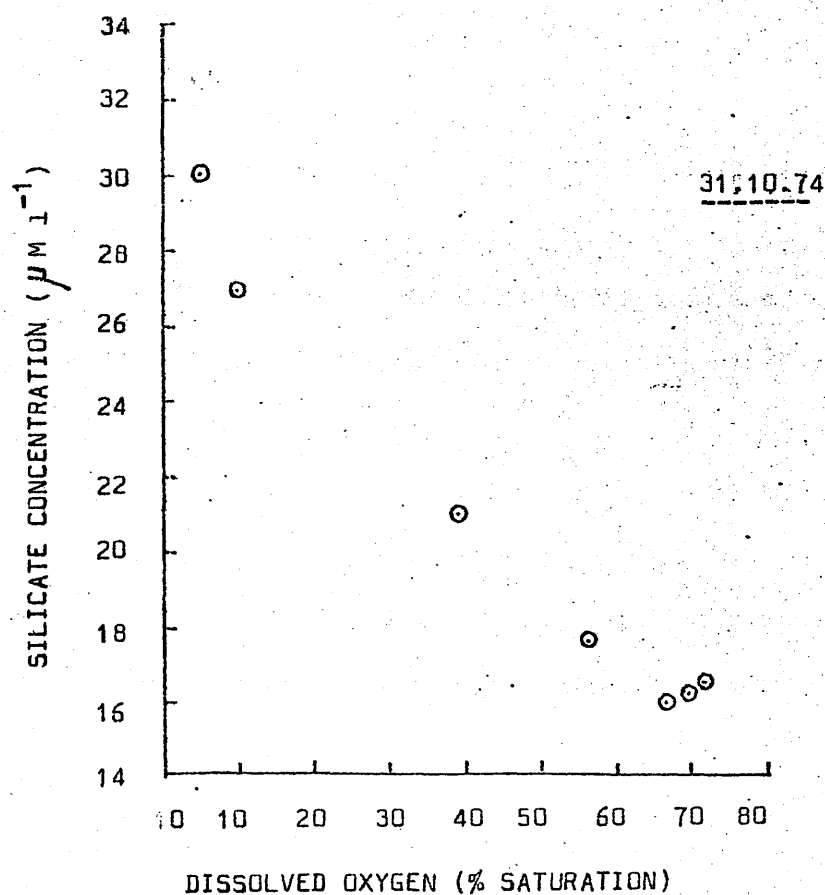
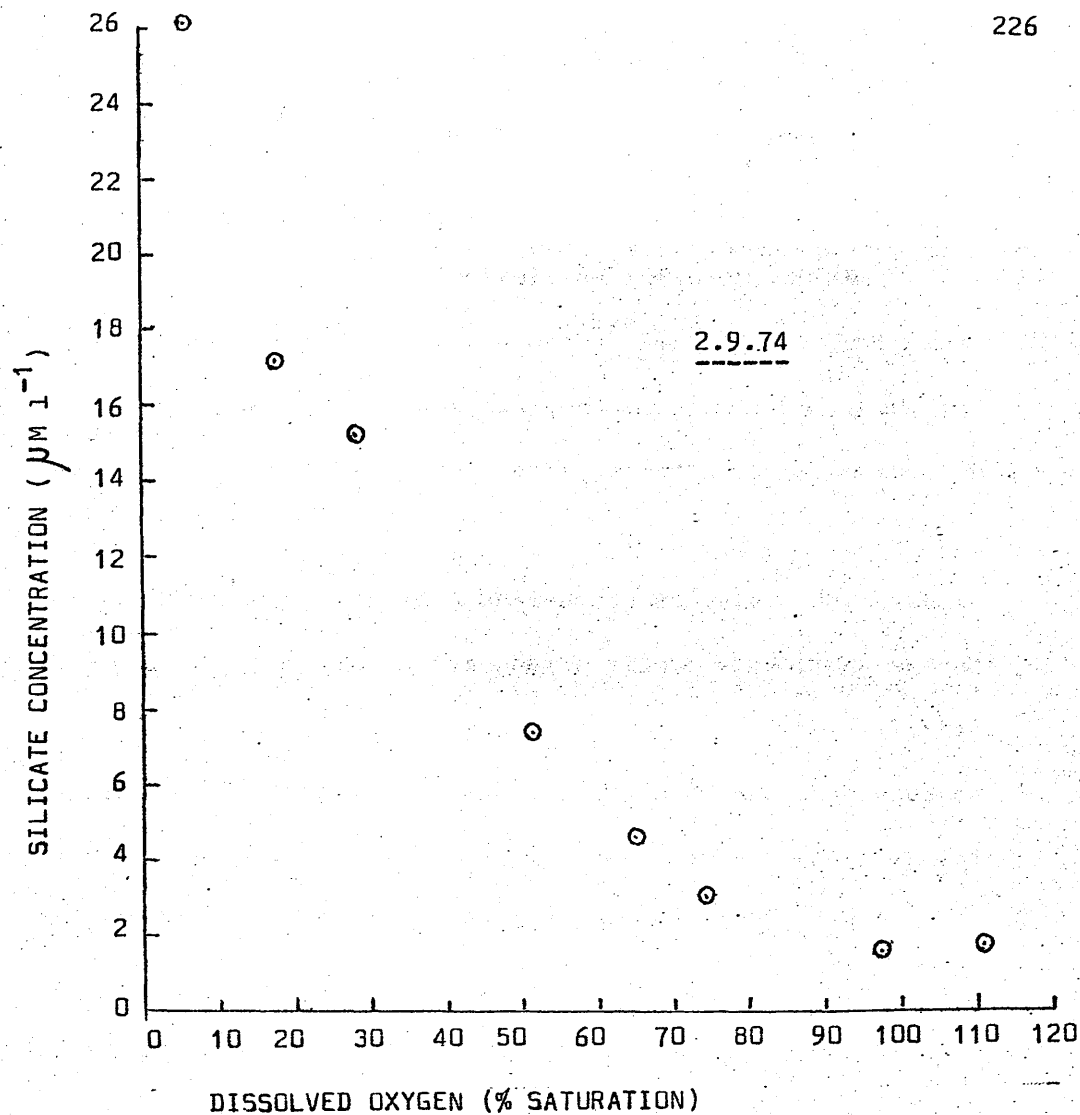


FIGURE 74. Silicate concentration versus dissolved oxygen for Loch Goil during 1974.

of new water into the system.

This detailed study of Loch Goil therefore indicates that biological activity can exert a controlling influence in the determination of radium concentrations and $^{228}\text{Ra}/^{226}\text{Ra}$ activity ratios in inshore water, the latter point being especially significant in that activity ratios might be erroneously regarded as being independent of biological effects.

In conclusion, Loch Goil is a semi-enclosed water body with an almost entirely retained deep water when a strong pycnocline extends below 20m. When the pycnocline below 20m is weak however, flushing occurs in less than a month. It is also apparent that a contained water body of this type can prove to be a very useful system in which to perform specific marine geochemical investigations.

4.4. Radium and radiocaesium concentrations in Clyde Sea Area sediments.

In interpretation of sediment results it is again advantageous to consider the caesium data before the radium data. From the caesium results, it is immediately apparent that the Craib corer satisfies the objectives behind its special construction by retaining undisturbed surface sediment samples. Comparison of cores LGC2 and LGG 5, however, indicate that the gravity corer probably loses about 8cm of surface sediment. Thus where a continuous sediment profile from the surface to greater than about 15cm is required, a Craib core and gravity core must be used in conjunction.

Core LGC2 indicates a fairly definite sedimentation pattern with high ^{137}Cs concentrations in the first 4cm and a $^{134}\text{Cs}/^{137}\text{Cs}$ activity ratio in the range 0.07 to 0.13. Below this depth, ^{137}Cs concentrations show a steady decrease while no ^{134}Cs is present. This caesium distribution suggests a fairly thorough mixing of the upper 4cm of sediment with a relatively stable structure below this depth. This

conclusion has been substantiated by more recent work at Glasgow in which X-ray photographs clearly show 'worm holes' giving rise to disturbance of the top 4-5cm of sediment in Loch Goil. This model is therefore in agreement with that proposed for the sedimentation pattern in the Great Lakes by Robbins and Edgington (1975). The general decrease in ^{137}Cs concentrations below 4cm must reflect the general trend in Windscale output of ^{137}Cs prior to 8.4.75. Thus assuming the first significant input of ^{137}Cs to the sediment occurred in 1955, the sediment depth accumulated since then must be at least 6cm, giving a sedimentation rate of at least 3mm y^{-1} . However, gravity core analyses for ^{210}Pb by Swan (1976) indicate a sedimentation rate of about 1mm y^{-1} . The presence of substantial amounts of ^{137}Cs at 10cm depth therefore indicates either that ^{137}Cs migration within the core, as well as surface mixing, is occurring or else that an increase in sedimentation rate has occurred in recent years.

Assuming the top 1cm concentration of $25.7\text{ dpm }^{137}\text{Cs/g}$ of dry sediment is representative of the equilibrium concentration of sediment in contact with the overlying water and assuming a ^{137}Cs concentration of 80 dpm l^{-1} for the water a concentration factor of 320 is obtained. This corresponds to a concentration factor of 55 for wet sediment, in good agreement with literature values.

A markedly different sedimentation pattern is indicated for Gareloch by core GLC1 in which ^{134}Cs is present down to 10cm. Since Gareloch and Loch Goil have fairly similar sediments at the two coring sites used, caesium diffusion in the sediment can be assumed to be of the same order of magnitude for both. The ^{134}Cs distribution in GLC1 therefore implies substantial, but not total, mixing to a depth of at least 10cm in Gareloch sediment. ^{137}Cs concentrations again show a steady increase towards the surface in accordance with the increasing

Windscale output. As a result of the high degree of mixing, no meaningful estimation of sedimentation rate can be derived from the caesium data.

Assuming a ^{137}Cs concentration of 85 dpm l^{-1} for Gareloch water in conjunction with a surface sediment concentration of 58.2 dpm/g dry sediment gives a concentration factor of 685 corresponding to a wet sediment concentration factor of 150. The apparent greater enrichment of ^{137}Cs in Gareloch sediments relative to Loch Goil sediments could arise from the different particulate flux in the two lochs. Gareloch, experiencing a considerable influence from the Clyde River system, has a mean total suspended solid content for the water of 3.2 mg l^{-1} composed of equal amounts of organic and inorganic material. Loch Goil has a lower mean total suspended solids content of 1.4 mg l^{-1} , composed of 0.9 mg l^{-1} organic and 0.5 mg l^{-1} inorganic material (Leatherland, 1976). Francis and Brinkley (1976) have observed that adsorption of ^{137}Cs onto micaceous minerals occurs in fresh water so that if a similar scavenging mechanism is proposed for salt water, the different nature of the particulate flux in the two lochs could account for the observed enrichments of radiocaesium in the sediments.

The radium data also indicate a contrast between Gareloch and Loch Goil sediment. Cores GLG1, GLG2 and GLC1 exhibit a typical 'inshore sediment' distribution of ^{226}Ra for Gareloch with concentrations ranging from 0.7 to 2.0 dpm/g dry sediment. This is in good agreement with ^{210}Pb results for Gareloch which show relatively constant values of about 8 dpm g^{-1} in the upper few cm (verifying the mixing indicated by $^{134}\text{Cs}/^{137}\text{Cs}$ data) and then decrease exponentially to about 1 dpm g^{-1} by 30cm (Swan, 1976). In contrast, Loch Goil shows a distinct maximum in ^{226}Ra concentrations in the upper 10cm with values rising exponentially

from typical inshore sediment concentrations of about 1 dpm g^{-1} at 10cm to 11 dpm g^{-1} at 4-5cm and then decreasing again to about 7 dpm g^{-1} at the surface. ^{210}Pb concentrations also show an unusual distribution for this core with a maximum of about 16 dpm g^{-1} being observed at 1-2 cm. Below this depth, ^{210}Pb values decrease but do not follow an exponential trend as might be expected since there is virtually no mixing below 4cm. The cause of this unusual distribution of the natural decay series nuclides is undefined. A change in the chemical environment of the sediment at 4cm depth could give rise to such a concentration profile as a result of localization of radium in the upper 4cm. The sediment however had a uniform appearance with no obvious colour changes in this region so that if such a change in chemical environment does exist, further chemical analyses of the sediment and pore water would be required to prove it. A second possibility is that a change in the nature of material being deposited has occurred in recent years. The development of the Argyll Forest was considered as a possible cause of such an effect via alteration of the natural drainage of the surrounding land. However assuming a sedimentation rate of 1 mm y^{-1} in conjunction with a mixed zone of 4cm implies that any change in the nature of the material being deposited would have occurred between 1968 and 1975, a period not corresponding to any major new planting in the area. A further possible cause of the anomaly is a direct input of radium as a pollutant. Upon enquiry, the only disposal of radioactive waste into the Clyde Sea Area which could be discovered was the dumping at Garroch Head of radioactively contaminated material from the site of a former luminizing factory at Balloch. The factory lay derelict from its closure in 1925 until the site was excavated in 1963, the excavated material containing an estimated 0.2 Ci of ^{226}Ra being deposited at Garroch Head (Lenihan, 1976).

This appears to be an unlikely source of the Loch Goil anomalous radium since any transport of radium from Garroch Head to Loch Goil would almost certainly have influenced Gareloch. Furthermore even if all 0.2 Ci was added to Loch Goil it would only increase the ^{226}Ra content of the sediment by about 5 dpm cm^{-2} , considerably less than the observed excess. On the basis of the available evidence it is therefore impossible to define either the nature or the extent of the anomalous ^{226}Ra distribution in Loch Goil sediments.

In conclusion, the results of sediment analyses reveal that neither radium nor radiocaesium provides a reliable indicator for use in geochronological studies within this area but that both can be used to establish patterns of sedimentation and can provide valuable information for use in conjunction with ^{210}Pb measurements.

4.5. Radiocaesium budget for the Clyde Sea Area.

Since only a limited amount of information is available for sediment concentrations, the calculation of a total ^{137}Cs budget for the Clyde Sea Area is subject to some degree of uncertainty. However as a result of the relative simplicity of the system and the low enrichment of caesium in sediments, the effects of this uncertainty on the calculation should be small.

It can firstly be stated that, from the observed results, the dominant input of ^{137}Cs to the area is from the Windscale effluent and for practical purposes all other inputs can be ignored. Thus considering the period December 1975 - March 1976 and assuming a mean ^{137}Cs concentration for Clyde Sea water of 110 dpm l^{-1} gives a total activity in the area of $1.82 \times 10^{16} \text{ dpm}$ ie. $8.2 \times 10^3 \text{ Ci}$. Assuming a residence time of 3.9 months for the Clyde Sea Area then the corresponding discharge from Windscale is $3.5 \times 10^4 \text{ Ci}$ (based on a mean monthly discharge for 1975 of $9 \times 10^3 \text{ Ci/month}$). These results

therefore imply that 23% of the ^{137}Cs discharged from Windscale passes through the Clyde Sea Area. Assuming a homogeneous distribution of ^{137}Cs in the Stranraer-Larne region (Jefferies, 1976) means that at least 23% of the net northwards flow of water across this line passes through the Clyde Sea Area. This is in general agreement with recent $^{134}\text{Cs}/^{137}\text{Cs}$ analyses by McKinley (1976) which indicate that between the Irish coast and Islay there is an inflow of Atlantic water along the Irish coast and a corresponding outflow of 'Irish Sea' water on the Scottish side.

If the amount of ^{137}Cs below 10cm in the sediment is regarded as small then an estimation of the fraction of the Windscale discharge remaining in the area can be made from the Loch Goil and Gareloch cores. The Loch Goil core LGC2 yields a value of $19.9 \text{ dpm } ^{137}\text{Cs cm}^{-2}$ giving a total burden of $4.98 \times 10^{14} \text{ dpm}$ or 224 Ci for the total area. The total Windscale discharge of ^{137}Cs up to April 1975 can be estimated as $3 \times 10^5 \text{ Ci}$ with 93% in the period 1970-1975. Thus applying a decay correction of 2.5y to the Clyde sediments burden gives a value of 237 Ci ie. 0.08% of the total Windscale output. A similar treatment of the data for Gareloch core GLC1 gives a decay corrected Clyde sediment burden of ^{137}Cs of 1556 Ci from a total Windscale output (to November 1975) of $3.8 \times 10^5 \text{ Ci}$ ie. 0.4%.

The best model at present for the total ^{137}Cs budget of the Clyde Sea Area is therefore that all of the radiocaesium entering the area is produced by Windscale, that about 23% of the Windscale discharge passes through the area and that between 0.08% and 0.4% remains in the sediments.

4.6. Radium budget for the Clyde Sea Area.

As a result of its complex geochemical and biogeochemical behaviour and lack of information on Irish Sea concentrations, a detailed budget for radium cannot be calculated for the Clyde Sea Area.

However a number of observations concerning relative input can be made. An apparent flux of $4 \times 10^{-13} \text{ g } ^{226}\text{Ra cm}^{-2} \text{ y}^{-1}$ from the sediments was calculated but subsequent detailed studies of Loch Goil revealed that the biological cycling of silicate may be the dominant factor controlling ^{226}Ra concentrations. This is in good agreement with Shannon and Cherry (1971) who estimated that the silicate controlled flux of ^{226}Ra could be as high as $4.6 \times 10^{-13} \text{ g } ^{226}\text{Ra cm}^{-2} \text{ y}^{-1}$, but somewhat higher than the value of $1.2 \times 10^{-14} \text{ g } ^{226}\text{Ra cm}^{-2} \text{ y}^{-1}$ reported by Bacon and Edmond (1972). This large biological effect means that the water 'residence times' previously calculated from the ^{226}Ra data are subject to a considerable error and should probably be regarded as lower limits. However no matter what the source, the 'flux' of $4 \times 10^{-13} \text{ g } ^{226}\text{Ra cm}^{-2} \text{ y}^{-1}$ does represent the variation in concentration of ^{226}Ra which can occur in the area and can be used

for comparative purposes to assess the importance of river input.

Assuming a mean (50% exceedence) river flow of $80 \text{ m}^3 \text{ sec}^{-1}$ gives a total input figure of $2.5 \times 10^{12} \text{ ly}^{-1}$ and taking a mean ^{226}Ra concentration of 60 dpm/1000 l yields an input of $2.8 \times 10^{-15} \text{ g } ^{226}\text{Ra cm}^{-2} \text{ y}^{-1}$ ie. less than 1% of the estimated combined biological and sediment flux.

The total radium budget for the Clyde Sea Area therefore appears to have a very small river input and to be controlled by three main factors : (1) The radium flux from the sediments (2) Biological cycling by silicate (3) The relative proportions of Atlantic and Irish Sea water present in the North Channel.

A more rigorous definition of the radium budget would require investigations of radium concentrations in the North Channel and the Irish Sea.

4.7. General conclusions.

The general conclusions from the foregoing discussion may be summarized as follows.

(1) Radium:

^{228}Ra and ^{226}Ra have a limited usefulness as tracers in this particular area, their distributions being indicative of a rapidly flushed coastal system. While the predicted enrichment of both isotopes was observed, the rapid time-scale of water renewal and the complex biological and geochemical behaviour of radium mean that little detailed information on water movement or residence can be unambiguously defined from the observed data. These isotopes would however probably provide useful tracers for water movement in the North Channel where mixing of Atlantic and Irish Sea water occurs. The survey proved a useful investigation of the coastal marine geochemistry of radium indicating that river input provides only a small contribution (probably about 1%) to the radium budget of the area so that the observed enrichments must occur via diffusion from sediments. The biological cycling of silicate was, however, demonstrated to be capable of exerting a dominant influence on radium concentrations. The observed 'flux' of about $4 \times 10^{-13} \text{ g } ^{226}\text{Ra cm}^{-2} \text{ y}^{-1}$ must therefore be regarded as a combined effect of biological cycling and diffusion from sediments. ^{226}Ra shows relatively conservative behaviour over a wide range of salinity along the length of the estuary.

These conclusions are in general agreement with the presently accepted model for the marine geochemical behaviour of radium.

Gareloch sediment has a ^{226}Ra distribution typical of inshore areas but Loch Goil sediment exhibits anomalously high ^{226}Ra concentrations in the upper 10cm. No satisfactory explanation could be discovered for this anomaly.

(2) Radiocaesium.

There is one dominant source of radiocaesium to the Clyde Sea Area, namely the effluent from the Windscale nuclear fuel reprocessing plant.

^{134}Cs and ^{137}Cs provide useful tracers for water movement and residence time studies in the area. The use of appropriate approximations enables evaluation of water transit times and residence times despite major variations in the concentrations of both radiocaesium isotopes in the Windscale discharge. Approximately 23% of the ^{137}Cs discharged from Windscale is estimated to pass through the Clyde Sea Area with 0.08% to 0.4% being incorporated into the sediment. ^{137}Cs exhibits conservative behaviour over the range of salinities observed in the estuary. ^{134}Cs and ^{137}Cs are good indicators of the degree of mixing in marine sediment but cannot be used to establish reliable chronologies.

(3) The Clyde Sea Area.

With the exception of Loch Goil, the Clyde Sea is vertically well mixed and has a mean water residence time in the order of 3.9 months. Salt water exchange with the North Channel is in the order of $10^9 \text{ m}^3 \text{ day}^{-1}$, much larger than the estimated freshwater and sewage inputs of 10^7 and $10^6 \text{ m}^3 \text{ day}^{-1}$. New water entering the area is typified by that in the Stranraer-Larne region and at least 23% of the water flowing northwards across this line is estimated to pass through the Clyde Sea Area. A variable proportion of Atlantic to Irish Sea water enters the area depending on the prevailing rate of outflow of water from the Irish Sea.

Loch Goil is the only part of the system exhibiting a long residence time and even here, this is a transient situation pertaining only when a strong pycnocline is present to greater than 20m depth. When this does not apply, total flushing of the loch occurs in less than 29 days.

Gareloch sediments are partially mixed to at least 10cm while Loch Goil sediments are well mixed to about 4cm depth below which the material is relatively stable.

In conclusion it should be noted that the above results and discussion are, as for any initial survey, of a somewhat tentative nature and are subject to reappraisal in the light of continuing research. However the agreement in a number of cases, as specified in the discussion, with results and trends in related parameters reported by other laboratories gives a considerable degree of support to the results of this research. The survey does indicate that useful information can be derived from this type of radiotracer study in the Clyde Sea Area and that this investigation could be profitably extended to the general Irish Sea and north east Atlantic.

APPENDIX 1

Since this dissertation is presented through a chemistry department some of the oceanographic terms used may be unfamiliar to the reader. To avoid unnecessary confusion, the following is intended as a brief glossary of some of the terms used in the text. A brief description of the dominant circulation patterns of the upper waters of the North Atlantic is also given.

Salinity can be regarded as the total weight in grams of dissolved solids in one kilogram of sea water and is defined by relationship to the conductivity of sea water via the expression:

$$S\% = -0.08996 + 28.29720R_{15} + 12.80832R_{15}^2 - 10.67869R_{15}^3 + 5.9862R_{15}^4 - 1.32311R_{15}^5$$

where the conductivity ratio R_t is the ratio of the conductivity of a water sample to that of one having a salinity of 35‰ with both samples being at the same temperature (15°C as defined above) and at a pressure of one atmosphere (Wallace, 1974).

A Thermocline is a vertical section of water in which there is a large rate of decrease of temperature with increasing depth. The main oceanic thermocline exists as a permanent feature from between 50 and 200m for a depth of about 500m in low and middle latitudes. Small scale thermoclines are induced as a transient feature in the Clyde Sea Area due to heating of surface waters.

A Holocline is a ^{zone of} large rate of increase of salinity with increasing depth /a

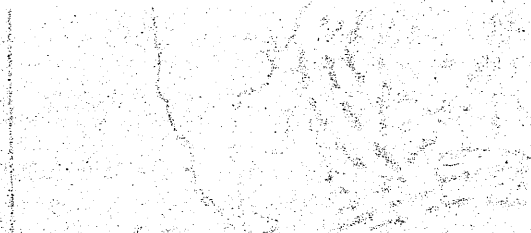
A Pycnocline is a ^{zone of} large rate of increase of density with increasing depth.

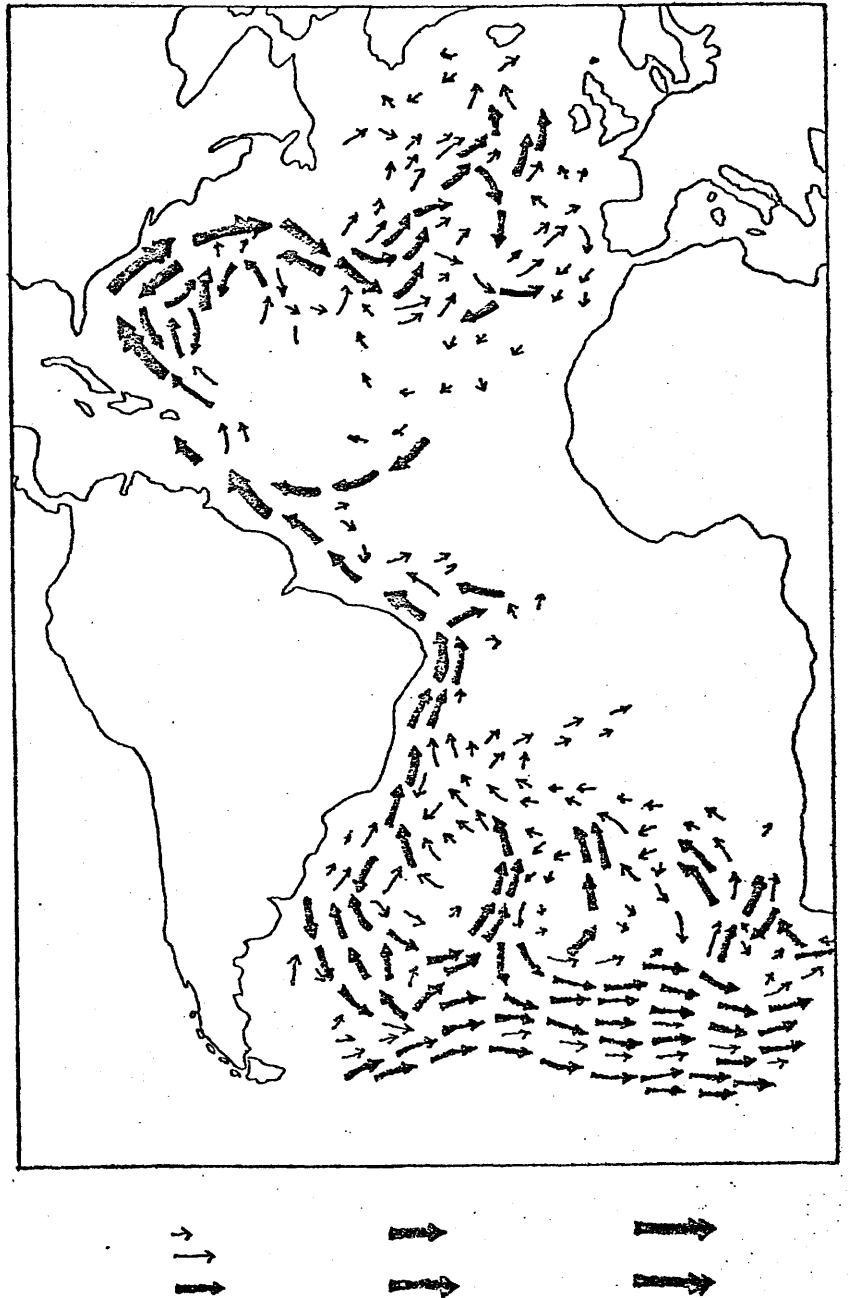
A species in seawater is said to exhibit conservative behaviour when

there is no significant process by which its concentration is changed other than by water mixing. (Pickard, 1975)

General circulation of the North Atlantic.

The circulation of upper waters in the oceans is governed by wind action, rotation of the earth and the positions of the continental land masses. The net result of this is a cyclonic circulation of upper ocean waters - clockwise in oceans in the northern hemisphere, counterclockwise in the southern hemisphere. The major features of surface circulation in the Atlantic Ocean are shown in Figure 75, showing that the dominant regime round the British Isles is a strong flow from the south west.





Relative water flow in upper waters.

FIGURE 75. Surface currents in the Atlantic Ocean (Defant, 1961)

APPENDIX 2.

Extraction of trace metals from sea water using manganese dioxide impregnated acrylic fibre.

The technique of using finely dispersed manganese dioxide supported on cation exchange acrylic fibre as a scavenging material for the removal of trace elements from sea water evolved from earlier work by Lal et al (1964) in which natural sponges and jute fibres were used as a support for finely dispersed ferric hydroxide. While these materials were demonstrated to be highly efficient in the adsorption of ^{32}Si , thorium and uranium from sea water, their value as the basis of an analytical procedure was limited by the inherently high blank values of radionuclide concentrations coupled with a high efficiency for the removal of particulate matter from the water being extracted. These problems were largely overcome by changing the support material for the ferric hydroxide to base treated acrylic fibre (Krishnaswami et al, 1972). This medium gave low blank concentrations and high extraction efficiencies for the uptake of ^{234}Th and ^{210}Pb from sea water, observed enrichment factors being in the range $10^3 - 10^4$. Enrichment factors for ^{226}Ra and ^{32}Si were lower, being in the ranges 200 to 900 and 200 to 500 respectively. To improve the efficiency of radium extraction, Moore and Reid (1973) investigated the properties of a number of adsorbants dispersed on acrylic fibre and selected manganese dioxide as a suitable material, having the desired properties of low blank concentrations and high extraction efficiency. Enrichment factors ranged from 10^4 to 3×10^4 for ^{226}Ra while a value of about 10^3 was observed from cobalt, copper, nickel and zinc.

As described in chapter 2, a method based on manganese dioxide impregnated acrylic fibre was developed for the investigation of

radium concentrations in the Clyde Sea Area. In this work it was verified that a slow pass of small volume solutions through a 75g column of fibre produces virtually quantitative uptake of radium but it was also found that rapid flow of large volume (60 l) samples resulted in only about 50% extraction efficiency. The following observations were also made on the nature of the fibre and its efficiency for extraction of other metals.

Activation analysis investigations indicated that a single pass of small volume (100 - 200ml) solutions through a 75g column of the manganese dioxide impregnated fibre resulted in about 30% uptake of thorium, cobalt, scandium and iron but less than 10% uptake of Europium. Retention of these elements (and radium) on untreated or base-treated acrylic fibre was less than 1%. A sample of MnO_2 from manganese dioxide impregnated fibre exposed to Clyde River Water at Broomielaw, Glasgow was analysed by activation analysis and showed four major species present, namely iron (0.38%), chromium (4.5 ppm), cobalt (1.53 ppm) and scandium (0.17 ppm).

Investigations by Dr. T. Baird in the electron microscopy unit of Glasgow University revealed that the MnO_2 is present in a widely varying range of crystal sizes with the crystals forming a thin coating on the intact acrylic fibres. Electron diffraction patterns produced by MnO_2 from fibre did not match those of MnO_2 prepared in the absence of fibre, nor did they match patterns produced from regular MnO_2 crystal structures as defined in literature sources. ESCA analysis however provided an identical binding energy trace for MnO_2 from the fibre and a pure sample of MnO_2 .

It can therefore be concluded that the fibre consists of finely - dispersed, poorly - crystallized, hydrated MnO_2 adhering to the surface of the acrylic fibre, the principal function of which is simply as a support to present a large surface area of MnO_2 . The fibre may have a

secondary effect in being partially instrumental in establishing the defective nature of the MnO_2 crystals. The mechanism of uptake of metal ions is probably by adsorption onto surface defects on the MnO_2 . Such incorporation of trace metals into manganese dioxide in the marine environment is a well established phenomenon and a large body of literature exists concerning both laboratory investigations (eg. Anderson et al, 1973) and analyses of manganese nodules (eg. Krishnaswami and Lal, 1972 ; Calvert and Price, 1970 ; Buchowiecki and Cherry, 1967).

APPENDIX 3

CALCULATIONS AND COMPUTER PROGRAMS

The following calculations for ^{226}Ra and $^{134}\text{Cs}/^{137}\text{Cs}$ concentrations are applicable to 20 l and 10 l sea water samples respectively. Simple modification of the latter stages of both calculations renders them applicable to water samples of different volume or to sediment samples. The ^{228}Ra calculation is applicable to all samples provided the appropriate value of ^{226}Ra concentration is used to calculate the $^{228}\text{Ra}/^{226}\text{Ra}$ activity ratio. 1 σ errors based purely on counting statistics are derived.

(1) Calculation of ^{226}Ra concentration.

Let $A \pm \sigma_A$ = observed count rate (cpm) at time t(h).

$B \pm \sigma_B$ = background count rate (cpm).

$C \pm \sigma_C$ = blank count rate (cpm) corrected to time zero.

E = % efficiency for collection and counting of ^{222}Rn based on three α emissions per ^{222}Rn decay

Background correction:

$$D = A - B \quad ; \quad \sigma_D = \sqrt{\sigma_A^2 + \sigma_B^2}$$

Correct to time zero:

$$F = D e^{\lambda^{222}\text{Rn} t} \quad ; \quad \sigma_F = \sigma_D \cdot \frac{F}{D}$$

Blank correction:

$$G = F - C \quad ; \quad \sigma_G = \sqrt{\sigma_F^2 + \sigma_C^2}$$

But efficiency = $E\%$ and each ^{222}Rn decay gives rise to three emissions.

$$H = \frac{100}{3E} G \quad ; \quad \sigma_H = \sigma_G \cdot \frac{H}{G}$$

But this is for a 20 l sample.

^{226}Ra concentration, $J = 500 H \text{ dpm}/1000 \text{ l}$

$$\sigma_J = 500 \sigma_H$$

(2) ^{228}Ra calculation.

Let $A \pm \sigma_A$ = observed count rate (cpm) at time t_1 (h).

$B \pm \sigma_B$ = observed count rate (cpm) at time t_2 (h).

$C \pm \sigma_C$ = observed count rate (cpm) at time t_3 (h).

where t_1 , t_2 and t_3 are approximately 5, 70 and 700 hours after isolation of ^{228}Ac respectively.

D = background count rate (cpm).

E = % efficiency for extraction and β^- counting of ^{228}Ac .

Background correction:

$$\begin{aligned} F &= A - D & ; & \quad \sigma_F = \sqrt{\sigma_A^2 + \sigma_D^2} \\ G &= B - D & ; & \quad \sigma_G = \sqrt{\sigma_B^2 + \sigma_D^2} \\ H &= C - D & ; & \quad \sigma_H = \sqrt{\sigma_C^2 + \sigma_D^2} \end{aligned}$$

Residual correction:

$$\begin{aligned} I &= F - H & ; & \quad \sigma_I = \sqrt{\sigma_F^2 + \sigma_H^2} \\ J &= G - H & ; & \quad \sigma_J = \sqrt{\sigma_G^2 + \sigma_H^2} \end{aligned}$$

(I represents the $^{228}\text{Ac} + ^{90}\text{Y}$ (if present) activity at time t_1 while J represents the ^{90}Y activity (if any) at time t_2)

Correction of ^{228}Ac activity at time t_1 for ^{90}Y contribution:

$$\begin{aligned} K &= J e^{(t_2 - t_1) \lambda_{^{90}\text{Y}}} & ; & \quad \sigma_K = \sigma_J \cdot \frac{K}{J} \\ L &= I - K & ; & \quad \sigma_L = \sqrt{\sigma_I^2 + \sigma_K^2} \end{aligned}$$

Correction of ^{228}Ac activity to time zero;

$$M = L e^{t_1 \lambda_{^{228}\text{Ac}}} & ; & \quad \sigma_M = \sigma_L \cdot \frac{M}{L}$$

Efficiency correction:

$$N = \frac{100}{E} M & ; & \quad \sigma_N = \sigma_M \cdot \frac{M}{N}$$

Correction for ^{228}Ra decay since sampling:

$$P = N e^{t_4 \lambda} {}^{228}\text{Ac} \quad ; \quad \sigma_P = \sigma_N \cdot \frac{P}{N}$$

The ^{228}Ra activity of the sample at time of collection is obtained via the $^{228}\text{Ra}/^{226}\text{Ra}$ activity ratio P/R where R is the appropriate ^{226}Ra content of the sample, the error on the ratio by

$$\sigma_{\text{ratio}} = \sqrt{\frac{\sigma_P^2}{R^2} + \left(\frac{P}{R^2}\right)^2 \sigma_R^2}$$

(3) A computer program in Fortran 1V for the solution of the above

^{228}Ra calculation.

```

C   TO CALCULATE THE RADIUM 228 ACTIVITY
C   TOT IS TOTAL ACTIVITY AT TIME T1
C   STOT IS ERROR ON TOT
C   YT IS TOTAL ACTIVITY AT TIME T2
C   SYT IS ERROR ON YT
C   RES IS TOTAL ACTIVITY AT TIME T3
C   SRES IS ERROR ON RES
C   TSAMP IS TIME SINCE SAMPLING
10  READ (5,20)TOT,STOT,T1,YT,SYT,T2,RES,SRES,T3,TSAMP
20  FORMAT(F6.2,4F5.2,F6.1,2F5.2,2F7.1)
    IF(TOT.EQ.0.0)GO TO 160
    BCKD=0.36
    SBCKD=0.03
    TOTBC=TOT-BCKD
    YTBC=YT-BCKD
    RESBC=RES-BCKD
    STOTBC=SQRT(SBCKD**2+STOT**2)
    SYTBC=SQRT(SBCKD**2+SYT**2)
    SRESBC=SQRT(SBCKD**2+SRES**2)
    ACYTI=TOTBC-RESBC
    YTT2=YTBC-RESBC
    SACYTI=SQRT(STOTBC**2+SRESBC**2)
    SYTT2=SQRT(SYTBC**2+SRESBC**2)
    DT=T2-T1
    YTLMDA=0.01083
    YTT1=YTT2*EXP(DT*YTLMDA)
    SYTT1=SYTT2*YTT1/YTT2
    ACT1=ACYTI-YTT1
    SACT1=SQRT(SACYTI**2+SYTT1**2)
    ACLMDA=0.11308
    ACT0=ACT1*EXP(ACLMDA*T1)
    SACT0=SACT1*ACT0/ACT1
    EC=3.125

```

```

ACEC=ACTO*EC
SACEC=SACTO*ACEC/ACTO
RALMDA=0.000283
RA=ACEC*EXP(RALMDA TSAMP)
SRA=SACEC*RA/ACEC
READ(5,30)
WRITE(6,30)
30 FORMAT(IHI,50H
WRITE(6,40)
40 FORMAT(IHO,5X,'TOTAL      SIGMA TOTAL      TI')
WRITE(6,50)TOT,STOT,TI
50 FORMAT(5X,F6.2,2X,F5.2,9X,F5.2)
WRITE(6,60)
60 FORMAT(IHO,5X,'YT ACTIVITY      SIGMA YT      T2')
WRITE(6,70)YT,SYT,T2
70 FORMAT(5X,F5.2,9X,F5.2,6X,F6.1)
WRITE(6,80)
80 FORMAT(IHO,5X,'RESIDUAL      SIGMA RESIDUAL      T3')
WRITE(6,90)RES,SRES,T3
90 FORMAT(5X,F5.2,6X,F5.2,12X,F7.1)
WRITE(6,100)
100 FORMAT(IHO,5X,'TIME SINCE SAMPLING')
WRITE(6,110)TSAMP
110 FORMAT(5X,F7.1)
WRITE(6,120)
120 FORMAT(IHO,5X,'RADIUM 228 ACTIVITY D.P.M.')
WRITE(6,130)RA
130 FORMAT(5X,F6.2)
WRITE(6,140)
140 FORMAT(IHO,5X,'RA 228 ERROR PLUS OR MINUS TWO SIGMA')
WRITE(6,150)SRA
150 FORMAT(5X,F5.2)
GO TO 10
160 STOP
END

```

(4) Calculation of caesium concentrations:

Let $A \pm \sigma_A$ = count rate (cpm) in ^{137}Cs region of spectrum.

$B \pm \sigma_B$ = count rate (cpm) in ^{134}Cs region of spectrum.

$C \pm \sigma_C$ = combined background and KCFC Blank count rate (cpm) in ^{137}Cs region of spectrum.

$D \pm \sigma_D$ = combined background and KCFC blank count rate (cpm) in ^{134}Cs region of spectrum.

E = % efficiency for extraction and counting of ^{137}Cs

F = % efficiency for extraction and counting of ^{134}Cs

Background and blank correction:

$$G = A - C \quad ; \quad \sigma_G = \sqrt{\sigma_A^2 + \sigma_C^2}$$

$$H = B - D \quad ; \quad \sigma_H = \sqrt{\sigma_B^2 + \sigma_D^2}$$

Empirically it has been derived that the ratio of the number of ^{134}Cs counts in the ^{137}Cs region to the number of ^{134}Cs counts in the ^{134}Cs region is 1.45. Correction of the ^{137}Cs count rate for ^{134}Cs contribution is therefore achieved by:

$$I = G - 1.45H \quad ; \quad \sigma_I = \sqrt{\sigma_G^2 + (1.45\sigma_H)^2}$$

Efficiency correction:

$$J = \frac{100}{E} I \quad ; \quad \sigma_J = \sigma_I \cdot \frac{J}{I}$$

$$K = \frac{100}{F} H \quad ; \quad \sigma_K = \sigma_H \cdot \frac{K}{H}$$

But this is for a 10 l water sample therefore ^{137}Cs and ^{134}Cs concentrations are given by:

$$L = 0.1J \quad ; \quad \sigma_L = 0.1 \sigma_J$$

$$M = 0.1K \quad ; \quad \sigma_M = 0.1 \sigma_K$$

The error on the $^{134}\text{Cs}/^{137}\text{Cs}$ activity ratio M/L is given by:

$$\sigma_{\text{ratio}} = \sqrt{\frac{\sigma_M^2}{L^2} + \left(\frac{M}{L^2}\right)^2 \sigma_L^2}$$

(5) A computer program in Fortran 1V for the solution of the above caesium concentration calculation.

(Written by I.G. McKinley).

```

C  CS137/134 PEAK INTEGRATION PROGRAM
C  LIST
C  DIMENSION A(300),B(300),C(300),L1(300),P2(300),L3(300),D1(300)
C  ID2(300),D3(300)
C  I=0
C  BK137=11034.0
C  BK134=6462.0
10 READ(5,20)CS137,CS134,TIME,TNUM,VOL
   READ(5,21)LOC,AT,ION,DA,YAND,DATE
   IF(CS137.EQ.CS134)GO TO 100
   IF(CS134.EQ.BK134)CS134=BK134+0.1
   IF(VOL.EQ.0.0)VOL=10.0
   F137D=(0.02244*((CS137-BK137)-1.45*(CS134-BK134)))/VOL
   F137C=F137D/2.22
   S137D=(0.02244*SQRT((CS137+BK137)+1.45*(CS134+BK134)))/VOL
   S137C=S137D/2.22
   F134D=(0.02622*(CS134-BK134))/VOL
   F134C=F134D/2.22
   S134D=(0.02622*SQRT(CS134+BK134))/VOL
   S134C=S134D/2.22
   F1370D=F137D*EXP(0.000063*TIME)
   F1370C=F1370D/2.22
   S1370D=(S137D*F1370D)/F137D
   S1370C=S1370D/2.22
   F1340D=F134D*EXP(0.000904*TIME)
   F1340C=F1340D/2.22
   S1340D=(S134D*F1340D)/F134D
   S1340C=S1340D/2.22
   RATIO=F1340D/F1370D

```

```

SRATO=SQRT((S1340D/F1370D)**2+(F1340D*S1370D/F1370D**2)**2)
IA=IFIX(CS137)
IB=IFIX(BK137)
IC=IFIX(CS134)
ID=IFIX(BK134)
KT=IFIX(TIME)
KN=IFIX(TNUM)
11 FORMAT(40X,6H GAMMA,I4/40X,12(IH*))
12 FORMAT(IH0,5X,45H PEAK INTEGRALS,BACKGROUNDS,COUNT TIME VOLUME)
13 FORMAT(IH0,5X,42H CS 137 INTEGRAL----DPM/L,SIGMA,PCI/L,SIGMA)
14 FORMAT(IH0,5X,42H CS 134 INTEGRAL----DPM/L,SIGMA,PCI/L,SIGMA)
15 FORMAT(IH0,5X,42H CS 1340INTEGRAL----DPM/L,SIGMA,PCI/L,SIGMA)
16 FORMAT(IH0,5X,12H.RATIO,SIGMA)
17 FORMAT(IH0,6X,3(80(IH*)/7X))
18 FORMAT(IH0,5X,42H.CS 1370INTEGRAL----DPM/L,SIGMA,PCI/L,SIGMA)
20 FORMAT(2(F10*2),10X),2F10.2,F10.5)
21 FORMAT(3(A4),2X,3(A4))
50 FORMAT(40X,F15.7)
55 FORMAT(10X,5I15,F15.3)
60 FORMAT(10X,5F15.7)
70 FORMAT(IH0,20X.3A4.30X.3A4)
75 FORMAT(IH1,6X,80(IH*))
76 FORMAT(IH0,5X,35H CS-134 BELOW LIMITS OF MEASUREMENT)
J=I/2
IF(I.EQ.2*J)WRITE(6,75)
C LOCATION,DATE

```


REFERENCES

- Anderson B.S., Jenne E.A. and Chao T.T., 1973. "The sorption of silver by poorly crystallized manganese oxide." ; *Geochim. Cosmochim. Acta*, 37,61.
- Arrhenius G.O.S. and Goldberg E.D., 1955. *Tellus*, 7, 226.
- Arrhenius G.O.S., Bramlette M.N. and Picciotto E., 1957. "Localization of radionuclides and stable heavy nuclides in ocean sediments." ; *Nature*, 180, 85.
- Bacon M.P. and Edmond J.M., 1972. "Barium at Geosecs 111 in the southwest Pacific." ; *Earth Planet. Sci. Lett.*, 16,66.
- Baker C.W., 1975. "The determination of radiocaesium in sea and fresh water." ; Ministry of Agriculture, Fisheries and Food, Fisheries Laboratory technical reports series number 16.
- Baker C.W., 1976. Personal communication.
- Barnes H and Goodley, 1961. "The general hydrography of the Clyde Sea Area, Scotland. Part 1." ; *Bull. Marine Ecol.*, 5,112.
- Baxter M.S. and Harkness D.D., 1975. " $^{14}\text{C}/^{12}\text{C}$ ratios as tracers of urban pollution." "Proc. IAEA and FAO cmf. "Isotope ratios as pollutant source and behaviour indicators", 135.
- Boni A.L., "Rapid ion exchange analysis of radiocaesium in milk, urine, sea water and environmental samples." ; *Anal.Chem.*,38,89.
- Bowden K.F., 1955. Fisheries Investigations Series 11, 18,67, HMSO.
- Bowden K.F., 1965. "Currents and mixing in the ocean" in "Chemical Oceanography" ; Eds. Riley J.P. and Skirrow G., Academic Press.
- Bowen V.T. and Sugihara T.T., 1960. "Strontium - 90 in the mixed layer of the Atlantic Ocean." ; *Nature*, 186,71.

- Bowen V.T., Noshkin V.E., Volchok H.L., Livingston H.D. and Wong K.M., 1974. "Caesium - 137 to strontium - 90 ratios in the Atlantic Ocean 1966 through 1972. "Limnol. Oceanog., 19,670.
- Broecker W.S., 1974. "Chemical Oceanography." ; Harcourt, Brace, Jovanovich inc.
- Broecker W.S., Bonebakker E.R. and Rocco G.E., 1966. "The vertical distribution of caesium - 137 and strontium - 90 in the oceans 2." J. Geophys. Res., 71,1999.
- Broecker W.S., Kaufman A and Trier R.M., 1973. "The residence time of thorium in surface sea water and its implications regarding the rate of reactive pollutants." ; Earth Planet. Sci. Lett., 20,35.
- Buchanan J.Y., 1891. "On the composition of oceanic and littoral manganese nodules." ; Trans. Roy. Soc. Edinburgh, 36,459.
- Buchowiecki J and Cherry R.D., 1967. "Thorium, radium and potassium in manganese nodules." ; Chem. Geol., 3,111.
- Burton J.D., 1965. "Radioactive nuclides in sea water, marine sediments and marine organisms" in "Chemical Oceanography" (vol 2) ; Eds. Riley J.P. and Skirrow G., Academic Press.
- Calvert S.E. and Price N.B., 1970. "Composition of manganese nodules and manganese carbonates from Loch Fyne, Scotland." Contr. Miner. Petrol., 29,215.
- Cambray R.S., Jefferies D.F. and Topping G., 1975. "An estimate of the input of atmospheric trace elements into the North Sea and the Clyde Sea (1972 - 3)." UKAEA Publication AERE - R 7733, HMSO.
- Chow T.J. and Goldberg E.D., 1960. "On the marine geochemistry of barium." ; Geochim Cosmochim Acta, 20,192.
- Chung Y, 1973a. "Excess radon in the Santa Barbara Basin." ; Earth Planet. Sci. Lett., 17,319.

- Chung Y, 1973b. "Transient excess radon profiles in Pacific bottom waters." ; Earth Planet Sci. Lett., 21,295.
- Chung Y, 1974. "Radium - 226 and Ra - Ba relationships in Antarctic and Pacific waters." ; Earth Planet Sci. Lett., 23,125.
- Chung Y. and Craig H., 1973. "Radium - 226 in the Eastern Equatorial Pacific." Earth Planet. Sci. Lett., 17,306.
- Chung Y, Craig H., Ku T.L., Goddard J. and Broecker W.S., 1974. "Radium - 226 measurements from three Geosecs intercalibration stations." ; Earth Planet. Sci. Lett., 23,116.
- Clyde River Purification Board, 1972. 17th Annual Report.
- Clyde River Purification Board, 1973. 18th Annual Report.
- Clyde River Purification Board, 1974a. 19th Annual Report.
- Clyde River Purification Board, 1974b. "Pollution in the Clyde" in "The Clyde Estuary and Firth. An assessment of present knowledge compiled by members of the Clyde Study Group." ; Natural Environment Research Council Publications Series C, number 11,24.
- Collar R.H.F., 1974. "The River Clyde Estuary. Current knowledge of water and sediment movement" in "The Clyde Estuary and Firth. An assessment of present knowledge compiled by members of the Clyde Study Group." ; Natural Environment Research Council Publications Series C. number 11,10.
- Conlan B., Henderson P. and Walton A., 1969. "A simplified procedure for the assay of picocurie concentrations of Radium - 226 and its application to a study of the natural radioactivity in surface water in Scotland." ; Analyst, 94,15.
- Cotton F.A. and Wilkinson G., 1968. "Advanced Inorganic Chemistry" (2nd edition) ; Interscience.
- Craib J.S., 1965. "A sampler for taking short undisturbed marine cores." ; J. Cons. Perm. Int. Explor. Med., 1,34.

- Craig H.E., 1969. "Abyssal carbon and radiocarbon in the Pacific." ;
J. Geophys. Res., 74,5491.
- Craig R.E., 1959. "Hydrography of Scottish coastal water." ; Mar. Res.,
20,30.
- Damon P.E. and Hyde H.I., 1952. "Scintillation tube for the measurement
of radioactive gases." ; Rev. Sci. Instr., 23,766.
- Deegan C.E., Kirby R., Rae I. and Floyd R., 1973. "The superficial
deposits of the Firth of Clyde and its sea lochs." ; Institute
of Geological Sciences Report number 73/9. HMSO.
- Defant A., 1961. "Physical Oceanography" (volume 1) ; Pergamon Press.
- Dooley H.D. and Steele J.H., 1969. "Wind driven currents near a coast," ;
Dt. Hydrogr. Z., 22,213.
- Doursma E.K. and Gross M.G., 1971. "Marine sediments and radioactivity"
in "Radioactivity in the marine environment." ; National Academy
of Sciences.
- Edmond J.M., 1970. "Comments on the paper by T.L. Ku, Y.H. Li,
G.G. Mathieu and H.K. Wong, "Radium in the Indian - Antarctic Ocean
south of Australia." ; J. Geophys. Res., 75,6878.
- Evans R.D. and Kip A.F., 1938. "The Ra content of marine sediments
from the E. Indies, the Phillipines and Japan, and of the
mesozoic fossil clays of the E. Indies." ; Am. J. Sci., 36,321.
- Evans R.D., Kip A.F. and Moberg E.G., 1938. "The Ra and Rn content of
Pacific Ocean water." ; Am. J. Sci., 36,241.
- Eve A.S., 1907. "The ionization of the atmosphere over the ocean." ;
Phil. Mag., 13,248.
- Eve A.S., 1909. "On the amount of Ra present in sea water." ; Phil Mag,
18,102.
- Ferrante E.R., Gourski E. and Boulenger R.R., 1964. "Detector for
radon - 222 measurements at very low level" in "The natural
radiation environment" Eds Adams J.A.S. and Lowder W.M. ;
Chicago University Press, 353.

- Fleming G, 1969. "The Clyde Basin : hydrology and sediment transport." Ph.D. Thesis. Univ. Strathclyde
- Food and Agriculture Organisation (United Nations), 1971. "Report on the seminar on methods of detection, measurement and monitoring of pollution in the marine environment." ; Panel 7, Radioactivity Fish. Rep. FAO, number 99, suppl 1, 87.
- Francis C.W. and Brinkley F.S., 1976 "Preferential adsorption of ^{137}Cs to micaceous minerals in contaminated freshwater sediments." ; Nature, 260, 511.
- Friedlander G., Kennedy J.W. and Millar J.M., 1964. "Nuclear and radiochemistry" (2nd edition). John Wiley, New York.
- Gair R., 1967. "Clyde sediments : rheological properties and movement." Ph.D. Thesis. Univ. Strathclyde.
- Goldberg E.G. and Bruland K, 1974. "Radioactive Geochronologies" in "The Sea (volume 5). Marine Chemistry" ed. Goldberg E.D. ; John Wiley, 451.
- Halcrow W., Mackay D.W. and Thornton I., 1973. "The distribution of trace metals and fauna in the Firth of Clyde in relation to the disposal of sewage sludge" J. Mar. Biol. Ass. U.K., 53, 721.
- Hall G.P.D., 1973. Royal Navy Hydrography chart 2000. Gareloch.
- Hammond D.E., Simpson H.J. and Mathieu G.M., 1975. "Methane and ^{222}Rn as tracers for exchange across the sediment-water interface in the Hudson River Estuary" in "Marine chemistry in the coastal environment", ACS symposium series 18, 119.
- Haslam D.W., 1975. Royal Navy Hydrography chart 3746. Loch Long and Loch Goil.
- Heath R.L., 1974. "Table of the isotopes" in "Handbook of chemistry and Physics." ; 55th edition 1974-75. CRC Press, B248.

- Hoffman B.W. and Van Camerik S.B., 1967. "A table and method for determining the true time representing a count rate observed in radionuclear counting." ; Anal. Chem., 39,1198.
- Howells H., 1976. Personal communication.
- Jefferies D.F., 1976. Personal communication.
- Jefferies D.F., Preston A. and Steele A.K., 1973. "Distribution of ^{137}Cs in British coastal waters." ; Mar. Poll. Bull., 4, 118.
- Johnson J.O., 1971. "Determination of ^{228}Ra in natural waters." ; United States Geological Survey Water - Supply Paper 1696-G.
- Johnston R., Adams J.A. and Dooley H.D., 1974. "Some observations on the hydrography, chemistry and plankton of the Firth of Clyde in relation to nitrate rich effluents" in "The Clyde Estuary and Firth. An assessment of present knowledge compiled by members of the Clyde Study Group." Natural Environment Research Council Publication Series C, number 11, 16.
- Johnstone G.S., Read H.H. and MacGregor A.G., 1966. "The Grampian Highlands" (3rd edition) : Institute of Geological Sciences handbook on the regional geology of Great Britain, HMSO.
- Joly J., 1908a. "The radioactivity of sea water." ; Phil. Mag., 15, 385.
- Joly J., 1908b. "On the radium content of deep sea sediments" ; Phil. Mag., 16, 190.
- Kaufman A., Trier R.M., Broecker W.S. and Feely H.W., 1973. "Distribution of ^{228}Ra in the world ocean." ; J. Geophys. Res., 78, 8827.
- Kawamura S., Shibata S. and Kurotaki K., 1971. "Adsorption characteristics of radionuclides on zirconium hexacyanoferrate (11)" Anal. Chim. Acta., 56, 405.
- Koczy F.F., 1954. in "Nuclear Geology", Wiley, 120.
- Koczy F.F., 1958. "Natural radium as a tracer in the ocean." ; Proc 2nd United Nations Int. Conf. 'Peaceful Uses of Atomic Energy', 18, 351.

Koczy F.F., 1965. Progr. in Oceanog., 3, 155.

Koczy F.F. and Titze H., 1958. "Radium content of carbonate shells." ;
J. Mar. Res., 17, 302.

Koide M., Bruland K. and Goldberg E.D., 1976. "²²⁶Ra chronology of a
coastal marine sediment." ; Earth Planet. Sci. Lett., 31, 31.

Krishnaswami S. Lal D., Martin J.M. and Meybeck M., 1971. "Geochronology
of lake sediments." ; Earth Planet. Sci. Lett., 11, 407.

Krishnaswami S., Lal D., Somayajulu B.L.K., Dixon F.S., Stonecipher S.A.
Craig H., 1972. "Silicon, radium, thorium and lead in sea water ;
in-situ extraction by synthetic fibre." Earth Planet. Sci. Lett., 16, 84.

Krishnaswami S. and Lal D., 1972. "Manganese nodules and budget of trace
solubles in oceans." in Nobel Symposium 20; "The changing chemistry
of the oceans." , 307.

Krishnaswami S., Lal D., Amin B.S. and Soutar A., 1973, "Geochronological
studies in Santa Barbara Basin : ⁵⁵Fe as a unique tracer for
particulate settling." ; Limnol. Oceanog., 18, 763.

Kroll V. St., 1953. "Vertical distribution of radium in deep sea sediments."
Nature, 171, 742.

Kroll V. St., 1954. Deep Sea Res. 1, 211.

Kroll V. St., 1955. Rep. Swed. Deep Sea Exped., 10. 1.

Ku T.L., Li Y.J., Mathieu G.G. and Wong H.K., 1970. "Radium in the
Indian-Antarctic Ocean south of Australia." ; J. Geophys. Res, 75, 5286.

Kuznetsov Y.V., Lisitsyn A.P., Simonyak Z.N. and Elizarova A.N., 1973.
"Distribution of ²²⁶Ra in waters of equatorial part of the Pacific
Ocean." ; Radiokhimiya, 15, 704.

Lal D., Arnold J.R. and Somayajulu B.L.K., 1964. "A method for the
extraction of trace elements from sea water." ; Geochim Cosmochim
Acta, 28, 1111.

Leatherland T.M., 1976. Personal communication.

Lederer C.M., Hollander J.M. and Perlman I., 1967. "Table of Isotopes"
(6th edition), Wiley.

- Lerman A. and Lietzke T.A., 1975. "Uptake and migration of tracers in lake sediments." ; *Limnol. Oceanog.*, 20, 497.
- Li Y.H., Ku T.L., Mathieu G.G. and Wolgemuth K., 1973. "Barium in the Antarctic Ocean and implications regarding the marine geochemistry of Ba and ^{226}Ra ." ; *Earth Planet Sci. Lett.*, 19, 352.
- Lietzke T.A., Lerman A. and Tanigucki H., 1973. "Cesium-137 and strontium-90 : similarities and differences in transport models in sediments." *EOS Trans. Am. Geophys Union*, 54, 341.
- Lowton R.J., Martin J.H. and Talbot J.W., 1966. "Dilution, dispersion and sedimentation in some British Estuaries." ; *Proc. IAEA conf. on 'Disposal of Radioactive Wastes into seas, oceans and surface waters*, 189
- MacGregor M. and MacGregor A.G., 1948. "The Midland Valley of Scotland" (2nd edition). Institute of Geological Sciences handbook on the regional geology of Great Britain, HMSO.
- Mackay D.W. and Gilligan J., 1972. "The relative importance of freshwater input, temperature and tidal range in determining levels of dissolved oxygen in a polluted estuary." ; *Water Res.*, 6, 183.
- Mackay D.W., Halcrow W. and Thornton I., 1972. "Sludge dumping in the Firth of Clyde." ; *Mar. Poll. Bull.*, 3, 7.
- Marshall S. 1974. "Plankton in the Firth of Clyde." in "The Clyde Estuary and Firth. An assessment of present knowledge compiled by members of the Clyde Study Group." ; Natural Environment Research Council Publications Series C. number 11, 32.
- McKinley I.G., 1976. Personal communication.
- Mill H.R., 1892. "The Clyde Sea Area, Parts 1 and 2." *Trans. Roy. Soc. Edinburgh*, 36, 641.
- Milne P.H., 1974. "Physical characteristics and tides of the Clyde Sea Area" in "The Clyde Estuary and Firth. An assessment of present knowledge compiled by members of the Clyde Study Group." ; Natural Environment Research Council Publications Series C, number 11, 14.

- Mitchell N.T., 1975. "Radioactivity in surface and coastal waters of the British Isles 1972-73." ; Ministry of Agriculture, Fisheries and Food, Fisheries Radiobiological Laboratory Technical Report FRL10.
- Moore H.B., 1931. "The muds of the Clyde Sea Area 111. Chemical and physical conditions, rates and nature of sedimentation and fauna." ; J. Mar. Biol. Ass. U.K., 17, 325.
- Moore W.S., 1969a. Ph.D. Thesis. State University of New York.
- Moore W.S., 1969b. "Measurement of ^{228}Ra and ^{228}Th in sea water." ; J. Geophys. Res., 74, 694.
- Moore W.S., 1969c. "Oceanic concentrations of ^{228}Ra ." ; Earth Planet Sci. Lett., 6, 437.
- Moore W.S., 1972. "Radium-228 : application to thermocline mixing studies." ; Earth Planet. Sci. Lett., 16, 422.
- Moore W.S. and Reid D.F., 1973. "Extraction of radium from natural waters using manganese-impregnated acrylic fibres." ; J. Geophys. Res., 78, 8880.
- Moore W.S. and Cook L.M., 1975. "Radium removal from drinking water." ; Nature, 253, 262.
- Natural Environment Research Council, 1974. "The Clyde Estuary and Firth. An assessment of present knowledge compiled by members of the Clyde Study Group." ; Natural Environment Research Council Publications Series C, number 11.
- Noshkin V.E. and Bowen V.T., 1972. "Concentration and distribution of long-lived fallout radionuclides in open ocean sediments." ; Proc. IAEA symposium on 'The interaction of radioactive contaminants with the constituents of the marine environment.'

- Osterberg C.L., Cutshall N., Johnson V., Cronin J., Jennings D. and Frederick K., 1966. "Some non-biological aspects of Columbia River radioactivity." ; Proc. IAEA conf. on 'Disposal of Radioactive Wastes into seas, oceans and surface waters.' 321.
- Pennington W., Cambray R.S. and Fisher E.M., 1973. "Observations on lake sediments using fallout ^{137}Cs as a tracer." ; Nature, 242, 324.
- Pettersson H., 1930. Result. Camp. Scient. Prince Albert 1, 81.
- Pettersson H., 1937. Mitt. Inst. Radiumforsch., Wien, 400a.
- Pettersson H., 1939. Meddn. Oceanogr. Inst. Goteborg, 1, 12.
- Pickard G.L. 1975. "Descriptive Physical Oceanography." ; (2nd edition), Pergamon Press.
- Piggott C.S. and Urry W.D., 1941. J. Mar. Res., 7, 618.
- Poskanzer A.M. and Foreman B.M., 1961. "A summary of TTA extraction coefficients." ; J. Inorg. Nucl. Chem., 16, 323.
- Preston A., 1974. "Artificial radioactivity in the sea." ; in "The Sea volume 5, Marine chemistry," ed. Goldberg E.D., 817.
- Preston A., Woodhead D.S., Mitchell N.T. and Penreath R.J., 1972. "The impact of artificial radioactivity on the oceans and on oceanography." ; Proc. Roy. Soc. Edinburgh, B, 72, 412.
- Proudman J., 1948. "On the mixing of sea water by turbulence." ; Proc. Roy. Soc., A, 195, 300.
- Prout W.E., Russel E.R. and Groh H.J., 1965. "Ion exchange absorption of caesium by potassium hexacyanocobalt (11) ferrate (11). " ; J. Inorg. Nucl. chem., 27, 473.
- Riley J.P., 1965. "Analytical chemistry of sea water" in "Chemical Oceanography" (volume 2). Eds. Riley J.P. and Skirrow G. ; Academic Press
- Riley J.P. and Skirrow G., 1975. "Chemical Oceanography (2nd edition)" (vol. 3) ; Academic Press, 523.
- Ritchie J.C. McHenry J.R. and Gill A.C., 1973. "Dating recent reservoir sediments." ; Limnol Oceanog. 18, 254.

- Robbins J.A. and Edgington D.N., 1975. "Determination of recent sedimentation in Lake Michigan using ^{210}Pb and ^{137}Cs ." ; *Geochim. Cosmochim. Acta*, 39, 285.
- Rocco G.G. and Broecker W.S., 1963. "The vertical distribution of cesium-137 and strontium-90 in the oceans." ; *J. Geophys. Res.*, 68, 4501.
- Shannon L.V. and Cherry R.D., 1971. "Radium-226 in marine phytoplankton." ; *Earth Planet. Sci. Lett.*, 11, 339.
- Strutt R.J., 1906. "On the distribution of radium in the earth's crust." ; *Proc. Roy. Soc., A*, 78, 150.
- Sverdrup H.V., Johnson M.W. and Fleming R.H., 1942. "The Oceans. Their Physics, chemistry and General Biology", Prentice Hall.
- Swan D.S., 1976. Personal communication.
- Szabo B.J., 1967. "Radium content in plankton and sea water in the Bahamas." ; *Geochim. Cosmochim. Acta*, 31, 1321.
- Thiebaux M.L. and Thiebaux H.J., 1974. "Radioactive decay in a steady state reservoir." ; *Water Research*, 8, 447.
- Thiebaux H.J., 1975. Personal communication.
- Thomson A. 1969. "A hydraulic investigation of the Clyde." ; Ph.D. Thesis. Univ. Strathclyde.
- Thomson J., 1971. Ph.D. Thesis. Univ. Glasgow.
- Thomson J. and Walton A., 1972. "Natural radioactive decay series elements in the oceans and sediments." ; *Proc. Roy. Soc. Edinburgh (b)*, 72/73, 169.
- Topping G., 1974. "The atmospheric input of some heavy metals to the Firth of Clyde and its relation to other inputs." ; *ICES CM 1974/E32*.
- Trier R.M., Broecker W.S. and Feely H.W., 1972. "Radium-228 profile at the second Geosecs intercalibration station, 1970, in the North Atlantic." ; *Earth Planet. Sci. Lett.*, 16, 141.
- Turekian K.K. and Johnson D.G., 1966. "The barium distribution in sea water." ; *Geochim. Cosmochim. Acta*, 30, 1153.

United Nations, 1972. "Ionizing radiation : levels and effects. volumes 1 and 2." ; A report of the U.N. Science Committee on the effects of atomic radiation to the General Assembly, U.N. Publication E72,1X,17.

Urry W.D., 1948. J. Mar. Res., 7, 618.

Wallace J.W., 1974. "The development of the chlorinity/salinity concept in oceanography." ; Elsevier oceanography series, volume 7.

Wilson T.S.R., 1974. "Caesium-137 as a water movement tracer in the St. Georges channel." ; Nature, 248, 125.

Wolgemuth K., 1970. "Barium analyses from the first Geosecs test cruise." ; J. Geophys. Res., 76, 7686.

Wolgemuth K. and Broecker W.S., 1970. "Barium in sea water." ; Earth Planet. Sci. Lett., 8, 372.

Katz J.J. and Seaborg G.T., 1957. "The chemistry of the actinide elements." (Methuen), 7.

Lenihan J., 1976. Personal communication.

Lucas H.F., 1957. "Improved low level alpha-scintillation counter for radon." Rev. Sci. Instr., 28, 680.

Miyake T, Saruhashi K, Katsuragi Y and Kunazawa T, 1962. "Penetration of ^{90}Sr and ^{137}Cs in deep layers of the Pacific and vertical diffusion rate of deep waters." J. Radiation. Res., 3, 161.

Pettersson H, 1951. "Radium and deep sea chronology." Nature, 167, 942.

Thom A.S., 1949. "Investigations of tidal phenomena in the Clyde estuary using a scale model." J. Inst. Civ. Eng., 33, 100.